



UNIVERSITÀ DEGLI STUDI DI MILANO
Scuola di Dottorato in Scienze Biologiche e Molecolari
XXVII Ciclo

**A PROTEOMIC APPROACH TO IDENTIFY PROTEIN
INTERACTORS RESPONSIBLE OF FLOWERING TIME
DETERMINATION IN THE MODEL SPECIES *ARABIDOPSIS
THALIANA***

Fabio Rossi

PhD Thesis

Scientific tutor: Paolo Pesaresi

Academic year: 2013-2014

SSD: BIO/04 Fisiologia Vegetale, BIO/18 Genetica

Thesis performed at the Department of Biosciences,
Università degli Studi di Milano, via Celoria 26, 20133 Milano

CONTENTS

1. SUMMARY	6
2. INTRODUCTION	8
2.1 The model species <i>Arabidopsis thaliana</i>	8
2.2 Meristems.....	9
2.3 The floral transition	10
2.4 The photoperiodic pathway	12
2.5 The vernalization pathway	14
2.6 The autonomous pathway.....	15
2.7 The thermosensory pathway.....	16
2.8 The GA pathway	17
2.9 MADS-box transcription factors	18
2.10 MADS-Domain and Chromatin remodeling.....	19
2.11 Role of SVP during the floral transition	20
3. AIM OF THE PH.D. PROJECT	22
4. MATERIALS AND METHODS.....	23
4.1 Plant material and growth conditions	23
4.2 Yeast Two hybrid assay.....	23
4.3 RNA isolation, Reverse Transcription-PCR and quantitative Real-Time (qRT-PCR) analysis	23
4.4 Crosslinking of plant material.....	24
4.5 Nuclear proteins isolation	25
4.6 Coimmunoprecipitation	26
4.7 Trypsin digestion	27
4.7.1 In gel trypsin digestion:	27
4.7.2 In solution trypsin digestion:	28
4.8 Mass spectrometry data analysis	29
4.8.1 Bioinformatics analysis: (Smaczniak, Li, et al. 2012)	30
4.9 Segregation analysis and primer combinations	32
5. RESULTS	34
5.1 The transgenic line CaMV-35S:: <i>SVP-GFP</i>	34
5.2 The native line <i>SVP</i> :: <i>SVP-GFP</i>	35
5.3 Nuclei isolation	36
5.4 Co-Immunoprecipitation	38
5.4.1 Dynabeads® Protein A:	38

5.4.2 GFP-Trap®:	39
5.5 Cross-Linking method for protein interaction analysis (Klockenbusch & Kast 2010).....	40
5.6 Analysis of the Mass Spectrometry data	41
5.6.1 Coimmunoprecipitation from seedling:	43
5.6.2 Coimmunoprecipitation from inflorescence:	43
5.7 Analysis of the putative interactors	45
5.8 SDG2 and GCN5 as putative interactors.....	46
5.8.1 SET domain protein 2 (SDG2):	46
5.8.2 Histone Acetyltransferase GCN5: (GENERAL CONTROL NON-REPRESSIBLE 5)	48
5.9 <i>In vivo</i> validation of the candidates selected from the MS output	49
5.10 <i>In planta</i> validation of proteomics data	50
6. DISCUSSION	52
6.1 The SVP::SVP-GFP and the 35S::SVP-GFP lines.....	52
6.2 The nuclei isolation protocol	52
6.3 The coimmunoprecipitation strategy	53
6.4 The Mass Spectrometry data.....	54
6.5 The putative interactors	54
6.6 SDG2 and GCN5 as a putative interactors.....	55
6.7 <i>In vivo</i> validation.....	55
7. CONCLUSIONS	56
8. FUTURE PROSPECTIVE	58
9. REFERENCES.....	59
10. PUBLICATIONS	71
10.1 List of publications:.....	72
11. ACKNOWLEDGEMENTS.....	126

I believe the sacrifices in life
give more than they take

[D.T.]

1. SUMMARY

Reproductive success in plants is dependent on the timing of the switch from vegetative to reproductive phase coinciding with optimal environmental and developmental conditions. This is a key step that dramatically influences plant productivity, one of the most important aspects in agriculture. Plants have evolved an elaborate regulatory network that integrates endogenous and environmental signals to ensure that flowering occurs when conditions are most favorable. During the last two decades, functional genomics studies have revealed the existence of a complex network of genetic interactions responsible of integrating the different types of signals, both internal and external, that plants receive and that define when plants can enter into the reproductive phase (Liu et al. 2009). However, the molecular characterization of the floral transition process is far from being completed, therefore new studies flanked by new research methods are needed to identify and characterize the proteins and protein complexes that play a key role in the transition to the reproductive phase (Jang et al. 2009). One of these proteins involved in floral transition is SVP (Short Vegetative Phase), a MADS-Box transcription factor studied for a long time at genetic level. It has been reported (Liu et al. 2007) that the ectopic expression of this transcription factor causes a late flowering phenotype in transgenic plants. Moreover, this line develops abnormal leaves and also the flower structure is altered. It is known that many, if not all transcription factors, play their biological role as part of multi-subunit protein complexes, on the other side knowledge on those protein complexes is scarce. In the case of SVP, some interacting partners have been identified via yeast-2-hybrid assays (Gregis et al. 2009), however *in planta* evidences of such interactions have not been provided, yet. During the last two years, in our laboratory we developed a protocol that enable us to coimmunoprecipitate protein complexes using an antibody against GFP fused to SVP, in order to identify the putative partners that interact together, with SVP, in controlling the flowering time. The analysis of the first data generated a large number of putative candidates involved in acetylation, deacetylation and methylation of histones (Cohen et al. 2009; Berr et al. 2010). A major conclusion that can be drawn from our findings, in agreement with recent publications in this field, is that SVP controls flowering time in Arabidopsis by a chromatin-dependent expression regulation of genes involved in the process. The aim of this project was the validation of the results, by using different methods, and the characterization of these putative partners in order to identify the right composition of different complexes in which SVP interacts with, and the mechanisms behind

the regulation of flowering time. The flowering time analysis of mutants of the two most promising candidates *GCN5* (GENERAL CONTROL NON-REPRESSIBLE 5) and *SDG2* (SET domain protein 2) revealed, in agreement with already published data, their involvement in this mechanism (Bertrand et al. 2003; Guo et al. 2010; Berr et al. 2010). Moreover, preliminary data obtained by analyzing the *35S::SVP-GFP svp/svp SDG2/sdg2* plants, indicate that the floral defect caused by the overexpression of *SVP*, needs also the presence of *SDG2* protein.

2. INTRODUCTION

Floral transition is a key step in the life cycle of plants since it determines the period of flower development, thus defining the transition from vegetative to reproductive phase, a crucial process that dramatically influences plant productivity. Clearly, the possibility to control this process has an estimable value in agriculture, since it will allow plants to flower under optimal environmental conditions, thus enabling maximal crop yield, every year, independently from the environmental conditions (Kang et al. 2011). To reach this ambitious goal, it is extremely important to gain a deep knowledge of all the molecular processes responsible of the flower transition process. During the last two decades, functional genomics studies have revealed the existence of a complex network of genetic interactions responsible of integrating the different types of signals, both internal and external, that plant receives and that define when plants can enter into the reproductive phase (Liu et al. 2009). However, the molecular characterization of the floral transition process is far from being completed, therefore new studies flanked by new research methods are needed to identify and characterize the proteins and protein complexes playing key roles in the transition to the reproductive phase (Jang et al. 2009), on the model species *Arabidopsis thaliana* is necessary.

2.1 The model species *Arabidopsis thaliana*

Arabidopsis thaliana (Figure 1) is a small herbaceous eudicot, member of the family of the *Brassicaceae*, that can be found in temperate areas. This plant is the first of which the genome was completely sequenced at the end of year 2000 thanks to the Arabidopsis Genome Initiative. Arabidopsis present a lot of characteristics that makes it the best plant model organism used to study developmental, biochemical and physiological processes. The knowledge obtained from these studies can often be transferred to other plants with economical relevance like Rice, Barley, Maize etc. Genetic engineering it's very easy, since plants can be transformed by using *Agrobacterium tumefaciens* through a simple procedure called "floral dipping", that doesn't require plant regeneration. Another advantage of this plant is the availability of many different mutants, both single nucleotide mutants obtained by EMS mutagenesis, and insertional mutants obtained by T-DNA or transposon insertions. To date 320.000 insertional mutants, covering more or less all the genome, are available in

the NASC (Nottingham Arabidopsis Stock Center) and ABRC (Arabidopsis Biological Resource Center) stock center. Other important characteristics of Arabidopsis that makes it an ideal model organism are the life-cycle very short (from seed to seed in 6 weeks), its small genome (146Mb), its little dimension and the abundance of seed produced by every single plant. The most commonly used ecotypes are *Columbia* (Col) and *Landsberg erecta* (Ler), and both of them have been sequenced. One of the main features of the Arabidopsis genome is the large amount of genetic redundancy, in fact about 60% of the entire genome is thought to be derived from a single event of duplication. Subsequently a process of specialization took place accumulating mutations in the coding sequence of the duplicated genes, thus conferring different gene functions and expression profiles.

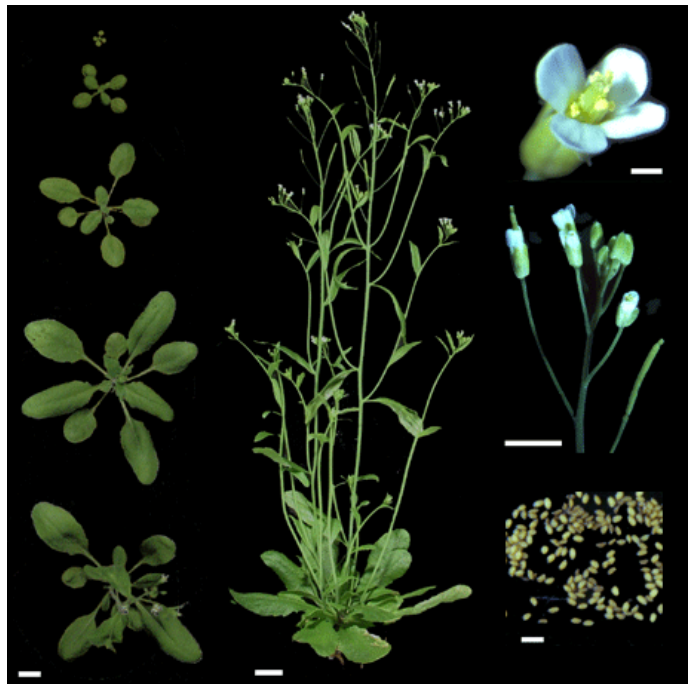


Figure 1. In this picture is represented the life cycle of the model plant *Arabidopsis Thaliana*.

2.2 Meristems

In *Arabidopsis thaliana* the primary meristems (root and shoot meristems) are formed during embryogenesis and form primary tissues from which all organs develop. Meristems can be classified into determinate or indeterminate: a determinate meristem is a meristem in which the stem cell reservoir is transient and its maintenance must be stopped at the correct stage of development. An indeterminate meristem, instead, grows indefinitely and its stem cell reservoir is maintained constantly. Meristem cells can produce daughter cells that differentiate to produce organs and to maintain the indeterminate meristem. Cytological and histological studies have shown that the angiosperm indeterminate shoot apical meristem (SAM) consist of dividing cells laid out in an organized manner (Evans & Barton 1997). Three positions have been recognized within the SAM (Figure 2). The central zone (CZ), localized at the apex of the SAM, is a small cluster of enlarged, highly vacuolated cells with a slow

rate of division as they are the reservoir of pluripotent stem cells. The peripheral zone (PZ) surrounds the central zone and is the site of organ formation, with small cells and fast division. The rib zone (RZ) is beneath to the central zone, constitutes the meristem pith and contributes to the bulk of the meristem. In *Arabidopsis*, the SAM gives rise to different tissues during the different phases of plant life cycle. During the vegetative growth phase the SAM proliferates to produce vegetative structures such as leaves and secondary shoots. A wild-type plants produces a rosette of 13-15 leaves in long day (LD) conditions (Hartmann et al. 2000). Upon environmental and endogenous signals, the floral transition occurs triggering the transformation of the SAM into an inflorescence meristem (IM). The *Arabidopsis* IM is an indeterminate meristem and develops in a spiral manner multiple determinate floral meristems (FMs) that produce a precise number of floral organs arranged in a whorled pattern (Irish 1999). Every FM is committed to form a single flower, composed of four sepals, four petals, six stamens and one pistil in a whorled pattern.

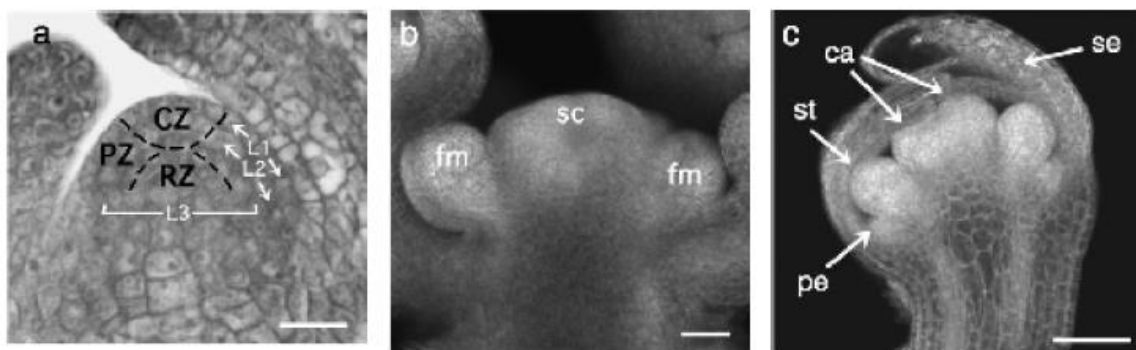


Figure 2. Structural features of *Arabidopsis* shoot apical and floral meristems. (a) Section through a vegetative SAM showing the cell layers (L1, L2, and L3) and the histologically defined domains. CZ, central zone; PZ, peripheral zone; RZ, rib zone. (b) Confocal micrograph of an indeterminate SAM. The stem cell reservoir (sc) is at the apex constituting the inflorescence meristem, and floral meristems (fm) arise from the flanks. (c) Confocal micrograph of a determinate flower, after the floral meristem has produced sepals (se), petals (pe), stamens (st), and two carpels (ca) in the center of the flower (Fletcher 2002).

2.3 The floral transition

The floral transition is a key step in the life cycle of plants, as it determines the switch from vegetative phase, where only leaves are produced by the SAM, to reproductive phase, during which flowers are formed. The flower contains both male and female gametes that are essential for plant reproduction. The decision to flower is one of the most important events during plant's life cycle and must be fine regulated. In *Arabidopsis thaliana* there are

five different pathways that control the floral transition in order to produce flowers and then seed and fruits (Figure 3), under the best environmental conditions (temperature, light). Three of these pathways are influenced by environmental stimuli: the photoperiodic pathway is regulated by day length, the vernalization pathway is regulated by low temperature, and the thermosensory pathway that is regulated by sub-optimal but not freezing temperature. The remaining two pathways, the autonomous pathway and the one controlled by plant hormone gibberellins, are dependent on internal signals. The signals generated from these different pathways are then integrated at the level of so called Floral Pathway Integrator genes which are *LEAFY (LFY)*, *FLOWERING LOCUS T (FT)*, and *SOPPRESSOR OF OVEREXPRESSION OF CONSTANS (SOC1)* (Kardailsky et al. 1999; Blázquez & Weigel 2000; Simpson & Dean 2002). *LFY* encodes a protein present only in the plant kingdom, it is expressed in young leaf primordia with a maximum expression peak in young flower meristems (Blázquez et al. 1997) where it is involved in the establishment of floral meristem identity. Its multiple role is responsible of different phenotypes in the plant. Overexpression of *LFY* confers an early flowering phenotype, while the *lfy* mutant shows the conversion of flowers into leaf-like structures with few inflorescence-like structures (Weigel, 1992). *LFY* integrates the photoperiodic and gibberellin pathways, through separate cis elements present on its own promoter (Blázquez & Weigel 2000). *FT* encodes a protein similar to phosphatidylethanolamine binding protein (PEBP) and Raf kinase inhibitor protein (RKIP) in animals (Kardailsky et al. 1999; Kobayashi et al. 1999) and its mRNA has been detected in all plant organs. Since the *ft* mutant flowers late in long day (LD) conditions but it is only slightly affected in short day (SD) conditions, *FT* has been attributed to the photoperiodic pathway (Koornneef et al. 1991). *SOC1* encodes a MADS box transcription factor that belongs to a gene family of four members: *SOC1*, *AGL42*, *AGL71* and *AGL72* (Parenicová et al. 2003). *SOC1* is expressed mostly in leaves and in the shoot apex, it is absent from stage 1 flower meristems and it reappears in the center of older flower meristems. *SOC1* integrates autonomous, vernalization and GA pathways (Moon et al. 2003). Working together with another MADS box transcription factor *AGAMOUS-LIKE24 (AGL24)*, *SOC1* is able to bind each other's promoters generating an auto-regulatory feedback loop and it is responsible of *LFY* activation (Lee et al. 2008).

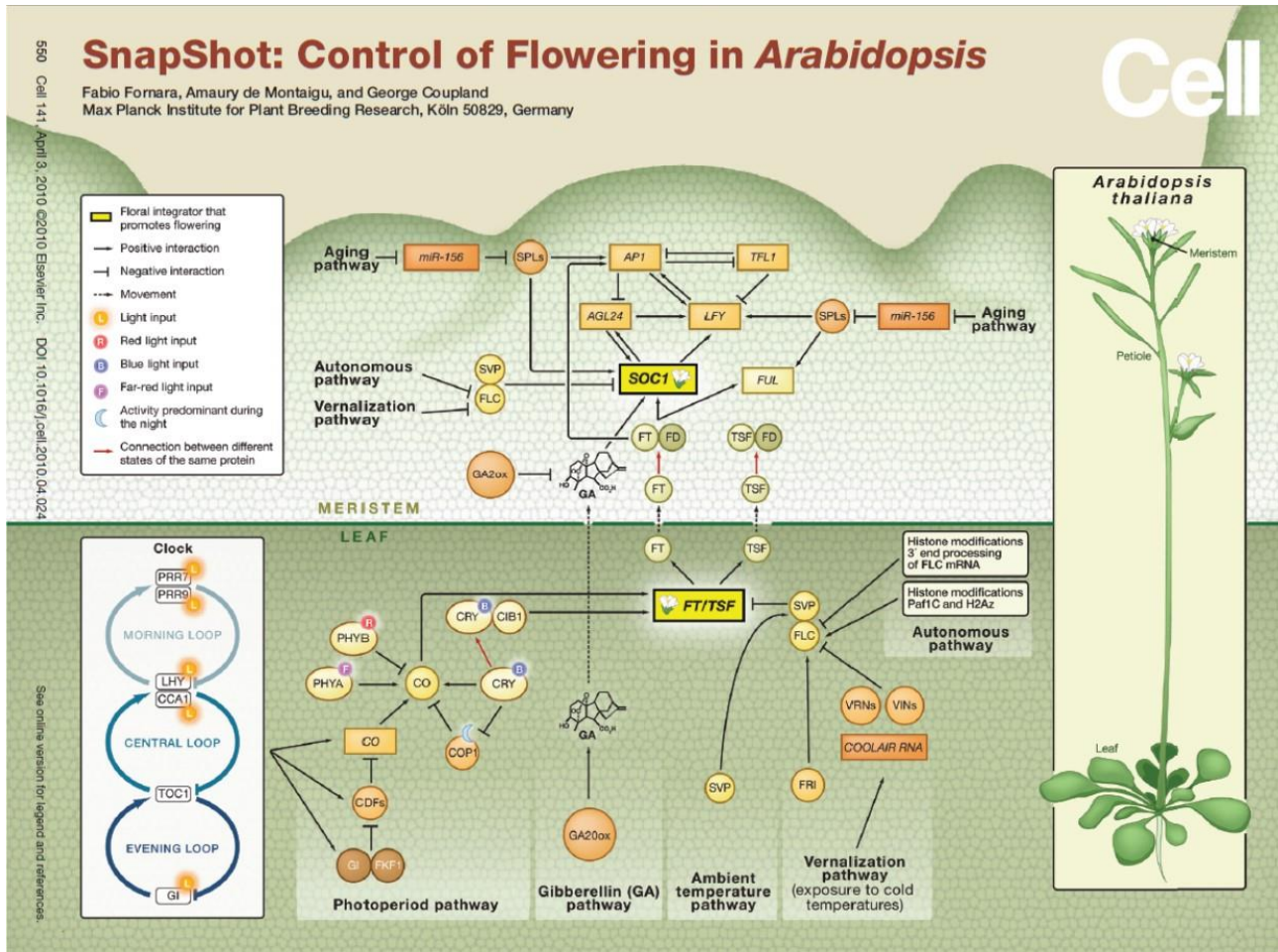


Figure 3. Here is represented the regulatory network that controls flowering in *Arabidopsis* (Fornara et al. 2010).

2.4 The photoperiodic pathway

Arabidopsis thaliana is a facultative long day plant: it flowers under long-day conditions, that is when spring and summer are coming. Studying mutants with altered photoperiodic flowering resulted in the identification of many genes that regulate flowering in response to long-day signal. These include light (photo) receptors, circadian clock components and clock- and light-regulated genes (Nakamichi et al. 2007; Takase et al. 2007).

For instance, mutations in *CONSTANS* (*CO*), *GIGANTEA* (*GI*), *FLOWERING LOCUS T* (*FT*), *FLOWERING LOCUS D* (*FD*), *FLOWERING WAGENINGEN* (*FWA*), *CRYPTOCHROME 2* (*FHA*) and *FE* cause lateness in flowering under long-days, but they have little effect under short-day; so all these genes have been placed in the photoperiodic pathway (Abe et al. 2005; Fowler et al. 1999).

One of the main players in this pathway is *CO*, a B-box zinc finger protein that promotes transcription of downstream flowering time genes (Putterill et al. 1995; Robson et al. 2001).

Alteration of *CO* expression has been observed in a number of circadian mutants. In fact the circadian clock controls expression of *CO* in the vascular tissue of leaves: *CO* mRNA level rises around 12 hours after dawn and it stays high throughout the night (Park et al. 1999; Fowler et al. 1999; Suárez-López et al. 2001). *CO* is also regulated at the post-translational level: cryptochrome and phytochrome A photoreceptors act at the end of the day to stabilize the *CO* protein (Valverde et al. 2004), while in darkness the protein is rapidly degraded. Under short-days the *CO* mRNA is only expressed during the dark hours, so the protein can never accumulate.

The major targets of *CO* are *FT*, a floral pathways integrator, and *TSF* (TWIN SISTER OF *FT*). *CO* promotes their expression in the leaves and their transport throughout the phloem system to the shoot apex (Figure 4) (Corbesier et al. 2007). It has been discovered that the

double mutant *ft-10 tsf-1* is photoperiod-insensitive and that the inactivation of these genes fully suppresses the early-flowering phenotype caused by over-expression of *CO*. Moreover both these genes are repressed by *SVP* in leaves (Lee et al. 2007; Li et al. 2008; Jang et al. 2009). It has been shown that in yeast *FT* and *TSF* can interact with the bZIP transcription factor *FD* (Abe et al. 2005; Wigge et al. 2005; Jang et al. 2009). In the SAM the complex *FT*/*FD* is involved in the

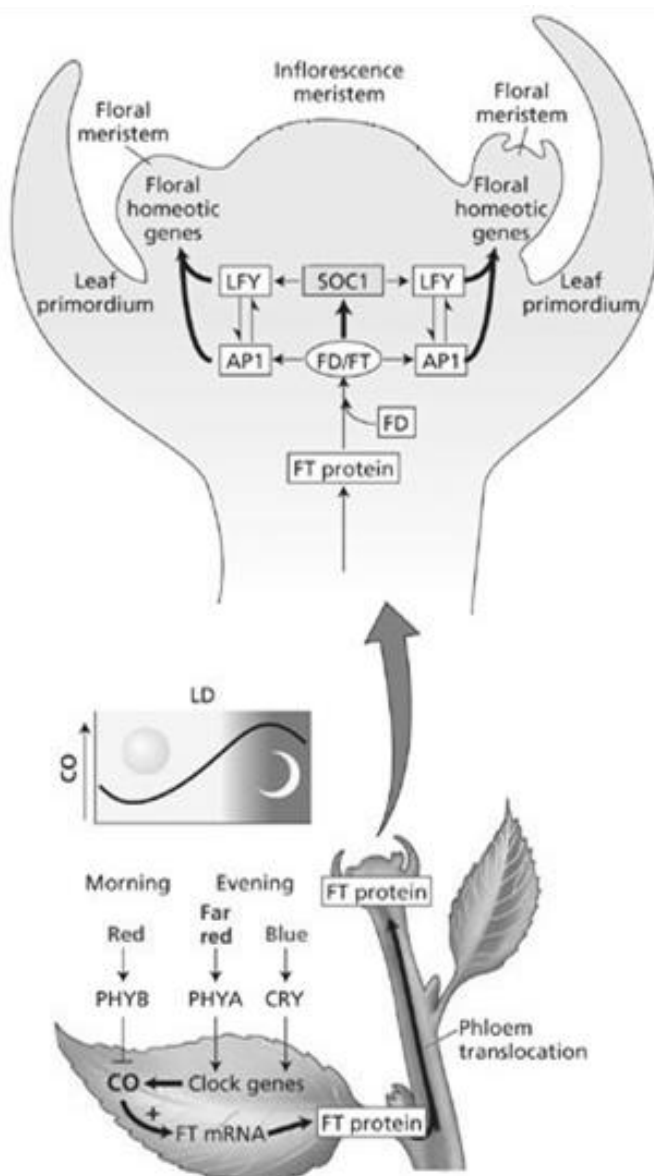


Figure 4. The photoperiodic pathway. Appropriate day length allows the accumulation of the transcription factor *CO* that controls expression of *FT* in the leaf. *FT* protein moves through the phloem to the shoot apex where it interacts with the transcription factor *FD* to activate key genes such as *AP1* and *SOC1*. *SOC1* then activates *LFY*, a transcription factor required for *AP1* expression in wild-type plants (Lee & Zeevaart 2007).

activation of *SOC1* (Searle et al. 2006), while it directly activates the MADS-box transcription factor *AP1* in the floral meristem (Abe et al. 2005; Wigge et al. 2005). An ectopic expression of *AP1* (*APETALA 1*) is observed in the over-expression of either FT or FD driven by the control of the CaMV 35S promoter (Kobayashi et al. 1999). In *Arabidopsis thaliana* an FT-independent photoperiodic pathway exists, but it is still not well characterized. The main player is *AGL17* (*AGAMOUS-LIKE 17*), a gene which is positively regulated by CO and that can influence *LFY* and *AP1* expression, since the expression of both these genes are reduced in the *agl17* mutant (Han et al. 2008).

2.5 The vernalization pathway

The vernalization pathway, which acts redundantly with the autonomous pathway, accelerates flowering upon exposure to a long period of cold (three to eight weeks). The requirement for vernalization is an adaptation to temperate climates that prevents flowering before winter and permits flowering in the favourable conditions during spring.

Arabidopsis plants can be summer-annual, if they are rapid-flowering and usually complete their reproductive cycle in one growing season, or winter-annual, if they may not complete their life cycle until the second growing season after an intervening winter.

To discover the genes involved in the vernalization pathway, winter- and summer-annual *Arabidopsis* plants were crossed and their progeny was analyzed using molecular markers. Two genes were found to be involved in this process: *FLOWERING LOCUS C* (*FLC*), a MADS-box transcription factor mostly expressed in meristems and leaves, and *FRIGIDA* (*FRI*), a nuclear protein found only in plants (Lee & Amasino 1995). In fact, in all the summer-annual *Arabidopsis* plants, these genes carry mutations that reduce their expression however *FLC* is expressed at high levels only in the presence of *FRI* (Johanson et al. 2000). In winter-annual *Arabidopsis*, vernalization promotes flowering by causing a down-regulation of *FLC*, which normally represses genes required for the transition to flowering (Michaels & Amasino 1999).

Screenings on mutagenized winter-annual plants were performed: plants that showed acquired insensitivity to vernalization were analysed to find the site of the mutation. Many different genes were discovered through these studies, such as *VERNALIZATION 1* (*VRN1*), *VERNALIZATION 2* (*VRN2*), *VERNALIZATION INSENSITIVE 3* (*VIN3*), *VRN5*

VIN3-LIKE 1 (VIL1), and *atPRMT5* (Levy et al. 2002; Bastow et al. 2004; Sung et al. 2006; Sung & Amasino 2004; Greb et al. 2007).

All these genes seem to be involved in remodelling *FLC* chromatin. The vernalization effect, in fact, is due to repressive histone modifications in the *FLC* locus, in particular to histone H3 Lys9 (H3K9) and histone H3 Lys27 (H3K27) methylation (Bastow et al. 2004; Sung & Amasino 2004).

However it has been shown that vernalization may act also through an *FLC*-independent pathway; for example, vernalization clearly promotes flowering in *flc* null mutants in SD (Scortecci et al. 2001). This is probably due to the repressive activity of *FLC* paralogs. In fact, in *Arabidopsis* five paralogs of *FLC* have been identified: *FLOWERING LOCUS M (FLM)/MADS AFFECTING FLOWERING 1 (MAF1)*, *MAF2*, *MAF3*, *MAF4*, and *MAF5*. *FLM/MAF1*, *MAF2*, and *MAF*. All these genes act as floral repressors, probably in a manner similar to what *FLC* does (Ratcliffe et al. 2001; Scortecci et al. 2003).

It has been shown that in plants with high *FLC* expression, *FT* and *SOC1* genes are repressed (Lee et al. 2000; Michaels et al. 2005). Moreover it has been demonstrated that *FLC* directly represses *SOC1* and *FD*, by binding their promoting regions, and *FT*, by binding a region in its first intron (Hepworth et al. 2002; Helliwell et al. 2006; Searle et al. 2006).

It has recently been discovered that the regions of *SOC1* and *FT* that are bound by *FLC* are also recognized by *SVP*. Coimmunoprecipitation analysis demonstrated that *SVP* and *FLC* interact in a repressive complex to delay the floral transition in *Arabidopsis* (Li et al. 2008). Although *SVP* interacts with *FLC* to repress flowering, *SVP* mRNA levels are not affected by vernalization, while vernalization results in the stable repression of *FLC* (Bastow et al. 2004; Sung & Amasino 2004). Recently it has been shown that the circadian clock has an influence on *SVP* levels, in fact in a double mutant of two clock components, *LATE ELONGATED HYPOCOTYL (LHY)* and *CIRCADIAN CLOCK ASSOCIATED 1 (CCA1)*, *SVP* protein accumulates to higher levels than in wild type plants (Fujiwara et al. 2008). This suggests that there may be a cross-talk between the photoperiodic pathway and the vernalization pathway.

2.6 The autonomous pathway

The autonomous pathway acts in parallel with the vernalization pathway as it also culminates in the repression of *FLC*. The mutants in this pathway are characterized by

delayed flowering in both LD and SD, in contrast to the mutants of the photoperiodic pathway that show delayed flowering only in LD conditions. Several genes have been associated to the autonomous pathway: *LUMINIDEPENDENS (LD)*, *FCA*, *FY*, *FPA*, *FLOWERING LOCUS D (FLD)*, *FVE*, *FLOWERING LATE KH MOTIF (FLK)*, *REF6* and *FLOWERING LOCUS D (FLD)* (Lee et al. 1994; Macknight et al. 1997; Schomburg et al. 2001; Simpson et al. 2003; Simpson et al. 2004; Sanda & Amasino 1996).

FCA, *FPA*, *FY*, and *FLK* proteins are predicted to be involved in RNA metabolism (Macknight et al. 1997; Schomburg et al. 2001; Simpson et al. 2003), while *FVE*, *FLD*, and *REF6* have domains that usually are associated with chromatin-modifying components, for example *FLD* and *REF6* are predicted to be histone demethylases (Noh et al. 2004; Jiang et al. 2007). Even if there is no evidence that these proteins directly interact with *FLC* mRNA or with the *FLC* locus, it has been demonstrated that mutations in the *FLC* locus completely suppress the delayed flowering phenotypes of autonomous pathway mutants (Michaels & Amasino 2001).

2.7 The thermosensory pathway

Ambient growth temperature is a very important regulator of many plant processes, as it affects the rates of metabolic reactions and morphogenesis. Flowering, in particular, is largely influenced by changes in ambient temperature. For example wild-type plants grown at 16°C are late flowering (Blázquez et al. 2003). To date only a few information are available about the thermosensory pathway. To discover the genes involved in this process, genetic screens have been performed to identified mutants whose flowering time isn't affected by temperature changes (Blázquez et al. 2003). These analyses evidenced that some genes, namely *FCA* and *FVE*, which had previously been attributed to the autonomous pathway, are also involved in the thermosensory process (Blázquez et al. 2003). Moreover, it was found that also the *svp* mutant fails to respond to low temperature, suggesting that *SVP* is part of this pathway (Lee et al. 2007). In particular this gene seems to act as a repressor downstream of *FCA* and *FVE* and upstream of *FT*. ChIP experiments demonstrated a preferential binding of *SVP* on the *FT* 5' promoter (Lee et al. 2007). Another gene that can possibly be involved in the thermosensory pathway is *SOC1*, as it was shown that the double mutant *soc1 ft* has a reduced response to temperature changes, when compared to *ft* single mutant (Lee et al. 2007).

Likely, in the apex *SOC1* is regulated by TERMINAL FLOWER1 (TFL1), a member of the FT family, that usually acts as a repressor downstream of FCA and FVE (Strasser et al. 2009).

Recently it was demonstrated that six small RNAs (miR156, miR163, miR169, miR172, miR398 and miR399) are ambient temperature-responsive and that the expression of one of them (miR172) is altered in the *svp* mutant (Lee et al. 2010).

2.8 The GA pathway

The gibberellin pathway is necessary to promote flowering especially under SD conditions (Wilson et al. 1992). In fact, mutations that disrupt either GA biosynthesis or signaling show alterations in flowering time. For example, a mutation in *GA1*, the enzyme that catalyzes the first step in the biosynthesis of GA, completely suppresses flowering under SD conditions (Moon et al. 2003).

The gibberellin pathway acts, at least in part, by up-regulating the floral meristem identity gene *LFY* since it has been shown that *LFY* activity is reduced in the *ga1-3* mutant and that it increases when exogenous GA is applied to both wild-type and *ga1-3* mutant plants (Blázquez et al. 1998; Blázquez & Weigel 2000). Moreover a cis-element has been found in the *LFY* promoter that abolishes its response to GA without affecting *LFY* induction by photoperiod, indicating that the two different pathways are integrated at the level of the *LFY* promoter (Blázquez & Weigel 2000). GA may also be involved in inducing *FT* expression, even if it has not been clearly demonstrated. What is known so far is that, both in LD and in SD, gibberellins promote *FT* expression in wild-type and in *ga1-3* plants (Hisamatsu & King 2008).

Finally gibberellins are able to induce *SOC1*, in fact over-expression of *SOC1* rescued the non-flowering phenotype of *ga1-3* and the *soc1* mutant showed reduced sensitivity to GA (Moon et al. 2003).

It is likely that gibberellins regulate flowering in *Arabidopsis* through the activation of the two flowering pathway integrators *SOC1* and *LFY* independently, but the existence of other factors involved in this process has been proposed (Moon et al. 2003). Moreover, it has been shown that *SOC1* and *AGL24* up-regulate each other in response to GA and synergistically determine flowering time under SD conditions (Li et al. 2008).

2.9 MADS-box transcription factors

A major gene involved in the regulation of the floral transition is *SHORT VEGETATIVE PHASE (SVP)*, a MADS-box transcription factor that is involved in the autonomous, thermosensory and GA pathways that negatively regulate flowering (Hartmann et al. 2000). The MADS-box transcription factors family comprises 107 members (Parenicová et al. 2003). The MADS domain is highly conserved in all eukaryotes and the term MADS derives from its first four discovered members: MCM1 (Yeast), AGAMOUS (Arabidopsis), DEFICIENS (Antirrhinum) and SRF (Human) (Schwarz-Sommer et al. 1992; Messenguy & Dubois 2003). In plants, two different classes of MADS-box transcription factors have been identified: the type I, divided into M α , M β and M γ clades, and type II, that comprises the M δ and MIKC clades (Alvarez-Buylla et al. 2000; Parenicová et al. 2003). Around 60 members compose the type I subfamily and they do not share any sequence similarity with the type II class, except for the MADS-box domain (De Bodt et al. 2003). Only a little part of these transcription factors has been functionally characterized, and recent studies suggest their involvement in gametophyte and seed development (Köhler et al. 2003; Bemer et al. 2008; Colombo et al. 2008; Kang et al. 2008). Concerning the type II MADS-box genes, the M δ class has not been well characterized, while many members of the MIKC clade have been intensively studied. The MIKC transcription factors share a conserved structure formed by the MADS domain (M), the intervening domain (I), the keratin-like domain (K) and the C-terminal domain (C) (Becker & Theissen 2003). The MADS domain is located in the N-terminus of the protein and is highly conserved; it is composed of 58 aminoacids and functions as a DNA binding domain that recognizes a specific sequence in the promoter regions called CA_nG-box (CC(A/T)₆GG) (Schwarz-Sommer et al. 1992; Huang et al. 1993; Shiraishi et al. 1993; Riechmann & Meyerowitz 1997). The MADS domain is also involved in nuclear localization and protein dimerization carried out through two antiparallel β -sheets that are present within the MADS domain, while an α -helix facilitates contact with the DNA (Messenguy & Dubois 2003). The intervening domain is involved in dimer formation (Riechmann & Meyerowitz 1997), together with the keratin-like domain. (Kaufmann et al. 2005). The C-terminal domain, that is the most variable, is involved in ternary complex formation and transcriptional activation (De Bodt et al. 2003; Masiero et al. 2002). The capacity of MADS-box proteins to form different heterodimers and ternary complexes, increases the complexity of their regulation; forming different complexes, with different activities (de Folter et al. 2005). Since many floral organ and floral meristem identity genes

belong to the MADS-box transcription factor family (Parenicová et al. 2003), the study of their functions is central to the comprehension of the molecular mechanisms responsible of plant development and plant reproduction, with important commercial outcome.

2.10 MADS-Domain and Chromatin remodeling

Floral organs identity is specified by the combinatorial action of MADS-domain transcription factors, but the mechanisms by which MADS-domain proteins activate or repress the expression of their target genes is still largely unknown. From affinity purification and mass spectrometry studies, it was shown that five major floral homeotic MADS-domain proteins (AP1, AP3, PI, AG, and SEP3) interact in the floral tissues as proposed in the “floral quartet” model (Smaczniak, Immink, et al. 2012). Furthermore, the results of this study indicate that the MADS-domain proteins interact not only with each other but also with a large number of non-MADS transcriptional regulators. Chromatin remodeling and modifying factors represent the most prominent group among these interactors. Several IP and MS analysis performed on floral tissues using as baits either AP1, AP3, AG, or SEP3 fused to a GFP at their C-terminus (de Folter et al. 2007; Urbanus et al. 2009), identified large protein complexes whose molecular mass is far from that of a MADS-protein heterotetramer. SOC1 and FUL were identified as interactors of AP1-GFP supporting the existence of a FUL/SOC1 protein complex active in floral transition. Therefore it was analyzed also the enrichment of non-MADS proteins, and several classes of nucleosome-remodeling factors were found, like RELATIVE OF EARLY FLOWERING 6 (REF6), recently characterized as histone H3K27demethylase (Lu et al. 2011). This suggests that the MADS-domain proteins can recruit or redirect the basic chromatin remodeling machinery to modulate the promoter structure of their target genes. Several others MADS-domain proteins, such as SHORT VEGETATIVE PHASE (SVP), are also binding partners of AP1 according to Y2H studies (de Folter et al. 2005), but they were not detected by the MS analysis probably for their very low abundance and their limited overlap in expression with AP1. The interaction between MADS-proteins with chromatin remodeling proteins is important for the regulation of gene expression by the MADS-domain factors (Smaczniak, Immink, et al. 2012), and their physical interaction suggests an important role of these TFs in controlling chromatin dynamics during plant development. Recent studies on chromatin accessibility during plant

development, suggest that MADS-domain TFs may act as pioneer factors that directly or indirectly trigger changes in the chromatin state (Zaret & Carroll 2011).

2.11 Role of SVP during the floral transition

Besides the floral pathway integrator genes described above, *SHORT VEGETATIVE PHASE (SVP)* belonging to the MADS-box transcription factor family, plays a central role together with its closely related MADS-box *AGAMOUS LIKE 24 (AGL24)* in the control of floral transition. *SVP* is a repressor of the floral transition since the *svp* mutant shows an early flowering phenotype compared with wild-type plants. In the opposite side, *AGL24* is a promoter of flowering and the *agl24* mutant displays a delay of flowering (Yu et al. 2002; Hartmann et al. 2000; Michaels et al. 2003). *SVP* and *AGL24* show high similarity in their primary amino acid sequences and their expression is detected during the vegetative phase before the floral transition (Parenicová et al. 2003; Hartmann et al. 2000; Michaels et al. 2003; Yu et al. 2002). *In situ* analysis shows the expression of *SVP* in whole vegetative seedlings and its expression gradually decrease during the floral transition until it disappears from the inflorescence meristem (Hartmann et al. 2000). *AGL24* is expressed in the shoot apical meristem and in the leaves during the vegetative phase, increasing its expression in the emerging floral meristem (Michaels et al. 2003; Yu et al. 2002). In the floral meristem both *SVP* and *AGL24* proteins are co-expressed and play a redundant role in controlling homeotic genes responsible for the formation of floral organs. *SVP* and *AGL24* play their role during the floral transition by interacting with the floral pathways integrator genes and by receiving signals from the pathways controlling flowering time. *SVP* for example plays an important role in the response of plants to changes in the ambient temperature because the mutant *svp* is insensitive to temperature changes (Lee et al. 2007). Recently, it has been demonstrated that *SVP* interacts *in vivo* with the protein *FLC* during vegetative growth where they bind the same promoter regions of *FT* and *SOC1* forming a multimeric complex (Hartmann et al. 2000; Li et al. 2008). *SVP* is also regulated by GA treatments that reduce its expression in SD conditions in wild-type plants (Li et al. 2008). According to these data, *SVP* regulates flowering by receiving stimuli from different pathways (autonomous, thermosensory and GA) underlining the relevance of this gene in the control of the floral transition (Li et al. 2008). Finally, recent studies with chromatin-immunoprecipitation analysis

have shown that both *SVP* and *AGL24* directly promote and repress, respectively, the expression of *SOC1* binding elements within the *SOC1* promoter (Li et al. 2008).

3. AIM OF THE PH.D. PROJECT

During my PhD project, I contributed to shed light into the flower transition process applying functional genomics and proteomics tools to the study of the model species *Arabidopsis thaliana*. Based on data already published I chose *SVP* transcription factor as a good candidate to investigate at protein level the floral transition mechanisms. The first aim of the project was to generate a transgenic line carrying the chimeric protein SVP-GFP under the control of the constitutive promoter *CaMV35S*. With this line I was able to get to the heart of the project, starting with proteomic studies. During the first year I was able to set up a protocol for the isolation of intact nuclei from different tissues of *Arabidopsis*, and to obtain nuclear protein complexes in their native state. This protocol was very important for the continuation of the project, in fact the skills and the results obtained were essential to perform coimmunoprecipitation assays of nuclear protein complexes in which different putative interactors of *SVP*, possibly involved in the control of the floral transition, were identified. The last goal of the project was the validation of results that took the end of second year and the large part of the third year. A functional genomics approach, including isolation of *Arabidopsis* mutants silenced in the candidate genes as well as gene expression analyses were exploited to confirm the relationships between *SVP* and its putative interactors. The obtained results, together with information already available about the putative interactors, allowed us to shed light on the biochemical mechanisms responsible of *SVP*-mediated inhibition of floral transition. In addition, we were able to develop a powerful biochemical approach that could be used for further studies, on nuclear transcription factors that act as part of protein complexes.

4. MATERIALS AND METHODS

4.1 Plant material and growth conditions

The *Arabidopsis thaliana* ecotype used in this work is Columbia 0 (Col-0). For the coimmunoprecipitations from seedling material, the plants were directly sown on soil and kept under short day conditions for three weeks (22°C, 8 h light and 16 h dark). While for the inflorescence material, the plants were directly sown on soil and kept under long-day conditions, until the inflorescence appears (22°C, 16 h light and 8 h dark). The T-DNA mutant plants studied during the validation of MS analysis were ordered from NASC collection and their line identification code is reported in the table 8.

4.2 Yeast Two hybrid assay

The two hybrid assays were performed at 28°C in the yeast strain AH109 (Clontech), using the co-transformation technique. The coding sequences of SVP, and GCN5 were cloned in the Gateway vector GAL4 system (pGADT7 and pGBKT7, Clontech) passing through pDONOR207 (Life Technologies). Yeast two hybrid assays were tested on selective YSD medium lacking leucine, tryptophan, adenine and histidine supplemented with different concentrations of 3-aminotriazole (1-3 mM 3-AT).

4.3 RNA isolation, Reverse Transcription-PCR and quantitative Real-Time (qRT-PCR) analysis

Total RNA was extracted using the LiCl method (Verwoerd et al. 1989) for all the expression analyses. Total RNA was treated with the Ambion TURBO DNA-free DNase kit and then retro-transcribed using the ImProm-II™ Reverse Transcription System (Promega). The cDNAs were standardized relative to UBIQUITIN10 (UBI10) and PROTEIN PHOSPHATASE 2A SUBUNIT A3 (PP2A- At1g13320) transcripts and the gene expression analyses was performed using the iQ5 Multi Colour Real-Time PCR detection system (Bio-Rad) with a SYBR Green PCR Master Mix (Biorad). Baseline and threshold levels were set according to the manufacturer's instructions.

4.4 Crosslinking of plant material

During the first part of this thesis work, different strategies were used to improve the Co-IP protocol. Especially for the first trials, formaldehyde crosslinking was the method used to stabilize protein-protein complexes before the nuclei isolation and the immunoprecipitation steps. The material was crosslinked following the protocol described in (Gregis et al. 2013) and according to other previous papers describing the crosslinking procedures (Klockenbusch & Kast 2010). All the steps have to be done at low temperature in order to reduce the activity of proteases that can digest the proteins and protein complexes. It is important to work with fresh material, only. Up to 1 g of plant material is collected into a falcon tube and kept in ice, then the fixation can start as below:

- 25 ml of MC buffer and 1% of formaldehyde are added to the sample, followed by 20 minutes of incubation under vacuum
- The reaction is stopped by adding glycine to a final concentration of 0.125 M and by incubating 2 minutes under vacuum followed by 5 minutes on ice
- The tissues are washed 3 times with MC buffer to eliminate formaldehyde residues, and the fixed material is dried on paper to eliminate water as much as possible
- The samples are frozen using liquid nitrogen and grinded to a fine powder
- At this point the samples can be stored at -80°C or used directly for the nuclear extraction steps

Once the immunoprecipitation is done, the crosslinking needs to be reverted in order to separate the single proteins from the complexes and to run either the immunoblotting or the mass spectrometry analysis. The crosslinking reversion occurs by heating the IP samples at 99 °C for 10-15 minutes, according to Klockenbusch & Kast, 2010 protocol.

MC Buffer:

- 10 mM NaPi pH 7
- 50 mM NaCl
- 0.1% Sucrose

4.5 Nuclear proteins isolation

All the information about the protocol developed during my first year are hereinafter described in detail:

- 0.5 g of Arabidopsis material seedlings/inflorescences are broken in a 15 cm mortar and a large pestle in nitrogen to a very fine powder.
- 30 ml of Buffer 1 are added into the mortar in presence of nitrogen and the powder under gently shaking. The buffer will freeze and form blocks. The buffer will be then broken and mix with the powder to obtain a very fine powder
- Let the frozen powder to melt into the mortar
- Pour the melted powder into a 50 um mesh placed with a funnel on top of a centrifuge tube
- Let the solution get into the tube and squeeze the remaining solution in the mesh
- Centrifuge at 6000 rpm in the JA25.50 rotor (4000 xg) for 20 min at 4 C. The pellet will consist of nuclei whereas the supernatant will be the cytosol.
- Collect 1 ml of cytosol, add 2 ul of Protease inhibitor cocktail and centrifuge at maximum speed in a bench-top centrifuge for 30' at 4 C. Take the supernatant as a extranuclei fraction.
- Resuspend the nuclei pellet in 10 ml of buffer 1 by using a 5 ml pipette
- Centrifuge at 5.000 rpm for 10 min at 4 C with the same rotor/centrifuge as above
- Resuspend the nuclei pellet in 10 ml buffer 1 by using a 5 ml pipette
- Centrifuge at 4.000 rpm for 10 min at 4 C.
- Resuspend the pellet in 1 ml buffer 2 by using a 5 ml pipette
- Centrifuge in a bench-top centrifuge at 2000 x g for 8 min at 4 C. The pellet obtained is made of intact nuclei in their native state.
- Add buffer 3 (high salt buffer), 2/3 of the nuclei pellet, to the nuclei
- Keep under shaking for 45' at 4 C

- Sonicate for 20" twice at amplitude of 15%
- Centrifuge at 5.000 rpm 4 C for 15'
- Collect the supernatant, made of nuclear proteins in their native state, in new tubes

Buffer 1 (Nuclei extraction buffer): 50 mM MES pH 8.5, 25 mM KCl, 5 mM MgCl₂, 30% glycerol, 5% sucrose.

To be added fresh: 10 mM betamercapto-ethanol (70 ul/100 ml), 1 mM DTT (1M stock; store at -20 C), 1 mM PMSF (0.1 M stock in ethanol; store at -20 C), 5 ug/ml, Chymostatin (1000x stock in DMSO; store at -20 C), 5 ug/ml Leupeptin (1000x stock; store at -20 C), 5 ug/ml Antiparin (1000x stock; store at -20 C)B-mercapto ethanol (70 ul in 100ml), 0.3% Triton (25% stock; store at 4 C)

Buffer 2 (Nuclei extraction buffer without triton): As buffer 1 without triton

Buffer 3 (Native extraction buffer): High salt solution from Sigma, 5 mM DTT, 1:200 Protease inhibitor cocktail (Serva protease inhibitor Mix #39103, 64.2 mg dissolve in DMSO) as an alternative: 1.6 M KCl, 25% glycerol, 50 mM Hepes pH 8.0, 3 mM MgCl₂, 0.2 mM EDTA, 5 mM DTT, 1:200 protease inhibitor cocktail

4.6 Coimmunoprecipitation

For the coimmunoprecipitation step were used two different systems; for the first CoIP was used the Dynabeads system, while for all the others coimmunoprecipitations was used the GFP-Trap system.

Dynabeads system (Invitrogen):

Dynabeads® Protein A Immunoprecipitation Kit (Catalog Number 10006D)

GFP-Trap® system (Chromotek):

GFP-Trap_MA (magnetic version, Catalog Number gtma-20)

All the information about the procedures and the buffer compositions are available online for the respectively company. No changes or variation in the procedure suggested from the company were made for the coimmunoprecipitation steps.

4.7 Trypsin digestion

4.7.1 In gel trypsin digestion:

This kind of trypsin digestion was required for the MALDI-TOF analysis that we used for the first coimmunoprecipitation made through Dynabeads system.

1. Washing

- Cut out the gel bands or slices and cut them into small pieces of ca. 1 mm². Use a sharp clean scalpel on a clean piece of parafilm. The smaller the gel pieces, the faster and better the digestion but more protein loss will occur when you make them too small. Transfer the gel pieces to clean low binding micro centrifuge tubes
- Wash gel pieces 2X in 50 ul water when you have not done so yet.

Remark: Some (most) protocols use a 50% acetonitril wash but this is not necessary when the sample is measured by LC-MSMS.

2. Cysteines reduction and alkylation

- Add 15 ul 50 mM Dithiotreitol in 50 mM NH₄HCO₃ or more, enough to cover the gel pieces (e.g. you will need 50 ul for a gel slice).
- Gently shake for 1 hr at 60 °C to reduce all disulfide bridges.
- Centrifuge shortly, cool to room temperature and replace the DTT by 15 ul 100 mM Iodoacetamide in 50 mM NH₄HCO₃ or more, enough to cover the gel pieces.
- Incubate at room temperature in the dark while gently shaking for 1 hour.
- Centrifuge shortly and remove the reagent. Wash the gel pieces 1 time with 50 ul 50 mM NH₄HCO₃ pH 8.
- At this point you may freeze + de-freeze the gel pieces to further increase the Trypsin accessible area.

3. Enzymatic digestion

- Add 10 – 20 ul cold freshly prepared Trypsin solution (10 ng/ul).
- When there is still some gel piece sticking out of the solution, then add extra 50 mM NH₄HCO₃ (but NO Trypsin) to completely cover the gel pieces.
- Incubate overnight while shaking at room temperature (20 °C) or 4 hours at 37 °C or 2 hours at 45 °C.

4. Extraction of peptides

Volumes described are for one narrow protein band. You will have to use larger volumes when you have used a gel slice.

- Sonicate for 2 (one ep) to 30 (series of eps) min.
- Centrifuge shortly and use a narrow 20 ul pipet tip to transfer the basic supernatant to a clean low binding tube.
- Add 10 ul 5% TFA/H₂O to the gel pieces
- Sonicate for 2 (one ep) to 30 (series of eps) minutes and transfer the acidic supernatant to the same tube with the same narrow 20 ul pipet tip used above.
- Add 10 ul of 15% AcNi / 1% TFA to the gel pieces
- Sonicate for 1 min and transfer the supernatant to the same tube with the same narrow 20 ul pipet tip used above.
- The total sample volume is now approximately 25 ul (with 5% AcNi) and the pH is about 2

4.7.2 In solution trypsin digestion:

This kind of treatment was use to prepare all the other coimmunoprecipitated samples for the Orbitrap LC-MS/MS machine.

- Weigh 0,2g NH₄HCO₃ and dissolve in 50 ml to obtain 50mM NH₄HCO₃ pH8.
- Weigh 7,7 mg DTT (dithiotreitol) in a 1,5 ml tube and keep on ice
- Weigh 19 mg iodocetamide in a 1,5 ml tube and keep on ice
- Weigh 24 mg cysteine in a 1,5 ml tube and keep on ice

- Add 1 ml 50 mM NH₄HCO₃ to the DTT, iodoacetamide and the cysteine just before use.

- Use the first 50 µl of the eluate of the immunoprecipitation (which contains most magnetic beads) to prepare for MS.
- Add 1 µl 50 mM DTT (dithiothreitol) in 50 mM NH₄HCO₃ pH8 (7,7 mg/l) to each IP sample and incubate 1-2 hours at 37°C.
- Add 1 µl 100 mM iodoacetamide in 50 mM NH₄HCO₃ pH8 (19 mg/l) to each IP sample and incubate at least 1 hour at room temperature in the dark.
- Add 1 µl 200 mM cysteine in 50 mM NH₄HCO₃ pH8 (24 mg/l) to each IP sample to stop the alkylation.
- Add 1 µl trypsin sequencing grade (0,5 µg/µl in 1 mM HCl) to each IP sample and incubate overnight at 20°C on a shaker. Do not incubate longer than approximately 16 hours because this will increase the amount of chymotrypsinic cleavages.
- The next morning add approximately 1,5-3 µl 10% TFA to make the pH approximately pH 3. Check the pH with a pH paper (try to avoid a pH of 1 or 4).
- Centrifuge 5 min. at maximum speed and pipet the supernatant into a new Low Bind tube. Repeat this 4-5 times to make sure that there are no beads in the samples anymore.
- The samples are ready to inject into the MS. Store the samples at -20.

4.8 Mass spectrometry data analysis

All the MS analysis were made using triplicate samples, in particular it has been used *wt* plants as a negative control and the native line *SVP::SVP-GFP* or the overexpression line *35S::SVP-GFP*. The raw data were obtained using Orbitrap mass spectrometry instrument. The data obtained from the *wt* samples were considered as nonspecific interactors, and used to clean up the data obtained from the tagged lines mentioned before, in order to obtain a short list of real putative SVP interactors. Moreover, nuclear protein coimmunoprecipitated samples can be easily contaminated by cytosolic and/or chloroplast proteins. For this reason, the data obtained after the comparison between the negative control and the tagged

lines, were further cleaned up from all these contaminants. The list obtained was based on the number of peptides generated by the MS machine, that match with a known protein present in the database. The analysis of the raw output based on the peptides, were performed by bioinformatics using proper software as mentioned below. Based on information already available in literature was generated a short list of putative SVP candidates that can have a biological relevance with the role of SVP. This short list represented the starting point to verify in different ways the role of these candidates in controlling the floral transition mechanisms together with SVP.

4.8.1 Bioinformatics analysis: (Smaczniak, Li, et al. 2012)

The Orbitrap type of mass spectrometers generate high-resolution data with a large dynamic range, and thus they are able to detect very-low-abundance proteins in complex samples. This is important for the identification of interaction partners of natively expressed transcription factors or signaling proteins. Identification of peptides in the eluates, after digesting the proteins with trypsin, revealed a large number of proteins in the IP samples on the basis of the MaxQuant/Andromeda19 peptide database search and initial filtering, thereby suggesting a substantial amount of background proteins in the eluates. To distinguish specifically immunoprecipitated proteins from the background, we applied a LFQ strategy and compared protein abundances between IP samples and IP controls. There are two LFQ methods that are often used in quantitative proteomics. First is the spectral counting method, which compares the number of identified MS/MS (MS2) spectra for peptides of a particular protein and can be used with the data obtained with any type of mass spectrometer. The second method is quantification using the MS (MS1) peak intensity/abundance (extracted ion chromatogram) measurement that allows the separation of the identification process, which uses both MS2 and MS1 data, from the quantification process that takes place only at the MS1 level. Both methods are suitable for analyzing protein abundance changes in large-scale proteomics experiments. In our experiments, we used MS1 peptide peak intensities/abundances for quantification, as the MS1 data also contain complete peak elution profiles required for relative protein quantification. Proper alignment of high-resolution MS1 peaks from several LC-MS runs is essential for accurate quantification. In addition, when MS1 peptide peak alignment is correct, it is not necessary to identify all MS1 peaks from every LC-MS run (in contrast to the spectral counting method), as a single identification can characterize well-aligned peptide peaks in other runs, ultimately

allowing for proper abundance comparison between those peptide peaks. We tested software packages for protein LFQ: MaxQuant (v1.2.2.5, Max Planck Institute of Biochemistry, Martinsried, Germany) and Progenesis LC-MS (v2.6, Nonlinear Dynamic). MaxQuant is freeware that was developed especially to process high-resolution, Orbitrap-type data. At the current stage of software development, MaxQuant is unable to process data obtained from other types of mass spectrometers. Progenesis LC-MS, in contrast, is a commercial software package that processes data obtained from many different types of mass spectrometers directly or in standard formats (e.g., .mzXML or .mzML). To correct for the variability in total protein amount in the IP samples and controls, we used a normalization approach assuming that most background proteins were unaffected by our experimental conditions. The normalization procedures are incorporated into both software applications. Low or zero MS1 intensity values in the control data sets can strongly impair the ratio calculation for low abundance proteins, such as the interaction partners in our data sets. Therefore, there is a need for imputation of a minimal quantity value for peptides that were not quantified (could not be normalized) to calculate approximate protein ratios. We tested several imputation strategies of missing values before (peptide intensity noise imputation) or after (lowest protein abundance imputation) data normalization. We calculated protein ratios by dividing the combined and normalized peptide intensities/abundances of a particular protein in the IP samples with the corresponding values in the controls. Proteins identified with at least two peptides (including one unique peptide) that are markedly enriched in the sample at a permutation-based false discovery rate (FDR) of 0.01 were considered potential interaction partners of the bait protein.

4.9 Segregation analysis and primer combinations

All the plants used in this thesis were controlled by PCR in order to verify the correct genotype of the different mutants, transgenic lines and crosses (Tables 1 and 2). Both the *35S::SVP-GFP* and *SVP::SVP-GFP* lines have an *svp/svp* background, so to check this type of plants, and then their respective crosses with *sdg2* and *gcn5* mutants, it was necessary to control every time the state of the endogenous locus of *SVP*.

Gene name	Wild type allele	Mutant allele
DEK domain	DEK s / DEK as	DEK s / LBA1
ATHD2	ATHD2 s / ATHD2 as	LB3 / ATHD2 as
HTA5	HTA5 s / HTA5 as	LB161 / HTA5 as
SDG2	SDG2 s / SDG2 as	LBA1 / SDG2 as
ATHD2A	ATHD2A s / ATHD2A as	LB161 / ATHD2A as
GCN5	GCN5 s / GCN5 as	LBA1 / GCN5 as
HSP	HSP s / HSP as	LBA1 / HSP as
NAP1	NAP1 s / NAP1 as	LB161 / NAP1 as
SVP	SVP s / SVP as	SVP s / SVP as (MUT.)
35S::SVP-GFP	Vep 34 / Atp 1491	-
SVP::SVP-GFP	Atp 277 / eGFP as	-

Table 1. In this table are indicated the combination of primers for segregation analysis

Name	Sequence
DEK s	CCAAAAAGGGGAAATCTGG
DEK as	ATCGAACGAGGCTAAGCCTC
ATHD2 s	AAATAGCCCCAAACCCACTG
ATHD2 as	GATATTGCTCGATGTTGGGG
HTA5 s	AGCAAACCCCTAAAGCCCAC
HTA5 as	AACTCCTGAGAAGCAGATCC
SDG2 s	TCCCCTGCATCTAGTGATTC
SDG2 as	ACCAAAGCAAAACCGAGGAG
ATHD2A s	AAGCCAGTTACAGTGACTCC
ATHD2A as	GCTCTTCTCCTCAGAATCC
GCN5 s	AAGATTGTGCTAGTCGCTCC
GCN5 as	TTAGCACCCAGATTGGAGACC
HSP s	TTCGGGTTTTGTCCCATTCC
HSP as	TTCACCTCTGATACGACGAG
NAP1 s	TAAGTACGAGATGAAGGG
NAP1 as	CATCCTCATCATCTTCCTCG
SVP s	GACCCACTAGTTATCAGCTCAG
SVP as	AAGTTATGCCTCTCTAGGAC
SVP as (MUT.)	AAGTTATGCCTCTCTAGGTT
LB3	TAGCATCTGAATTTATAACCAATCTCGATACAC
LB161	GGGCTACACTGAATTGGTAGCTC
LBA1	TGGTTCACGTAGTGGCCATCG
Vep 34	GGATGACGCACAATCCCACATCC
eGFP as	AGTCGTGCTGCTTCATGTGG
Atp 277	GCAACTAACGGAAGAGAACGAG
Atp 1491	AGAGAACGGAGAGTTCTTCAGC

Table 2. In this table are indicated the sequence of primers for segregation analysis

5. RESULTS

5.1 The transgenic line CaMV-35S::*SVP-GFP*

As a member of the MADS-box transcription factors, the structure of *SVP* is very similar to many other members of this family, especially for particular regions with conserved domains. For this characteristic working at proteomic level with this transcription factor family is rather complex, especially when antibodies specific for each MADS-box, and Yeast two-hybrid assays are needed. This was true for the study of *SVP*, for which a specific antibody to be used for different immuno-based assays, including protein complex coimmunoprecipitation, was not available. A simple way to solve this problem was the generation of a chimeric protein obtained through the fusion of the protein of interest with either a tag or protein for which a specific antibody is commercially available. In our specific case, we chose the GREEN FLUORESCENT PROTEIN (GFP), because a good correspondent specific antibody was available. Using the Gateway Cloning system, *SVP* was fused to the *GFP* at the C-terminal in order to generate a chimeric protein which was functional both at the level of *SVP* activity and GFP fluorescence. The obtained construct was integrated in the genome of *svp* knock-out plants via *Agrobacterium tumefaciens* and the transformed events were selected based on the rescue of the *svp* phenotype (Figure 5), i.e. flowering time identical to WT plants under short- and long-day conditions, and the level of GFP fluorescence in the nuclei.



Figure 5. Phenotypes of WT (Col-0), *svp* knock-out and one of the selected transgenic line. Plants were grown for 4 weeks under long-day conditions in a growth chamber. The early flowering phenotype of the *svp* mutant

plant is clearly visible, whereas the transgenic line *35S::SVP-GFP* shows the same flowering time of the WT plant, thus indicating the complete rescue of the early flowering phenotype.

5.2 The native line *SVP::SVP-GFP*

The *SVP* overexpression line mentioned above represents a forced system in which the *SVP-GFP* chimeric gene is expressed through the whole life cycle of the plant and in all its tissues. This confers to the transformant line a late flowering phenotype and leads to defects in flower development. For this reason, we chose also the native line *SVP::SVP-GFP* to perform the same experiments and to compare the results with the overexpression ones. In fact the chimeric protein controlled by the native promoter of *SVP* allows us to reproduce and investigate both the real expression profile and the correct subcellular localization of the protein. This line was already available in the lab of Martin Kater group where it was used for genetic studies and for the identification of pathway directly regulated by *SVP* (Gregis et al. 2013). This chimeric line was generated using the Gateway cloning system in which a putative promoter region of *SVP* (around 1000 bp upstream the *SVP* ORF) and the full length genomic sequence were fused to the *GFP* to generate a chimeric protein *SVP::GFP* under the control of the native *SVP* promoter. The construct was integrated in *svp* null mutant plants via *Agrobacterium*-mediated transformation with the binary vector pGREENII that confers BASTA resistance to the transformed plants. The obtained *svp* defective, BASTA-resistant plants were complemented to the wild type phenotype (Figure 6), indicating that the *SVP-GFP* chimeric protein is functional and that those plants represent a good material to design genetic and biochemical analysis. Since in general the TFs are required at a very small amount in the cells to play their role, they are not easily detected with common biochemical approaches. Conversely, thanks to the fusion with fluorescent proteins we are normally able to detect a good signal of fluorescence and we are able to detect the chimeric protein via immunoblotting. These plants, together with the overexpression line, were used to perform the coimmunoprecipitation analysis described in this thesis.



Figure 6. Phenotypes of WT (Col-0), *svp* knock-out and one of the selected transgenic line *SVP::SVP-GFP* in *svp* background. Plants were grown for 4 weeks under long-day at 22°C. The early flowering phenotype of the *svp* mutant plants is clearly visible, whereas the transgenic complemented line shows the same flowering time phenotype of the WT plants, indicating the complete rescue of the *svp* early flowering phenotype.

5.3 Nuclei isolation

As a transcription factor, SVP is located into the nuclei of plant cells where it is able to bind specific sequences in the promoter region of its target genes, thus modulating the level of their expression. The localization of SVP was confirmed *in vivo* by analyzing the overexpression line *35S::SVP-GFP* at the fluorescence microscope, and a good signal of the chimeric protein was detected in the nuclei. In collaboration with Federico Valverde from the institute of Biochemistry and Photosynthesis of Seville, within the frame of the project titled “Azione integrata Italia-Spagna” and supported by MIUR, a specific protocol was developed aimed to purify intact nuclei from different tissues of *Arabidopsis*. This protocol allowed us to obtain nuclear proteins in their native state with almost no contamination of extra-nuclear proteins that could hamper our analyses, including the possibility of forming aspecific complexes with SVP. Since, we were interested in the regulation of flower transition mediated by SVP, we focused our attention in identifying the protein complexes that SVP can form into the nucleus at two different stages of the *Arabidopsis* life cycle: the seedling (2 cotyledons and first two leaves) and inflorescence meristem stages. The material collected is ground using liquid nitrogen and with crystals of frozen buffer in order to obtain a fine powder that will melt in its own buffer. A series of centrifugations with decreasing speed, are then required to separate the organelles that remains in suspension from a pellet made of a intact nuclei. These purified nuclei can be broken by sonication in order to release

their protein content and eliminate nuclear membranes. The material obtained from purified nuclei was checked for the presence of contaminants deriving from other cell compartments especially from the cytosolic fraction. As shown in Figure 7, through SDS-PAGE stained with Blue Coomassie staining, and Western Blotting analyses, we were able to show that such purified nuclear fractions did not contain major contaminants as RUBISCO, which was almost undetectable and were enriched with histones.

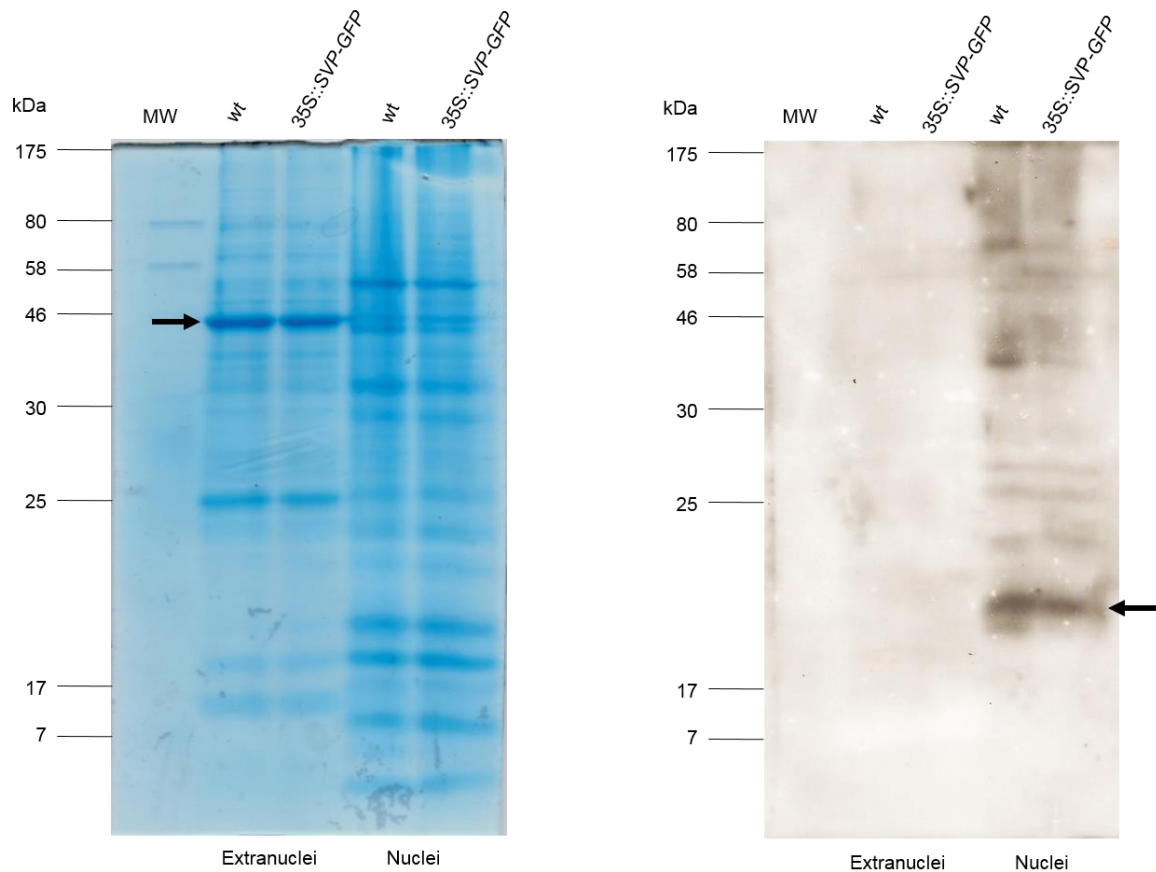


Figure 7. Quality check of nuclear protein isolation compared with the extranuclei fraction composed for the large part of cytosolic and organellar proteins. On the left the SDS-PAGE stained with Blue Coomassie shows (black arrow) the presence of large subunit of Rubisco only in the extranuclear fraction, whereas the protein is almost absent in the nuclear fraction. On the right is shown the immuno-decoration of a replica filter using an antibody against Histones H3.

5.4 Co-Immunoprecipitation

5.4.1 Dynabeads® Protein A:

Reached the desired quality of the nuclear preparation, we proceeded with the break of the nuclear envelope in order to release the protein content. The nuclei can be broken by two different ways: either in the presence of denaturing conditions like high concentration of Urea that denatures all the proteins and disrupts all the complexes interactions, or in the presence of high salt concentration which is able to break the nuclei maintaining the protein structures and protein-protein interactions in their native state. The latter procedure is essential to immunoprecipitate the protein of interest together with its partners in the protein complex. There are many different strategies to perform the immunoprecipitation and to analyze the immuno-precipitated samples, therefore different trials were necessary to define the best conditions and the methods compatible with our kind of samples and their protein concentration. The first method that we tried was based on the use of magnetic beads (Dynabeads system from Invitrogen), coupled with protein A, and able to bind the GFP specific antibody. The bead-associated GFP antibody was then used to recognize the chimeric SVP-GFP protein and to immunoprecipitate it together with its putative interactors. Unfortunately, this method did not work for our purpose; in fact, the interaction between the protein A covalently associated to the beads and the GFP antibody was not strong enough, and during the elution step large part of the GFP antibody was found in the immunoprecipitated samples, thus hampering downstream analyses, including immunoblottings and mass spectrometry (Figure 8).

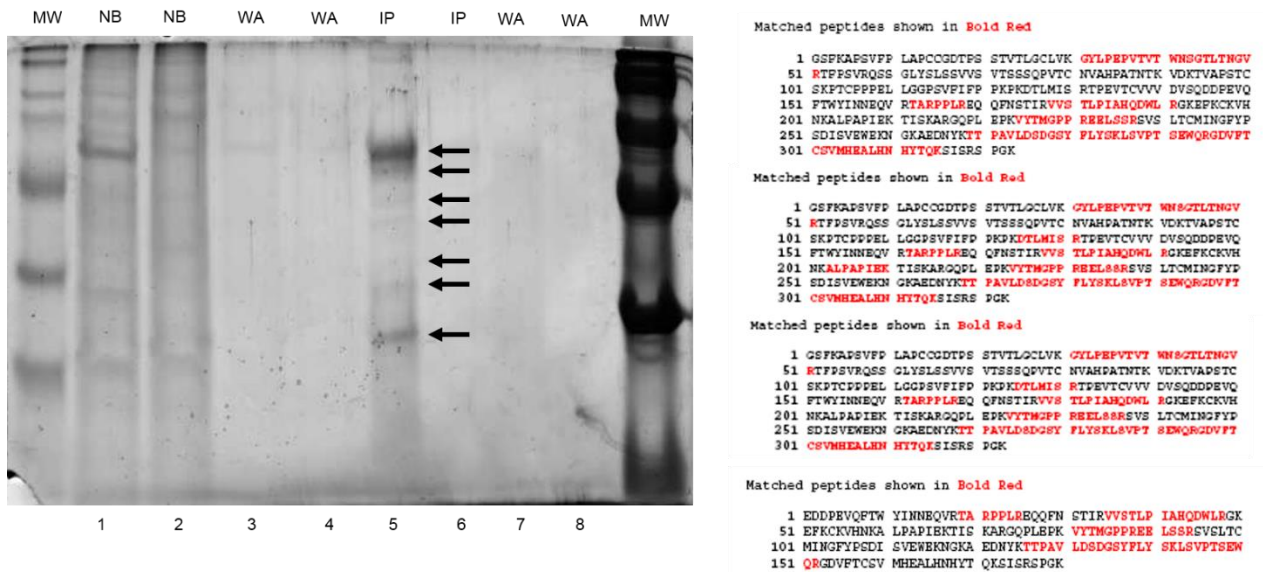


Figure 8. Immunoprecipitated sample fractionation and MS-analyses. On the left is reported the SDS-PAGE stained with colloidal coomassie in which all the fractions obtained during the coimmunoprecipitation procedure in both 35S::SVP-GFP (lane 1-3-5-7) and WT material (lane 2-4-6-8) were fractionated.: NB, Not Bound is made by all the proteins that did not bind the beads (lanes 1 and 2); WA, Washing fractions, obtained both before and after the elution step, composed of proteins that aspecifically interact with the beads (lanes 3-4-7-8); IP, Eluted fraction composed of proteins that were specifically bound to the beads (lanes 5-6), possibly containing SVP and its interacting partners. Interesting immunoprecipitated proteins were visible only in the transgenic line (lane 5), while they were totally absent in the control sample (lane 6). On the right mass spectrometry data, obtained from the analyses of bands excises in lane 5 are reported. As mentioned before, with this method we obtained a lot of antibody contamination and the mass spectrometry analysis was only able to detect peptides belonging to the GFP antibody used to immunoprecipitate SVP.

5.4.2 GFP-Trap®:

Because of the problems caused by the Dynabeads method, we decide to move to another coimmunoprecipitation procedure named GFP-Trap® and developed by Chromotek. The advantage of this new procedure is that the antibody is covalently coupled to the magnetic beads (Figure 9). This kit allowed us to elute from the beads the immunoprecipitated proteins without any kind of contamination generated by the antibodies detached during the elution step. Furthermore, exploiting this feature, we were also able to increase the strength of the washing buffers before the elution step in order to eliminate as many contaminations as possible. Thus, this approach allowed us to obtain high quality IP samples, suitable for Mass Spectrometry (MS) analysis. The MS analysis requires a preliminary trypsin digestion, necessary to cut the proteins into short polypeptides. The analysis of all the peptides, allows

then to identify all the proteins contained in IP samples. In the case of the Dynabeads method the IP samples were fractionated in a SDS PAGE and only the visible bands were

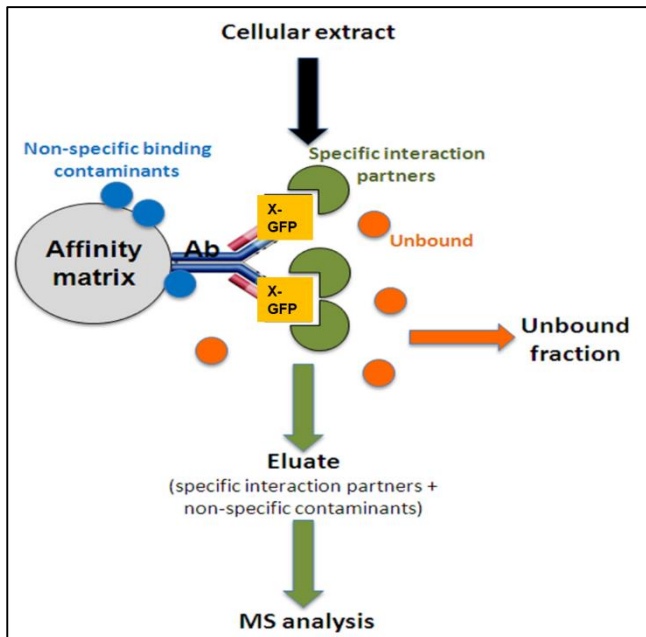


Figure 9. A scheme of the common coimmunoprecipitation procedure. The difference between Dynabead and Chromotek system is the binding of the antibody to the affinity matrix

excised and subjected to in-gel trypsin digestion (Figure 8), while the IP samples obtained by the new way, were directly digested, avoiding the SDS-PAGE fractionation step. In the first case, the detection of putative protein partners is limited to the very low number of bands visible after the colloidal coomassie staining, losing for instance all the putative interactors present at very low amount and not visible in the stained gel. On the other hand, through an in solution-digestion of the whole IP samples, it is possible to detect much more proteins, even those present at lower abundance.

5.5 Cross-Linking method for protein interaction analysis (Klockenbusch & Kast 2010)

Protein-protein interactions are at the basis of most cellular processes, including signal transduction, protein synthesis and gene transcription. In plants, knowledge of these protein interactions network is important to better understand the molecular mechanisms at the basis of those processes, that nowadays remain well studied only at the genetic level. At present, protein-protein interactions are investigated by different strategies including yeast-two-hybrid and by *in vitro* binding assays (Young 1998; Willander & Al-Hilli 2009). However, even if these approaches are very fast and easy to use, they are also prone to false positive identifications because they do not take into account the temporal and spatial separations that occur in a living system. A powerful technique that can solve this problem is an affinity enrichment of the protein of interest followed by detection of its binding partners by means of mass spectrometry. This technique has two main drawbacks: weak interactions could be missed in stringent washing conditions, while nonstringent conditions lead to a high number

of false positives. One method to solve this problem is to treat intact cells with a covalent cross-linking agent, to stabilize all the occurring protein-protein interactions, including the very weak and transient ones. The shortest and cheapest cross-linker available is formaldehyde, that has been used for long time in histology as fixing agent. Low concentration requirement and especially short reaction time allow the utilization of formaldehyde as a cross-linker to analyze protein-protein interactions. Formaldehyde is a very small molecule and thus the cross-linking occurs only for proteins closely associated. Furthermore, its high permeability through cell membranes enables to treat intact cells, without using any kind of solvent, otherwise needed for others cross-linkers. Even if the cross-linking seems to be a powerful method to detect protein-protein interactions, it is still not able to identify all the possible complexes that the protein of interest can form with its partners. This is due to the possibility that hidden epitopes are generated by the formation of the large complex in which such protein can take part. In any case, after the coimmunoprecipitation of the complexes, the cross-linking need to be reverted to separate each single protein that will be digested with trypsin and analysed in mass spectrometry. Also in this case formaldehyde remarks its versatility for its type of cross-linking that can be easily and completely reverted by heating the sample at 99°C for just 5 minutes. Formaldehyde-mediated cross-linking seems to be a promising method to analyse protein-protein interactions and can be coupled with the conventional methods mentioned before, to refine the result obtained with all the different techniques.

5.6 Analysis of the Mass Spectrometry data

Before being subjected to the MS analysis, the coimmunoprecipitated samples need to be digested with Trypsin in order to generate shorter polypeptides, able to be recognized by the MS technique. The methods used for Trypsin digestion mentioned in the previous paragraph, are strictly linked to the type of Mass Spectrometry device that we wanted to use. In our case we tried two different kind of MS; the MALDI-TOF (Matrix-assisted laser desorption/ionization coupled with a Time of Flight analyzer) and the Orbitrap (Ion Trap Mass Analyzer) (Makarov 2000; Hu et al. 2005). For MALDI-TOF analysis, it is recommended the In-gel Trypsin digestion, well described in the methods paragraph, while for the Orbitrap analysis is required a direct Trypsin digestion (see materials and methods). The MALDI-TOF spectrometer was only used for the samples obtained through the

Dynabeads procedure in which unfortunately, only the heavy chains of the GFP antibody were detected, while for all the other coimmunoprecipitations we moved to the Orbitrap system. Once analyzed, the output generated by the Orbitrap MS machine is made for a huge list of polypeptides recognized by analysis. As described before, the Mass Spectrometry is a very sensitive technique, able to recognize peptides present in a very low concentration. We must keep in mind that all the aspecific proteins immunoprecipitated together with the real interactors of SVP, and also the human protein contaminations belonging to the operators that prepare the samples are recognized by the MS and they will be found in the output. The cleanup of the raw output of the sample of interest is made by eliminating all the peptides found also in the WT sample (negative control) and excluding all proteins belonging from different organisms for example trypsin used to digest the samples and human keratin. From the cleaned list generated, other criteria of selection are applied in order to reduce the number of candidates to a short list of strong putative interactors. Generally, this last selection is based on the number of times that a peptide is detected in the sample, coupled with literature documentation about the pertinence of the result. For example, a chloroplast protein found in large amount in our nuclear protein samples is for sure a contaminant and eliminated from the list of putative interactors. The first table (Table 3) shown below contains a selection of the putative interactors obtained by analyzing seedling material of the transgenic line *35S::SVP-GFP*. The other tables (Tables 4-5-6-7) contain results obtained from inflorescence material, crossing the MS output of both *35S::SVP-GFP* and the native line *SVP::SVP-GFP* already available in the group of professor Martin Kater. This kind of selection allowed us to generate a very short list of real putative interactors that can be analyzed to verify if they are part of a SVP complex.

5.6.1 Coimmunoprecipitation from seedling:


Gene ID	Description	
AT1G55990	Glycine-rich protein	
AT1G50140	P-loop containing nucleoside triphosphate hydrolases superfamily protein	
AT1G19700	Encodes a member of the BEL family of homeodomain proteins	
AT3G14890	Phosphoesterase; FUNCTIONS IN: DNA binding, catalytic activity, zinc ion binding	
AT4G31730	Glutamine dumper1 is a putative transmembrane protein. It is involved in glutamine secretion	
AT3G06340	DNA heat shock N-terminal domain-containing protein	
AT4G25960	P-glycoprotein 2 (PGP2)	
AT5G60760	P-loop containing nucleoside triphosphate hydrolases superfamily protein	
AT5G17620	CONTAINS InterPro DOMAIN/s	
AT5G65760	Serine carboxypeptidase S28 family protein	
AT4G14250	Structural constituent of ribosome	

Table 3. In the table are reported the results of MS analysis performed on seedling material

5.6.2 Coimmunoprecipitation from inflorescence:


Gene ID	Description	
AT1G51060	P-loop containing nucleoside triphosphate hydrolases superfamily protein; FUNCTIONS IN: helicase activity	
AT2G45810	DEA(D/H)-box RNA helicase family protein; FUNCTIONS IN: helicase activity	
AT2G33730	P-loop containing nucleoside triphosphate hydrolases superfamily protein; FUNCTIONS IN: helicase activity	
AT3G06480	DEAD box RNA helicase family protein; FUNCTIONS IN: helicase activity	
AT2G42520	P-loop containing nucleoside triphosphate hydrolases superfamily protein; FUNCTIONS IN: helicase activity	
AT5G05450	P-loop containing nucleoside triphosphate hydrolases superfamily protein; FUNCTIONS IN: helicase activity	
AT5G51280	DEAD-box protein abstrakt, putative; FUNCTIONS IN: helicase activity	
AT3G01540	RNA HELICASE DRH1 protein_coding DEAD BOX RNA HELICASE 1 (DRH1)	
AT5G62190	DEAD/DEAH box RNA helicase PRH75	
AT3G19760	RNA helicase that may be a component of the Exon Junction Complex.	
AT3G58510	DEA(D/H)-box RNA helicase family protein; FUNCTIONS IN: helicase activity	
AT5G11170	DEAD/DEAH box RNA helicase family protein ; FUNCTIONS IN: helicase activity	

Table 4. RNA Helicases found via MS analysis of samples from inflorescence tissues.


Gene ID	Description	
AT1G08880	HTA5, a histone H2A protein.	
AT3G20670	HTA13, a histone H2A protein.	
AT3G45980	Histone 2B (H2B) protein.	
AT3G44750	Histone deacetylase. Controls the development of adaxial/abaxial leaf polarity.	
AT3G53650	Histone superfamily protein; INVOLVED IN: nucleosome assembly;	
AT5G02570	Histone superfamily protein; INVOLVED IN: nucleosome assembly.	
AT3G54610	Histone acetyltransferase required to regulate the floral meristem activity	

Table 5. Histones modification proteins found via MS analysis, using inflorescence tissues.


Gene ID	Description	
AT5G58470	TBP-associated factor 15B (TAF15b); nucleic acid binding.	
AT5G42520	BASIC PENTACYSTEINE 6 DNA binding	
AT5G63550	DEK domain-containing chromatin associated protein	
AT5G22650	ARABIDOPSIS HISTONE DEACETYLASE 2	
AT4G15180	SET domain protein 2 (SDG2)	
AT4G40030	Histone superfamily protein	
AT2G19480	NUCLEOSOME ASSEMBLY PROTEIN 1	

Table 6. Proteins found via MS analysis, using inflorescence tissues.


Gene ID	Description	
AT1G33811	GDSL-like Lipase/Acylhydrolase superfamily protein; FUNCTIONS IN: hydrolase activity	
AT3G48290	Putative cytochrome P450	
AT3G60360	EMBRYO SAC DEVELOPMENT ARREST 14	
AT4G33250	Initiation factor 3k (EIF3k)	
AT3G51070	S-adenosyl-L-methionine-dependent methyltransferases superfamily protein	
AT3G57290	Protein that is found in not only the eif3 complex but also in association with subunits of the COP9	
AT5G14920	Gibberellin-regulated family protein; INVOLVED IN: response to gibberellin stimulus	

Table 7. Proteins found via MS analysis, using inflorescence tissues.

5.7 Analysis of the putative interactors

Based on the short list of the putative interactors of SVP showed before, eight candidates were chosen in order to investigate further the putative interaction with SVP (Table 8). Those candidates were involved in different aspect of chromatin remodeling, including histones modifications (acetylation and methylation) and nucleosome assembly. These candidates were also selected, based on the common notion that transcription factors, including SVP, act as part of large protein complexes that include chromatin remodeling factors in order to modulate the expression of their own target genes. For each of the eight candidate genes that we chose, the corresponding knock-out mutants were ordered to verify their possible involvement in flowering time determination.

Gene ID	Gene name	Description	NASC Code
AT5G63550	DEK domain	DEK domain-containing chromatin associated protein	SALK_137152.43.05.x
AT5G22650	ATHD2	Arabidopsis Histone Deacetylase 2	SAIL_1247 A02
AT1G08880	HTA5	Histone H2A Protein	GABI_097F11
AT4G15180	SDG2	SET Domain Protein 2	SALK_021008.5600.x
AT3G44750	ATHD2A	Histone Deacetylase	GABI_355H03
AT3G54610	GCN5	Histone Acetyltransferase	SALK_106557.46.80.x
AT4G40030	HSP	Histone Superfamily Protein	SALK_082765.35.95.n
AT2G19480	NAP1	Nucleosome Assembly Protein 1	GABI_273H07

Table 8. The Gene ID, gene name and T-DNA insertion codes of the eight candidate genes are listed.

For each of the ordered lines, homozygous lines for the T-DNA insertion were selected and analyzed at phenotypic level. Only two of them, namely *gcn5* altered in histone H3 acetyl transferase and *sdg2* affected in histone H3 lysine 4 methylation, displayed a clearly visible phenotype compared with WT plants, reported in the Figure 10.

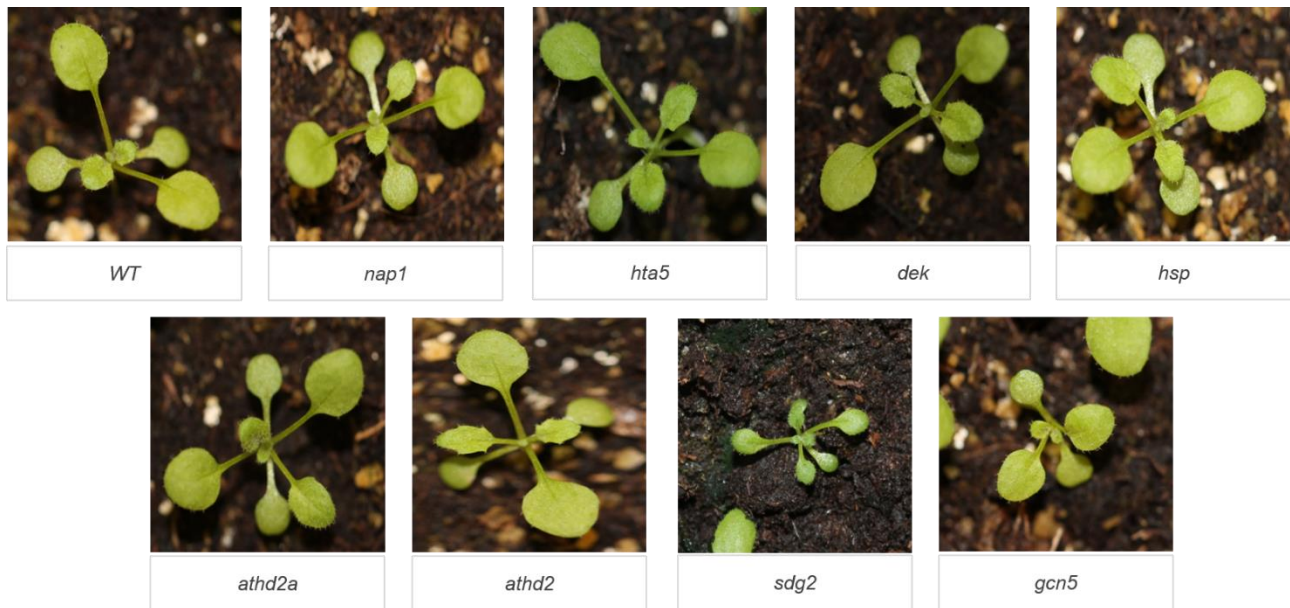


Figure 10. Phenotypes of each knock-out mutant compared with the *WT* plants grown for 4 weeks under green-house conditions. As it can be observed, only *sdg2* and *gcn5* display altered phenotypes characterized by a reduced size of the rosette. At later stages these mutants show also flower sterility as already published and for the case of *gcn5* a low percentage displays also a three-cotyledons phenotype (described in detail in the next paragraph). For all the other mutants, there are no differences compared with the control.

5.8 SDG2 and GCN5 as putative interactors

From the phenotypic analysis of the eight candidates, only two of them (*gcn5* and *sdg2*) showed a different rate of growth compared to the *WT*, and thus were subsequently chosen to better investigate their relationship with *SVP*. Both of them are completely sterile, so is not possible work with a pure homozygous line, but only with a segregating progeny that contains a quarter of homozygous plants.

5.8.1 SET domain protein 2 (SDG2):

Four types of histone modifications have been described in plants, namely methylation, acetylation, phosphorylation and ubiquitination (Zhang et al. 2007; Johnson et al. 2004). Four lysine residues in *Arabidopsis* core histones can be specifically methylated, histone H3 lysine4 (H3K4), H3K9, H3K27, and H3K36 (Zhang et al. 2007). The *Arabidopsis* SET domain group 2 (*SDG2*) is part of the SDGs class III, that is the class of the SDGs able to

modifying H3K4me2/3 (Jackson et al. 2002). The morphological defects in *sdg2* first become apparent at 6–8 days after germination, when *sdg2* seedlings are smaller with curly leaves and have significantly shorter roots. *sdg2* plants remain dwarf, with smaller rosettes throughout the whole vegetative growth, and they flower significantly earlier in all photoperiods tested (i.e., short day, long day, and constitutive light). This early transition from vegetative to reproductive growth is accompanied by the down-regulation of flowering repressor gene *FLC*. Moreover, although the correct number of floral organs (sepal, petal, stamen, and carpel) is formed in *sdg2* flowers, *sdg2* mutants are completely sterile (Guo et al. 2010).

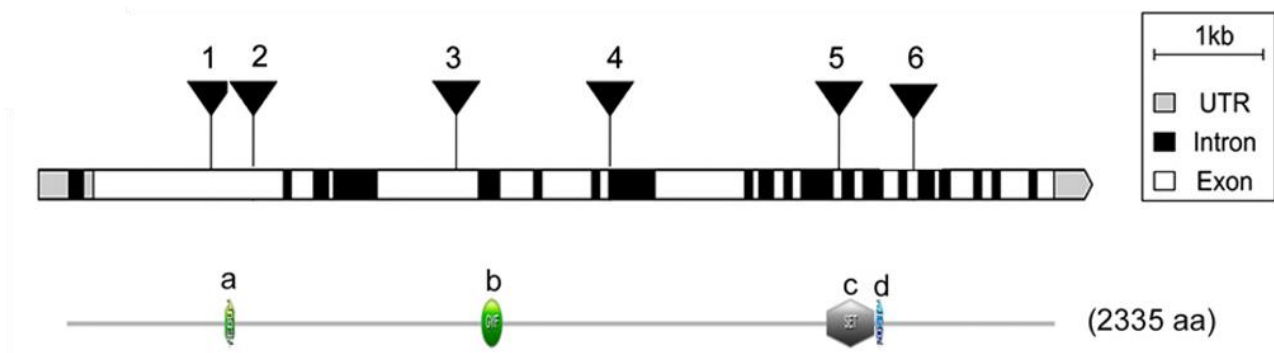


Figure 11. The structure of the *SDG2* gene with the position of all T-DNA insertions available, and the protein structure are shown (Berr et al. 2010).

Considering the phenotypes and the information already published in literature that link both *SDG2* and *GCN5* to mechanisms related to the regulation of the flowering time, it was clear that we were in the right way using our coimmunoprecipitation and MS methods. Analysis made in our laboratories confirmed the data present in literature showing a dwarf phenotype, curly leaves and an early flowering compared with the *WT* plants (Figure 12).

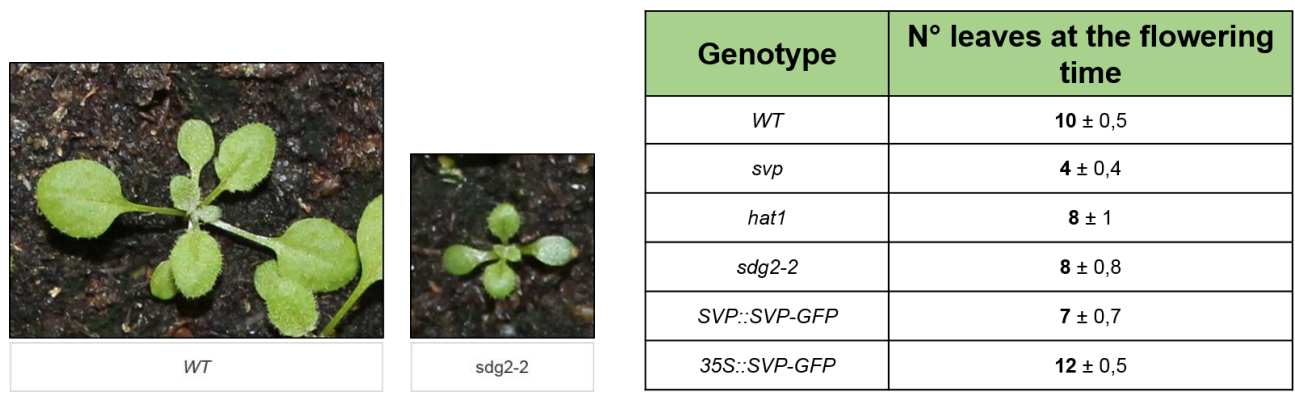


Figure 12. The pictures on the left shows the phenotype of the mutant line *sdg2-2* analyzed in laboratory and compared with the *WT* plant. The table on the right reports the flowering time analysis made in long day

conditions comparing all the mutants and transgenic lines available in our lab. It is visible the early flowering of *sdg2-2* compared with *WT*.

5.8.2 Histone Acetyltransferase GCN5: (GENERAL CONTROL NON-REPRESSIBLE 5)

The developmental transition of a plant from a vegetative to reproductive stage is regulated in response to a variety of external stimuli and endogenous cues. To ensure that flowering occurs in favorable conditions, many plants flower only after an extended period of cold, known as vernalization (Bond et al. 2009). One of the major player in controlling cold response is *FLC* (Michaels & Amasino 2001; Sheldon et al. 1999) and modification of chromatin state can modulate the expression of known and unknown factors upstream of *FLC* through histone acetylation (Deng et al. 2007). Histone acetylation is altered by the antagonistic actions of histone acetyltransferases (HATs) and histone deacetylases (HDACs), which add or remove acetyl groups on lysine residues of histone tails (Shahbazian & Grunstein 2007). *GCN5* is one of the 12 putative HATs present in Arabidopsis genome, and is able to acetylate lysine residues of histone tails. It plays a role in numerous biological processes such as floral development, embryonic cell-fate patterning and promotion of light-regulated genes (Bertrand et al. 2003; Long et al. 2006; Benhamed et al. 2006). Histone acetyltransferases also play a role in the regulation of flowering time in Arabidopsis. Taken together all these information tell us that *GCN5* represents a good candidate in controlling the flowering time processes and its role must be deeply investigated. As for the *SDG2* gene described before, also for *GCN5* we studied the phenotype and also in this case the homozygous mutant plants were completely sterile, with dwarfism and early flowering (Figure 14). In addition a certain percentage (10%) of the homozygous plants displays pleiotropic phenotypes such a three cotyledons seedling and a gradient of plant sizes.

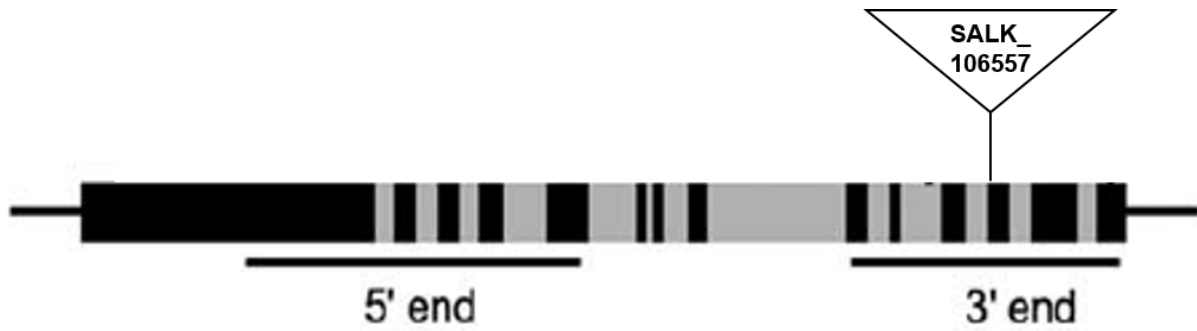


Figure 13. Scheme of *GCN5* gene with the position of the T-DNA insertion in the *gcn5* mutant allele.



Figure 14. Phenotypes of *gcn5* mutants compared with *WT* control. The two pictures in the center, shows the gradient of the *gcn5* phenotypes while the picture on the right showing a tri-cotyledons phenotype that is present for a low percentage of *gcn5* homozygous plants.

Also in the case of *gcn5* the flowering time was analyzed to see if in the mutants are early flowering like the *svp* mutant, in order to connect their action in the same flowering control pathway (Figure 12).

5.9 *In vivo* validation of the candidates selected from the MS output

After the phenotypical analysis of the two putative interactors GCN5 and SDG2, an approach to verify *in vivo* their interaction with SVP was employed. The most common way to validate the *in vivo* interactions is the Yeast two hybrid assay (Y2H). The open reading frame encoding SVP was fused to the activation domain (AD) and GCN5 open reading frame was fused to both the binding domain (BD) and AD, and tested for interaction. We were not able to obtain the entire open reading frame of SDG2 because of the huge length of its CDS sequence (ca. 7k base pairs). Therefore, only the SVP-GCN5 and GCN5-GCN5 interactions were tested, and both of them resulted to be negative. The negative result obtained was not

surprising (Table 9), because Y2H can only detect a direct interaction between two proteins. With high probability GCN5 and also SDG2 take part to a multimeric complex together with SVP, but they are not directly bound to SVP that is probably linked with them via other protein partners. Clearly, other approaches will have to be used to validate these interactions *in planta*, including FRET.

	GCN5-BD
SVP-AD	-
GCN5-AD	-

Table 9. This matrix reports the protein interactions tested via yeast Two Hybrid assay.

5.10 *In planta* validation of proteomics data

By means of yeast two hybrid assays we were only able to test the interaction between SVP and GCN5, while other approaches have been planned in order to validate the mass spectrometry data. The negative results obtained by the yeast two-hybrid assay do not discard the hypothesis that GCN5 and SDG2 can have a role, together with SVP, in the chromatin remodeling controlling the floral transition. The idea is that they work in a large complex composed by different factors, in which GCN5, SDG2 and SVP are physically separated by other factors. This scenario could explain why via yeast two hybrid we were not able to confirm the direct interaction. To establish whether there is a relation between these three factors we introduced the single *sdg2* and *gcn5* mutations in the overexpression line *35S::SVP-GFP* background, looking for differences from the overexpression phenotype. The strong phenotype of both the single mutants described before suggests an important role of these chromatin remodeling factors for the correct development of the plant. The idea is that the late flowering phenotype and the flower defects in the *SVP* overexpression will be reverted to the wild type or better to the *svp* phenotype although the levels of *SVP* transcript and protein are very high. As reported in literature, the MADS-domain TFs as pioneer factors in DNA binding can act as a platform for the chromatin remodeling factors that, by modulating the chromatin structure, can promote or repress the transcription of the target

genes (Pajoro et al. 2014). Due to the sterility of both the single mutants *sdg2* and *gcn5* already described, we performed the crosses using pollen of the heterozygous plants for these two mutants, while homozygous plants for the *SVP* overexpression were used as a mother. This procedure took long time and preliminary data are available only for *SDG2*. In the F2 generation, a *35S::SVP-GFP svp/svp SDG2/sdg2* plant was isolated, which lacked the floral defect caused by the overexpression of *SVP*, suggesting also a sort of dosage effect of *sdg2* mutation. Even if this first result supports our idea about the connection between *SVP* and *SDG2*, other analyses need to be made to confirm this evidence, starting from the evaluation of the flowering time of this line.

6. DISCUSSION

6.1 The SVP::SVP-GFP and the 35S::SVP-GFP lines

This plant material played a central role in all the experiments performed during this thesis work. As a starting point for the project, these two lines were used both for the set-up of the experiments of nuclear proteins isolation and coimmunoprecipitation, as well as for the crosses made with the putative interactors of SVP identified by the Mass Spectrometry analysis. The transgenic line *35S::SVP-GFP* in *svp/svp* background, generated during the first year of the Ph.D. project showed the same phenotype of the overexpression line *35S::SVP* in the WT background, characterized by a delay in flowering time and floral organs defects, indicating that the chimeric protein is functional. Furthermore, when the chimeric protein localization was investigated by *in vivo* fluorescent microscopy observations of Arabidopsis leaves tissues, it was detected within the nuclei of the observed cells, consistently with the notion that SVP is a transcription factor. These data were also supported by the immunoblotting assays performed on the purified nuclear proteins, with an antibody against the GFP protein. Further support comes from the information that the native line *SVP::SVP-GFP* already available in our lab (Gregis et al. 2013), was able to complement the *svp/svp* mutant, shifting its flowering time back to values similar to the wild type. The *SVP::SVP-GFP* chimera was also localized in the nucleus by the same *in vivo* fluorescence microscopy study. These data confirm that also in the line *SVP::SVP-GFP* *svp/svp* the chimeric protein is functional.

6.2 The nuclei isolation protocol

Our goal was to isolate nuclei from the inflorescence tissues of the *SVP::SVP-GFP* and the *35S::SVP-GFP* lines, in comparison with the wild type. After the generation and the validation of the plant material necessary for our experiments, we realized through coomassie staining and western blot analysis, that the protocol of nuclei isolation represented a limiting step in term of quality of the material to analyze by MS. As reported in the results chapter, the immunoprecipitated proteins analyzed via Mass Spectrometry can contain many extranuclear contaminant proteins. The design of a robust method able to

purify as much as possible the nuclear protein fraction, was crucial for the generation of a high quality material that would yield a clean MS outcoming list, with the lowest amount of extranuclear (which are likely to be false positives) putative interactors. After different adjustments and modifications of various steps of a general protocol for nuclei isolation from Arabidopsis tissues, we were able to develop a robust protocol that makes it possible to isolate only the nuclear protein fraction without any contamination of proteins from other cellular compartments. The quality of the nuclei isolation was checked by coomassie staining, in which the major cytosolic contaminant protein RUBISCO, was not observed in the nuclei protein fraction and by immunoblotting with antibodies specific for histones, that were highly enriched in the nuclear fraction.

6.3 The coimmunoprecipitation strategy

As the improvement of the nuclei isolation protocol, the design of a tailored coimmunoprecipitation experiment was crucial for the quality of the results, and time demanding. The goal/difficulty was to devise a good strategy to immunoprecipitate the tagged proteins (the chimeric protein SVP-GFP) together with their interactors, with the highest efficiency i.e. reducing the loss of tagged proteins and their own interactors, while maintaining high the stringency of the elution conditions and without any kind of contamination due to the adopted immunoprecipitation system. As it happened during first trials, the non-covalently bound antibody detached from the magnetic beads used for the CoIP, and it represented the major contaminant of our IP samples. After different trials, we decided to adopt a new tool for IP analysis where the GFP-specific antibody was covalently linked to the magnetic beads, therefore it was not released into the IP samples after elution. We checked the quality of the material resulting from the IP experiment before going ahead with the mass spectrometry. Western blotting analysis performed with an antibody against the GFP detected in the IP samples a large amount of chimeric protein, and no GFP-specific antibody contamination, indicating that the immunoprecipitation strategy worked properly, and that we had established a good protocol to identify SVP interactors.

6.4 The Mass Spectrometry data

The material resulting from the IP performed on both the *SVP::SVP-GFP* and the *35S::SVP-GFP* lines was analyzed either by a MALDI-TOF or a ORBITRAP mass spectrometer (Makarov 2000; Hu et al. 2005), the latter providing much better results in term of sensitivity. Moreover, the trypsin digestion of the protein samples was initially performed “in gel”: samples were run into a SDS PAGE, and the slice of gel containing all the proteins was excised, subjected to trypsin treatment and MS-analyzed. This procedure unluckily reduced the quality and the number of proteins identified within the sample, as the list of peptides identified by MS was far too short to be reliable. This could be due by the presence of acrylamide that might represent an obstacle to protein digestion and peptide release. Better results were obtained when a protocol based on “in solution” trypsin digestion, in which the IP samples were directly digested without the SDS-PAGE step, was adopted. After this treatment, a relatively large list of putative protein interactors was obtained, and many of the interactors were shared between the two output lists. By comparing the IP-MS lists, we were able to generate a short list of strong putative SVP interactors, to be validated through functional genomics studies.

6.5 The putative interactors

Looking through the short list of putative interactors, generated applying the different filters described above, a main group of proteins could be recognized. A large part of the putative interactors found in the IP samples, indeed, is involved in chromatin remodeling indicating a strong interaction between SVP and chromatin modifications. It has been already shown that MADS-box TFs are able to interact with this class of proteins, in order to modify the chromatin structure promoting or repressing the transcription of the target genes (Lu et al. 2011; Smaczniak, Immink, et al. 2012). The high number of chromatin modifying factors, like histone acetyltransferase, deacetylase and methyltransferase, suggest the capacity of SVP to form different types of complexes interacting with different chromatin remodeling factors, possibly playing different roles. The corresponding knock-out mutants of eight of these putative candidates did not show a relevant phenotype compared with the wild type, however other two knock-out mutants altered in *SDG2* and *GCN5* genes showed a flowering-time phenotype. It possible that these chromatin remodeling factors, play their role

in a large protein complex and with SDG2 and GCN5 playing a crucial role in SVP-dependent flowering time determination.

6.6 SDG2 and GCN5 as a putative interactors

The analysis of the two single mutants *sdg2* and *gcn5*, showed a marked alteration of the flowering time, compared with wild type plants (Guo et al. 2010; Bertrand et al. 2003), indicating that *sdg2* and *gcn5* may be needed for the perfect functionality of SVP and part of the molecular network that controls the flowering time process. Beside this important finding, the data also represent a strong evidence of the goodness of our co-immunoprecipitation and MS analysis strategies, thus validating the work made until now. These two interactors were used to deep investigate their role in controlling the flowering time mechanisms, and their interaction with SVP.

6.7 *In vivo* validation

Driven by the results obtained during the analysis of the single mutants and the data present in literature, we started to deep investigate the role of SDG2 and GCN5 during the flowering time. Different strategies were used in order to validate the interaction between these factors and SVP. Among them, we started with the yeast two hybrid assay by which we were not able to confirm the direct interaction between GCN5 and SVP, whereas SDG2 could not be tested because the CDS is not available. Our hypothesis is that SVP is part of a large complex that binds to the promoter region of the SVP target genes, where it modulates nuclear gene expression by changing chromatin structure. Moreover, it is not necessary that all the identify factors directly interact with SVP, since other proteins can be interposed between them and SVP. Moreover, crosses between the single mutant *sdg2* and *gcn5* whit the *35S::SVP-GFP* line were performed to identify other functional interactions between these factors and *SVP*. Preliminary data available for *sdg2*, revealed that the *35S::SVP-GFP svp/svp SDG2/sdg2* plants, lacks the flower defect caused by the overexpression of *SVP*. Even if further analyses are required, these data strongly correlate *SDG2* to the *SVP* role in influencing flower morphology.

7. CONCLUSIONS

During the three years of my PhD I contributed to shed light into the floral transition mechanisms. In the first part of my work, I focused my attention to define a proteomic approach able to identify the protein partners of SVP. Even if during the last decade the SVP was very well studied at genomic level, only a few information are available at the proteomic level. The genetic network in which *SVP* play a role, promoting or repressing the expression of their target genes in controlling the flowering time mechanism, was deep investigate (Lee et al. 2007; Li et al. 2008; Jang et al. 2009). About the protein partners of SVP, forming a complex responsible to control flowering time, only few interactors were identified by yeast two-hybrid assay (de Folter et al. 2005). The complex mechanisms of the floral transition, is probably controlled by different complexes in which SVP takes part. The protein composition of these complexes is still unknown and their identification can allow us to attribute to SVP different functions depending on the type of complex in which it takes part. A new strategy and new tools are required in order to identify the components of these complexes, reducing the amount of work, and the time used to analyze and validate the data obtained. The protocol developed during the first year was a starting point to deep investigate the proteins interactors of SVP. As a transcription factor, SVP play its role at the nuclear level, interacting with others protein classes. The protocol was therefore focused to purify the nuclear protein fraction, maintaining the proteins in their native state to preserve the protein-protein interactions. The nuclear purification coupled with the Mass Spectrometry analysis, allowed us to define a lists of putative interactors. The large part of these putative interactors are involved in histone modifications, such as acetyltransferases, deacetylases and methyltransferases. This suggests that the MADS-domain proteins can recruit or redirect the basic chromatin remodeling machinery to modulate the promoter structure of their target genes. The interaction between MADS-proteins with chromatin remodeling proteins is important for the regulation of gene expression by the MADS-domain factors (Smaczniak, Immink, et al. 2012), and their physical interaction suggests an important role of these TFs in controlling chromatin dynamics during plant development. The two promising candidate found in our MS analysis, *GCN5* and *SDG2*, seems to represent a good validation of the procedure on which our work is based. In fact, data already published in literature report a connection between *GCN5*, *SDG2* and the flowering time processes especially in the repression of flowering caused by SVP. *GCN5* and *SDG2* are involved respectively in

histone acetyltransferase and histone methyltransferase and as reported in literature we confirmed their flowering delay compared with the *WT* plants. Another important evidence that link these two proteins to SVP, belong to the phenotype observation in the *35S::SVP-GFP* background in which the single mutation *sdg2*, and *gcn5* were introgressed. First evidence were showed in the case of *SDG2*, where the isolated plants *35S::SVP-GFP svp/svp SDG2/sdg2* lacked the floral defect caused by the overexpression of SVP, suggesting also a sort of dosage effect of *sdg2* mutation. Even if more analysis are needed to better investigate their role in flowering time and their interaction with SVP, the results obtained during my work also opened a new windows into the world of flowering time, suggesting a strong interaction between chromatin modification factors and the floral transition, in accordance with literature data (Smaczniak, Immink, et al. 2012). Our hypothesis is that SVP binds the promoter regions of the target genes and then recruits the different protein interactors, acting as a platform for the chromatin remodeling complexes that modulates the transcription of the downstream gene. Probably the activation or repression activity of a transcription factor depends on the different composition of the chromatin remodeling complex driven by endogenous and exogenous stimuli such a developmental stage, temperature, light and hormones. Going on with this project, in the future, we aim to identify the composition of all the different complexes generated by each kind of stimuli and the action of each different complexes in the flowering time related processes.

8. FUTURE PROSPECTIVE

All the work made during these three years of my PhD allowed us to set up a good strategy in the identification of protein complexes. Especially for SVP we were able to identify a putative mechanism based on chromatin remodeling that can control the flowering time in Arabidopsis. Nevertheless, we spent a lot of time setting the protocols and making trials. At this time a lot of work is needed to better validate the preliminary results obtained and for deep study of the mechanisms in which SVP is involved in controlling flowering time. Next work to finish this part and going on with the project, are articulated in many validation experiments and new methods that can be placed side by side at the currently strategies in use.

- BiFC (Bimolecular Fluorescence Complementation) and FRET (Fluorescence Resonance Energy Transfer) to validate *in vivo* interaction in substitution of Yeast Two Hybrid assay.
- Cross the transgenic lines *35S::SVP-GFP* and *svp* mutant with the two mutants *sdg2-2* and *gcn5* to verify some difference in flowering time.
- Real-time PCR of the mutant plants *sdg2-2* and *gcn5* to check the expression of the SVP gene targets.
- Blue native Gel electrophoresis and Sucrose gradients of IP fractions in order to separate the different complexes and analyze the protein composition of each one.
- Perform new Coimmunoprecipitation in collaboration with the Gerko group and work together to find new interactors of SVP.
- Studies on chromatin modification involved in the flowering time mechanisms.

9. REFERENCES

- Abe, M. et al., 2005. FD, a bZIP protein mediating signals from the floral pathway integrator FT at the shoot apex. *Science (New York, N. Y.)*, 309(5737), pp.1052–6. Available at: <http://www.ncbi.nlm.nih.gov/pubmed/16099979> [Accessed September 3, 2014].
- Allahverdiyeva, Y. et al., 2013. Arabidopsis plants lacking PsbQ and PsbR subunits of the oxygen-evolving complex show altered PSII super-complex organization and short-term adaptive mechanisms. *Plant Journal*, 75(4), pp.671–684.
- Alvarez-Buylla, E.R. et al., 2000. An ancestral MADS-box gene duplication occurred before the divergence of plants and animals. *Proceedings of the National Academy of Sciences of the United States of America*, 97(10), pp.5328–33. Available at: <http://www.pubmedcentral.nih.gov/articlerender.fcgi?artid=25828&tool=pmcentrez&rendertype=abstract> [Accessed October 15, 2014].
- Bastow, R. et al., 2004. Vernalization requires epigenetic silencing of FLC by histone methylation. *Nature*, 427(6970), pp.164–7. Available at: <http://www.ncbi.nlm.nih.gov/pubmed/14712277> [Accessed October 24, 2014].
- Becker, A. & Theissen, G., 2003. The major clades of MADS-box genes and their role in the development and evolution of flowering plants. *Molecular phylogenetics and evolution*, 29(3), pp.464–89. Available at: <http://www.ncbi.nlm.nih.gov/pubmed/14615187> [Accessed October 15, 2014].
- Bemer, M. et al., 2008. The MADS domain protein DIANA acts together with AGAMOUS-LIKE80 to specify the central cell in Arabidopsis ovules. *The Plant cell*, 20(8), pp.2088–101. Available at: <http://www.pubmedcentral.nih.gov/articlerender.fcgi?artid=2553608&tool=pmcentrez&rendertype=abstract> [Accessed October 15, 2014].
- Benhamed, M. et al., 2006. Arabidopsis GCN5, HD1, and TAF1/HAF2 interact to regulate histone acetylation required for light-responsive gene expression. *The Plant cell*, 18(11), pp.2893–903. Available at: <http://www.pubmedcentral.nih.gov/articlerender.fcgi?artid=1693931&tool=pmcentrez&rendertype=abstract> [Accessed October 14, 2014].
- Berr, A. et al., 2010. Arabidopsis SET DOMAIN GROUP2 is required for H3K4 trimethylation and is crucial for both sporophyte and gametophyte development. *The Plant cell*, 22(10), pp.3232–48. Available at: <http://www.pubmedcentral.nih.gov/articlerender.fcgi?artid=2990135&tool=pmcentrez&rendertype=abstract> [Accessed October 17, 2014].
- Bertrand, C. et al., 2003. Arabidopsis histone acetyltransferase AtGCN5 regulates the floral meristem activity through the WUSCHEL/AGAMOUS pathway. *The Journal of biological chemistry*, 278(30), pp.28246–51. Available at: <http://www.ncbi.nlm.nih.gov/pubmed/12740375> [Accessed November 2, 2014].

- Blázquez, M. et al., 1998. Gibberellins promote flowering of Arabidopsis by activating the LEAFY promoter. *The Plant Cell*, 10(5), pp.791–800. Available at: <http://www.pubmedcentral.nih.gov/articlerender.fcgi?artid=144373&tool=pmcentrez&endertype=abstract> [Accessed October 27, 2014].
- Blázquez, M.A. et al., 1997. LEAFY expression and flower initiation in Arabidopsis. *Development (Cambridge, England)*, 124(19), pp.3835–44. Available at: <http://www.ncbi.nlm.nih.gov/pubmed/9367439> [Accessed October 14, 2014].
- Blázquez, M.A., Ahn, J.H. & Weigel, D., 2003. A thermosensory pathway controlling flowering time in Arabidopsis thaliana. *Nature genetics*, 33(2), pp.168–71. Available at: <http://www.ncbi.nlm.nih.gov/pubmed/12548286> [Accessed October 14, 2014].
- Blázquez, M.A. & Weigel, D., 2000. Integration of floral inductive signals in Arabidopsis. *Nature*, 404(6780), pp.889–92. Available at: <http://www.ncbi.nlm.nih.gov/pubmed/10786797> [Accessed October 9, 2014].
- De Bodt, S. et al., 2003. Genomewide structural annotation and evolutionary analysis of the type I MADS-box genes in plants. *Journal of molecular evolution*, 56(5), pp.573–86. Available at: <http://www.ncbi.nlm.nih.gov/pubmed/12698294> [Accessed October 15, 2014].
- Bond, D.M. et al., 2009. Histone acetylation, VERNALIZATION INSENSITIVE 3, FLOWERING LOCUS C, and the vernalization response. *Molecular plant*, 2(4), pp.724–37. Available at: <http://www.ncbi.nlm.nih.gov/pubmed/19825652> [Accessed November 2, 2014].
- Cohen, R. et al., 2009. The histone acetyltransferase GCN5 affects the inflorescence meristem and stamen development in Arabidopsis. *Planta*, 230(6), pp.1207–21. Available at: <http://www.ncbi.nlm.nih.gov/pubmed/19771450> [Accessed November 3, 2014].
- Colombo, M. et al., 2008. AGL23, a type I MADS-box gene that controls female gametophyte and embryo development in Arabidopsis. *The Plant journal : for cell and molecular biology*, 54(6), pp.1037–48. Available at: <http://www.ncbi.nlm.nih.gov/pubmed/18346189> [Accessed October 15, 2014].
- Corbesier, L. et al., 2007. FT protein movement contributes to long-distance signaling in floral induction of Arabidopsis. *Science (New York, N.Y.)*, 316(5827), pp.1030–3. Available at: <http://www.ncbi.nlm.nih.gov/pubmed/17446353> [Accessed July 16, 2014].
- Deng, W. et al., 2007. Involvement of the histone acetyltransferase AtHAC1 in the regulation of flowering time via repression of FLOWERING LOCUS C in Arabidopsis. *Plant physiology*, 143(4), pp.1660–8. Available at: <http://www.pubmedcentral.nih.gov/articlerender.fcgi?artid=1851829&tool=pmcentrez&rendertype=abstract> [Accessed November 2, 2014].
- Evans, M.M.S. & Barton, M.K., 1997. GENETICS OF ANGIOSPERM SHOOT APICAL MERISTEM DEVELOPMENT. *Annual review of plant physiology and plant molecular*

biology, 48, pp.673–701. Available at: <http://www.ncbi.nlm.nih.gov/pubmed/15012278> [Accessed October 7, 2014].

Fletcher, J.C., 2002. Shoot and floral meristem maintenance in arabidopsis. *Annual review of plant biology*, 53, pp.45–66. Available at: <http://www.ncbi.nlm.nih.gov/pubmed/12221985> [Accessed May 5, 2015].

De Folter, S. et al., 2005. Comprehensive interaction map of the Arabidopsis MADS Box transcription factors. *The Plant cell*, 17(5), pp.1424–33. Available at: <http://www.pubmedcentral.nih.gov/articlerender.fcgi?artid=1091765&tool=pmcentrez&rendertype=abstract> [Accessed October 15, 2014].

De Folter, S. et al., 2007. Tagging of MADS domain proteins for chromatin immunoprecipitation. *BMC plant biology*, 7, p.47. Available at: <http://www.pubmedcentral.nih.gov/articlerender.fcgi?artid=2071916&tool=pmcentrez&rendertype=abstract> [Accessed April 16, 2015].

Fornara, F., de Montaigu, A. & Coupland, G., 2010. SnapShot: Control of flowering in Arabidopsis. *Cell*, 141(3), pp.550, 550.e1–2. Available at: <http://www.ncbi.nlm.nih.gov/pubmed/20434991> [Accessed October 9, 2014].

Fowler, S. et al., 1999. GIGANTEA: a circadian clock-controlled gene that regulates photoperiodic flowering in Arabidopsis and encodes a protein with several possible membrane-spanning domains. *The EMBO journal*, 18(17), pp.4679–88. Available at: <http://www.pubmedcentral.nih.gov/articlerender.fcgi?artid=1171541&tool=pmcentrez&rendertype=abstract> [Accessed October 17, 2014].

Fujiwara, S. et al., 2008. Circadian clock proteins LHY and CCA1 regulate SVP protein accumulation to control flowering in Arabidopsis. *The Plant cell*, 20(11), pp.2960–71. Available at: <http://www.pubmedcentral.nih.gov/articlerender.fcgi?artid=2613671&tool=pmcentrez&rendertype=abstract> [Accessed October 27, 2014].

Greb, T. et al., 2007. The PHD finger protein VRN5 functions in the epigenetic silencing of Arabidopsis FLC. *Current biology : CB*, 17(1), pp.73–8. Available at: <http://www.ncbi.nlm.nih.gov/pubmed/17174094> [Accessed October 3, 2014].

Gregis, V. et al., 2013. Identification of pathways directly regulated by SHORT VEGETATIVE PHASE during vegetative and reproductive development in Arabidopsis. *Genome biology*, 14(6), p.R56. Available at: <http://www.pubmedcentral.nih.gov/articlerender.fcgi?artid=3706845&tool=pmcentrez&rendertype=abstract> [Accessed April 27, 2015].

Gregis, V. et al., 2009. The Arabidopsis floral meristem identity genes AP1, AGL24 and SVP directly repress class B and C floral homeotic genes. *The Plant journal : for cell and molecular biology*, 60(4), pp.626–37. Available at: <http://www.ncbi.nlm.nih.gov/pubmed/19656343> [Accessed October 27, 2014].

Guo, L. et al., 2010. SET DOMAIN GROUP2 is the major histone H3 lysine [corrected] 4 trimethyltransferase in Arabidopsis. *Proceedings of the National Academy of Sciences*

of the United States of America, 107(43), pp.18557–62. Available at: <http://www.pubmedcentral.nih.gov/articlerender.fcgi?artid=2972934&tool=pmcentrez&rendertype=abstract> [Accessed November 2, 2014].

- Han, P. et al., 2008. AGAMOUS-LIKE 17, a novel flowering promoter, acts in a FT-independent photoperiod pathway. *The Plant journal : for cell and molecular biology*, 55(2), pp.253–65. Available at: <http://www.ncbi.nlm.nih.gov/pubmed/18363787> [Accessed October 24, 2014].
- Hartmann, U. et al., 2000. Molecular cloning of SVP: a negative regulator of the floral transition in Arabidopsis. *The Plant journal : for cell and molecular biology*, 21(4), pp.351–60. Available at: <http://www.ncbi.nlm.nih.gov/pubmed/10758486> [Accessed October 7, 2014].
- Helliwell, C.A. et al., 2006. The Arabidopsis FLC protein interacts directly in vivo with SOC1 and FT chromatin and is part of a high-molecular-weight protein complex. *The Plant journal : for cell and molecular biology*, 46(2), pp.183–92. Available at: <http://www.ncbi.nlm.nih.gov/pubmed/16623882> [Accessed October 24, 2014].
- Hepworth, S.R. et al., 2002. Antagonistic regulation of flowering-time gene SOC1 by CONSTANS and FLC via separate promoter motifs. *The EMBO journal*, 21(16), pp.4327–37. Available at: <http://www.pubmedcentral.nih.gov/articlerender.fcgi?artid=126170&tool=pmcentrez&rendertype=abstract> [Accessed October 24, 2014].
- Hisamatsu, T. & King, R.W., 2008. The nature of floral signals in Arabidopsis. II. Roles for FLOWERING LOCUS T (FT) and gibberellin. *Journal of experimental botany*, 59(14), pp.3821–9. Available at: <http://www.pubmedcentral.nih.gov/articlerender.fcgi?artid=2576629&tool=pmcentrez&rendertype=abstract> [Accessed October 27, 2014].
- Hu, Q. et al., 2005. The Orbitrap: a new mass spectrometer. *Journal of mass spectrometry : JMS*, 40(4), pp.430–43. Available at: <http://www.ncbi.nlm.nih.gov/pubmed/15838939> [Accessed July 10, 2014].
- Huang, H. et al., 1993. Isolation and characterization of the binding sequences for the product of the Arabidopsis floral homeotic gene AGAMOUS. *Nucleic acids research*, 21(20), pp.4769–76. Available at: <http://www.pubmedcentral.nih.gov/articlerender.fcgi?artid=331504&tool=pmcentrez&rendertype=abstract> [Accessed October 15, 2014].
- Irish, V.F., 1999. Patterning the flower. *Developmental biology*, 209(2), pp.211–20. Available at: <http://www.ncbi.nlm.nih.gov/pubmed/10328916> [Accessed October 7, 2014].
- Jackson, J.P. et al., 2002. Control of CpNpG DNA methylation by the KRYPTONITE histone H3 methyltransferase. *Nature*, 416(6880), pp.556–60. Available at: <http://www.ncbi.nlm.nih.gov/pubmed/11898023> [Accessed October 27, 2014].

- Jang, S., Torti, S. & Coupland, G., 2009. Genetic and spatial interactions between FT, TSF and SVP during the early stages of floral induction in Arabidopsis. *The Plant journal : for cell and molecular biology*, 60(4), pp.614–25. Available at: <http://www.ncbi.nlm.nih.gov/pubmed/19656342> [Accessed October 3, 2014].
- Jiang, D. et al., 2007. Arabidopsis relatives of the human lysine-specific Demethylase1 repress the expression of FWA and FLOWERING LOCUS C and thus promote the floral transition. *The Plant cell*, 19(10), pp.2975–87. Available at: <http://www.pubmedcentral.nih.gov/articlerender.fcgi?artid=2174716&tool=pmcentrez&rendertype=abstract> [Accessed October 27, 2014].
- Johanson, U. et al., 2000. Molecular analysis of FRIGIDA, a major determinant of natural variation in Arabidopsis flowering time. *Science (New York, N.Y.)*, 290(5490), pp.344–7. Available at: <http://www.ncbi.nlm.nih.gov/pubmed/11030654> [Accessed October 24, 2014].
- Johnson, L. et al., 2004. Mass spectrometry analysis of Arabidopsis histone H3 reveals distinct combinations of post-translational modifications. *Nucleic acids research*, 32(22), pp.6511–8. Available at: <http://www.pubmedcentral.nih.gov/articlerender.fcgi?artid=545460&tool=pmcentrez&rendertype=abstract> [Accessed November 2, 2014].
- Kang, H.-G. et al., 2011. Overexpression of FTL1/DDF1, an AP2 transcription factor, enhances tolerance to cold, drought, and heat stresses in Arabidopsis thaliana. *Plant science : an international journal of experimental plant biology*, 180(4), pp.634–41. Available at: <http://www.ncbi.nlm.nih.gov/pubmed/21421412> [Accessed October 27, 2014].
- Kang, I.-H. et al., 2008. The AGL62 MADS domain protein regulates cellularization during endosperm development in Arabidopsis. *The Plant cell*, 20(3), pp.635–47. Available at: <http://www.pubmedcentral.nih.gov/articlerender.fcgi?artid=2329934&tool=pmcentrez&rendertype=abstract> [Accessed October 15, 2014].
- Kardailsky, I. et al., 1999. Activation tagging of the floral inducer FT. *Science (New York, N.Y.)*, 286(5446), pp.1962–5. Available at: <http://www.ncbi.nlm.nih.gov/pubmed/10583961> [Accessed October 2, 2014].
- Kaufmann, K., Melzer, R. & Theissen, G., 2005. MIKC-type MADS-domain proteins: structural modularity, protein interactions and network evolution in land plants. *Gene*, 347(2), pp.183–98. Available at: <http://www.ncbi.nlm.nih.gov/pubmed/15777618> [Accessed August 25, 2014].
- Klockenbusch, C. & Kast, J., 2010. Optimization of formaldehyde cross-linking for protein interaction analysis of non-tagged integrin beta1. *Journal of biomedicine & biotechnology*, 2010, p.927585. Available at: <http://www.pubmedcentral.nih.gov/articlerender.fcgi?artid=2896913&tool=pmcentrez&rendertype=abstract> [Accessed July 10, 2014].

- Kobayashi, Y. et al., 1999. A pair of related genes with antagonistic roles in mediating flowering signals. *Science (New York, N.Y.)*, 286(5446), pp.1960–2. Available at: <http://www.ncbi.nlm.nih.gov/pubmed/10583960> [Accessed October 2, 2014].
- Köhler, C. et al., 2003. The Polycomb-group protein MEDEA regulates seed development by controlling expression of the MADS-box gene PHERES1. *Genes & development*, 17(12), pp.1540–53. Available at: <http://www.pubmedcentral.nih.gov/articlerender.fcgi?artid=196083&tool=pmcentrez&endertype=abstract> [Accessed October 11, 2014].
- Koornneef, M., Hanhart, C.J. & van der Veen, J.H., 1991. A genetic and physiological analysis of late flowering mutants in *Arabidopsis thaliana*. *Molecular & general genetics : MGG*, 229(1), pp.57–66. Available at: <http://www.ncbi.nlm.nih.gov/pubmed/1896021> [Accessed October 14, 2014].
- Lee, D.J. & Zeevaart, J.A.D., 2007. Regulation of gibberellin 20-oxidase1 expression in spinach by photoperiod. *Planta*, 226(1), pp.35–44. Available at: <http://www.ncbi.nlm.nih.gov/pubmed/17216482> [Accessed October 27, 2014].
- Lee, H. et al., 2010. Genetic framework for flowering-time regulation by ambient temperature-responsive miRNAs in *Arabidopsis*. *Nucleic acids research*, 38(9), pp.3081–93. Available at: <http://www.pubmedcentral.nih.gov/articlerender.fcgi?artid=2875011&tool=pmcentrez&rendertype=abstract> [Accessed October 26, 2014].
- Lee, H. et al., 2000. The AGAMOUS-LIKE 20 MADS domain protein integrates floral inductive pathways in *Arabidopsis*. *Genes & development*, 14(18), pp.2366–76. Available at: <http://www.pubmedcentral.nih.gov/articlerender.fcgi?artid=316936&tool=pmcentrez&endertype=abstract> [Accessed October 24, 2014].
- Lee, I. et al., 1994. Isolation of LUMINIDEPENDENS: a gene involved in the control of flowering time in *Arabidopsis*. *The Plant cell*, 6(1), pp.75–83. Available at: <http://www.pubmedcentral.nih.gov/articlerender.fcgi?artid=160417&tool=pmcentrez&endertype=abstract> [Accessed October 27, 2014].
- Lee, I. & Amasino, R.M., 1995. Effect of Vernalization, Photoperiod, and Light Quality on the Flowering Phenotype of *Arabidopsis* Plants Containing the FRIGIDA Gene. *Plant physiology*, 108(1), pp.157–162. Available at: <http://www.pubmedcentral.nih.gov/articlerender.fcgi?artid=157316&tool=pmcentrez&endertype=abstract> [Accessed October 24, 2014].
- Lee, J. et al., 2008. SOC1 translocated to the nucleus by interaction with AGL24 directly regulates leafy. *The Plant journal : for cell and molecular biology*, 55(5), pp.832–43. Available at: <http://www.ncbi.nlm.nih.gov/pubmed/18466303> [Accessed October 14, 2014].
- Lee, J.H. et al., 2007. Role of SVP in the control of flowering time by ambient temperature in *Arabidopsis*. *Genes & development*, 21(4), pp.397–402. Available at:

<http://www.pubmedcentral.nih.gov/articlerender.fcgi?artid=1804328&tool=pmcentrez&rendertype=abstract> [Accessed October 14, 2014].

- Levy, Y.Y. et al., 2002. Multiple roles of Arabidopsis VRN1 in vernalization and flowering time control. *Science (New York, N.Y.)*, 297(5579), pp.243–6. Available at: <http://www.ncbi.nlm.nih.gov/pubmed/12114624> [Accessed October 24, 2014].
- Li, D. et al., 2008. A repressor complex governs the integration of flowering signals in Arabidopsis. *Developmental cell*, 15(1), pp.110–20. Available at: <http://www.ncbi.nlm.nih.gov/pubmed/18606145> [Accessed September 7, 2014].
- Liu, C. et al., 2009. Regulation of floral patterning by flowering time genes. *Developmental cell*, 16(5), pp.711–22. Available at: <http://www.ncbi.nlm.nih.gov/pubmed/19460347> [Accessed October 27, 2014].
- Liu, C. et al., 2007. Specification of Arabidopsis floral meristem identity by repression of flowering time genes. *Development (Cambridge, England)*, 134(10), pp.1901–10. Available at: <http://www.ncbi.nlm.nih.gov/pubmed/17428825> [Accessed October 27, 2014].
- Long, J.A. et al., 2006. TOPLESS regulates apical embryonic fate in Arabidopsis. *Science (New York, N.Y.)*, 312(5779), pp.1520–3. Available at: <http://www.ncbi.nlm.nih.gov/pubmed/16763149> [Accessed October 30, 2014].
- Lu, F. et al., 2011. Arabidopsis REF6 is a histone H3 lysine 27 demethylase. *Nature Genetics*, 43(7), pp.715–719. Available at: <http://www.ncbi.nlm.nih.gov/pubmed/21642989> [Accessed March 18, 2015].
- Macknight, R. et al., 1997. FCA, a gene controlling flowering time in Arabidopsis, encodes a protein containing RNA-binding domains. *Cell*, 89(5), pp.737–45. Available at: <http://www.ncbi.nlm.nih.gov/pubmed/9182761> [Accessed October 27, 2014].
- Makarov, A., 2000. Electrostatic axially harmonic orbital trapping: a high-performance technique of mass analysis. *Analytical chemistry*, 72(6), pp.1156–62. Available at: <http://www.ncbi.nlm.nih.gov/pubmed/10740853> [Accessed November 1, 2014].
- Masiero, S. et al., 2002. Ternary complex formation between MADS-box transcription factors and the histone fold protein NF-YB. *The Journal of biological chemistry*, 277(29), pp.26429–35. Available at: <http://www.ncbi.nlm.nih.gov/pubmed/11971906> [Accessed October 15, 2014].
- Messenguy, F. & Dubois, E., 2003. Role of MADS box proteins and their cofactors in combinatorial control of gene expression and cell development. *Gene*, 316, pp.1–21. Available at: <http://www.ncbi.nlm.nih.gov/pubmed/14563547> [Accessed October 14, 2014].
- Michaels, S.D. et al., 2003. AGL24 acts as a promoter of flowering in Arabidopsis and is positively regulated by vernalization. *The Plant journal : for cell and molecular biology*, 33(5), pp.867–74. Available at: <http://www.ncbi.nlm.nih.gov/pubmed/12609028> [Accessed October 16, 2014].

- Michaels, S.D. et al., 2005. Integration of flowering signals in winter-annual Arabidopsis. *Plant physiology*, 137(1), pp.149–56. Available at: <http://www.pubmedcentral.nih.gov/articlerender.fcgi?artid=548846&tool=pmcentrez&endertype=abstract> [Accessed October 24, 2014].
- Michaels, S.D. & Amasino, R.M., 1999. FLOWERING LOCUS C encodes a novel MADS domain protein that acts as a repressor of flowering. *The Plant cell*, 11(5), pp.949–56. Available at: <http://www.pubmedcentral.nih.gov/articlerender.fcgi?artid=144226&tool=pmcentrez&endertype=abstract> [Accessed October 24, 2014].
- Michaels, S.D. & Amasino, R.M., 2001. Loss of FLOWERING LOCUS C activity eliminates the late-flowering phenotype of FRIGIDA and autonomous pathway mutations but not responsiveness to vernalization. *The Plant cell*, 13(4), pp.935–41. Available at: <http://www.pubmedcentral.nih.gov/articlerender.fcgi?artid=135534&tool=pmcentrez&endertype=abstract> [Accessed October 27, 2014].
- Moon, J. et al., 2003. The SOC1 MADS-box gene integrates vernalization and gibberellin signals for flowering in Arabidopsis. *The Plant journal : for cell and molecular biology*, 35(5), pp.613–23. Available at: <http://www.ncbi.nlm.nih.gov/pubmed/12940954> [Accessed October 14, 2014].
- Nakamichi, N. et al., 2007. Arabidopsis clock-associated pseudo-response regulators PRR9, PRR7 and PRR5 coordinately and positively regulate flowering time through the canonical CONSTANS-dependent photoperiodic pathway. *Plant & cell physiology*, 48(6), pp.822–32. Available at: <http://www.ncbi.nlm.nih.gov/pubmed/17504813> [Accessed October 17, 2014].
- Noh, Y.-S. et al., 2004. EARLY FLOWERING 5 acts as a floral repressor in Arabidopsis. *The Plant journal : for cell and molecular biology*, 38(4), pp.664–72. Available at: <http://www.ncbi.nlm.nih.gov/pubmed/15125772> [Accessed October 27, 2014].
- Pajoro, A. et al., 2014. Dynamics of chromatin accessibility and gene regulation by MADS-domain transcription factors in flower development. *Genome Biology*, 15(3), p.R41. Available at: <http://www.pubmedcentral.nih.gov/articlerender.fcgi?artid=4054849&tool=pmcentrez&endertype=abstract> [Accessed March 30, 2015].
- Parenicová, L. et al., 2003. Molecular and phylogenetic analyses of the complete MADS-box transcription factor family in Arabidopsis: new openings to the MADS world. *The Plant cell*, 15(7), pp.1538–51. Available at: <http://www.pubmedcentral.nih.gov/articlerender.fcgi?artid=165399&tool=pmcentrez&endertype=abstract> [Accessed October 14, 2014].
- Park, D.H. et al., 1999. Control of circadian rhythms and photoperiodic flowering by the Arabidopsis GIGANTEA gene. *Science (New York, N. Y.)*, 285(5433), pp.1579–82. Available at: <http://www.ncbi.nlm.nih.gov/pubmed/10477524> [Accessed October 20, 2014].

- Putterill, J. et al., 1995. The CONSTANS gene of Arabidopsis promotes flowering and encodes a protein showing similarities to zinc finger transcription factors. *Cell*, 80(6), pp.847–57. Available at: <http://www.ncbi.nlm.nih.gov/pubmed/7697715> [Accessed October 17, 2014].
- Ratcliffe, O.J. et al., 2001. Regulation of flowering in Arabidopsis by an FLC homologue. *Plant physiology*, 126(1), pp.122–32. Available at: <http://www.pubmedcentral.nih.gov/articlerender.fcgi?artid=102287&tool=pmcentrez&endertype=abstract> [Accessed October 24, 2014].
- Riechmann, J.L. & Meyerowitz, E.M., 1997. MADS domain proteins in plant development. *Biological chemistry*, 378(10), pp.1079–101. Available at: <http://www.ncbi.nlm.nih.gov/pubmed/9372178> [Accessed October 15, 2014].
- Robson, F. et al., 2001. Functional importance of conserved domains in the flowering-time gene CONSTANS demonstrated by analysis of mutant alleles and transgenic plants. *The Plant journal : for cell and molecular biology*, 28(6), pp.619–31. Available at: <http://www.ncbi.nlm.nih.gov/pubmed/11851908> [Accessed October 17, 2014].
- Romani, I. et al., 2012. Versatile roles of Arabidopsis plastid ribosomal proteins in plant growth and development. *Plant Journal*, 72(6), pp.922–934.
- Sanda, S.L. & Amasino, R.M., 1996. Interaction of FLC and late-flowering mutations in Arabidopsis thaliana. *Molecular & general genetics : MGG*, 251(1), pp.69–74. Available at: <http://www.ncbi.nlm.nih.gov/pubmed/8628249> [Accessed October 27, 2014].
- Schomburg, F.M. et al., 2001. FPA, a gene involved in floral induction in Arabidopsis, encodes a protein containing RNA-recognition motifs. *The Plant cell*, 13(6), pp.1427–36. Available at: <http://www.pubmedcentral.nih.gov/articlerender.fcgi?artid=135578&tool=pmcentrez&endertype=abstract> [Accessed October 27, 2014].
- Schwarz-Sommer, Z. et al., 1992. Characterization of the Antirrhinum floral homeotic MADS-box gene *deficiens*: evidence for DNA binding and autoregulation of its persistent expression throughout flower development. *The EMBO journal*, 11(1), pp.251–63. Available at: <http://www.pubmedcentral.nih.gov/articlerender.fcgi?artid=556446&tool=pmcentrez&endertype=abstract> [Accessed October 14, 2014].
- Scortecci, K., Michaels, S.D. & Amasino, R.M., 2003. Genetic interactions between FLM and other flowering-time genes in Arabidopsis thaliana. *Plant molecular biology*, 52(5), pp.915–22. Available at: <http://www.ncbi.nlm.nih.gov/pubmed/14558654> [Accessed October 24, 2014].
- Scortecci, K.C., Michaels, S.D. & Amasino, R.M., 2001. Identification of a MADS-box gene, FLOWERING LOCUS M, that represses flowering. *The Plant journal : for cell and molecular biology*, 26(2), pp.229–36. Available at: <http://www.ncbi.nlm.nih.gov/pubmed/11389763> [Accessed October 24, 2014].

- Searle, I. et al., 2006. The transcription factor FLC confers a flowering response to vernalization by repressing meristem competence and systemic signaling in *Arabidopsis*. *Genes & development*, 20(7), pp.898–912. Available at: <http://www.pubmedcentral.nih.gov/articlerender.fcgi?artid=1472290&tool=pmcentrez&rendertype=abstract> [Accessed October 15, 2014].
- Shahbazian, M.D. & Grunstein, M., 2007. Functions of site-specific histone acetylation and deacetylation. *Annual review of biochemistry*, 76, pp.75–100. Available at: <http://www.ncbi.nlm.nih.gov/pubmed/17362198> [Accessed July 15, 2014].
- Sheldon, C.C. et al., 1999. The FLF MADS box gene: a repressor of flowering in *Arabidopsis* regulated by vernalization and methylation. *The Plant cell*, 11(3), pp.445–58. Available at: <http://www.pubmedcentral.nih.gov/articlerender.fcgi?artid=144185&tool=pmcentrez&rendertype=abstract> [Accessed October 31, 2014].
- Shiraishi, H., Okada, K. & Shimura, Y., 1993. Nucleotide sequences recognized by the AGAMOUS MADS domain of *Arabidopsis thaliana* in vitro. *The Plant journal : for cell and molecular biology*, 4(2), pp.385–98. Available at: <http://www.ncbi.nlm.nih.gov/pubmed/8106084> [Accessed October 15, 2014].
- Simpson, G.G. et al., 2003. FY is an RNA 3' end-processing factor that interacts with FCA to control the *Arabidopsis* floral transition. *Cell*, 113(6), pp.777–87. Available at: <http://www.ncbi.nlm.nih.gov/pubmed/12809608> [Accessed October 27, 2014].
- Simpson, G.G. et al., 2004. RNA processing and *Arabidopsis* flowering time control. *Biochemical Society transactions*, 32(Pt 4), pp.565–6. Available at: <http://www.ncbi.nlm.nih.gov/pubmed/15270676> [Accessed October 27, 2014].
- Simpson, G.G. & Dean, C., 2002. *Arabidopsis*, the Rosetta stone of flowering time? *Science (New York, N.Y.)*, 296(5566), pp.285–9. Available at: <http://www.ncbi.nlm.nih.gov/pubmed/11951029> [Accessed October 7, 2014].
- Smaczniak, C., Immink, R.G.H., et al., 2012. Characterization of MADS-domain transcription factor complexes in *Arabidopsis* flower development. *Proceedings of the National Academy of Sciences of the United States of America*, 109(5), pp.1560–5. Available at: <http://www.pubmedcentral.nih.gov/articlerender.fcgi?artid=3277181&tool=pmcentrez&rendertype=abstract> [Accessed April 8, 2015].
- Smaczniak, C., Li, N., et al., 2012. Proteomics-based identification of low-abundance signaling and regulatory protein complexes in native plant tissues. *Nature protocols*, 7(12), pp.2144–58. Available at: <http://www.ncbi.nlm.nih.gov/pubmed/23196971> [Accessed March 17, 2015].
- Strasser, B. et al., 2009. A complementary role for ELF3 and TFL1 in the regulation of flowering time by ambient temperature. *The Plant journal : for cell and molecular biology*, 58(4), pp.629–40. Available at: <http://www.ncbi.nlm.nih.gov/pubmed/19187043> [Accessed October 27, 2014].

- Suárez-López, P. et al., 2001. CONSTANS mediates between the circadian clock and the control of flowering in *Arabidopsis*. *Nature*, 410(6832), pp.1116–20. Available at: <http://www.ncbi.nlm.nih.gov/pubmed/11323677> [Accessed October 9, 2014].
- Sung, S. & Amasino, R.M., 2004. Vernalization in *Arabidopsis thaliana* is mediated by the PHD finger protein VIN3. *Nature*, 427(6970), pp.159–64. Available at: <http://www.ncbi.nlm.nih.gov/pubmed/14712276> [Accessed October 24, 2014].
- Sung, S., Schmitz, R.J. & Amasino, R.M., 2006. A PHD finger protein involved in both the vernalization and photoperiod pathways in *Arabidopsis*. *Genes & development*, 20(23), pp.3244–8. Available at: <http://www.ncbi.nlm.nih.gov/pubmed/17114575> [Accessed October 24, 2014].
- Tadini, L. et al., 1871. Plastid signaling involves GUN1-dependent formation of complexes containing plastid ribosomal protein S1 and Mg chelatase subunit D.
- Takase, T. et al., 2007. Overexpression of the chimeric gene of the floral regulator CONSTANS and the EAR motif repressor causes late flowering in *Arabidopsis*. *Plant cell reports*, 26(6), pp.815–21. Available at: <http://www.ncbi.nlm.nih.gov/pubmed/17219103> [Accessed October 17, 2014].
- Urbanus, S.L. et al., 2009. In planta localisation patterns of MADS domain proteins during floral development in *Arabidopsis thaliana*. *BMC plant biology*, 9, p.5. Available at: <http://www.pubmedcentral.nih.gov/articlerender.fcgi?artid=2630930&tool=pmcentrez&rendertype=abstract> [Accessed April 16, 2015].
- Valverde, F. et al., 2004. Photoreceptor regulation of CONSTANS protein in photoperiodic flowering. *Science (New York, N.Y.)*, 303(5660), pp.1003–6. Available at: <http://www.ncbi.nlm.nih.gov/pubmed/14963328> [Accessed October 20, 2014].
- Verwoerd, T.C., Dekker, B.M. & Hoekema, A., 1989. A small-scale procedure for the rapid isolation of plant RNAs. *Nucleic acids research*, 17(6), p.2362. Available at: <http://www.pubmedcentral.nih.gov/articlerender.fcgi?artid=317610&tool=pmcentrez&rendertype=abstract> [Accessed November 3, 2014].
- Weigel, D. et al., 1992. LEAFY controls floral meristem identity in *Arabidopsis*. *Cell*, 69(5), pp.843–59. Available at: <http://www.ncbi.nlm.nih.gov/pubmed/1350515> [Accessed October 14, 2014].
- Wigge, P.A. et al., 2005. Integration of spatial and temporal information during floral induction in *Arabidopsis*. *Science (New York, N.Y.)*, 309(5737), pp.1056–9. Available at: <http://www.ncbi.nlm.nih.gov/pubmed/16099980> [Accessed October 15, 2014].
- Willander, M. & Al-Hilli, S., 2009. *Micro and Nano Technologies in Bioanalysis* R. S. Foote & J. W. Lee, eds., Totowa, NJ: Humana Press. Available at: <http://www.ncbi.nlm.nih.gov/pubmed/19488702> [Accessed April 15, 2015].
- Wilson, R.N., Heckman, J.W. & Somerville, C.R., 1992. Gibberellin Is Required for Flowering in *Arabidopsis thaliana* under Short Days. *Plant physiology*, 100(1), pp.403–8. Available at:

<http://www.pubmedcentral.nih.gov/articlerender.fcgi?artid=1075565&tool=pmcentrez&rendertype=abstract> [Accessed October 27, 2014].

Young, K.H., 1998. Yeast two-hybrid: so many interactions, (in) so little time... *Biology of reproduction*, 58(2), pp.302–11. Available at: <http://www.ncbi.nlm.nih.gov/pubmed/9475380> [Accessed April 15, 2015].

Yu, H. et al., 2002. AGAMOUS-LIKE 24, a dosage-dependent mediator of the flowering signals. *Proceedings of the National Academy of Sciences of the United States of America*, 99(25), pp.16336–41. Available at: <http://www.pubmedcentral.nih.gov/articlerender.fcgi?artid=138612&tool=pmcentrez&rendertype=abstract> [Accessed October 16, 2014].

Zaret, K.S. & Carroll, J.S., 2011. Pioneer transcription factors: establishing competence for gene expression. *Genes & development*, 25(21), pp.2227–41. Available at: <http://www.pubmedcentral.nih.gov/articlerender.fcgi?artid=3219227&tool=pmcentrez&rendertype=abstract> [Accessed July 13, 2014].

Zhang, K. et al., 2007. Distinctive core histone post-translational modification patterns in *Arabidopsis thaliana*. *PloS one*, 2(11), p.e1210. Available at: <http://www.pubmedcentral.nih.gov/articlerender.fcgi?artid=2075165&tool=pmcentrez&rendertype=abstract> [Accessed November 2, 2014].

10. PUBLICATIONS

During the three years of my Ph.D., I was also involved in other projects focused on the short-term and long-term regulation of photosynthesis and more in general of chloroplast activities. The long-term regulation studies were mainly focused on nuclear-chloroplast communication, in particular the retrograde signaling, that controls chloroplast biogenesis and chloroplast functionality. These projects were concluded with two publications, respectively on 2012 and 2014, and one manuscript has been recently submitted. Regarding the long-term regulation and retrograde signaling, the first manuscript published on 2012 demonstrated the importance of individual plastid ribosomal proteins (PRPs) in *Arabidopsis thaliana* development (Romani et al. 2012). Plants devoid of specific PRPs showed different phenotypes ranging from embryo lethality to compromised vitality, with the latter being associated with photosynthetic lesions and decreases in the expression of plastid proteins. The *prps* mutants were then used to investigate the molecular details of the plastid gene expression (PGE)-dependent retrograde signaling pathway (Tadini et al., 2015). In particular, we have been able to identify a novel protein complex, named Retrosome, where the PRPS1 protein interacts with GUN1 and enzymes of the tetrapyrrole biosynthesis pathway, and that is responsible to coordinate the assembly of protein complexes within the thylakoid membranes. Concerning the short-term regulation, during the three years of my PhD we have started a project focused on the analysis of mutants affected in the Oxygen Evolving Complex (OEC) protein composition, with the aim to obtain plants with reduced linear electron transport and enhanced alternative electron transport pathways, including Cyclic Electron Transport (CET). In Allahverdiyeva et al., (2013), plants devoid of PsbQ and PsbR subunits have been generated and their phenotypes have been investigated at molecular and physiological level. Currently, we have generated plants with a minimal OEC complex devoid of PsbO1, PsbP2, PsbQ1, PsbQ2 and PsbR subunits where we could show that under limited Linear Electron Transport (LET) plants enhance the CET pathway essential to induce the NPQ and to regulate LET itself (manuscript in preparation).

10.1 List of publications:

1. Romani, I., Tadini, L., Rossi, F., Masiero, S., Pribil, M., Jahns, P., ... Pesaresi, P. (2012). Versatile roles of Arabidopsis plastid ribosomal proteins in plant growth and development. *Plant Journal*, 72(6), 922–934.
2. Allahverdiyeva, Y., Suorsa, M., Rossi, F., Pavesi, A., Kater, M. M., Antonacci, A., ... Pesaresi, P. (2013). Arabidopsis plants lacking PsbQ and PsbR subunits of the oxygen-evolving complex show altered PSII super-complex organization and short-term adaptive mechanisms. *Plant Journal*, 75(4), 671–684.
3. Tadini, L., Pesaresi, P., Kleine, T., Rossi, F., Guljamow, A., Pribil, M., ... Leister, D. (2015) Plastid signaling involves GUN1-dependent formation of complexes containing plastid ribosomal protein S1 and Mg chelatase subunit D, submitted.

Versatile roles of Arabidopsis plastid ribosomal proteins in plant growth and development

Isidora Romani^{1,†,‡}, Luca Tadini^{2,†}, Fabio Rossi¹, Simona Masiero¹, Mathias Pribil², Peter Jahns³, Martin Kater¹, Dario Leister^{2,*} and Paolo Pesaresi¹

¹Dipartimento di Bioscienze, Università degli studi di Milano, I-20133 Milano, Italy,

²Lehrstuhl für Molekularbiologie der Pflanzen (Botanik), Department Biologie I, Ludwig-Maximilians-Universität München, D-82152 Planegg-Martinsried, Germany, and

³Plant Biochemistry, Heinrich-Heine-University Düsseldorf, Universitätsstrasse 1, D-40225 Düsseldorf, Germany

Received 1 June 2012; revised 23 July 2012; accepted 14 August 2012; published online 12 October 2012.

*For correspondence (e-mail leister@lrz.uni-muenchen.de).

†These authors contributed equally to this work.

‡Present Address: Lehrstuhl für Molekularbiologie der Pflanzen (Botanik), Department Biologie I, Ludwig-Maximilians-Universität München, D-82152 Planegg-Martinsried, Germany.

SUMMARY

A lack of individual plastid ribosomal proteins (PRPs) can have diverse phenotypic effects in *Arabidopsis thaliana*, ranging from embryo lethality to compromised vitality, with the latter being associated with photosynthetic lesions and decreases in the expression of plastid proteins. In this study, reverse genetics was employed to study the function of eight PRPs, five of which (PRPS1, -S20, -L27, -L28 and -L35) have not been functionally characterised before. In the case of PRPS17, only leaky alleles or RNA interference lines had been analysed previously. PRPL1 and PRPL4 have been described as essential for embryo development, but their mutant phenotypes are analysed in detail here. We found that PRPS20, -L1, -L4, -L27 and -L35 are required for basal ribosome activity, which becomes crucial at the globular stage and during the transition from the globular to the heart stage of embryogenesis. Thus, lack of any of these PRPs leads to alterations in cell division patterns, and embryo development ceases prior to the heart stage. PRPL28 is essential at the latest stages of embryo–seedling development, during the greening process. PRPS1, -S17 and -L24 appear not to be required for basal ribosome activity and the organism can complete its entire life cycle in their absence. Interestingly, despite the prokaryotic origin of plastids, the significance of individual PRPs for plant development cannot be predicted from the relative phenotypic severity of the corresponding mutants in prokaryotic systems.

Keywords: ribosome, plastid, embryo, development, photosynthesis, *Arabidopsis thaliana*.

INTRODUCTION

Plant growth and development are controlled by the concerted actions of many signalling pathways, which are triggered by developmental and metabolic cues. Plastids play an important role in plant development. On the one hand, they display a variety of interconvertible differentiated forms which are closely associated with different cell types (Waters and Pyke, 2005; Hsu *et al.*, 2010). In addition, many essential metabolic processes take place in plastids (Neuhaus and Emes, 2000; Yamaguchi and Kamiya, 2000; Seo and Koshiba, 2002; DellaPenna and Pogson, 2006) that also serve as sources of signals to the nucleus (plastid or retrograde signalling) which regulate plastid biogenesis and coordinate cell differentiation and tissue architecture (Lopez-Juez and Pyke, 2005; Lopez-Juez, 2007; Pesaresi *et al.*, 2007; Tejos *et al.*, 2010).

Embryogenesis also depends on plastid function and differentiation, and is usually divided into two phases. During embryo morphogenesis, the basic body plan is established, whereas embryo maturation includes cell growth and expansion together with the accumulation of macromolecules that allow the embryo to withstand the desiccation that accompanies seed formation and enable seedling growth after germination (Goldberg *et al.*, 1994). Embryo morphogenesis begins with a single-celled zygote which, in *Arabidopsis thaliana*, undergoes a stereotypical series of cell divisions giving rise in turn to pre-globular, globular, heart and torpedo, linear- and bent-cotyledon stages and mature green embryos. Plastids in embryonic cells of *A. thaliana* remain undifferentiated and non-photosynthetic until the late globular stage, when grana

become visible (Hsu *et al.*, 2010; Tejos *et al.*, 2010). Subsequently, the number of chloroplasts increases at the torpedo stage, before entry into the maturation phase, during which chloroplasts contribute to seed metabolism by producing NADPH and ATP for fatty acid biosynthesis, supplying oxygen to otherwise hypoxic seeds and refixing respiratory CO₂ via the Calvin cycle (Rolletschek *et al.*, 2002; Ruuska *et al.*, 2004).

The precise roles of proplastids and chloroplasts during embryogenesis are not fully understood. Nevertheless, genetic screens in *Arabidopsis* have demonstrated that impairment of plastid functions can perturb embryogenesis and even result in embryo lethality (Hsu *et al.*, 2010; Bryant *et al.*, 2011; Muralla *et al.*, 2011; Lloyd and Meinke, 2012). Indeed, among the 400 *Arabidopsis* genes so far identified as essential for embryo development, about 30% encode chloroplast-localised proteins (see the SeedGenes Project database, <http://www.seedgenes.org/>). Such plastid proteins are frequently involved in metabolite biosynthesis or, like aminoacyl-tRNA synthetases and plastid ribosomal proteins (PRPs), play a role in plastid protein synthesis. Thus, of the nuclear-encoded elements of the plastid ribosome, three components of the small subunit (PRPS5, -S9 and -S13) and eight of the large subunit (PRPL1, -L4, -L6, -L10, -L13, -L18, -L21 and -L31) have been suggested to be essential for embryogenesis (Hsu *et al.*, 2010; Bryant *et al.*, 2011; Muralla *et al.*, 2011; Lloyd and Meinke, 2012; Yin *et al.*, 2012). However, only in five cases (PRPS5, -S13, -L1, -L6 and -L21) has the gene–phenotype relationship been unambiguously confirmed by allelism tests or genetic complementation assays (Bryant *et al.*, 2011; Lloyd and Meinke, 2012; Yin *et al.*, 2012). In the absence of PRPL21, embryo development is arrested at the globular stage (Yin *et al.*, 2012), whereas the loss-of-function phenotypes of PRPS5, -S13, -L1 and -L6 were analysed in the course of large reverse genetics screens without further detailed characterisation. Nevertheless, these four PRPs are annotated in the SeedGenes Project database as essential at the pre-globular or globular stage of embryo development, similar to mutants defective in other aspects of plastid protein synthesis (Berg *et al.*, 2005; Muralla *et al.*, 2011).

Interestingly, not all ribosomal subunits are equally important for embryo development. For instance, *Arabidopsis* lines without PRPL11 show normal germination rates and are characterised by reduced photosynthetic performance, pale green leaf colour and a drastic reduction in growth rate under greenhouse conditions, in association with diminished levels of protein synthesis in plastids (Pesaresi *et al.*, 2001). Similarly, lack of PRPS21 in the *ghs1* (*glucose hypersensitive1*) mutant increases sensitivity to glucose, together with a reduction in plastid protein synthesis, altered photosynthetic performance and impaired chloroplast development (Morita-Yamamuro *et al.*, 2004). The *Arabidopsis ore4-1* mutant was identified on the basis of its

extended leaf longevity, and shown to exhibit reduced expression of the *PRPS17* gene (Woo *et al.*, 2002). In this mutant, as well as in lines lacking PRPL24 (Tiller *et al.*, 2012), growth rate and leaf pigment content are decreased, as a consequence of altered plastid protein synthesis. Although analysis of the five plant-specific ribosomal proteins PSRP2–6 is hampered by the lack of knock-out lines for PSRP2, -4 and -5, preliminary analyses have indicated that none of the five is essential for embryo development (Tiller *et al.*, 2012).

In the present study, a reverse genetic approach targeted to several PRPs associated with different ribosome domains was employed to further dissect the function of plastid ribosomes during embryogenesis and plant development. Interestingly, although plastids originated from free-living prokaryotes, we found little correlation in phenotypic severity between homologous plastid and prokaryotic mutants.

RESULTS

Isolation of mutants for PRPS and PRPL proteins in *Arabidopsis*

Arabidopsis lines carrying T-DNA insertions in single-copy nuclear genes coding for a total of nine protein components of the small (PRPS proteins) and large (PRPL proteins) subunits of the plastid ribosome were identified. Of these, five (PRPS1, -S20, -L27, -L28 and -L35) have not been functionally characterised previously in *A. thaliana*. PRPS17 had been analysed using leaky alleles or RNA interference (RNAi) lines only (Woo *et al.*, 2002; Tiller *et al.*, 2012), while PRPL1 and PRPL4 have been reported to be essential for embryo development (Bryant *et al.*, 2011) but their mutant phenotypes have not been subjected to thorough investigation. Only *prpl24-1* has been characterised in detail before (Tiller *et al.*, 2012), and is used here as a control.

One insertion mutant allele only was found for each of three PRPS genes (*PRPS1/At5g30510*, *PRPS17/At1g79850* and *PRPS20/At3g15190*) and four PRPL genes (*PRPL24/At5g54600*, *PRPL27/At5g40950*, *PRPL28/At2g33450* and *PRPL35/At2g24090*) (Figure 1). Two mutant alleles each were obtained for *PRPL1/At3g63490* and *PRPL4/At1g07320*.

Interestingly, two splicing variants have been reported for *PRPL1* and *PRPL24*, and up to four different transcripts have been predicted for *PRPL4* (see <http://www.arabidopsis.org/>). Real-time PCR analyses indicate that both *PRPL1* splicing variants are present in leaves and developing siliques, with *PRPL1.1* being more abundant than *PRPL1.2* (Figure S1 in Supporting Information). Conversely, only one transcript variant was detectable for *PRPL4* (*PRPL4.1*) and *PRPL24* (*PRPL24.1*) in both leaves and siliques.

Mutations in PRPS1, PRPS17 and PRPL24 affect growth and photosynthesis

Only in the case of *PRPS1* and *PRPS17*, and the *prpl24-1* allele used as a control for lines with a reduced plastid

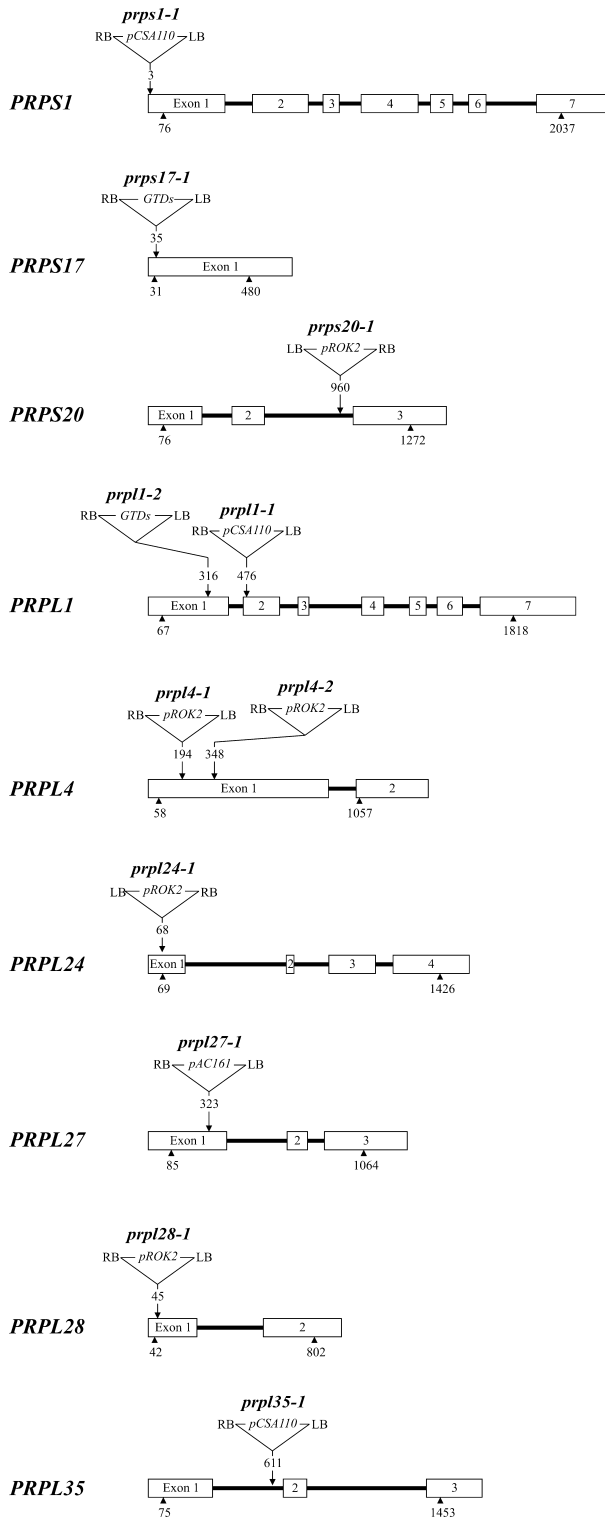


Figure 1. T-DNA tagging of *PRPS* and *PRPL* genes. Exons are indicated as numbered white boxes, introns as black lines. Arrowheads indicate the positions of translation initiation and stop codons. Sites, designations and orientations of T-DNA insertions are indicated (RB, right border; LB, left border). For *PRPL1*, *PRPL4* and *PRPL24*, the intron–exon structures of the most abundant transcript variants are indicated. The T-DNA insertions are not drawn to scale.

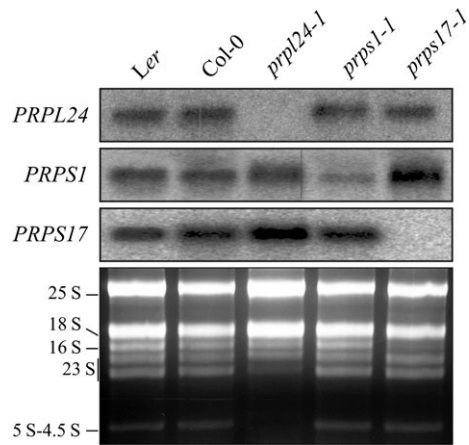


Figure 2. Northern analyses of wild type (Col-0 and *Ler*) and mutant (*prpl24-1*, *prps1-1* and *prps17-1*) plants. Total leaf RNA was fractionated on a denaturing agarose gel, transferred to a nylon membrane, and hybridised with the corresponding *PRP* cDNA probes, reported on the left side of the panel. An agarose gel stained with ethidium bromide and showing the different rRNA molecules (from 25S to 4.5S; Zybailov *et al.*, 2009) was used as a loading control.

translation efficiency (Tiller *et al.*, 2012), could homozygous mutants be identified by PCR-based genotyping. The T-DNA insertions in the *PRPS17* and *PRPL24* loci completely suppressed the accumulation of the corresponding transcripts, whereas residual amounts [about 8% of the level in Columbia-0 (Col-0)] of *PRPS1* transcripts were detected by Northern analysis in *prps1-1* homozygotes (Figure 2). An agarose gel stained with ethidium bromide and showing the different rRNA molecules was used as a loading control, allowing us to discern any effects of loss of *PRPL24* or *PRPS17* on rRNA accumulation. Indeed, specific reductions in levels of 23S rRNA and 5S-4.5S rRNA were found in *prpl24-1* leaves, whereas the amount of 16S rRNA was decreased in *prps17-1* leaves (Figure 2).

All three *prp* homozygotes were characterised by pale green cotyledons and leaves, and reduction in overall size (Figure 3a), and the mutant phenotype segregated as a single-locus recessive trait. Quantification of growth rates by non-invasive image analyses under optimal growth-chamber conditions showed that the size of 4-week-old *prpl24-1* and *prps1-1* mutant plants was reduced by about 80% and 60%, respectively, relative to the corresponding wild type (WT) background (Col-0) (Figure 3b). For *prps17-1*, a reduction of approximately 55% in size in comparison to the WT [*Landsberg erecta* (*Ler*)] was measured.

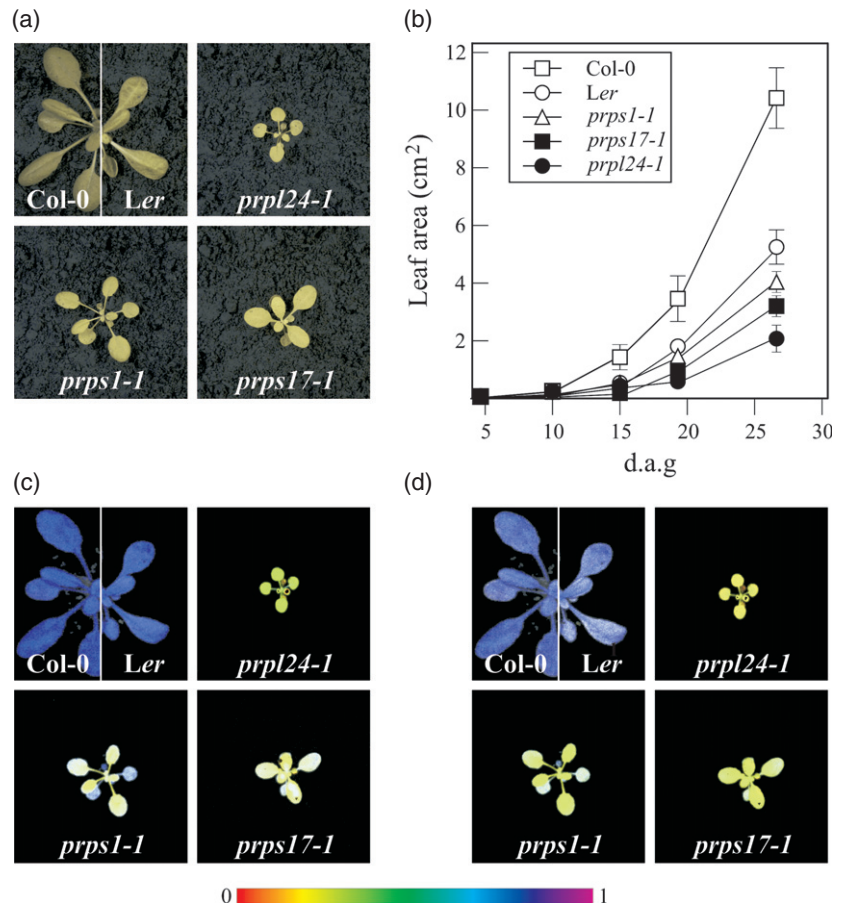
Photosynthetic performance was characterised by monitoring chlorophyll (Chl) *a* fluorescence. The data showed a clear decrease in maximum quantum yield of photosystem II (PSII) (F_V/F_M , ratio of variable to maximum fluorescence) in *prpl24-1* and a somewhat less pronounced effect in *prps1-1* and *prps17-1* plants (Col-0, 0.83 ± 0.01 ; *Ler*, 0.83 ± 0.01 ; *prpl24-1*, 0.47 ± 0.03 ; *prps1-1*, 0.69 ± 0.01 ; *prps17-1*, 0.66 ± 0.01 ; see also Figure 3c). A similar picture emerged when the

Figure 3. Phenotypes of mutant (*prpl24-1*, *prps1-1* and *prps17-1*) and wild-type (Col-0 and *Ler*) plants.

(a) The different genotypes were grown for 4 weeks in a growth chamber.

(b) The growth kinetics of the different genotypes was measured from 4 to 28 days after germination (d.a.g.). Each point is based on the determination of mean leaf area from at least 10 individuals ($n \geq 10$). Bars indicate standard deviations.

(c,d) The photosynthetic parameter F_v/F_M (c) and Φ_{II} (d) of the different genotypes were measured as described in the Experimental Procedures. Signal intensities for F_v/F_M and Φ_{II} are indicated according to the colour scale at the bottom of the figure.



effective quantum yield of PSII (Φ_{II}) was taken into account. In this case too, *prpl24-1* plants were markedly impaired with respect to Col-0, whereas differences between *prps1-1* and *prps17-1* and the corresponding WT plants were less marked (Col-0, 0.77 ± 0.01 ; *Ler*, 0.77 ± 0.01 ; *prpl24-1*, 0.43 ± 0.02 ; *prps1-1*, 0.63 ± 0.01 ; *prps17-1*, 0.60 ± 0.02 ; see also Figure 3d). To quantify the alteration in leaf coloration in *prpl24-1*, *prps1-1* and *prps17-1* plants, leaf pigments were analysed by HPLC. As expected, mutant plants contained only 58% (*prps1-1*), 50% (*prps17-1*) and 68% (*prpl24-1*) of WT levels of total chlorophyll (Chl *a* + *b*) (Table 1). The Chl *a/b* ratio was also clearly decreased in *prpl24-1*, and to a lesser extent in *prps1-1* (Table 1), indicating either a higher PSII/PSI ratio or, rather more likely in light of the nature of the mutations, an increase in the size of the Chl *b*-binding peripheral antenna (which is made of nuclear-encoded subunits) relative to the Chl *a*-binding reaction centres, synthesis of which requires plastid ribosomes. Interestingly, the Chl *a/b* ratio was not markedly altered in *prps17-1* with respect to *Ler* plants, suggesting that in this case the reduction in amounts of plastid-encoded reaction centres might be accompanied by a similar decrease in antenna complexes.

All mutant phenotypes could be rescued by *Agrobacterium tumefaciens*-mediated transformation of homozygous

mutants with either the appropriate coding sequence (*PRPS1* and *PRPS17*) fused to the 35S promoter of cauliflower mosaic virus (35S-CaMV), or the genomic sequence including a 1-kbp fragment of the promoter (*PRPL24*), corroborating a direct correspondence between genotype and phenotype (see Table S1). Thus, when *PRPS1* and *PRPL24* were introduced into the corresponding mutants, a complete rescue of the mutant phenotype was observed, whereas a marginal reduction of Φ_{II} values and leaf pigment content with respect to WT remained after complementation of *prps17-1* lines with the WT *PRPS17* gene (Table S1). Taken together, the data indicate that *PRPS1*, *PRPS17* and *PRPL24* are required for optimal plastid performance in terms of photosynthesis and growth, but their loss is compatible with plant viability.

Plastid protein synthesis and thylakoid composition are perturbed in *prps1-1*, *prps17-1* and *prpl24-1* plants

To determine whether the defect in photosynthetic performance described above is associated with alterations in the protein composition of thylakoids, two-dimensional blue native (2D BN)/SDS-PAGE and one-dimensional (1D) SDS-PAGE were performed on thylakoids and total protein extracts, respectively (Figure 4). Quantification of banding

Table 1 Levels of leaf pigments in light-adapted mutant (*prpl24-1*, *prps1-1*, *prps17-1*) and wild-type (Col-0 and *Ler*) plants at the six-leaf rosette stage. Leaf pigments were determined by HPLC and are reported in pmol mg⁻¹ leaf fresh weight. Mean values ± SD are shown

	Leaf pigment content (pmol mg ⁻¹ leaf fresh weigh)							
	Nx	Lut	Chl <i>b</i>	Chl <i>a</i>	β-Car	VAZ	Chl <i>a</i> + <i>b</i>	Chl <i>a/b</i>
<i>Ler</i>	36 ± 3	117 ± 13	249 ± 22	1007 ± 95	100 ± 10	51 ± 4	1251 ± 98	4.05 ± 0.03
Col-0	39 ± 4	124 ± 11	246 ± 23	952 ± 76	985 ± 8	43 ± 4	1198 ± 98	3.87 ± 0.03
<i>prpl24-1</i>	39 ± 4	1075 ± 11	191 ± 20	625 ± 61	32 ± 2	53 ± 5	815 ± 79	3.27 ± 0.11
<i>prps1-1</i>	30 ± 2	87 ± 9	146 ± 10	549 ± 53	37 ± 3	44 ± 4	694 ± 63	3.76 ± 0.09
<i>prps17-1</i>	26 ± 2	77 ± 6	123 ± 11	497 ± 39	34 ± 3	50 ± 1	619 ± 51	4.04 ± 0.06

Nx, neoxanthin; Lut, lutein; Chl *b*, chlorophyll *b*; Chl *a*, chlorophyll *a*; β-Car, β-carotene; VAZ, violaxanthin + antheraxanthin + zeaxanthin.

patterns on Coomassie-stained 2D BN/SDS polyacrylamide (PA) gels revealed marked reductions in levels of the plastid-encoded PSII core subunits PsbA, PsbB, PsbC and PsbD in *prpl24-1*, *prps1-1* and *prps17-1* thylakoids, with amounts corresponding to 25–27, 51–59 and 40–44%, respectively, of those seen in the WT (Figure 4a, Table 2). Accumulation of PsbB was also quantified by 1D SDS-PAGE and immunoblot analysis, and values comparable to those from stained 2D SDS-PA gels were obtained (Figure 4b, Table 2). Other plastid-encoded subunits of thylakoid multiprotein complexes, including the reaction centre of PSI (PsaA/B), the β-subunit of ATPase (ATPase β), cytochrome *b₆* (PetB) and the large subunit of Rubisco (RbcL) also showed marked declines in level in mutant plants, particularly in *prpl24-1* homozygotes. The reduced accumulation of the PSI reaction centre was accompanied by a decrease in amounts of nuclear-encoded PSI subunits, such as PsaD, PsaF and PsaO, indicating that the entire PSI complex is destabilised as a result of the mutations (Figure 4b, Table 2). Other nuclear-encoded thylakoid proteins, including the PSI antenna protein Lhca2, and Lhcb4 and Lhcb6 (the minor antenna of PSII), behaved like PSI and PSII, while the nuclear-encoded components of LHCII (Lhcb1-3) were least affected (Figure 4a, Table 2), most probably because they can accumulate independently of PSI and PSII (Caffarri *et al.*, 2005).

To study whether the putative defects in plastid protein synthesis which, in the case of *prps17-1* and *prpl24-1*, are already suggested by the changes in rRNA accumulation (see Figure 2), might be mitigated by adaptive mechanisms at the transcriptional and/or post-transcriptional level, the effects of *prps1-1*, *prps17-1* and *prpl24-1* mutations on accumulation and processing of plastid transcripts were studied by Northern analysis (Figure 5a). The steady-state level of the *psbA* transcript was increased by a factor of almost two in mutant leaves relative to WT plants. A similar increase was also observed for *rbcL* mRNA and for transcripts of the *psaA-psaB* and *atpB-atpE* operons, monitored by employing *psaB*- and *atpB*-specific probes. These results exclude the possibility that the reduced accumulation of plastid-encoded proteins (see Figure 4) can be ascribed to

reduced transcription of plastid genes. To investigate this issue further, plastid protein synthesis was measured by monitoring the rate of incorporation of [³⁵S]methionine into plastid proteins in young leaves of WT and mutant (*prps1-1*, *prps17-1* and *prpl24-1*) plants in the presence of light and inhibitors of cytoplasmic protein synthesis for 5, 15 and 30 min. Subsequently, total leaf proteins were extracted and fractionated by SDS-PAGE (Figure 5b). In three independent experiments, the amount of PsbA and RbcL labelled in *prpl24-1* plants was decreased on average to 20% of WT levels after 30 min of [³⁵S]methionine incubation. More moderate reductions in the levels of labelled PsbA and RbcL proteins (to about 40 and 30% of WT) were observed in *prps1-1* and *prps17-1* leaves, respectively.

Taken together, our results imply that the phenotypic behaviour of *prpl24-1*, *prps1-1* and *prps17-1* mutants with respect to the reduction in growth rate and photosynthesis is caused by a decrease in the accumulation of photosynthetic proteins. This can be attributed to defects in ribosome function, as indicated by reductions in rRNA levels and translation of plastid mRNAs.

PRPS20, -L1, -L4, -L27, -L28 and -L35 are required for normal embryonic development

Unlike the three ribosomal mutations described above, no homozygous mutant plants could be identified in the case of *prps20-1*, *prpl4-1*, *prpl27-1*, *prpl35-1* and *prpl1-1*, the last of which was used as a control for an embryo-lethal phenotype (Bryant *et al.*, 2011). Homozygous WT (*PRP/PRP*) and heterozygous mutant (*PRP/prp*) plants segregated in a 1:2 manner, indicating that the corresponding gene products are essential during the early stages of embryo and/or seed development.

To further characterise the developmental phenotype of these mutant lines, silique length, seed-setting numbers and the ratio of normal to abnormal seeds in siliques were quantified in homozygous WT (*PRP/PRP*) and heterozygous mutant plants (*PRP/prp*). Whereas seed set and silique morphology were very similar in all *PRP/PRP* and *PRP/prp* plants (Table S2), albino seeds were readily distinguishable

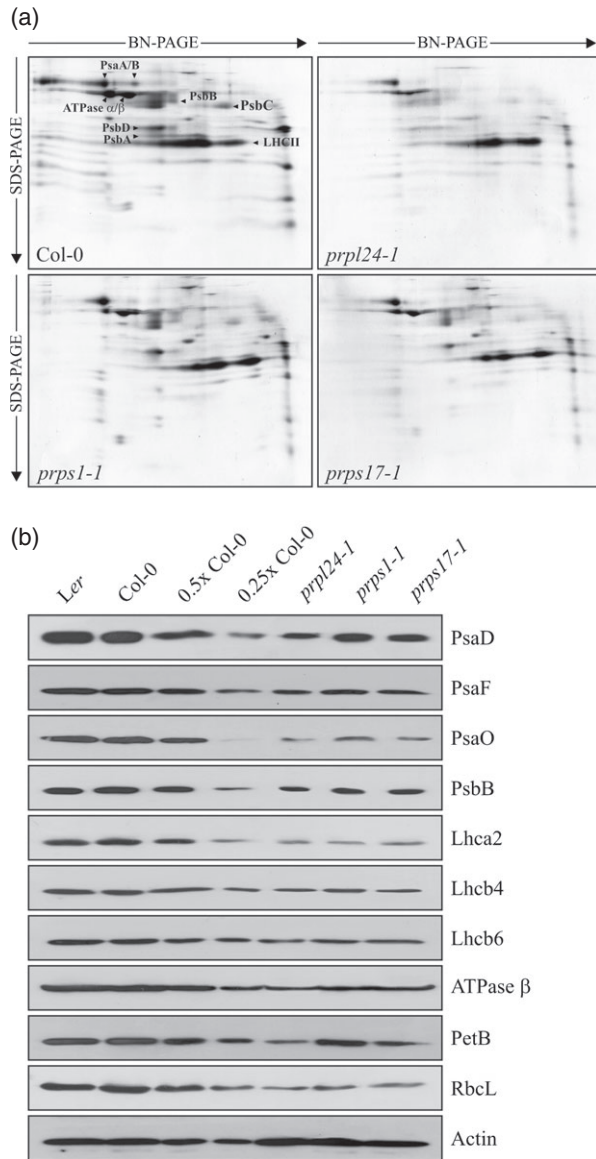


Figure 4. Two-dimensional blue native (BN) SDS-PAGE separation and one-dimensional SDS-PAGE analysis of thylakoid proteins from wild-type (Col-0 and *Ler*) and mutant (*prps1-1*, *prps17-1* and *prpl24-1*) leaves. (a) Thylakoid protein complexes were fractionated by BN-PAGE in the first dimension and then by 15% SDS-PAGE, followed by staining with colloidal Coomassie Blue (G 250). The identity of relevant proteins is indicated by arrows. Note that *Ler* behaved like Col-0. (b) Total leaf proteins were fractionated by SDS-PAGE, and blots were probed with antibodies raised against individual subunits of photosystem I (PsaD, PsaF, PsaO), photosystem II (PsbB), LHCI (Lhca2), the minor antenna of photosystem II (Lhcb4, Lhcb6), the chloroplast ATP synthase (β -subunit), the Cyt *b₆/f* complex (PetB) and the large subunit of Rubisco (RbcL). Decreasing levels of wild-type proteins were loaded in the lanes marked 0.5x Col-0 and 0.25x Col-0. Immunodecoration with an actin-specific antibody was employed to control for equal loading.

at 6–7 days after fertilisation (DAF) in all siliques of *PRP/prp* plants bearing each of the five different mutant alleles (Figure 6a, left panel). In mature siliques, the albino seeds eventually turned into shrunken, dark brown structures that

were unable to germinate on either MS medium or soil (Figure 6a, right panel). In all mutant plants analysed, the mean percentage of albino/aborted seeds ranged between 23.7 and 26.9%, whereas only 1.7 and 2.1% aborted seeds were observed in WT *Ler* and Col-0 sister plants, respectively (Table S2). These values are consistent with a 3:1 (normal:aborted seeds) segregation ratio, indicating that the abnormal seed phenotype is a recessive trait controlled by a single locus. To confirm that the abnormal seed phenotypes were indeed caused by mutation of the *PRP* genes, an additional mutant allele (in the case of *PRPL1* and *PRPL4*) was phenotypically characterised or the respective WT *PRP* gene was introduced into heterozygous mutant plants to obtain in the next generation homozygous mutants containing the transgenic *PRP* gene. As expected, the *prpl1-2* and *prpl4-2* alleles behaved phenotypically like the *prpl1-1* and *prpl4-1* alleles, respectively (Table S2). Moreover, viable plants with normal seeds and WT-like photosynthetic performance and leaf pigment content were obtained by introducing the WT *PRP* genes into the homozygous mutant background, demonstrating that the seed phenotypes are indeed caused by mutation of the *PRP* genes (Tables S1 and S2).

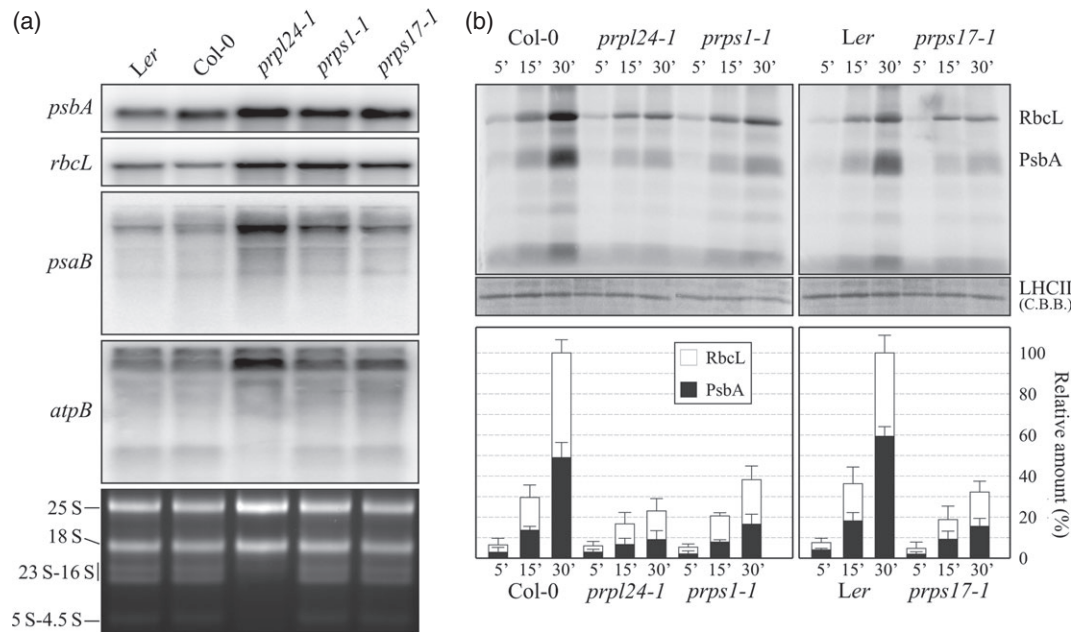
To determine whether embryo development was affected in the *prps20*, *prpl1*, *prpl4*, *prpl27* and *prpl35* mutants, optical sections of cleared seed whole-mounts at different developmental stages were analysed by microscopy (Figure 6b). At 3–4 DAF, WT embryos had reached the heart stage (Figure 6b, top panel), whereas about 25% of the seeds from *PRP/prp* plants were retarded in their development and the embryos arrested at the globular stage (Figure 6b, bottom panel, left picture of each genotype). In the WT, heart-stage embryos undergo an ordered series of cell divisions that allow them to traverse through the torpedo and linear cotyledon stages to the fully mature embryo stage (Figure 6b, top panel). In contrast, although they retained the capacity for cell division, mutant embryos at 4–5 DAF exhibited a disordered globular-like structure (Figure 6b, bottom panel, right picture of each mutant), and began to disintegrate at about 15 DAF. To visualise the cellular organisation of mutant and WT embryos, representative siliques of heterozygous *PRPS20/prps20-1* plants at 3–4 DAF were subjected to a modified pseudo-Schiff propidium iodide (mPS-PI) staining technique (Figure 6c; see Experimental procedures). The mutant embryos showed a disordered globular-like organisation marked by abnormal cell division patterns. In particular, mutant globular embryos showed additional transverse cell division planes (Figure 6c, arrowheads) while lacking the usual two longitudinal division planes (Figure 6c, inset). Therefore, it appears that while the epidermis, the first element of embryo radial pattern (Jenik *et al.*, 2007) which becomes visible in the 16-cell embryo (early globular), can differentiate in mutant embryos, provascular cells fail to differentiate. Similar

Table 2 Quantification of thylakoid proteins in light-adapted mutant plants (*prps1-1*, *prps17-1* and *prpl24-1*). Wild-type levels are set to 100%. Average values were calculated from three independent 2D polyacrylamide gels and protein gel blots (see Figure 4)

Protein	<i>prpl24-1</i>		<i>prps1-1</i>		<i>prps17-1</i>	
	2D PAGE	Immunoblot	2D PAGE	Immunoblot	2D PAGE	Immunoblot
PsaA/B ^a	0.31 ± 0.03	nd	0.59 ± 0.05	nd	0.46 ± 0.04	nd
PsaD	nd	0.32 ± 0.03	nd	0.44 ± 0.04	nd	0.39 ± 0.04
PsaF	nd	0.34 ± 0.03	nd	0.52 ± 0.04	nd	0.45 ± 0.03
PsaO	nd	0.28 ± 0.02	nd	0.37 ± 0.03	nd	0.32 ± 0.04
PsbA ^a	0.27 ± 0.02	nd	0.51 ± 0.03	nd	0.42 ± 0.02	nd
PsbB ^a	0.25 ± 0.02	0.34 ± 0.03	0.54 ± 0.04	0.45 ± 0.04	0.41 ± 0.04	0.48 ± 0.04
PsbC ^a	0.25 ± 0.02	nd	0.55 ± 0.02	nd	0.40 ± 0.03	nd
PsbD ^a	0.27 ± 0.02	nd	0.59 ± 0.04	nd	0.44 ± 0.04	nd
Lhca2	nd	0.31 ± 0.03	nd	0.27 ± 0.02	nd	0.36 ± 0.02
Lhcb1/b2/b3	0.67 ± 0.04	nd	0.74 ± 0.05	nd	0.53 ± 0.04	nd
Lhcb4	nd	0.32 ± 0.03	nd	0.45 ± 0.04	nd	0.38 ± 0.03
Lhcb6	nd	0.39 ± 0.03	nb	0.48 ± 0.04	nd	0.45 ± 0.04
ATPase β ^a	0.29 ± 0.03	0.26 ± 0.03	0.51 ± 0.05	0.46 ± 0.04	0.42 ± 0.03	0.45 ± 0.04
PetB ^a	nd	0.18 ± 0.02	nd	0.79 ± 0.05	nd	0.39 ± 0.03
RbcL ^a	nd	0.19 ± 0.02	nd	0.27 ± 0.03	nd	0.21 ± 0.02

nd, not determined.

^aProteins encoded by plastid genes.

**Figure 5.** Translation efficiency of chloroplast-encoded proteins in wild-type (WT; Col-0 and *Ler*) and mutant (*prps1-1*, *prps17-1* and *prpl24-1*) leaves.

(a) Analysis of transcripts from WT and mutant leaves. Total leaf RNA was fractionated by denaturing agarose gel electrophoresis, blotted onto nylon membrane, and hybridised with the probes reported on the left side of the panel. A replicate agarose gel, stained with ethidium bromide and showing the different rRNA molecules, was used as a loading control.

(b) Incorporation of [³⁵S]methionine into total leaf proteins isolated from six-leaf-rosette plants at low light (20 μmol photons m⁻² sec⁻¹). After pulse labelling with [³⁵S]methionine for 5, 15 and 30 min in the presence of cycloheximide, total leaf proteins were isolated, fractionated by SDS-PAGE and detected by autoradiography. As loading control, a portion of the Coomassie Brilliant Blue (C.B.B.)-stained SDS-PAGE, corresponding to the LHCII migration region, is shown. Levels of [³⁵S]methionine incorporation into RbcL and PsbA proteins were quantified and reported in the bar-plot. Values were normalised to the maximal signal intensities obtained in WT leaves (Col-0 and *Ler*) after 30-min labelling.

differences were also observed in the other mutant genotypes, indicating that, in the absence of PRPS20, -L1, -L4, -L27 or -L35, embryo development is perturbed due to a

change in cell division patterns, which prevents embryos from progressing through the globular to the heart stage and beyond.

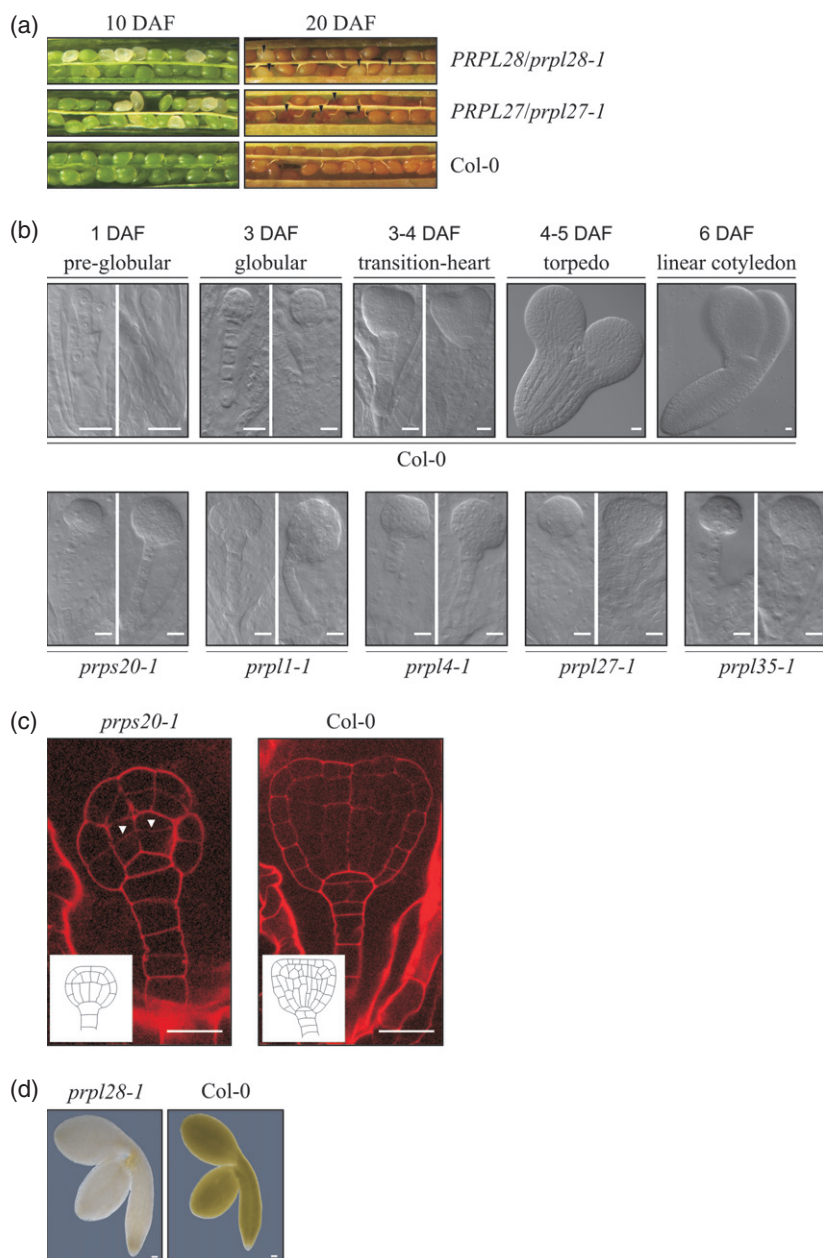
Figure 6. Effects of loss of plastid ribosomal proteins (PRPs) on early plant development.

(a) Morphological characterisation of seed development in siliques of wild-type (WT; Col-0) and heterozygous *PRPL27/prpl27-1* and *PRPL28/prpl28-1* plants. In WT siliques at 10 days after fertilisation (DAF), all developing seeds are green, whereas in *PRPL27/prpl27-1* and *PRPL28/prpl28-1* siliques around 25% of seeds are albino. A very similar phenotype was observed in heterozygous *PRPS20/prps20-1*, *PRPL1/prpl1-1*, *PRPL4/prpl4-1* and *PRPL35/prpl35-1* plants. In mature WT siliques (at 20 DAF) all seeds are round and yellowish, whereas 25% of seeds are shrunken and aborted (in *PRPL27/prpl27-1*) or much paler (in *PRPL28/prpl28-1*). Note that *PRPS20/prps20-1*, *PRPL1/prpl1-1*, *PRPL4/prpl4-1* and *PRPL35/prpl35-1* siliques behaved like *PRPL27/prpl27-1* siliques.

(b) Characterisation of different stages of embryo development. Top panel, cleared whole mount of WT (Col-0) seeds containing embryos at different developmental stages including pre-globular (1 DAF), globular (3 DAF), transition globular to heart (3–4 DAF), torpedo (4–5 DAF) and linear cotyledons (6 DAF). Bottom panel, 25% of embryos from *PRPS20/prps20-1*, *PRPL1/prpl1-1*, *PRPL4/prpl4-1*, *PRPL27/prpl27-1* and *PRPL35/prpl35-1* siliques stopped developing, although they retained the capacity for cell division, and remained arrested at a disordered globular stage. For each genotype, the left image was taken at 3–4 DAF and the right picture at 4–5 DAF. Bars = 20 μ m.

(c) Analysis of cell division pattern of mutant embryos from WT (Col-0) and heterozygous *PRPS20/prps20-1* plants. Siliques were subjected to a modified pseudo-Schiff propidium iodide (mPS-PI) staining technique aimed at visualising the cellular organisation of embryos. The transverse cell division plane in the mutant is indicated by arrowheads. Insets show the cell division planes typical of WT embryos. Note that the cell division pattern of *prpl1-1*, *prpl4-1*, *prpl27-1* and *prpl35-1* mutant embryos was very similar to the one of *prps20-1* mutant embryos. Bars = 20 μ m.

(d) Images of isolated fully mature embryos (bent cotyledon stage) from WT (Col-0) and *prpl28-1* seeds. Bars = 20 μ m.



Mutation of the gene coding for PRPL28 results in a phenotype which differs from that described above. Although siliques of heterozygous *PRPL28/prpl28-1* plants were also characterised by the presence of albino seeds at 6–7 DAF (Figure 6a, left panel), these seeds retained their very pale colour even in mature siliques (Figure 6a, right panel) and accounted for about one-quarter of all seeds, which is typical of a monogenic recessive trait (Table S2). The pale seeds contained fully mature albino embryos (Figure 6d) that were able to germinate on both soil and MS medium, but they did not survive past the cotyledon stage when grown under photoautotrophic conditions (Figure S2). This observation, together with the complete restoration of the WT

phenotype by introduction of the WT *PRPL28* gene into the *prpl28-1* background (see Table S1), implies that PRPL28 is essential for the latest stages of embryo–seedling development, during the greening process.

DISCUSSION

Decreases in plastid translation rates can affect photosynthesis

Certain ribosomal proteins are not essential for ribosomal function, but their removal reduces the translational capacity and decreases the photosynthetic performance of plastids. Thus, Arabidopsis mutants that lack PRPS21, -L11

or -L24, or have reduced amounts of PRPS17, are viable but display a marked drop in rates of photosynthesis and growth (Pesaresi *et al.*, 2001; Woo *et al.*, 2002; Morita-Yamamuro *et al.*, 2004; Tiller *et al.*, 2012). In this study, characterisation of Arabidopsis lines lacking PRPS1 or -S17, together with the *prpl24-1* mutant as a control, confirmed that these loss-of-function mutants are able to complete their entire life cycle (Figure 7), although all three mutant genotypes showed reductions in growth rate, leaf pigment content and photosynthetic performance. The altered photosynthetic performance is attributable to the marked decrease in chloroplast translational activity in these mutants, as shown by reduced incorporation of [³⁵S]methionine into PsbA and RbcL. Are PRPS17 and PRPL24 dispensable for the basal activity of plastid ribosomes (for PRPS1 this cannot be unequivocally concluded because residual expression of *PRPS1* remains in *prps1-1* homozygotes) or are there alternative explanations available for the viability of these *prp* mutants? Theoretically, dual targeting of their nuclear-encoded mitochondrial counterparts (At1g49400 and At3g18880 in the case of PRPS17; At5g23535 in the case of PRPL24) to mitochondria and chloroplasts could account for the viability of *prps17* and *prpl24* mutants. However, the Ambiguous Targeting Predictor (<http://www.cosmoss.org/bm/ATP>; Mitschke *et al.*, 2009), a machine-learning implementation that predicts dual-targeted organelle proteins, attributed very low scores to At1g49400 (0.53), At3g18880 (0.53) and At5g23535 (0.44), whereas PRORS1, an experimentally verified dual-located protein (Pesaresi *et al.*, 2006), was unambiguously predicted into both plastids and mitochondria (0.95). Moreover, proteomic studies failed to detect At1g49400, At3g18880 and At5g23535 within chloroplasts [see also 'The Subcellular Location of Proteins in Arabidopsis Database (SUBA; <http://suba.plantenergy.uwa.edu.au/flatfile.php?>) and the Plant Proteome Database (<http://ppdb.tc.cornell.edu/dbsearch/gene.aspx?>)]. Therefore, it is unlikely that dual targeting of

nuclear-encoded mitochondrial ribosomal proteins contributes to the phenotypes observed for the *prps17* and *prpl24* mutants.

Plastid translation is required for embryo development in Arabidopsis

Plastid differentiation during embryogenesis, which generates specific patterns of chloroplast-containing cells in specific cell layers at specific stages of embryogenesis, must be tightly regulated (Tejos *et al.*, 2010), but how this is achieved at the molecular level remains unclear. Functional plastids are certainly essential for embryogenesis in Arabidopsis. Thus, based on the work of Bryant *et al.* (2011) and Yin *et al.* (2012), and the data in the present study, it can be concluded that at least nine nuclear-encoded PRPs (PRPS5, -S13, -S20, -L1, -L4, -L6, -L21, -L27 and -L35) are essential for embryo development in Arabidopsis. Our analysis of lines lacking PRPS20, -L1, -L4, -L27 or -L35 indicate that these PRPs become indispensable at the globular stage of embryo development (see Figures 6 and 7), corroborating previous analyses of lines lacking PRPL21 (Yin *et al.*, 2012). Moreover, such mutant embryos are characterised by perturbations in cell division patterns, leading to the formation of highly disordered globular-like structures. The resulting failure to differentiate specific cell layers prevents the progression of embryo development beyond this stage. This defect in the patterning of cell division could be due to the lack of specific molecules, such as hormones produced by plastids (Peltier *et al.*, 2006; Santner and Estelle, 2009; Santner *et al.*, 2009) that either directly influence cell division or are involved in the coordination of nuclear and plastid gene expression.

Which plastid process is essential for embryogenesis in Arabidopsis?

The possibility that the embryo lethality observed in some *prp* mutants is caused by interference with the photosyn-

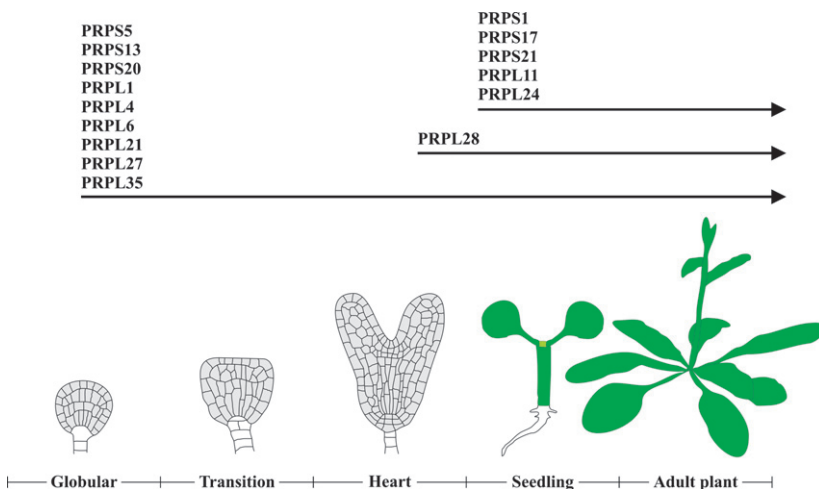


Figure 7. Schematic representation of functions of plastid ribosomal proteins (PRPs). The proteins PRPS5, -S13, -S20, -L1, -L4, -L6, -L21, -L27 and -L35 allow the transition from the globular to the heart stage. PRPL28 is essential for the greening of embryos and seedlings, whereas PRPS1, -S17, -S21, -L11 and -L24 play a major role in adult plants, being pivotal for optimal ribosome activity. Note that the role of the following subunits has been reported in previous publications: PRPS5, -S13, -L1, -L6 (Bryant *et al.*, 2011; Lloyd and Meinke, 2012); PRPL21 (Yin *et al.*, 2012); PRPS21 (Morita-Yamamuro *et al.*, 2004); PRPL11 (Pesaresi *et al.*, 2001) and PRPL24 (Tiller *et al.*, 2012).

thetic process can be excluded, because mutants devoid of components essential for thylakoid electron flow can still reach the seedling stage (see, for instance, Maiwald *et al.*, 2003; Weigel *et al.*, 2003; Ilnatowicz *et al.*, 2004). Intraspecific variation with respect to the sensitivity of plant embryogenesis to the loss of plastid translation has shed further light on the role of plastids in embryogenesis. In most cases, mutations that interfere with chloroplast translation efficiency in barley, maize or *Brassica napus* generally do not disrupt embryogenesis, but allow the formation of albino seedlings instead (Hess *et al.*, 1994; Zubko and Day, 1998). For instance, lack of the plastid-encoded PRPS12 results in embryo lethality in Arabidopsis, whereas the corresponding maize mutant is able to germinate and produce albino seedlings (Ostheimer *et al.*, 2003; Asakura and Barkan, 2006). Several lines of evidence suggest that a relative lack of the plastid-encoded accD-subunit of the multimeric acetyl-CoA carboxylase required for fatty acid biosynthesis might be one of the causes responsible for the lethality of Arabidopsis embryos defective in plastid translation (Bryant *et al.*, 2011). Indeed, grass species and *B. napus* contain a plastid-located monomeric acetyl-CoA carboxylase that, differently from Arabidopsis, is encoded in the nucleus and translated in the cytosol (Schulte *et al.*, 1997; Chalupska *et al.*, 2008). Therefore fatty acid biosynthesis (and embryogenesis) can continue even when plastid protein synthesis is affected in these species. The essential nature of fatty acid biosynthesis in embryo development is also known from the disruption of a nuclear-encoded subunit of the plastid multimeric acetyl-CoA carboxylase (At5g16390; Li *et al.*, 2011), as well as from the arrest of fatty acid biosynthesis by preventing the accumulation of the S-malonyltransferase enzyme (At2g30200; Bryant *et al.*, 2011). This, together with the observed block in embryogenesis at the globular stage in *prp* mutants (this study and Yin *et al.*, 2012), suggests that at the globular stage, when pro-plastids start to differentiate into chloroplasts (Mansfield and Briarty, 1991), fatty acid biosynthesis might become essential for embryo development (Kobayashi *et al.*, 2007). Certainly, disruption of other essential plastid functions can also lead to the arrest of embryogenesis. For instance, loss of function of key players in the TOC-TIC machinery required for plastid protein import, such as TOC75, TIC20, TIC110, results in embryo lethality (Jarvis, 2008; Inaba and Ito-Inaba, 2010; Kasmati *et al.*, 2011). Likewise, mutation in the gene encoding the key enzyme of galactolipid biosynthesis, MGD1, compromises proper embryogenesis. Mutation in other essential proteins, such as chaperons, proteases and aminoacyl-tRNA synthetases, in plastids also compromise embryogenesis (Inaba and Ito-Inaba, 2010). However, with the exception of the ClpP protease (Shikanai *et al.*, 2001), these genes are encoded by the nuclear genome; therefore disruption of plastid translation cannot directly interfere with their expression.

Can one predict which plastid ribosomal proteins are essential for embryogenesis?

The nine plastid ribosomal subunits identified so far as being essential for embryogenesis in Arabidopsis (PRPS5, -S13, -S20, -L1, -L4, -L6, -L21, -L27 and -L35) contribute to different ribosomal domains in either the 30S or the 50S subunit (Stelzl *et al.*, 2001). Moreover, the essential/non-essential nature of the role of PRPs in Arabidopsis embryogenesis cannot be predicted on the basis of studies on prokaryotes. This is outlined in the following three scenarios in which the phenotypic effects of the removal of individual subunits from *Escherichia coli* are compared with those of deletion of their counterparts in chloroplast ribosomes in Arabidopsis.

- 1 Lethality in *E. coli*/embryo lethality in Arabidopsis: (P)RPL4 and -L27 (this study; Table S3; Hashimoto *et al.*, 2005; Bryant *et al.*, 2011). Only in these cases is the essential nature of the Arabidopsis PRP reflected in the *E. coli* mutant phenotype.
- 2 Viability in *E. coli*/embryo lethality in Arabidopsis: (P)RPS20, -L1 and -L35 (this study; Table S3; Hashimoto *et al.*, 2005; Bryant *et al.*, 2011). Interestingly, loss of PRPL35 also results in aberrant embryo morphogenesis and non-viable seeds in maize (Magnard *et al.*, 2004), indicating that a certain level of plastid protein synthesis is also needed for normal embryo development in grasses.
- 3 Lethality in *E. coli*/unperturbed embryogenesis in Arabidopsis: (P)RPS1, -S17, -L24, -L28 (this study; Table S3; Hashimoto *et al.*, 2005). The Arabidopsis *prps1-1*, *prps17-1* and *prpl24-1* mutants are viable, albeit with reduced photosynthetic performance. However, a fundamental role of PRPS1 in Arabidopsis cannot be entirely excluded, because some residual *PRPS1* gene expression can still be observed in *prps1-1* plants. Interestingly, the maize *high chlorophyll fluorescence 60* mutant, which lacks PRPS17, displays a seedling-lethal phenotype (Schultes *et al.*, 2000), in contrast to the corresponding Arabidopsis mutant which can complete its life cycle. Although Arabidopsis plants without PRPL28 are seedling lethal, they still show embryo and seed formation (this study). Given the altered pigmentation of *prpl28-1* mutant seeds, it can be speculated that the formation of the photosynthetic machinery, which is associated with the greening process, is disturbed. For instance, a specific role of PRPL28 in the translation process on the surface of thylakoid membranes might be hypothesised (Minami and Watanabe, 1984; Hurewitz and Jagendorf, 1987; Zhang *et al.*, 1999). Indeed, stromal ribosomes are recruited into thylakoid polysomes, which are active in synthesising thylakoid proteins that are essential for the biogenesis of the photosynthetic apparatus. In this context, PRPL28 might play a major role in the recruitment of ribosomes to

thylakoids. Alternatively, the presence of PRPL28 might be specifically required for thylakoid-bound ribosomes.

Taken together, this cross-kingdom comparison of mutant phenotypes clearly suggests that the impact of specific ribosomal proteins on embryogenesis in *Arabidopsis* cannot be predicted on the basis of their mutant phenotypes in *E. coli*. In principle, this can be explained by changes in the function of these proteins during evolution of the chloroplast from a cyanobacterial endosymbiont, or more probably by the combination of changes in protein and rRNA sequences.

The sensitivity of embryogenesis to plastid gene expression in *Arabidopsis* allows one to identify PRPs which are essential for embryogenesis. Further studies have to clarify whether these PRPs are also essential for ribosomal function, or whether plastid ribosomes that lack such PRPs retain a basal activity that is insufficient to meet the need for plastid protein synthesis during embryogenesis.

EXPERIMENTAL PROCEDURES

Plant material, propagation and growth measurements

Mutant alleles were identified by searching the T-DNA Express database (<http://signal.salk.edu/cgi-bin/tdnaexpress>) and mutant lines were obtained from the SALK collection (Alonso *et al.*, 2003) (*prps20-1/Salk_094710*; *prpl4-1/Salk_117563*; *prpl4-2/Salk_094226*; *prpl24-1/Salk_010822*; *prpl28-1/Salk_142282*), the SAIL collection (Sessions *et al.*, 2002) (*prps1-1/Sail_560_B02*; *prpl1-1/Sail_295_A02*; *prpl35-1/Sail_367_E07*), the John Innes Centre collection (Tissier *et al.*, 1999) (*prps17-1/GT_5_19055*; *prpl1-2/GT_5_101962*) and the GABI-KAT collection (Rosso *et al.*, 2003) (*prpl27-1/GABI_123H12*). With two exceptions, mutant alleles are in the Col-0 genetic background; *prps17-1* and *prpl1-2* are derived from *Ler*. T-DNA insertions were confirmed by sequencing PCR products obtained using gene- and T-DNA-specific primers (Table S4). *Arabidopsis thaliana* Heynh. WT (Col-0 and *Ler*) and mutant plants were grown under controlled growth chamber conditions as described (Pesaresi *et al.*, 2009). Phenotypic analyses were also conducted on plants grown on Murashige and Skoog (MS) medium (Duchefa, <http://www.duchefa.com/>) with or without 1% (w/v) sucrose. Growth measurements are described elsewhere (Leister *et al.*, 1999).

Plant transformation and isolation of transgenic lines

For complementation analyses, the *PRPS1* and *PRPS17* coding sequences were recombined into the Gateway plant transformation destination vector pB2GW7 (Flanders Interuniversity Institute for Biotechnology, Gent, Belgium), under the control of the 35S promoter from the Cauliflower Mosaic Virus (CaMV) (see Table S5 for primer sequences). For *PRPS20*, *PRPL24*, *PRPL27*, *PRPL28* and *PRPL35* the corresponding genomic sequences, together with 1 kbp of promoter regions, were recombined into pB2GW7, devoid of the 35S-CaMV promoter. Plants were transformed according to Clough and Bent (1998) and independent transgenic plants were selected on the basis of their resistance to Basta.

Nucleic acid analysis

Arabidopsis thaliana DNA was isolated as described (Ihnatowicz *et al.*, 2004). For RNA analysis, total leaf RNA was extracted from

fresh tissue using the TRIzol reagent (Invitrogen, <http://www.invitrogen.com/>). Northern analysis was performed under stringent conditions, according to Sambrook and Russell (2001). Probes complementary to nuclear and chloroplast genes were used for the hybridisations. Primers used to amplify the probes are listed in Table S6. All probes used were cDNA fragments labelled with ³²P. Signals were quantified with a phosphorimager (Typhoon; GE Healthcare, <http://www3.gehealthcare.com/>) using the program IMAGEQUANT.

For quantitative real-time PCR (qRT-PCR) profiling, 4-µg aliquots of total RNA, treated with DNase I (Roche Applied Science, <http://www.roche-applied-science.com/>) for at least 30 min, were utilised for first-strand cDNA synthesis using iScript reverse transcriptase (Bio-Rad, <http://www.bio-rad.com/>) according to the supplier's instructions. The qRT-PCR profiling was carried out on an iCycler iQ5 real-time PCR system (Bio-Rad), using the oligonucleotide sequences reported in Table S6. Data from three biological and three technical replicates were analysed with Bio-Rad iQ5 software (version 2.0).

PAGE and immunoblot analyses

Leaves were harvested from plants at the six-leaf rosette stage, and thylakoids were prepared as described (Bassi *et al.*, 1985). For BN-PAGE, thylakoid samples equivalent to 100 mg of fresh leaf material were solubilised and fractionated as described in Pesaresi *et al.* (2009). For 2D PAGE, BN-PAGE lanes were subsequently fractionated on denaturing Tricine-SDS gels (15% PA gel) and the protein content was stained with colloidal Coomassie Blue (G 250).

For immunoblot analyses total proteins were prepared from plants at the six-leaf rosette stage (Martinez-Garcia *et al.*, 1999), then fractionated by SDS-PAGE (on 12% PA gels) (Schägger and von Jagow, 1987). Subsequently, proteins were transferred to poly(vinylidene difluoride) membranes (Ihnatowicz *et al.*, 2004), and replicate filters were immunodecorated with appropriate antibodies. Signals were detected by enhanced chemiluminescence (GE Healthcare) and quantified using IMAGE QUANT for Macintosh (version 1.2; Molecular Dynamics, <http://www.mdyn.com/>).

In-vivo translation assay

The *in-vivo* translational assay was performed essentially as in Pesaresi (2011). Twelve leaf discs of 4 cm diameter were incubated in a buffer containing 20 µg ml⁻¹ cycloheximide, 1 mM K₂HPO₄-KH₂PO₄ (pH 6.3), and 0.1% (w/v) Tween-20 to block cytosolic translation. The [³⁵S]methionine was added to the buffer (0.1 mCi ml⁻¹) and the material was vacuum-infiltrated. Leaves were exposed to light (20 µmol photons m⁻² s⁻¹) and four leaf discs were collected at each time point (5, 15 and 30 min). Total proteins were extracted as described above and loaded on Tricine SDS-PAGE (12% PA). Signals were detected and quantified using the phosphorimager and the IMAGEQUANT program as described above.

Chlorophyll fluorescence and pigment analyses

In vivo Chl *a* fluorescence of leaves was measured using the Dual-PAM-100 (Walz, <http://www.walz.com/>) as described (Pesaresi *et al.*, 2009). Five plants of each genotype were analysed and average values plus standard deviations were calculated. Plants were dark-adapted for 30 min and minimal fluorescence (F_0) was measured. Then pulses (0.8 sec) of saturating white light (5000 µmol photons m⁻² sec⁻¹) were used to determine the maximum fluorescence (F_M), and the ratio $(F_M - F_0)/F_M = F_V/F_M$ (maximum quantum yield of PSII) was calculated. A 10-min exposure to actinic light (80 µmol photons m⁻² sec⁻¹) served to drive electron transport between PSII and PSI. Then steady-state fluorescence (F_S) was

measured, and F'_M was determined after exposure to further saturation pulses (0.8 sec, 5000 $\mu\text{mol photons m}^{-2} \text{sec}^{-1}$). The effective quantum yield of PSII (Φ_{II}) was calculated as the ratio $(F'_M - F_S)/F'_M$.

In vivo Chl *a* fluorescence of whole plants was recorded using an imaging chlorophyll fluorometer (Imaging PAM; Walz) by exposing dark-adapted plants to a pulsed, blue measuring beam (1 Hz, intensity 4; F_0) and a saturating light flash (intensity 4) to obtain F_v/F_M . A 10-min exposure to actinic light (80 $\mu\text{mol photons m}^{-2} \text{sec}^{-1}$) was then used to calculate Φ_{II} .

Pigments were analysed by reverse-phase HPLC (Färber *et al.*, 1997).

Whole-mount preparation and microscopy

To analyse defects in seed development, siliques of WT and heterozygous *PRPS20/prps20-1*, *PRPL1/prpl1-1*, *PRPL4/prpl4-1*, *PRPL27/prpl27-1*, *PRPL28/prpl28-1* and *PRPL35/prpl35-1* plants were manually dissected and observed using a Zeiss LUMAR.V12 stereomicroscope (<http://www.zeiss.com/>). To follow defects during embryo development, siliques from the same genotypes were cleared as reported (Yadegari *et al.*, 1994). Developing seeds were observed using a Zeiss Axiophot D1 microscope equipped with differential interface contrast (DIC) optics. Images were recorded with an AxioCam MRC5 camera (Zeiss) using the Axiovision program (version 4.1). Modified pseudo-Schiff propidium iodide (mPS-PI) embryo staining was performed as described by Truernit *et al.* (2008). Whole seeds were observed with a Leica TCS-SP5 confocal laser scanning microscope (Leica Microsystems, <http://www.leica-microsystems.com/>). The excitation wavelength for mPS-PI-stained samples was 488 nm, and fluorescence emission was collected between 520 and 720 nm.

ACKNOWLEDGEMENTS

This work was supported by the Italian Ministry of Research, special fund for basic research (PRIN 2008XB7774B) to PP and by the Deutsche Forschungsgemeinschaft (SFB-TR1, TP B8 and FOR 804) to DL. We thank Paul Hardy for critical reading of the manuscript.

SUPPORTING INFORMATION

Additional Supporting Information may be found in the online version of this article:

Figure S1. Relative expression and intron-exon structures of *PRPL1*, *PRPL4* and *PRPL24* transcript variants quantified by real-time PCR.

Figure S2. Growth behaviour of *prpl28-1* albino mutants.

Table S1. Overview of the outcome of complementation experiments.

Table S2. Silique length, seed set and frequency of normal and aborted or (in case of *PRPL28/prpl28-1*) albino seeds observed in wild-type (Col-0) and heterozygous mutant siliques.

Table S3. Overview of the functions of the ribosomal protein studied in chloroplasts and the prokaryote *Escherichia coli*.

Table S4. Oligonucleotide sequences employed for genotyping insertion lines.

Table S5. Oligonucleotide sequences employed for complementation tests.

Table S6. Oligonucleotide sequences employed for gene expression analysis.

Please note: As a service to our authors and readers, this journal provides supporting information supplied by the authors. Such materials are peer-reviewed and may be re-organized for online delivery, but are not copy-edited or typeset. Technical support issues arising from supporting information (other than missing files) should be addressed to the authors.

REFERENCES

- Alonso, J.M., Stepanova, A.N., Leisse, T.J. *et al.* (2003) Genome-wide insertional mutagenesis of *Arabidopsis thaliana*. *Science*, **301**, 653–657.
- Asakura, Y. and Barkan, A. (2006) Arabidopsis orthologs of maize chloroplast splicing factors promote splicing of orthologous and species-specific group II introns. *Plant Physiol.* **142**, 1656–1663.
- Bassi, R., dal Belin Peruffo, A., Barbato, R. and Ghisi, R. (1985) Differences in chlorophyll-protein complexes and composition of polypeptides between thylakoids from bundle sheaths and mesophyll cells in maize. *Eur. J. Biochem.* **146**, 589–595.
- Berg, M., Rogers, R., Muralla, R. and Meinke, D. (2005) Requirement of aminoacyl-tRNA synthetases for gametogenesis and embryo development in *Arabidopsis*. *Plant J.* **44**, 866–878.
- Bryant, N., Lloyd, J., Sweeney, C., Myouga, F. and Meinke, D. (2011) Identification of nuclear genes encoding chloroplast-localized proteins required for embryo development in *Arabidopsis*. *Plant Physiol.* **155**, 1678–1689.
- Caffarri, S., Frigerio, S., Olivieri, E., Righetti, P.G. and Bassi, R. (2005) Differential accumulation of Lhcb gene products in thylakoid membranes of *Zea mays* plants grown under contrasting light and temperature conditions. *Proteomics*, **5**, 758–768.
- Chalupska, D., Lee, H.Y., Faris, J.D., Evrard, A., Chalhouh, B., Haselkorn, R. and Gornicki, P. (2008) Acc homeoeloci and the evolution of wheat genomes. *Proc. Natl Acad. Sci. U S A*, **105**, 9691–9696.
- Clough, S.J. and Bent, A.F. (1998) Floral dip: a simplified method for Agrobacterium-mediated transformation of *Arabidopsis thaliana*. *Plant J.* **16**, 735–743.
- DellaPenna, D. and Pogson, B.J. (2006) Vitamin synthesis in plants: tocopherols and carotenoids. *Annu. Rev. Plant Biol.* **57**, 711–738.
- Färber, A., Young, A.J., Ruban, A.V., Horton, P. and Jahns, P. (1997) Dynamics of xanthophyll-cycle activity in different antenna subcomplexes in the photosynthetic membranes of higher plants - The relationship between zeaxanthin conversion and nonphotochemical fluorescence quenching. *Plant Physiol.* **115**, 1609–1618.
- Goldberg, R.B., de Paiva, G. and Yadegari, R. (1994) Plant embryogenesis: zygote to seed. *Science*, **266**, 605–614.
- Hashimoto, M., Ichimura, T., Mizoguchi, H. *et al.* (2005) Cell size and nucleoid organization of engineered *Escherichia coli* cells with a reduced genome. *Mol. Microbiol.* **55**, 137–149.
- Hess, W.R., Hoch, B., Zeltz, P., Hubschmann, T., Kossel, H. and Börner, T. (1994) Inefficient rpl2 splicing in barley mutants with ribosome-deficient plastids. *Plant Cell*, **6**, 1455–1465.
- Hsu, S.C., Belmonte, M.F., Harada, J.J. and Inoue, K. (2010) Indispensable roles of plastids in *Arabidopsis thaliana* embryogenesis. *Curr. Genomics*, **11**, 338–349.
- Hurewitz, J. and Jagendorf, A.T. (1987) Further characterization of ribosome binding to thylakoid membranes. *Plant Physiol.* **84**, 31–34.
- Ihnatowicz, A., Pesaresi, P., Varotto, C., Richly, E., Schneider, A., Jahns, P., Salamini, F. and Leister, D. (2004) Mutants for photosystem I subunit D of *Arabidopsis thaliana*: effects on photosynthesis, photosystem I stability and expression of nuclear genes for chloroplast functions. *Plant J.* **37**, 839–852.
- Inaba, T. and Ito-Inaba, Y. (2010) Versatile roles of plastids in plant growth and development. *Plant Cell Physiol.* **51**, 1847–1853.
- Jarvis, P. (2008) Targeting of nucleus-encoded proteins to chloroplasts in plants. *New Phytol.* **179**, 275–285.
- Jenik, P.D., Gillmor, C.S. and Lukowitz, W. (2007) Embryonic patterning in *Arabidopsis thaliana*. *Annu. Rev. Cell Dev. Biol.* **23**, 207–236.
- Kasmati, A.R., Topel, M., Patel, R., Murtaza, G. and Jarvis, P. (2011) Molecular and genetic analyses of Tic20 homologues in *Arabidopsis thaliana* chloroplasts. *Plant J.* **66**, 877–889.
- Kobayashi, K., Kondo, M., Fukuda, H., Nishimura, M. and Ohta, H. (2007) Galactolipid synthesis in chloroplast inner envelope is essential for proper thylakoid biogenesis, photosynthesis, and embryogenesis. *Proc. Natl Acad. Sci. U S A*, **104**, 17216–17221.
- Leister, D., Varotto, C., Pesaresi, P., Niwergall, A. and Salamini, F. (1999) Large-scale evaluation of plant growth in *Arabidopsis thaliana* by non-invasive image analysis. *Plant Physiol. Biochem.* **37**, 671–678.
- Li, X., Ilarslan, H., Brachova, L., Qian, H.R., Li, L., Che, P., Wurtele, E.S. and Nikolau, B.J. (2011) Reverse-genetic analysis of the two biotin-containing subunit genes of the heteromeric acetyl-coenzyme A carboxylase in Ara-

- bidopsis indicates a unidirectional functional redundancy. *Plant Physiol.* **155**, 293–314.
- Lloyd, J. and Meinke, D. (2012) A comprehensive dataset of genes with a loss-of-function mutant phenotype in Arabidopsis. *Plant Physiol.* **158**, 1115–1129.
- Lopez-Juez, E. (2007) Plastid biogenesis, between light and shadows. *J. Exp. Bot.* **58**, 11–26.
- Lopez-Juez, E. and Pyke, K.A. (2005) Plastids unleashed: their development and their integration in plant development. *Int. J. Dev. Biol.* **49**, 557–577.
- Magnard, J.L., Heckel, T., Massonneau, A., Wisniewski, J.P., Cordelier, S., Lassagne, H., Perez, P., Dumas, C. and Rogowsky, P.M. (2004) Morphogenesis of maize embryos requires ZmPRPL35-1 encoding a plastid ribosomal protein. *Plant Physiol.* **134**, 649–663.
- Maiwald, D., Dietzmann, A., Jahns, P., Pesaresi, P., Joliot, P., Joliot, A., Levin, J.Z., Salamini, F. and Leister, D. (2003) Knock-out of the genes coding for the Rieske protein and the ATP-synthase δ -subunit of Arabidopsis. Effects on photosynthesis, thylakoid protein composition, and nuclear chloroplast gene expression. *Plant Physiol.* **133**, 191–202.
- Mansfield, S. and Briarty, L. (1991) Early embryogenesis in *Arabidopsis thaliana* II. The developing embryo. *Can. J. Bot.* **69**, 461–476.
- Martinez-Garcia, J.F., Monte, E. and Quail, P.H. (1999) A simple, rapid and quantitative method for preparing Arabidopsis protein extracts for immunoblot analysis. *Plant J.* **20**, 251–257.
- Minami, E. and Watanabe, A. (1984) Thylakoid membranes: the translational site of chloroplast DNA-regulated thylakoid polypeptides. *Arch. Biochem. Biophys.* **235**, 562–570.
- Mitschke, J., Fuss, J., Blum, T., Höglund, A., Reski, R., Kohlbacher, O. and Rensing, S.A. (2009) Prediction of dual protein targeting to plant organelles. *New Phytol.* **183**, 224–236.
- Morita-Yamamuro, C., Tsutsui, T., Tanaka, A. and Yamaguchi, J. (2004) Knock-out of the plastid ribosomal protein S21 causes impaired photosynthesis and sugar-response during germination and seedling development in *Arabidopsis thaliana*. *Plant Cell Physiol.* **45**, 781–788.
- Muralla, R., Lloyd, J. and Meinke, D. (2011) Molecular foundations of reproductive lethality in *Arabidopsis thaliana*. *PLoS One*, **6**, e28398.
- Neuhauss, H.E. and Emes, M.J. (2000) Nonphotosynthetic metabolism in plastids. *Annu. Rev. Plant Physiol. Plant Mol. Biol.* **51**, 111–140.
- Ostheimer, G.J., Williams-Carrier, R., Belcher, S., Osborne, E., Gierke, J. and Barkan, A. (2003) Group II intron splicing factors derived by diversification of an ancient RNA-binding domain. *EMBO J.* **22**, 3919–3929.
- Peltier, J.B., Cai, Y., Sun, Q., Zabrouskov, V., Giacomelli, L., Rudella, A., Ytterberg, A.J., Rutschow, H. and van Wijk, K.J. (2006) The oligomeric stromal proteome of *Arabidopsis thaliana* chloroplasts. *Mol. Cell. Proteomics*, **5**, 114–133.
- Pesaresi, P. (2011) Studying translation in Arabidopsis chloroplasts. *Methods Mol. Biol.* **774**, 209–224.
- Pesaresi, P., Varotto, C., Meurer, J., Jahns, P., Salamini, F. and Leister, D. (2001) Knock-out of the plastid ribosomal protein L11 in Arabidopsis: effects on mRNA translation and photosynthesis. *Plant J.* **27**, 179–189.
- Pesaresi, P., Masiero, S., Eubel, H., Braun, H.P., Bhushan, S., Glaser, E., Salamini, F. and Leister, D. (2006) Nuclear photosynthetic gene expression is synergistically modulated by rates of protein synthesis in chloroplasts and mitochondria. *Plant Cell*, **18**, 970–991.
- Pesaresi, P., Schneider, A., Kleine, T. and Leister, D. (2007) Interorganellar communication. *Curr. Opin. Plant Biol.* **10**, 600–606.
- Pesaresi, P., Hertle, A., Pribil, M. et al. (2009) Arabidopsis STN7 kinase provides a link between short- and long-term photosynthetic acclimation. *Plant Cell*, **21**, 2402–2423.
- Rolletschek, H., Borisiuk, L., Koschorreck, M., Wobus, U. and Weber, H. (2002) Legume embryos develop in a hypoxic environment. *J. Exp. Bot.* **53**, 1099–1107.
- Rosso, M.G., Li, Y., Strizhov, N., Reiss, B., Dekker, K. and Weisshaar, B. (2003) An Arabidopsis thaliana T-DNA mutagenized population (GABI-Kat) for flanking sequence tag-based reverse genetics. *Plant Mol. Biol.* **53**, 247–259.
- Ruuska, S.A., Schwender, J. and Ohlrogge, J.B. (2004) The capacity of green oilseeds to utilize photosynthesis to drive biosynthetic processes. *Plant Physiol.* **136**, 2700–2709.
- Sambrook, J. and Russell, D.W. (2001) *Molecular cloning: a laboratory manual*, 3rd edn. Cold Spring Harbor, NY: Cold Spring Harbor Laboratory Press.
- Santner, A. and Estelle, M. (2009) Recent advances and emerging trends in plant hormone signalling. *Nature*, **459**, 1071–1078.
- Santner, A., Calderon-Villalobos, L.I. and Estelle, M. (2009) Plant hormones are versatile chemical regulators of plant growth. *Nat. Chem. Biol.* **5**, 301–307.
- Schägger, H. and von Jagow, G. (1987) Tricine-sodium dodecyl sulfate-polyacrylamide gel electrophoresis for the separation of proteins in the range from 1 to 100 kDa. *Anal. Biochem.* **166**, 368–379.
- Schulte, W., Töpfer, R., Stracke, R., Schell, J. and Martini, N. (1997) Multi-functional acetyl-CoA carboxylase from *Brassica napus* is encoded by a multi-gene family: indication for plastidic localization of at least one isoform. *Proc. Natl Acad. Sci. U S A*, **94**, 3465–3470.
- Schultes, N.P., Savers, R.J., Brutnell, T.P. and Krueger, R.W. (2000) Maize high chlorophyll fluorescent 60 mutation is caused by an Ac disruption of the gene encoding the chloroplast ribosomal small subunit protein 17. *Plant J.* **21**, 317–327.
- Seo, M. and Koshida, T. (2002) Complex regulation of ABA biosynthesis in plants. *Trends Plant Sci.* **7**, 41–48.
- Sessions, A., Burke, E., Presting, G. et al. (2002) A high-throughput Arabidopsis reverse genetics system. *Plant Cell*, **14**, 2985–2994.
- Shikanai, T., Shimizu, K., Ueda, K., Nishimura, Y., Kuroiwa, T. and Hashimoto, T. (2001) The chloroplast *clpP* gene, encoding a proteolytic subunit of ATP-dependent protease, is indispensable for chloroplast development in tobacco. *Plant Cell Physiol.* **42**, 264–273.
- Stelzl, U., Connell, S., Nierhaus, K.H. and Wittmann-Liebold, B. (2001) Ribosomal proteins: role in ribosomal functions. *Encyclopedia of Life Sci.*, 1–12.
- Tejos, R.I., Mercado, A.V. and Meisel, L.A. (2010) Analysis of chlorophyll fluorescence reveals stage specific patterns of chloroplast-containing cells during Arabidopsis embryogenesis. *Biol. Res.* **43**, 99–111.
- Tiller, N., Weingartner, M., Thiele, W., Maximova, E., Schöttler, M.A. and Bock, R. (2012) The plastid-specific ribosomal proteins of *Arabidopsis thaliana* can be divided into non-essential proteins and genuine ribosomal proteins. *Plant J.* **69**, 302–316.
- Tissier, A.F., Marillonnet, S., Klimyuk, V., Patel, K., Torres, M.A., Murphy, G. and Jones, J.D. (1999) Multiple independent defective suppressor-mutator transposon insertions in Arabidopsis: a tool for functional genomics. *Plant Cell*, **11**, 1841–1852.
- Truernit, E., Bauby, H., Dubreucq, B., Grandjean, O., Runions, J., Barthelemy, J. and Palauqui, J.C. (2008) High-resolution whole-mount imaging of three-dimensional tissue organization and gene expression enables the study of phloem development and structure in Arabidopsis. *Plant Cell*, **20**, 1494–1503.
- Waters, M. and Pyke, K. (2005) Plastid development and differentiation. *Annu. Plant Rev. Plastids*, Moller, S.G., Ed. Blackwell: Oxford, **13**, 30–59.
- Weigel, M., Varotto, C., Pesaresi, P., Finazzi, G., Rappaport, F., Salamini, F. and Leister, D. (2003) Plastocyanin is indispensable for photosynthetic electron flow in *Arabidopsis thaliana*. *J. Biol. Chem.* **278**, 31286–31289.
- Woo, H.R., Gow, C.H., Park, J.H., Teysseidier de la Serve, B., Kim, J.H., Park, Y.I. and Nam, H.G. (2002) Extended leaf longevity in the *ored-1* mutant of Arabidopsis with a reduced expression of a plastid ribosomal protein gene. *Plant J.* **31**, 331–340.
- Yadegari, R., Paiva, G., Laux, T., Koltunow, A.M., Apuya, N., Zimmerman, J.L., Fischer, R.L., Harada, J.J. and Goldberg, R.B. (1994) Cell differentiation and morphogenesis are uncoupled in Arabidopsis raspberry embryos. *Plant Cell*, **6**, 1713–1729.
- Yamaguchi, S. and Kamiya, Y. (2000) Gibberellin biosynthesis: its regulation by endogenous and environmental signals. *Plant Cell Physiol.* **41**, 251–257.
- Yin, T., Pan, G., Liu, H., Wu, J., Li, Y., Zhao, Z., Fu, T. and Zhou, Y. (2012) The chloroplast ribosomal protein L21 gene is essential for plastid development and embryogenesis in Arabidopsis. *Planta*, **235**, 907–921.
- Zhang, L., Paakkari, V., van Wijk, K.J. and Aro, E.M. (1999) Co-translational assembly of the D1 protein into photosystem II. *J. Biol. Chem.* **274**, 16062–16067.
- Zubko, M.K. and Day, A. (1998) Stable albinism induced without mutagenesis: a model for ribosome-free plastid inheritance. *Plant J.* **15**, 265–271.
- Zybaïlov, B., Friso, G., Kim, J., Rudella, A., Rodriguez, V.R., Asakura, Y., Sun, Q. and van Wijk, K.J. (2009) Large scale comparative proteomics of a chloroplast Clp protease mutant reveals folding stress, altered protein homeostasis, and feedback regulation of metabolism. *Mol. Cell. Proteomics*, **8**, 1789–1810.

Arabidopsis plants lacking PsbQ and PsbR subunits of the oxygen-evolving complex show altered PSII super-complex organization and short-term adaptive mechanisms

Yagut Allahverdiyeva^{1,†}, Marjaana Suorsa^{1,†}, Fabio Rossi², Andrea Pavesi², Martin M. Kater², Alessia Antonacci³, Luca Tadini⁴, Mathias Pribil⁴, Anja Schneider⁴, Gerhard Wanner⁵, Dario Leister^{4,6,7}, Eva-Mari Aro¹, Roberto Barbato³ and Paolo Pesaresi^{2,*}

¹Molecular Plant Biology, Department of Biochemistry and Food Chemistry, University of Turku, FI-20014 Turku, Finland,

²Dipartimento di Bioscienze, Università degli Studi di Milano, I-20133, Milano, Italy,

³Dipartimento di Scienze dell'Ambiente e della Vita, Università del Piemonte Orientale, viale Teresa Michel 11, I-15121 Alessandria, Italy,

⁴Plant Molecular Biology (Botany), Department Biology I, Ludwig Maximilians Universität München, D-82152 Planegg-Martinsried, Germany,

⁵Ultrastrukturforschung, Department Biology I, Ludwig Maximilians Universität München, D-82152 Planegg-Martinsried, Germany,

⁶Centre for Integrative Biology, Università degli Studi di Trento, I-38123 Mattarello (Trento), Italy, and

⁷Istituto Agrario San Michele all'Adige, Research and Innovation Centre, Foundation Edmund Mach, via E. Mach 1, I-38010 San Michele all'Adige (Trento), Italy

Received 30 January 2013; revised 28 March 2013; accepted 1 May 2013.

*For correspondence (e-mail paolo.pesaresi@unimi.it).

†These authors contributed equally to this work.

SUMMARY

The oxygen-evolving complex of eukaryotic photosystem II (PSII) consists of four extrinsic subunits, PsbO (33 kDa), PsbP (23 kDa), PsbQ (17 kDa) and PsbR (10 kDa), encoded by seven nuclear genes, *PsbO1* (At5g66570), *PsbO2* (At3g50820), *PsbP1* (At1g06680), *PsbP2* (At2g30790), *PsbQ1* (At4g21280), *PsbQ2* (At4g05180) and *PsbR* (At1g79040). Using Arabidopsis insertion mutant lines, we show that PsbP1, but not PsbP2, is essential for photoautotrophic growth, whereas plants lacking both forms of PsbQ and/or PsbR show normal growth rates. Complete elimination of PsbQ has a minor effect on PSII function, but plants lacking PsbR or both PsbR and PsbQ are characterized by more pronounced defects in PSII activity. Gene expression and immunoblot analyses indicate that accumulation of each of these proteins is highly dependent on the presence of the others, and is controlled at the post-transcriptional level, whereas PsbO stability appears to be less sensitive to depletion of other subunits of the oxygen-evolving complex. In addition, comparison of levels of the PSII super-complex in wild-type and mutant leaves reveals the importance of the individual subunits of the oxygen-evolving complex for the supramolecular organization of PSII and their influence on the rate of state transitions.

Keywords: *Arabidopsis thaliana*, photosynthesis, oxygen-evolving complex, protein complex, NPQ, state transitions.

INTRODUCTION

Photosystem II (PSII) is a large pigment–protein complex found in the thylakoid membranes of plants, algae and cyanobacteria, which catalyzes light-induced electron transfer from water to the plastoquinone pool, with concomitant production of oxygen and protons. The core complex is made up of six major intrinsic proteins [D1/PsbA, D2/PsbD, CP47/PsbB, CP43/PsbC and the α and β

subunits (PsbE and PsbF) of cytochrome b_{559}] and a number of low molecular mass intrinsic membrane proteins, associated with an inorganic Mn_4O_5Ca cluster and a number of chloride ions. Together, these form the minimal unit that is capable of light-induced oxygen evolution (Bricker and Frankel, 2011; Ifuku *et al.*, 2011b; Bricker *et al.*, 2012).

For optimal oxygen evolution, plants and green algae require an additional set of four lumen-exposed extrinsic proteins with apparent molecular masses of 33, 23, 17 and 10 kDa (PsbO, PsbP, PsbQ and PsbR, respectively), which form the so-called oxygen-evolving complex (OEC). In *Arabidopsis thaliana*, two genes each code for PsbO (*PsbO1*, At5g66570; *PsbO2*, At3g50820), PsbP (*PsbP1*, At1g06680; *PsbP2*, At2g30790) and PsbQ (*PsbQ1*, At4g21280; *PsbQ2*, At4g05180), whereas PsbR is encoded by a single gene, *At1g79040* (Suorsa et al., 2006; Yi et al., 2008; <http://www.arabidopsis.org>).

These extrinsic proteins have been the subject of extensive investigation by numerous laboratories over the last 25 years, and high-resolution structures have been obtained for PsbP (Ifuku et al., 2004) and PsbQ (Calderone et al., 2003). Analysis of *psbo1* and *psbo2* insertional knockout mutants has yielded insights into their roles in photosynthesis (Murakami et al., 2002, 2005; Lundin et al., 2008; Allahverdiyeva et al., 2009). In particular, these two mutants differ in phenotype. *Arabidopsis psbo1* plants are characterized by retarded growth, low PSII activity, pale green leaves and enhanced susceptibility to photoinactivation, whereas *psbo2* knockout plants show wild-type (WT) levels of PSII activity, growth rate and pigment content. However, both PsbO subunits appear to be required for PSII assembly/stability and photoautotrophy, as shown by the observation that *Arabidopsis* RNAi lines in which expression of both genes are suppressed only grow on sucrose-supplemented medium (Yi et al., 2005). Insertional T-DNA mutants have also been used to provide insights into the function of the PsbR protein in *Arabidopsis* (Suorsa et al., 2006; Allahverdiyeva et al., 2007; Liu et al., 2009). Lack of PsbR was found to lead to decreased rates of oxygen evolution and quinone (Q_A⁻) re-oxidation (Allahverdiyeva et al., 2007). Moreover, *Arabidopsis psbr* mutants showed a reduced content of both PsbP and PsbQ proteins, and near-total depletion of these proteins was observed under steady-state low-light conditions, indicating that PsbR is required for the stable assembly of PsbP and, probably indirectly, of PsbQ (Suorsa et al., 2006). RNAi has also been used to investigate the role of the PsbP and PsbQ proteins (Ifuku et al., 2005b; Yi et al., 2007, 2008, 2009; Ido et al., 2009). Plants that lacked detectable amounts of PsbP were unable to survive in the absence of sucrose, and were characterized by extensive defects in the architecture of the thylakoid membrane (Yi et al., 2007, 2009). In addition, immunological analysis of the PSII protein complement showed marked reductions in CP47 and D2, and, to a lesser extent, in D1 and CP43 proteins, demonstrating that PsbP is essential for PSII core assembly and thylakoid organization (Yi et al., 2007). On the other hand, plants that lacked PsbQ were indistinguishable from WT, indicating that PsbQ is dispensable in higher plants, at least under optimal growth conditions (Ifuku et al., 2005b;

Yi et al., 2009). Moreover, a non-essential role for PsbQ has recently been corroborated by the finding that halophytes lack the PsbQ protein (Pagliano et al., 2009; Trotta et al., 2012).

Although RNAi-mediated silencing of the *PsbP* and *PsbQ* genes has clarified important aspects of their roles in oxygen evolution and PSII electron transport, the lack of stable T-DNA insertion lines has made it impossible to attribute specific functions to each of the two PsbP and PsbQ isoforms. This is unfortunate, particularly for the two isoforms of PsbP, which differ markedly in size (Goulas et al., 2006) and are differentially expressed under conditions of environmental stress. For example, *PsbP2*, unlike *PsbP1*, has been shown to be specifically repressed during cold acclimation (Vergnolle et al., 2005; Goulas et al., 2006). Moreover, the *PsbP2* gene, unlike *PsbP1*, shows a very low degree of co-expression with the majority of the genes encoding lumen proteins, perhaps implying a distinctive function for this subunit (Granlund et al., 2009). However, Ifuku et al. (2008) have proposed that the *PsbP2* gene does not produce a functional PsbP2 protein in the most commonly used *Arabidopsis* ecotype (Columbia-0, Col-0), due to a frameshift in its sequence.

Here, we report the isolation and characterization of insertional *psbp* and *psbq* mutants in *Arabidopsis*, and the generation of lines bearing various combinations of these mutations, including the *psbq1-1 psbq2-1* double mutant and the *psbq1-1 psbq2-1 psbr-1* triple mutant. We show that PsbP1 is essential during the early stages of seedling development, but becomes dispensable in mature plants. The *psbq1-1 psbq2-1 psbr-1* triple mutant accumulates functional PSII complexes, and shows a WT-like phenotype with respect to rates of growth and biomass accumulation under optimal greenhouse conditions, despite having lower steady-state levels of PSII super-complexes and displaying a markedly reduced rate of oxygen evolution, as well as alterations in thylakoid protein phosphorylation, state transitions and non-photochemical quenching.

RESULTS

Isolation of mutants for PsbP and PsbQ proteins in *Arabidopsis*

Lines bearing T-DNA or *Ds* transposon insertions in the nuclear genes coding for each of the PsbP and PsbQ isoforms were identified by targeted PCR. Two mutant alleles were isolated for each of the four genes (Figure 1). In the case of *PsbQ1*, *PsbQ2* and *PsbP1*, T-DNA or *Ds* insertions are located downstream of the predicted translation start codon, whereas the *PsbP2* insertions map to the 5' UTR region. The double mutant *psbq1-1 psbq2-1* was obtained by crossing single mutants and genotyping F₂ progeny. The single mutant *psbr-1* (Suorsa et al., 2006) was crossed with the *psbq1-1 psbq2-1* plants to generate the *psbq1-1*

psbq2-1 psbr-1 triple mutant. In each single mutant, the T-DNA and *Ds* insertions abolished gene expression completely, as revealed by quantitative real-time PCR analysis (Figure 2). No major changes in expression of the other OEC-encoding genes were noted, except in the case of *PsbQ1*, whose expression was increased by approximately 75% in *psbp2-1* and *psbq2-1* leaves, and by 50% in *psbr-1* leaves.

Interestingly, *psbq* and *psbr-1* single mutants, together with the corresponding double and triple mutants, showed no visually discernible phenotype when grown under optimal greenhouse conditions (Figure 3a). Similarly, plants homozygous for *psbp2* mutant alleles were indistinguishable from WT plants grown on soil and when plated on MS medium, whereas *psbp1* plants only grew on sucrose-supplemented medium (Figure 3b), supporting the notion that the PsbP1 protein is essential for photoautotrophy.

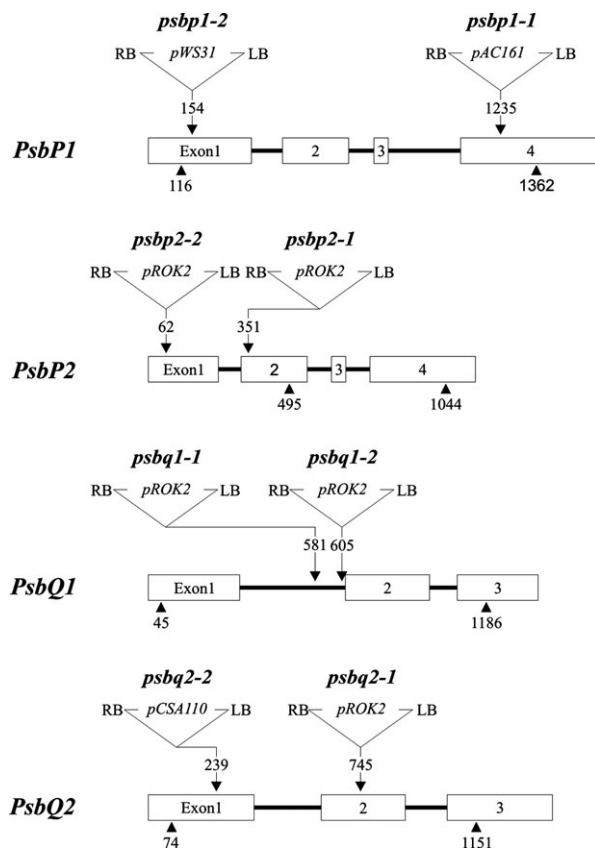


Figure 1. T-DNA tagging of *PSBQ* and *PSBP* genes.

Exons are indicated as numbered white boxes, while introns are shown as black lines. Arrowheads indicate the positions of translation initiation and stop codons. The locations, designations and orientations of T-DNA insertions are indicated (RB, right border; LB, left border). Note that, in the case of the *PsbQ1* and *PsbP1* genes, the intron–exon patterns reflect the composition of the transcript variants identified in leaves, and correspond to *At4g21280.1* and *At1g06680.1*, respectively (see also annotations at TAIR, <http://www.arabidopsis.org>). The T-DNA insertions are not drawn to scale.

Thylakoid protein composition is affected in the OEC mutants

Thylakoid polypeptide composition was investigated by immunoblot analysis in *psbp2-1*, *psbq1-1*, *psbq2-1* and *psbr-1* single mutants, together with the double mutant *psbq1-1 psbq2-1* and the triple mutant *psbq1-1 psbq2-1 psbr-1* (Figure 4 and Table 1). The *psbq* single mutants (*psbq1-1* and *psbq2-1*) were characterized by depletion of one of the two isoforms, which are electrophoretically distinguishable (Figure 4a), whereas the PsbQ protein was completely absent in *psbq1-1 psbq2-1* plants, confirming that the T-DNA insertions lead to complete silencing of the *PsbQ* genes. Similarly, the *psbr-1* mutant showed no accumulation of the PsbR subunit (Suorsa *et al.*, 2006; Figure 4a), and the seedling-lethal phenotype of mutants bearing both *psbp1-1* and *psbp1-2* alleles indicated complete inactivation of *PsbP1* gene. In contrast, no changes were observed in overall accumulation of the PsbP subunit, or in the levels of OEC or PSII core proteins, in *psbp2-1* plants (Figure 4b).

The depletion (*psbq1-1* and *psbq2-1*) or complete absence (*psbq1-1 psbq2-1*) of PsbQ was accompanied by a marked decrease in the abundance of PsbR and PsbP subunits, but no alteration in PsbO levels was observed. Similarly, the absence of PsbR (*psbr-1*) was associated with reduced accumulation of the PsbQ and PsbP proteins to 18% and 3% of the WT levels, respectively, with no concomitant change in PsbO abundance. Interestingly, the simultaneous absence of PsbQ and PsbR subunits led to the disappearance of PsbP from 4-week-old (eight-leaf rosette stage) *psbq1-1 psbq2-1 psbr-1* mutant plants, and reduced the amount of PsbO to approximately 30% of the WT level (Figure 4a).

The complete absence of PsbP1 in mature *psbq1-1 psbq2-1 psbr-1* plants, together with the seedling-lethal phenotype of the *psbp1* mutant, may indicate that the PsbP1 protein is required during the early stages of plant development, but becomes dispensable in mature plants. To clarify this point, the accumulation of PsbP protein was investigated in the rosettes of WT, *psbr-1* and *psbq1-1 psbq2-1 psbr-1* mutants at various stages of development and after exposure to low-light conditions for 5 h (Figure 4c; see also Experimental procedures). In particular, proteins were extracted from cotyledons/leaves and from both intact and ruptured thylakoids with the aim of monitoring whether the reduction of PsbP abundance may be ascribed to the PsbP luminal pool rather than to the PsbP fraction associated with PSII. Interestingly, steady-state levels of PsbP showed a marked decrease in WT plants at the eight-leaf rosette stage, independently of the isolation procedure, whereas it was already barely detectable during the six-leaf rosette phase in the triple mutant, and did not accumulate at all at the eight-leaf stage, when

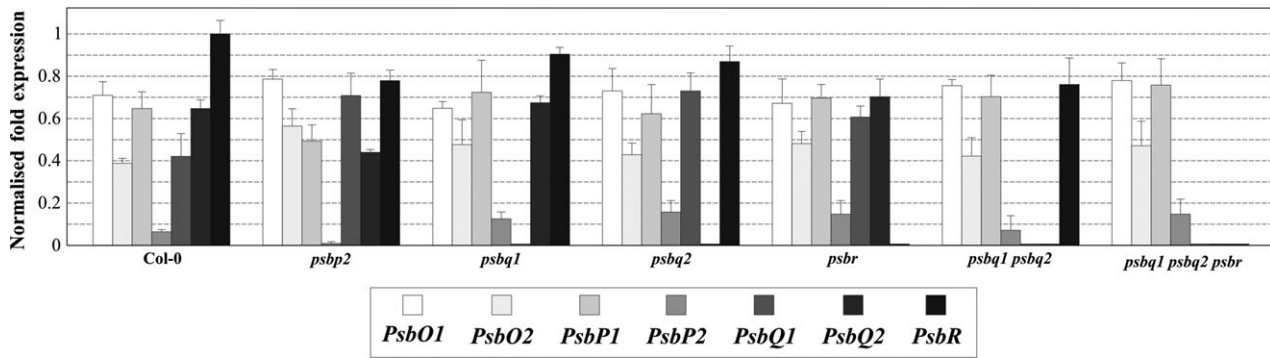


Figure 2. Relative expression levels of OEC-encoding genes in 4-week-old (eight-leaf rosette stage) WT (Col-0) and mutant plants. Levels of *PsbO1*, *PsbO2*, *PsbP1*, *PsbP2*, *PsbQ1*, *PsbQ2* and *PsbR* gene expression were ascertained by real-time PCR of cDNA obtained from leaves of WT and mutant plants. Gene expression was normalized with respect to the level of *PsbR* transcript in WT plants, and ubiquitin was used as an internal reference. The bars indicate standard deviations. Note that, in subsequent figures, data obtained from analyses of *psbp1-1*, *psbp2-1*, *psbq1-1*, *psbq2-1*, *psbr-1*, *psbq1-1 psbq2-1*, *psbq1-1 psbq2-1 psbr-1* alleles are shown; identical data were obtained for the corresponding second allele in each figure.

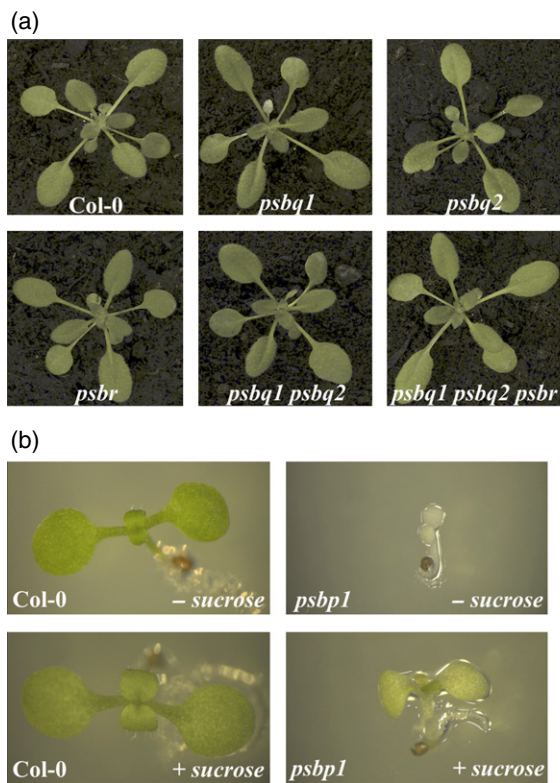


Figure 3. Phenotypes of WT (Col-0), single and multiple mutant plants grown either in a growth chamber or on MS medium. (a) Arabidopsis WT and mutant plants were grown for 4 weeks (eight-leaf rosette stage) in a growth chamber. (b) Col-0, *psbp1* and *psbp2* plants were grown for 10 days on MS medium supplemented or not with 1% sucrose.

plants were fully developed. Even more marked differences in PsbP accumulation were observed in the lumen of WT, *psbr-1* and the triple mutant, indicating that the pool of soluble (unassembled) PsbP is also affected by the absence of PsbR and PsbQ subunits.

To monitor the effects of altered OEC subunit composition on the thylakoid electron transport chain, patterns of accumulation of the major thylakoid protein complex subunits were also investigated (Figure 4d and Table 1). Interestingly, no marked decrease in thylakoid proteins was observed in any of the single mutants, with the exception of CP43 in *psbq2-1* (85% of WT levels) and D2 in *psbr-*

1 (84% of WT levels). Comparable reductions in PSII core subunits, except D1, were observed both in *psbq1-1 psbq2-1* and *psbq1-1 psbq2-1 psbr-1* thylakoid membranes. In addition, diminished amounts of the β -subunit of ATPase were detected in the double and triple mutant thylakoids. However, accumulation of PSI (Lhca2) and PSII (Lhcb2) antenna proteins was not affected, even in the case of *psbq1-1 psbq2-1 psbr-1* thylakoids, in which OEC formation is limited by the amount of PsbO available.

The abundance of key regulatory proteins, including the kinases STN7 and STN8 (Bonardi *et al.*, 2005), the phosphatase TAP38 (Pribil *et al.*, 2010), the PsbS protein (Li

Figure 4. Immunoblot analyses of PSII proteins in WT (Col-0) and mutant leaves.

(a) Nitrocellulose filters carrying fractionated thylakoid proteins, isolated from WT and mutant plants at the eight-leaf rosette stage, were probed with antibodies raised against individual subunits of the OEC (PsbO, PsbP, PsbQ and PsbR).

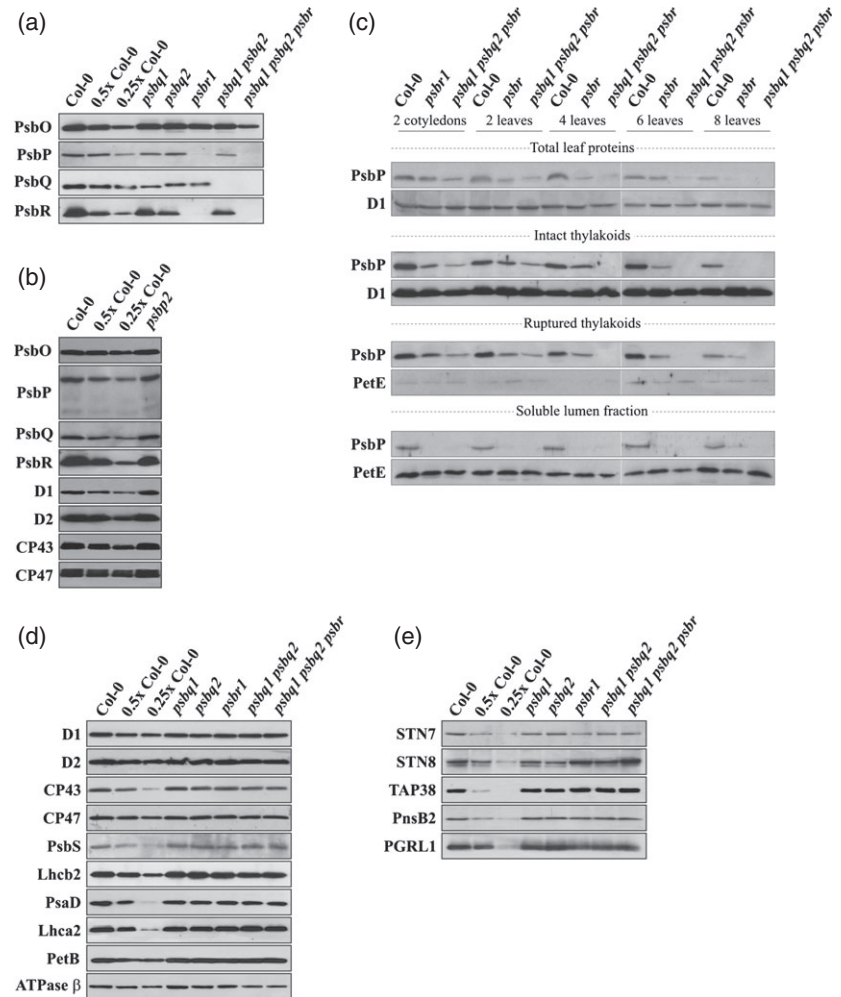
(b) Immunoblot analyses of WT and *psbp2* thylakoids using antibodies specific for OEC proteins and PSII core subunits (D1, D2, CP43 and CP47).

(c) Accumulation of PsbP protein in total cotyledons/leaves, intact thylakoids, ruptured thylakoids and the thylakoid lumen of WT and mutant plants at various stages after germination. A D1-specific antibody was used to verify the abundance of PSII core complexes. A plastocyanin-specific antibody (PetE) was used as a marker of the thylakoid lumen.

(d) Immunoblot analyses performed on the same set of genotypes as in (a) to monitor the accumulation of major thylakoid protein complexes using antibodies specific for PSI (PsaD), PSII (D1, D2, CP43, CP47 and PsbS), LHCI (Lhca2), LHCI (Lhcb2), the chloroplast ATP synthase (ATPase β) and the cytochrome *b₆/f* complex (PetB).

(e) Immunoblot analyses monitoring the accumulation of STN7 and STN8 kinases, the thylakoid-associated phosphatase TAP38 and the subunits responsible for cyclic electron transport (PnsB2 and PGRL1).

Decreasing levels of WT thylakoid proteins were loaded in the lanes marked 0.5 \times Col-0 and 0.25 \times Col-0.

**Table 1** Quantification of thylakoid proteins in light-adapted mutant plants

Protein	<i>psbp2</i>	<i>psbq1</i>	<i>psbq2</i>	<i>psbr</i>	<i>psbq1</i> <i>psbq2</i>	<i>psbq1</i> <i>psbq2 psbr</i>
PsbO	0.95 ± 0.21	0.91 ± 0.17	1.08 ± 0.28	0.92 ± 0.24	0.92 ± 0.27	0.29 ± 0.14
PsbP	1.00 ± 0.07	0.42 ± 0.11	0.44 ± 0.16	0.03 ± 0.02	0.35 ± 0.11	0
PsbQ	1.00 ± 0.03	0.28 ± 0.13	0.35 ± 0.09	0.18 ± 0.06	0	0
PsbR	0.92 ± 0.17	0.74 ± 0.24	0.51 ± 0.22	0	0.58 ± 0.27	0
D1	0.97 ± 0.09	1.11 ± 0.14	0.94 ± 0.14	1.00 ± 0.12	0.98 ± 0.13	1.17 ± 0.19
D2	1.08 ± 0.09	0.96 ± 0.14	1.06 ± 0.19	0.84 ± 0.18	0.64 ± 0.11	0.73 ± 0.13
CP43	1.08 ± 0.15	1.02 ± 0.14	0.85 ± 0.21	0.92 ± 0.23	0.69 ± 0.28	0.71 ± 0.23
CP47	0.96 ± 0.21	0.96 ± 0.14	0.94 ± 0.28	1.03 ± 0.18	0.65 ± 0.12	0.76 ± 0.14
PsbS	ND	1.12 ± 0.23	0.95 ± 0.31	0.91 ± 0.27	1.12 ± 0.26	0.97 ± 0.22
Lhcb2	ND	0.94 ± 0.14	1.11 ± 0.25	0.93 ± 0.22	0.94 ± 0.17	0.95 ± 0.23
PsaD	ND	0.97 ± 0.03	0.94 ± 0.04	0.98 ± 0.06	0.95 ± 0.06	0.95 ± 0.04
Lhca2	ND	0.93 ± 0.17	0.91 ± 0.24	1.05 ± 0.22	0.98 ± 0.04	0.96 ± 0.07
PetB	ND	0.97 ± 0.08	1.12 ± 0.15	0.96 ± 0.15	1.09 ± 0.24	1.08 ± 0.23
ATPase β	ND	1.03 ± 0.26	0.93 ± 0.24	0.94 ± 0.06	0.36 ± 0.16	0.42 ± 0.19
STN7	ND	0.93 ± 0.28	0.91 ± 0.27	0.49 ± 0.24	0.64 ± 0.23	0.63 ± 0.22
STN8	ND	0.81 ± 0.31	0.78 ± 0.26	1.82 ± 0.32	1.64 ± 0.25	1.88 ± 0.36
TAP38	ND	0.97 ± 0.23	1.06 ± 0.18	1.29 ± 0.29	1.31 ± 0.17	1.45 ± 0.08
PnsB2	ND	1.04 ± 0.25	1.03 ± 0.17	0.94 ± 0.17	0.96 ± 0.06	0.91 ± 0.25
PGRL1	ND	0.96 ± 0.11	1.078 ± 0.11	0.53 ± 0.13	0.55 ± 0.15	0.57 ± 0.22

WT (Col-0) levels are set to 1 (100%). Values are means \pm SD from five independent protein gel blots (see Figure 4). ND, not determined.

et al., 2000) required for non-photochemical quenching, as well as PnsB2 (Sirpiö *et al.*, 2009; Takabayashi *et al.*, 2009; Ifuku *et al.*, 2011a) and PGRL1 (DalCorso *et al.*, 2008), which are involved in cyclic electron transport, was also investigated to characterize how plants react to alterations in the subunit composition of the OEC (Figure 4e and Table 1). Interestingly, the STN7 and STN8 kinases responded in precisely opposite ways: the levels of STN7 fell by 40–50% and those of STN8 increased approximately twofold in *psbr-1*, *psbq1-1 psbq2-1* and *psbq1-1 psbq2-1 psbr-1* mutant thylakoids. An increase in TAP38 abundance was also observed in *psbr-1*, *psbq1-1 psbq2-1* and *psbq1-1 psbq2-1 psbr-1* plants, whereas a decrease of approximately 40–50% in PGRL1 was detected in the same set of mutants. Levels of PnsS and PnsB2 were unaltered in mutant thylakoids.

The OEC subunit composition influences PSII–LHCII organization and the dynamics of state transitions

In order to detect possible changes in the organization of thylakoid protein complexes in the mutants, thylakoid membranes were solubilized with β -dodecyl maltoside and analyzed by large-pore Blue Native PAGE in the first dimension (Figure 5a), and subsequently subjected to 2D SDS–PAGE (Figure 5b and Table 2). Prominent changes in protein complex organization were observed in *psbr-1*, *psbq1-1 psbq2-2* and *psbq1-1 psbq2-1 psbr-1* thylakoids. Compared to WT, a reduction of 36% in the amount of the PSII–Light Harvesting Complex of PSII (LHCII) super-complexes was noted in *psbr-1* thylakoids, and more pronounced effects were seen in both the *psbq1-1 psbq2-1* mutant (reduced by 58%) and the *psbq1-1 psbq2-1 psbr-1* mutant (reduced by 54%), indicating that OEC subunit composition has an effect on PSII–LHCII organization.

As *psbr-1*, *psbq1-1 psbq2-2* and *psbq1-1 psbq2-1 psbr-1* plants exhibited the most extensive defects, further analyses, including thylakoid phosphoprotein-specific immunoblot experiments, were performed on these mutant lines (Figure 6a). As expected, phosphorylation of almost all PSII core (P-D1, P-D2), LHCII (P-Lhcb) and Cas (P-Cas; Vainonen *et al.*, 2008) proteins increased in WT leaves under both standard (growth light, GL) and PSII-favoring light conditions, and decreased after incubation in the dark or under light conditions that favor excitation of PSI. The only exception is P-CP43, which accumulated to similar levels in dark-adapted and GL-adapted leaves. A similar pattern was observed in mutant plants, although phosphorylation of LHCII was markedly decreased in GL- and PSII light-adapted thylakoids isolated from *psbr-1* and *psbq1-1 psbq2-1 psbr-1* plants, but not from the *psbq1-1 psbq2-1* mutant (Figure 6a and Table 2). In addition, accumulation of P-D1 and P-D2 proteins was barely detectable in *psbq1-1 psbq2-1 psbr-1* leaves under all light conditions tested, whereas P-CP43 accumulated to levels lower than those seen in WT. Comparable decreases in phosphorylation of PSII core proteins, with the exception of

P-D2, were observed in thylakoids isolated from GL- and PSII light-adapted *psbr-1* and *psbq1-1 psbq2-1* leaves, although the reduction in PSII core protein phosphorylation was more pronounced in *psbq1-1 psbq2-1* than in *psbr-1* leaves in the dark and under PSI light conditions (Figure 6a and Table 2). Interestingly, P-Cas accumulation appeared to be more affected in *psbq1-1 psbq2-1* than in *psbq1-1 psbq2-1 psbr-1* thylakoids.

LHCII phosphorylation forms the basis for state transitions, a well-known short-term adaptive mechanism that involves the re-equilibration of excitation energy between the photosystems. The effects of OEC deficiencies on this mechanism were followed by monitoring the chlorophyll *a* fluorescence yield during state 1 to state 2 (Figure 6b, left panel) and state 2 to state 1 transitions (Figure 6b, right panel), which may be driven by irradiating plants at wavelengths that specifically excite PSII and PSI, respectively. Surprisingly, *psbr-1*, *psbq1-1 psbq2-1*, and, even more strikingly, *psbq1-1 psbq2-1 psbr-1* leaves were able to switch from one state to the other much more rapidly than WT (Figure 6b). Despite the altered kinetics, the extent of state transitions did not differ markedly between WT and mutant plants (WT, 0.11 ± 0.02 ; *psbr-1*, 0.11 ± 0.02 ; *psbq1-1 psbq2-1*, 0.12 ± 0.01 ; *psbq1-1 psbq2-1 psbr-1*, 0.09 ± 0.03 ; see also Figure S1).

Interestingly, the changes in thylakoid protein abundance and behavior in OEC mutant plants, i.e. the marked decrease in thylakoid protein accumulation, the relative inefficiency of PSII–LHCII super-complex formation and the alterations in protein phosphorylation levels, did not result in major modifications in thylakoid membrane architecture, as shown by ultrastructural comparisons of thylakoids in chloroplasts isolated from WT, *psbr-1*, *psbq1-1 psbq2-1* and *psbq1-1 psbq2-1 psbr-1* leaves (Figure S2).

The functional properties of the PSII complex depend on OEC subunit composition

To estimate the photochemical efficiency of PSII complexes, chlorophyll *a* fluorescence was monitored in WT and mutant leaves (Figure 7). The data shown in Figure 7(a) indicate a clear decrease in the maximum (F_V/F_M) and effective quantum yield of PSII (Φ_{II}) in *psbq1-1 psbq2-1 psbr-1*, and a somewhat less pronounced effect was also observed in *psbr-1* leaves, particularly under low and medium actinic light intensities, whereas *psbq1-1 psbq2-1* and WT plants had identical F_V/F_M and Φ_{II} values. In addition, the steady-state levels of non-photochemical quenching were reduced in mutant plants at light intensities higher than $100 \mu\text{mol photons m}^{-2} \text{sec}^{-1}$ (Figure 7b). In particular, at the highest light intensity used in the experiment ($920 \mu\text{mol photons m}^{-2} \text{sec}^{-1}$), non-photochemical quenching levels decreased by 32% in *psbq1-1 psbq2-1* leaves, and more drastic reductions were observed in *psbr-1* (46%) and *psbq1-1 psbq2-1 psbr-1* (55%) leaves, indicating reduced

Figure 5. Blue Native and 2D SDS-PAGE analyses of thylakoid membrane protein complexes in WT (Col-0), single and multiple mutant plants.

(a) Thylakoid membranes, isolated from WT (Col-0) and mutant plants at the eight-leaf rosette stage were solubilized with 1% w/v β -dodecyl maltoside prior to fractionation by Blue Native PAGE. NDH, NAD(P)H dehydrogenase; PS, photosystem; LHC, light-harvesting complex; Cyt *b₆/f*, cytochrome *b₆/f*.
(b) Native PAGE of dodecyl maltoside-solubilized membranes was followed by separation of protein complexes in the second dimension by SDS-PAGE and silver staining. Asterisks indicate the position of PSII-LHCII super-complexes.

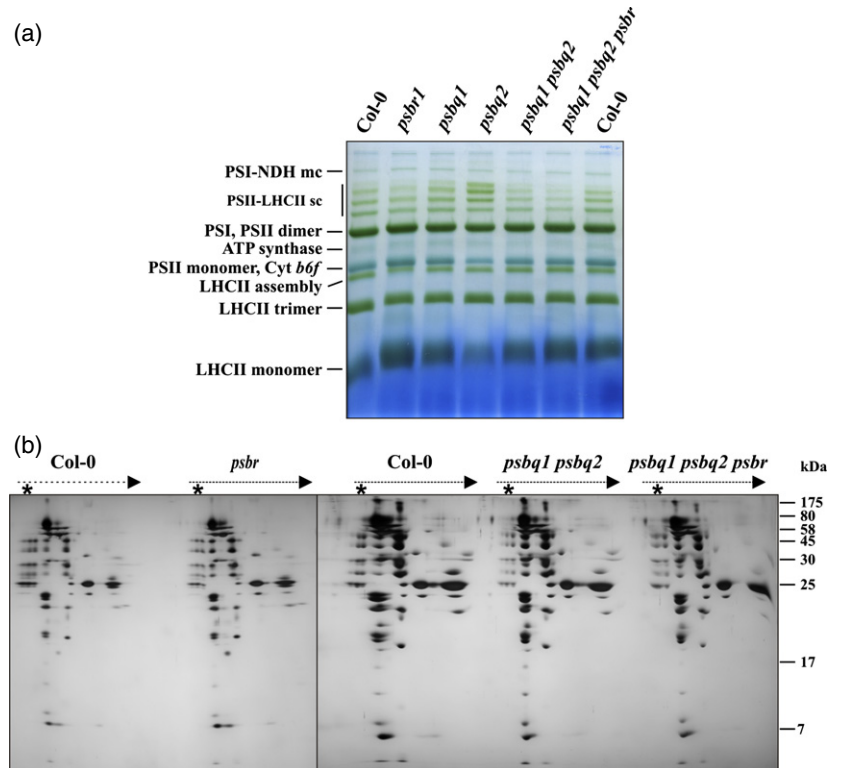
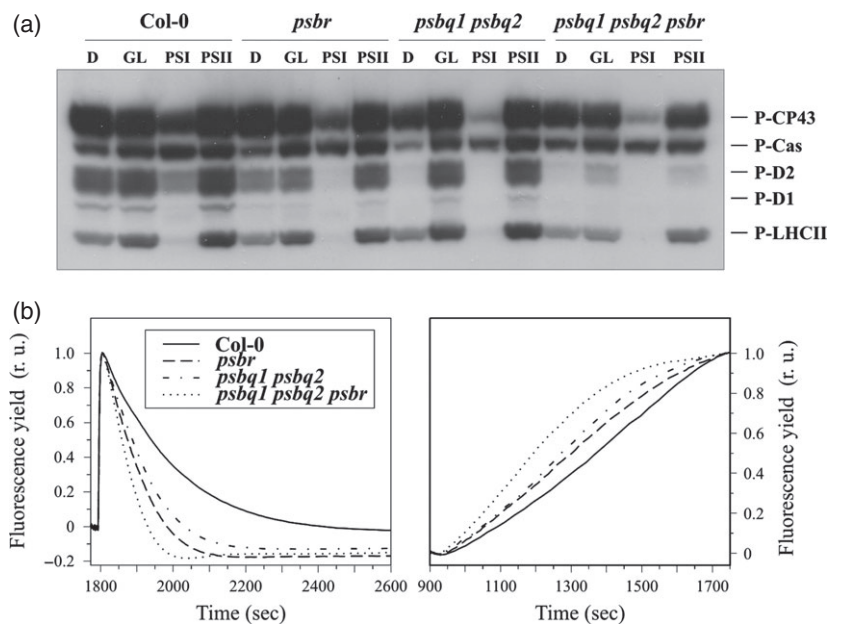


Figure 6. Thylakoid protein phosphorylation and state transitions in WT (Col-0) and mutant plants.

(a) Thylakoid proteins extracted from WT (Col-0) and mutant plants (eight-leaf rosette stage) kept in the dark (D), and subsequently exposed to growth light (GL), PSI-specific light (PSI) or PSII-specific light (PSII), were fractionated by SDS-PAGE. Phosphorylation of LHCII (P-Lhcb), PSII core proteins (P-D1, P-D2, P-CP43) and the Cas protein (P-Cas) was detected by immunoblot analysis using a phosphothreonine-specific antibody. One of three immunoblots for each genotype is shown.
(b) Fluorescence yield of WT and mutant leaves illuminated with PSII-specific light, which induces the state 1 to state 2 transition (left panel), and with PSI-specific light, which triggers the state 2 to state 1 transition (right panel). Each plot shows representative data for one of four replicates. See also Figure S1.



electron flow through the mutant thylakoid membranes. This was investigated further by measuring the rate of steady-state oxygen evolution in WT, *psbr-1*, *psbq1-1 psbq2-1* and *psbq1-1 psbq2-1 psbr-1* leaves under GL conditions in a CO₂-saturated atmosphere. The *psbr-1* and *psbq1-1 psbq2-1 psbr-1* leaves showed 23% and 35% decreases, respectively,

in the steady-state oxygen evolution rate relative to WT, in agreement with previous findings (Suorsa *et al.*, 2006; Allahverdiyeva *et al.*, 2007), whereas a 13% reduction was observed in the *psbq1-1 psbq2-1* double mutant (WT, 6.33 ± 0.43 ; *psbq1-1 psbq2-1*, 5.52 ± 0.23 ; *psbr-1*, 4.87 ± 0.33 ; *psbq1-1 psbq2-1 psbr-1*, $4.13 \pm 0.43 \mu\text{mol O}_2 \text{ m}^{-2} \text{ sec}^{-1}$).

Table 2 Quantification of PSII super-complex accumulation and thylakoid protein phosphorylation in *psbr-1*, *psbq1-1 psbq2-1* and *psbq1-1 psbq2-1 psbr-1* plants

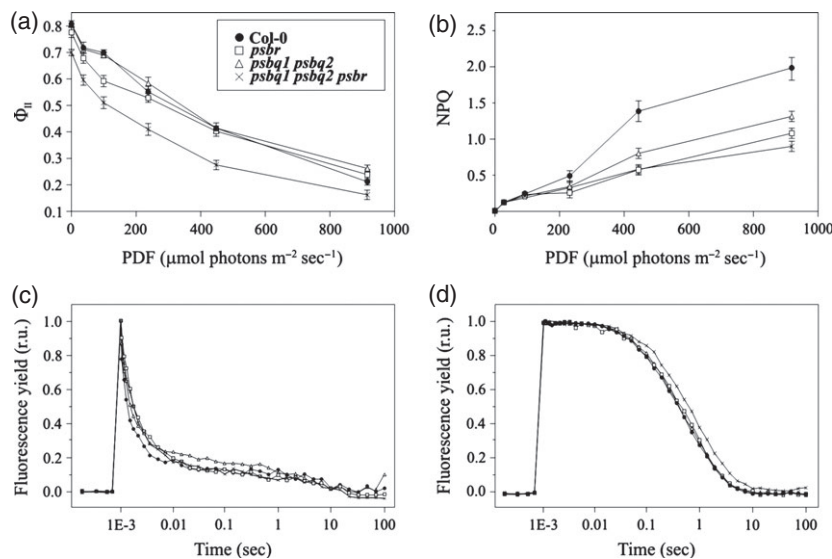
Protein complex/phospho-protein	<i>psbr</i>	<i>psbq1 psbq2</i>	<i>psbq1 psbq2 psbr</i>
PSII-LHCII super-complexes ^a	0.64 ± 0.19	0.42 ± 0.15	0.46 ± 0.18
P-CP43 ^b	0.95 ± 0.15 (D) 0.84 ± 0.21 (GL) 0.46 ± 0.19 (PSI) 0.81 ± 0.22 (PSII)	0.41 ± 0.16 (D) 0.96 ± 0.15 (GL) 0.09 ± 0.04 (PSI) 0.98 ± 0.25 (PSII)	0.67 ± 0.18 (D) 0.74 ± 0.21 (GL) 0.07 ± 0.04 (PSI) 0.67 ± 0.19 (PSII)
P-Cas	0.78 ± 0.18 (D) 0.98 ± 0.17 (GL) 0.69 ± 0.15 (PSI) 1.09 ± 0.23 (PSII)	0.15 ± 0.07 (D) 0.78 ± 0.18 (GL) 0.21 ± 0.13 (PSI) 1.18 ± 0.24 (PSII)	0.98 ± 0.18 (D) 0.93 ± 0.19 (GL) 0.72 ± 0.16 (PSI) 0.64 ± 0.17 (PSII)
P-D2 ^b	0.23 ± 0.09 (D) 0.29 ± 0.08 (GL) bdl (PSI) 0.54 ± 0.09 (PSII)	bdl (D) 0.84 ± 0.14 (GL) bdl (PSI) 0.61 ± 0.11 (PSII)	bdl (D) 0.04 ± 0.03 (GL) bdl (PSI) 0.03 ± 0.02 (PSII)
P-D1 ^b	bdl (D) bdl (GL) bdl (PSI) 0.04 ± 0.03 (PSII)	bdl (D) 0.06 ± 0.04 (GL) bdl (PSI) 0.09 ± 0.05 (PSII)	bdl (D) bdl (GL) bdl (PSI) bdl (PSII)
P-LHCII ^b	0.93 ± 0.24 (D) 0.78 ± 0.15 (GL) bdl (PSI) 0.67 ± 0.22 (PSII)	0.96 ± 0.14 (D) 1.21 ± 0.17 (GL) bdl (PSI) 1.11 ± 0.18 (PSII)	0.49 ± 0.16 (D) 0.27 ± 0.11 (GL) bdl (PSI) 0.39 ± 0.18 (PSII)

bdl, below detection limit. D, dark-adapted; GL, growth light-adapted; PSI, photosystem I-specific light-adapted; PSII, photosystem II-specific light-adapted (see also Experimental procedures).

WT (Col-0) levels are set to 1 (100%).

^aValues are means ± SD from three independent 2D SDS-PAGE experiments.

^bValues are means ± SD from three independent phosphothreonine-specific immunoblots (see also Figures 5b and 6a).

**Figure 7.** Photosynthetic performance of WT (Col-0) and mutant plants.

(a,b) The photosynthetic parameters F_V/F_M (dark-adapted), Φ_{II} (a) and non-photochemical quenching (NPQ) (b) were measured in WT and mutant plants at the eight-leaf rosette stage, grown under low light conditions ($80 \mu\text{mol photons m}^{-2} \text{sec}^{-1}$), dark-adapted for 30 min and illuminated for 15 min with various light intensities. Fluorescence was recorded after dark adaptation and at the end of each illumination period. PDF, photosynthetically active flux density.

(c, d) Relaxation of flash-induced chlorophyll fluorescence yield in leaves of WT (Col-0) and mutant plants. The measurements were performed after single-flash excitation of WT and mutant leaves in the absence (c) and presence (d) of $50 \mu\text{M}$ DCMU. For ease of comparison, the fluorescence relaxation curves were normalized to the F_{0h} and F_M values. Traces are based on the means of three replicates.

PSII complex activity was also investigated by monitoring the functional status of the donor and acceptor sides. The kinetics of flash-induced increase and the subsequent relaxation of the chlorophyll fluorescence yield (FF relaxation) were compared between WT and mutant leaf discs. In the absence of 3-(3,4-dichlorophenyl)-1, 1-dimethylurea (Figure 7c), the kinetics of relaxation in WT leaves were

dominated by the fast phase (0.38 ± 0.08 msec, relative amplitude $41.1\% \pm 4.3$), which arises from Q_A^- to Q_B/Q_B^- electron transfer (Figure 7c and Table 3). The contribution of the middle phase (4.7 ± 1.3 msec) to the whole relaxation curve amounted to $28.3 \pm 4.7\%$. This phase reflects the re-oxidation of Q_A^- in the PSII centers, which had an empty Q_B pocket at the moment of triggering the flash.

Table 3 Characteristic kinetic parameters of the FF relaxation curve in the WT and mutant leaves in the absence and presence of DCMU (see Figure 7c,d)

	Fast phase τ (msec)/Amp (%)	Middle phase τ (msec)/Amp (%)	Slow phase τ (sec)/Amp (%)
Without DCMU			
WT	$0.38 \pm 0.08/41.1 \pm 4.3$	$4.7 \pm 1.3/28.3 \pm 4.7$	$3.02 \pm 2.0/29.4 \pm 5.8$
<i>psbr</i>	$0.79 \pm 0.07/38.4 \pm 5.1$	$8.2 \pm 3.0/31.5 \pm 0.5$	$3.02 \pm 2.5/26.9 \pm 7.9$
<i>psbq1 psbq2</i>	$0.47 \pm 0.04/46.2 \pm 3.8$	$16.3 \pm 7.7/16.4 \pm 2.3$	$3.09 \pm 1.4/33.1 \pm 5.6$
<i>psbq1 psbq2 psbr</i>	$0.86 \pm 0.23/46.3 \pm 4.2$	$9.8 \pm 5.0/23.1 \pm 2.1$	$4.03 \pm 3.4/27.5 \pm 8.4$
With DCMU			
WT			$0.79 \pm 0.03/99 \pm 0.4$
<i>psbr</i>			$0.83 \pm 0.04/98 \pm 0.5$
<i>psbq1 psbq</i>			$0.80 \pm 0.04/98 \pm 0.3$
<i>psbq1 psbq2 psbr</i>			$1.10 \pm 0.05/97 \pm 0.4$

Values are means \pm SD from three independent measurements.

The relative amplitude of the slow phase (3.02 ± 2.0 sec), which arises from $S_2(Q_A Q_B)^-$ charge recombination, was $29.4 \pm 5.8\%$. In *psbr-1*, and *psbq1-1 psbq2-1 psbr-1* leaf discs, the overall FF relaxation kinetics were slower compared to *psbq1-1 psbq2-1* and WT. The fast phase showed slower time constants of 0.79 ± 0.07 and 0.86 ± 0.23 msec in *psbr-1* and *psbq1-1 psbq2-1 psbr-1* leaves, respectively. Moreover, *psbr-1*, *psbq1-1 psbq2-1 psbr-1*, and, even more clearly, *psbq1-1 psbq2-1* leaf discs were characterized by slower middle phases compared to WT, demonstrating significantly retarded electron transfer from Q_A^- to Q_B . In contrast, the slow phase of FF relaxation kinetics in WT and mutant thylakoids was characterized by rather similar time constants (Figure 7c and Table 3).

FF relaxation kinetics were also measured for WT and mutant leaf discs in the presence of DCMU (Figure 7d and Table 3), which blocks the re-oxidation of Q_A^- by forward electron transfer. Hence, this measurement mainly reveals the donor-side status of PSII complexes. Major modifications of FF relaxation kinetics were observed only in *psbq1-1 psbq2-1 psbr-1* leaf discs, in which the time constant and the amplitude of the dominant slow phase, arising from $S_2 Q_A^-$ relaxation, were 1.10 ± 0.05 sec and $97.0 \pm 0.4\%$, respectively, compared to 0.79 ± 0.03 sec and $99 \pm 0.4\%$ for WT leaf discs.

Interestingly, larger differences in the functional status of both the donor and acceptor sides of PSII were observed between isolated thylakoids prepared from WT and mutant plants, indicating that the defects in OEC make the PSII complexes so unstable that their function is prone to further deterioration during the thylakoid purification procedure (Figure S3).

DISCUSSION

PsbP1 is essential for photoautotrophic growth of Arabidopsis plants

Under normal physiological conditions, the absence of one or more of the extrinsic subunits of the OEC specifically

impairs both oxygen production capacity and photoautotrophic growth to a greater or lesser extent. Complete loss of PsbQ proteins in *psbq1-1 psbq2-1* plants results in only a marginal decrease in oxygen evolution and Φ_{II} values, without altering photoautotrophic growth. Similar results have been obtained in cyanobacteria, where PsbQ homologs are dispensable for PSII accumulation and photoautotrophic growth (Thornton *et al.*, 2004). Moreover, under normal light conditions (GL), knockdown of PsbQ expression by RNAi had no effect on photoautotrophic growth, PSII assembly or photosynthetic performance in tobacco (*Nicotiana tabacum*) (Ifuku *et al.*, 2005b) and Arabidopsis (Yi *et al.*, 2006), in agreement with our findings for the corresponding knockout mutants. However, a major phenotypic effect of PsbQ depletion was observed under low-light conditions in Arabidopsis (Yi *et al.*, 2006): RNAi plants progressively became chlorotic and died, most probably as a consequence of the reduced ability to produce oxygen under limiting light conditions.

In the absence of PsbR, oxygen evolution, but not photoautotrophic growth, is also impaired under optimal growth-chamber conditions (Figure 3), in agreement with previous findings (Stockhaus *et al.*, 1990; Suorsa *et al.*, 2006; Allahverdiyeva *et al.*, 2007; Liu *et al.*, 2009). This is further supported by the phenotypic characteristics of *psbq1-1 psbq2-1 psbr-1* plants. Even the concomitant absence of PsbQ and PsbR proteins does not preclude photoautotrophic growth, although the leaves of triple mutants are characterized by marked reductions in Φ_{II} and rates of oxygen evolution. Interestingly, no PsbP protein was detected in mature *psbq1-1 psbq2-1 psbr-1* leaves (eight-leaf rosette stage), whereas residual levels accumulated up to the four-leaf rosette stage in the triple mutant. This finding, together with the fact that complete suppression of *PsbP1* expression prevents photoautotrophic growth, in agreement with previous reports (Ifuku *et al.*, 2005a; Yi *et al.*, 2007; Ido *et al.*, 2009), and the observation that PsbP1 accumulation decreases in WT plants as leaves get older, is compatible with the assumption that PsbP1 has a

major role in PSII and OEC assembly, rather than simply being a structural component of the PSII–OEC complex. Interestingly, only PsbP1, but not PsbP2, is strictly required for photoautotrophic growth. Gene expression and immunoblot analyses (see Figures 2 and 4b) show that the *PsbP2* gene contributes very little to the total *PsbP* transcript level, and that the PsbP2 protein does not accumulate inside the thylakoid lumen, at least under optimal growth conditions. This result is compatible with the reported frameshift mutation in the *PsbP2* gene in the Columbia ecotype (Ifuku *et al.*, 2008), which is predicted to encode a 125-residue protein, corresponding to amino acids 129–263 of the PsbP1 protein. This truncated gene product is presumably non-functional, as it lacks the chloroplast transit peptide and is therefore incapable of being translocated into the thylakoid lumen.

Like PsbP1, the PsbO protein has been reported to be essential for photoautotrophic growth in both algae (Mayfield *et al.*, 1987) and Arabidopsis (Yi *et al.*, 2005), due to its vital role in stabilization of the Mn₄O₅Ca cluster. Its presence is sufficient to support WT-like photoautotrophic growth in mature *psbq1-1 psbq2-1 psbr-1* leaves that lack PsbP, PsbQ and PsbR.

OEC subunit composition influences PSII protein abundance and the organization of PSII super-complexes

Gene expression analyses based on quantitative real-time PCR clearly indicate that silencing of *PsbP*, *PsbQ* and *PsbR* genes, either individually or in combination, has only a marginal effect on the levels of transcripts deriving from the remaining OEC gene(s). However, a very different picture emerges when the accumulation of OEC proteins is monitored via immunoblot analyses in the various mutant backgrounds. Of the four OEC subunits, PsbO appears to be least sensitive to perturbation, as it is present in normal amounts in most of the mutants analyzed. The only exception is observed in *psbq1-1 psbq2-1 psbr-1* thylakoids, where a decrease to approximately 30% of WT levels was noted. The relative stability of PsbO is attributable to interaction of its N-terminal region with several PSII core subunits, including CP43, CP47, D1 and D2, as shown in the PSII crystal structure from *Thermosynechococcus vulcanus* (Umena *et al.*, 2011). Moreover, numerous cross-linking studies have indicated that the PsbO protein may be cross-linked to CP47 in higher plants (Bricker *et al.*, 1988; Enami *et al.*, 1989; Seidler *et al.*, 1996). Indeed, levels of CP47 (and to a lesser extent D2 and CP43) are significantly reduced in *psbq1-1 psbq2-1 psbr-1* thylakoids, but D1 levels are unaffected (Figure 4d).

Based on these findings, it appears that PsbO provides a basal structure for binding of the other OEC subunits to PSII. The levels of PsbP fell below the limits of detection only when a marked decrease in PsbO accumulation was

also observed, as in the case of mature *psbq1-1 psbq2-1 psbr-1* leaves. Indeed, the PsbP protein is known to interact with PsbO, and a variety of studies have shown that PsbO is required for binding of PsbP to PSII (Miyao and Murata, 1989; Kavelaki and Ghanotakis, 1991). Moreover, PsbP levels were also reduced in *psbq1-1 psbq2-1* thylakoids that totally lack PsbQ subunits but retain WT levels of PsbO, supporting the possibility that a major function of PsbQ is to stabilize the association of PsbP with PsbO in higher plants (Kakiuchi *et al.*, 2012). Previous studies had also indicated that PsbP is required for the association of PsbQ with PSII (Miyao and Murata, 1989; Kavelaki and Ghanotakis, 1991), in agreement with the standard model, in which PsbO binds to the PSII core and PsbP interacts with both PsbO and PsbQ (Bricker *et al.*, 2012). Characterization of the *psbr-1* mutant further confirms this molecular model, as both our immunoblot data (Figure 4) and previous results (Suorsa *et al.*, 2006) support a major role for PsbR protein in assembly of PsbP into the PSII complex. PsbP was barely detectable in *psbr-1* thylakoids, and the concomitant lack of PsbQ2 in this genotype is most probably a secondary effect of the absence of PsbP.

The OEC protein composition has a prominent effect on PSII assembly and accumulation, as shown by the lethal phenotype of *psbp1-1* plants. The decreased amounts of PSII core subunits, such as D2, CP43 and CP47, found in *psbq1-1 psbq2-1* and *psbq1-1 psbq2-1 psbr-1* plants, further support this inference (see Figure 4d). Moreover, defects in the assembly of the OEC, as seen in *psbr-1*, *psbq1-1 psbq2-1* and *psbq1-1 psbq2-1 psbr-1* plants, appear to lead to a more general re-adjustment of the entire thylakoid electron transport chain, particularly with respect to proteins involved in regulatory processes, such as PGRL1 (DalCorso *et al.*, 2008), the STN7 and STN8 kinases (Bonardi *et al.*, 2005) and the phosphatase TAP38 (Pribil *et al.*, 2010), i.e. the enzymes that are responsible for adaptation of photosynthetic function to varying environmental conditions.

The OEC also plays a key role in defining the architecture of PSII super-complexes in higher plants (Caffarri *et al.*, 2009; Ifuku *et al.*, 2011b). PsbP knockdown by RNAi in tobacco resulted in a severe decrease in the amount of PSII–LHCII super-complexes, while amounts of unattached LHCII trimers and minor LHCs were significantly increased (Ido *et al.*, 2009). Similarly, as shown here, the abundance of PSII–LHCII super-complexes decreased in *psbq1-1 psbq2-1* and *psbq1-1 psbq2-1 psbr-1*, and, albeit to a lesser extent, *psbr-1* thylakoids (Figure 5). One feature common to all these genotypes is the marked decrease and/or complete absence in their thylakoid membranes of PsbQ and PsbP subunits, indicating that these have specific and important roles in stabilizing PSII–LHCII super-complexes, but do not have major effects on thylakoid membrane organization (see also Figure S2).

Removal of OEC subunits alters PSII activity and short-term regulatory mechanisms

To obtain insights into the role of OEC subunits in the function of the PSII complex, we performed a detailed investigation of the behavior of chlorophyll fluorescence and electron transport in *psbr-1*, *psbq1-1 psbq2-1* and *psbq1-1 psbq2-1 psbr-1* mutant plants. The absence of either PsbR alone, or PsbR and PsbQ, was shown to lower the quantum yield of PSII, possibly due to impairment of electron transfer through the reaction centers, whereas the *psbq1-1 psbq2-1* mutant behaved like WT. These observations are supported by FF relaxation experiments, which revealed malfunctions on both the donor and acceptor sides of PSII in *psbq1-1 psbq2-1 psbr-1* leaves, and on the acceptor side in *psbr-1*. In particular, a characteristic feature of both *psbr-1* and *psbq1-1 psbq2-1 psbr-1* leaves was the slower rate of electron transfer from Q_A to Q_B , indicated by slower time constants for the fast and middle phases of the FF relaxation curve relative to WT (Table 3 and Figure 7). In contrast, the time constant and amplitude of the fast phase were only marginally increased in *psbq1-1 psbq2-1* leaves.

In the presence of DCMU, the FF relaxation curve is an indicator of the donor-side status of the PSII complex. Significant slow-down of FF relaxation kinetics, indicating a stabilization of the $S_2Q_A^-$ charge pair, was observed only in *psbq1-1 psbq2-1 psbr-1* leaves (Table 3 and Figure 7).

Based on these findings, together with the oxygen evolution rates observed in *psbr-1*, *psbq1-1 psbq2-1* and *psbq1-1 psbq2-1 psbr-1* leaves, it seems clear that the PsbR and PsbQ subunits play synergistic roles in the optimization of photosynthetic water splitting and electron transfer in PSII.

Interestingly, the less efficient thylakoid electron transport chain in *psbr-1* and *psbq1-1 psbq2-1 psbr-1*, which is reflected by the low phosphorylation levels of LHCII under various light conditions, impaired the kinetics but not the extent of state transitions (see Figure 6b and Figure S1). It may be hypothesized that the low LHCII phosphorylation levels are compensated for by the faster transitions from state 1 to state 2 (and vice versa) observed in mutant leaves, most probably facilitated by the increased availability of LHCII proteins loosely bound to photosystems that results from impaired formation of PSII–LHCII super-complexes. Similarly, the Arabidopsis *psb27* mutant, which cannot form PSII–LHCII super-complexes, has recently been shown to exhibit highly accelerated state transitions, indicating that dissociation of PSII–LHCII super-complexes is required for movement of antenna proteins (Dietzel *et al.*, 2011).

Taken together, our findings indicate that, in higher plants, the absence of PsbQ and PsbR results in only minor changes in the oxygen evolution rate and growth behavior

under optimal growth conditions. However, their depletion has a major effect on short-term regulatory mechanisms, such as state transitions and non-photochemical quenching, as a consequence of reduced PSII activity and defective PSII–LHCII super-complex accumulation.

EXPERIMENTAL PROCEDURES

Plant material and propagation

Arabidopsis thaliana mutant lines in the Columbia-0 (Col-0) background were obtained from the European Arabidopsis Stock Center (<http://arabidopsis.info/>) after searching the T-DNA Express database (<http://signal.salk.edu/cgi-bin/tdnaexpress>). The *psbq1-1* (SALK_082214), *psbq1-2* (SALK_082212), *psbq2-1* (SALK_002715), *psbp2-1* (SALK_012599), *psbp2-2* (SALK_073785) and *psbr-1* (SALK_114496) (Suorsa *et al.*, 2006;) lines were obtained from the SALK collection (Alonso *et al.*, 2003), *psbq2-2* (SAIL_229_A07) was obtained from the SAIL collection (Sessions *et al.*, 2002), *psbp1-1* (GABI_556E08) was obtained from the GABI-Kat collection (Rosso *et al.*, 2003) and *psbp1-2* (CSHL_ET12592) was obtained from the Martienssen Lab collection (Sundaresan *et al.*, 1995). T-DNA and *Ds* insertions were confirmed by sequencing PCR products obtained using gene- and insertion-specific primers (Table S1). Arabidopsis plants were grown under controlled growth chamber conditions as described previously (Pesaresi *et al.*, 2009). In addition, phenotypic analyses were performed on plants grown on Murashige and Skoog (MS) medium (Duchefa, <http://www.duchefa.com/>) with or without 1% w/v sucrose.

Nucleic acid analyses

Arabidopsis DNA was isolated as described previously (Ihnatowicz *et al.*, 2004). For gene expression analysis, total leaf RNA was extracted from fresh tissue using the LiCl method (Verwoerd *et al.*, 1989). For quantitative real-time PCR analysis, 4 μ g aliquots of total RNA, treated with DNase I (Roche Applied Science, <http://www.roche-applied-science.com/>) for at least 30 min, were utilized for first-strand cDNA synthesis using iScript reverse transcriptase (Bio-Rad, <http://www.bio-rad.com/>) according to the manufacturer's instructions. The quantitative real-time PCR profiling was performed on an iCycler iQ5 real-time PCR system (Bio-Rad), using the oligonucleotide sequences listed in Table S2. Data from three biological and three technical replicates were analyzed using Bio-Rad iQ5 software (version 2.0).

PAGE and immunoblot analyses

Thylakoid isolation was performed as described by Jarvi *et al.* (2011). Samples of thylakoid membranes, corresponding to 8 μ g chlorophyll, were solubilized in the presence of 1% β -dodecyl maltoside (Sigma-Aldrich, <http://www.sigmaaldrich.com/>), and optimal separation of the thylakoid membrane protein complexes was obtained by large-pore Blue Native PAGE (Jarvi *et al.*, 2011). For two-dimensional protein fractionation under denaturing conditions (2D SDS–PAGE), the denatured strips were transferred to the top of an SDS–PAGE (15% w/v acrylamide containing 6 M urea), and subjected to electrophoresis to determine the subunit composition of the complexes. For protein visualization, gels were stained with silver as described previously (Blum *et al.*, 1987).

For immunoblot analyses, total proteins were prepared as described by Martinez-Garcia *et al.* (1999), and ruptured thylakoids and the corresponding lumen fraction were obtained by sonica-

tion as described by Lennartz *et al.* (2001). Total proteins, intact and ruptured thylakoids, corresponding to 3 µg chlorophyll, as well as the lumen fraction were fractionated by SDS-PAGE (12% w/v acrylamide) (Schagger and von Jagow, 1987). Subsequently, proteins were transferred to polyvinylidene difluoride membranes (Ihnatowicz *et al.*, 2004), and replicate filters were immunodecorated using appropriate antibodies.

For phosphorylation analyses, thylakoids were isolated from WT and mutant plants kept overnight in the dark, or exposed to growth light (100 µmol photons m⁻² sec⁻¹), or PSI- or PSII-specific light conditions as described by Tikkanen *et al.* (2006). Thylakoids were isolated as described above, fractionated by SDS-PAGE, transferred to polyvinylidene difluoride membranes and immunodecorated with a polyclonal anti-phosphothreonine antibody (New England BioLabs, <http://www.neb.com/>).

Electron microscopy

Pieces of leaf tissue from light-adapted WT and mutant plants were fixed immediately with 2.5% glutaraldehyde in fixation buffer (75 mM sodium cacodylate, pH 7.0, 2 mM MgCl₂) for 1 h at room temperature, rinsed several times in the same buffer, and post-fixed for 2 h with 1% osmium tetroxide in fixation buffer at room temperature, as described previously (Aseeva *et al.*, 2007). All micrographs were taken using an EM 912 electron microscope (Zeiss, <http://zeiss.com>).

Chlorophyll *a* fluorescence and oxygen evolution analyses

In vivo chlorophyll *a* fluorescence of leaves was measured using a Dual-PAM-100 (Walz, <http://www.walz.com/>) as described previously (Pesaresi *et al.*, 2009), and the parameters F_V/F_M , Φ_{II} (Genty *et al.*, 1989) and non-photochemical quenching (Grasses *et al.*, 2002) were quantified.

State transitions were measured as described previously (Lunde *et al.*, 2000). Briefly, transition to state 2 was induced by PSII-favoring red light (635 nm, 25 µmol photons m⁻² sec⁻¹), whereas state 1 was reached using PSI-specific far-red light (720 nm, intensity step 15). FF relaxation kinetics in the absence or presence of DCMU were measured using a double-modulation fluorometer (Photon System Instruments, <http://www.psi.cz/>) in the 150 µsec–100 sec time range, as described previously (Allahverdiyeva *et al.*, 2007). Leaf discs were vacuum-infiltrated or not with DCMU (50 µM), and dark adapted for 5 min before fluorescence was measured. Similarly, thylakoid membranes, prepared as described above, were incubated or not with 10 µM DCMU, and dark-adapted for 5 min before fluorescence detection. Analysis of fluorescence spectra was performed as described by Vass *et al.* (1999).

Oxygen evolution rates were measured on leaf discs of approximately 6 mm diameter, isolated from 4-week-old WT and mutant plants. The discs were dark-adapted for 30 min in a buffer containing 1 M NaHCO₃ (pH 9) to provide a CO₂-saturated atmosphere (Chow *et al.*, 1989). A Clark-type O₂ electrode (Oxygraph, Hansatech, <http://www.hansatech-instruments.com/>) provided with an electrode conditioning unit was used for the measurements. At the end of the dark period, no O₂ was detectable in the chamber. Then the chamber was illuminated with white light, at a flux rate of approximately 80 µmol photons m⁻² sec⁻¹, and oxygen production was measured for 20 min.

Acknowledgments

This work was supported by funds from the Italian Ministry of Research (Special Fund for Basic Research; PRIN 2008XB7774B)

awarded to P.P. and R.B., from the 'International Mobility' project of the University of Piemonte Orientale to R.B., from the Academia of Finland (Center of Excellence project 118637 to E.-M.A. and project 138703 to M.S.) and from the Deutsche Forschungsgemeinschaft (SFB-TR1, TP B8 and FOR 804) to D.L. We thank Virpi Pakkarinen for the excellent technical assistance and Paul Hardy for critical reading of the manuscript.

SUPPORTING INFORMATION

Additional Supporting Information may be found in the online version of this article.

Figure S1. Measurements of state transitions in WT (Col-0), *psbr*, *psbq1 psbq2* and *psbq1 psbq2 psbr* plants.

Figure S2. Ultrastructure of WT (Col-0), *psbr*, *psbq1 psbq2* and *psbq1 psbq2 psbr* thylakoids.

Figure S3. Relaxation of flash-induced chlorophyll fluorescence yield in thylakoids of WT (Col-0) and mutant plants.

Table S1. Oligonucleotide sequences used for genotyping insertion lines.

Table S2. Oligonucleotide sequences used for gene expression analysis.

REFERENCES

- Allahverdiyeva, Y., Mamedov, F., Suorsa, M., Styring, S., Vass, I. and Aro, E.M. (2007) Insights into the function of PsbR protein in *Arabidopsis thaliana*. *Biochim. Biophys. Acta*, **1767**, 677–685.
- Allahverdiyeva, Y., Mamedov, F., Holmstrom, M., Nurmi, M., Lundin, B., Styring, S., Spetea, C. and Aro, E.M. (2009) Comparison of the electron transport properties of the *psbo1* and *psbo2* mutants of *Arabidopsis thaliana*. *Biochim. Biophys. Acta*, **1787**, 1230–1237.
- Alonso, J.M., Stepanova, A.N., Leisse, T.J. *et al.* (2003) Genome-wide insertional mutagenesis of *Arabidopsis thaliana*. *Science*, **301**, 653–657.
- Aseeva, E., Ossenhuhl, F., Sippel, C. *et al.* (2007) Vipp 1 is required for basic thylakoid membrane formation but not for the assembly of thylakoid protein complexes. *Plant Physiol. Biochem.* **45**, 119–128.
- Blum, H., Beier, H. and Gross, H.J. (1987) Improved silver staining of plant-proteins, RNA and DNA in polyacrylamide gels. *Electrophoresis*, **8**, 93–99.
- Bonardi, V., Pesaresi, P., Becker, T., Schleiff, E., Wagner, R., Pfanschmidt, T., Jahns, P. and Leister, D. (2005) Photosystem II core phosphorylation and photosynthetic acclimation require two different protein kinases. *Nature*, **437**, 1179–1182.
- Bricker, T.M. and Frankel, L.K. (2011) Auxiliary functions of the PsbO, PsbP and PsbQ proteins of higher plant photosystem II: a critical analysis. *J. Photochem. Photobiol., B*, **104**, 165–178.
- Bricker, T.M., Odum, W.R. and Queirolo, C.B. (1988) Close association of the 33-kDa extrinsic protein with the apoprotein of Cpa1 in photosystem II. *FEBS Lett.* **231**, 111–117.
- Bricker, T.M., Roose, J.L., Fagerlund, R.D., Frankel, L.K. and Eaton-Rye, J.J. (2012) The extrinsic proteins of photosystem II. *Biochim. Biophys. Acta*, **1817**, 121–142.
- Caffarri, S., Kouril, R., Kereiche, S., Boekema, E.J. and Croce, R. (2009) Functional architecture of higher plant photosystem II supercomplexes. *EMBO J.* **28**, 3052–3063.
- Calderone, V., Trabucco, M., Vujcic, A., Battistutta, R., Giacometti, G.M., Andreucci, F., Barbato, R. and Zanotti, G. (2003) Crystal structure of the PsbQ protein of photosystem II from higher plants. *EMBO Rep.* **4**, 900–905.
- Chow, W.S., Hope, A.B. and Anderson, J.M. (1989) Oxygen per flash from leaf-discs quantifies photosystem II. *Biochim. Biophys. Acta*, **973**, 105–108.
- DalCorso, G., Pesaresi, P., Masiero, S., Aseeva, E., Schunemann, D., Finazzi, G., Joliot, P., Barbato, R. and Leister, D. (2008) A complex containing PGRL1 and PGR5 is involved in the switch between linear and cyclic electron flow in *Arabidopsis*. *Cell*, **132**, 273–285.

- Dietzel, L., Brautigam, K., Steiner, S., Schuffler, K., Lepetit, B., Grimm, B., Schottler, M.A. and Pfannschmidt, T. (2011) Photosystem II supercomplex remodeling serves as an entry mechanism for state transitions in *Arabidopsis*. *Plant Cell*, **23**, 2964–2977.
- Enami, I., Miyaoka, T., Mochizuki, Y., Shen, J.R., Satoh, K. and Katoh, S. (1989) Nearest neighbor relationships among constituent proteins of oxygen-evolving photosystem II membranes – binding and function of the extrinsic 33 kDa protein. *Biochim. Biophys. Acta*, **973**, 35–40.
- Genty, B., Briantais, J.M. and Baker, N.R. (1989) The relationship between the quantum yield of photosynthetic electron-transport and quenching of chlorophyll fluorescence. *Biochim. Biophys. Acta*, **990**, 87–92.
- Goulas, E., Schubert, M., Kieselbach, T., Kleczkowski, L.A., Gardestrom, P., Schroder, W. and Hurry, V. (2006) The chloroplast lumen and stromal proteomes of *Arabidopsis thaliana* show differential sensitivity to short- and long-term exposure to low temperature. *Plant J.* **47**, 720–734.
- Granlund, I., Hall, M., Kieselbach, T. and Schroder, W.P. (2009) Light induced changes in protein expression and uniform regulation of transcription in the thylakoid lumen of *Arabidopsis thaliana*. *PLoS ONE*, **4**, e5649.
- Grasses, T., Pesaresi, P., Schiavon, F., Varotto, C., Salamini, F., Jahns, P. and Leister, D. (2002) The role of delta pH-dependent dissipation of excitation energy in protecting photosystem II against light-induced damage in *Arabidopsis thaliana*. *Plant Physiol. Biochem.* **40**, 41–49.
- Ido, K., Ifuku, K., Yamamoto, Y., Ishihara, S., Murakami, A., Takabe, K., Miyake, C. and Sato, F. (2009) Knockdown of the PsbP protein does not prevent assembly of the dimeric PSII core complex but impairs accumulation of photosystem II supercomplexes in tobacco. *Biochim. Biophys. Acta*, **1787**, 873–881.
- Ifuku, K., Nakatsu, T., Kato, H. and Sato, F. (2004) Crystal structure of the PsbP protein of photosystem II from *Nicotiana tabacum*. *EMBO Rep.* **5**, 362–367.
- Ifuku, K., Nakatsu, T., Shimamoto, R., Yamamoto, Y., Ishihara, S., Kato, H. and Sato, F. (2005a) Structure and function of the PsbP protein of photosystem II from higher plants. *Photosynth. Res.* **84**, 251–255.
- Ifuku, K., Yamamoto, Y., Ono, T.A., Ishihara, S. and Sato, F. (2005b) PsbP protein, but not PsbQ protein, is essential for the regulation and stabilization of photosystem II in higher plants. *Plant Physiol.* **139**, 1175–1184.
- Ifuku, K., Ishihara, S., Shimamoto, R., Ido, K. and Sato, F. (2008) Structure, function, and evolution of the PsbP protein family in higher plants. *Photosynth. Res.* **98**, 427–437.
- Ifuku, K., Endo, T., Shikanai, T. and Aro, E.M. (2011a) Structure of the chloroplast NADH dehydrogenase-like complex: nomenclature for nuclear-encoded subunits. *Plant Cell Physiol.* **52**, 1560–1568.
- Ifuku, K., Ido, K. and Sato, F. (2011b) Molecular functions of PsbP and PsbQ proteins in the photosystem II supercomplex. *J. Photochem. Photobiol. B*, **104**, 158–164.
- Ihnatowicz, A., Pesaresi, P., Varotto, C., Richly, E., Schneider, A., Jahns, P., Salamini, F. and Leister, D. (2004) Mutants for photosystem I subunit D of *Arabidopsis thaliana*: effects on photosynthesis, photosystem I stability and expression of nuclear genes for chloroplast functions. *Plant J.* **37**, 839–852.
- Jarvi, S., Suorsa, M., Paakkarinen, V. and Aro, E.M. (2011) Optimized native gel systems for separation of thylakoid protein complexes: novel super- and mega-complexes. *Biochem. J.* **439**, 207–214.
- Kakiuchi, S., Uno, C., Ido, K., Nishimura, T., Noguchi, T., Ifuku, K. and Sato, F. (2012) The PsbQ protein stabilizes the functional binding of the PsbP protein to photosystem II in higher plants. *Biochim. Biophys. Acta*, **1817**, 1346–1351.
- Kavelaki, K. and Ghanotakis, D.F. (1991) Effect of the manganese complex on the binding of the extrinsic proteins (17-kDa, 23-kDa and 33-kDa) of photosystem II. *Photosynth. Res.* **29**, 149–155.
- Lennartz, K., Plücker, H., Seidler, A., Westhoff, P., Bechtold, N. and Meierhoff, K. (2001) HCF164 encodes a thioredoxin-like protein involved in the biogenesis of the cytochrome *b₆f* complex in *Arabidopsis*. *Plant Cell*, **13**, 2539–2551.
- Li, X.P., Bjorkman, O., Shih, C., Grossman, A.R., Rosenquist, M., Jansson, S. and Niyogi, K.K. (2000) A pigment-binding protein essential for regulation of photosynthetic light harvesting. *Nature*, **403**, 391–395.
- Liu, H., Frankel, L.K. and Bricker, T.M. (2009) Characterization and complementation of a *psbR* mutant in *Arabidopsis thaliana*. *Arch. Biochem. Biophys.* **489**, 34–40.
- Lunde, C., Jensen, P.E., Haldrup, A., Knoetzel, J. and Scheller, H.V. (2000) The PSI-H subunit of photosystem I is essential for state transitions in plant photosynthesis. *Nature*, **408**, 613–615.
- Lundin, B., Nurmi, M., Rojas-Stuetz, M., Aro, E.M., Adamska, I. and Spetea, C. (2008) Towards understanding the functional difference between the two PsbO isoforms in *Arabidopsis thaliana* – insights from phenotypic analyses of *psbo* knockout mutants. *Photosynth. Res.* **98**, 405–414.
- Martinez-Garcia, J.F., Monte, E. and Quail, P.H. (1999) A simple, rapid and quantitative method for preparing *Arabidopsis* protein extracts for immunoblot analysis. *Plant J.* **20**, 251–257.
- Mayfield, S.P., Bennoun, P. and Rochaix, J.D. (1987) Expression of the nuclear encoded OEE1 protein is required for oxygen evolution and stability of photosystem II particles in *Chlamydomonas reinhardtii*. *EMBO J.* **6**, 313–318.
- Miyao, M. and Murata, N. (1989) The mode of binding of three extrinsic proteins of 33-kDa, 23-kDa and 18-kDa in the photosystem II complex of spinach. *Biochim. Biophys. Acta*, **977**, 315–321.
- Murakami, R., Ifuku, K., Takabayashi, A., Shikanai, T., Endo, T. and Sato, F. (2002) Characterization of an *Arabidopsis thaliana* mutant with impaired *PsbO*, one of two genes encoding extrinsic 33-kDa proteins in photosystem II. *FEBS Lett.* **523**, 138–142.
- Murakami, R., Ifuku, K., Takabayashi, A., Shikanai, T., Endo, T. and Sato, F. (2005) Functional dissection of two *Arabidopsis* PsbO proteins: PsbO1 and PsbO2. *FEBS J.* **272**, 2165–2175.
- Pagliano, C., La Rocca, N., Andreucci, F., Deak, Z., Vass, I., Rascio, N. and Barbato, R. (2009) The extreme halophyte *Salicornia veneta* is depleted of the extrinsic PsbQ and PsbP proteins of the oxygen-evolving complex without loss of functional activity. *Ann. Bot.* **103**, 505–515.
- Pesaresi, P., Hertle, A., Pribil, M. et al. (2009) *Arabidopsis* STN7 kinase provides a link between short- and long-term photosynthetic acclimation. *Plant Cell*, **21**, 2402–2423.
- Pribil, M., Pesaresi, P., Hertle, A., Barbato, R. and Leister, D. (2010) Role of plastid protein phosphatase TAP38 in LHClI dephosphorylation and thylakoid electron flow. *PLoS Biol.* **8**, e1000288.
- Rosso, M.G., Li, Y., Strizhov, N., Reiss, B., Dekker, K. and Weisshaar, B. (2003) An *Arabidopsis thaliana* T-DNA mutagenized population (GABI-Kat) for flanking sequence tag-based reverse genetics. *Plant Mol. Biol.* **53**, 247–259.
- Schagger, H. and von Jagow, G. (1987) Tricine-sodium dodecyl sulfate-polyacrylamide gel electrophoresis for the separation of proteins in the range from 1 to 100 kDa. *Anal. Biochem.* **166**, 368–379.
- Seidler, A., Rutherford, A.W. and Michel, H. (1996) On the role of the N-terminus of the extrinsic 33 kDa protein of photosystem II. *Plant Mol. Biol.* **31**, 183–188.
- Sessions, A., Burke, E., Presting, G. et al. (2002) A high-throughput *Arabidopsis* reverse genetics system. *Plant Cell*, **14**, 2985–2994.
- Sirpio, S., Allahverdiyeva, Y., Holmström, M., Khrouchtchova, A., Haldrup, A., Battchikova, N. and Aro, E.M. (2009) Novel nuclear-encoded subunits of the chloroplast NAD(P)H dehydrogenase complex. *J. Biol. Chem.* **284**, 905–912.
- Stockhaus, J., Hofer, M., Renger, G., Westhoff, P., Wydrzynski, T. and Willmitzer, L. (1990) Antisense RNA efficiently inhibits formation of the 10 kDa polypeptide of photosystem II in transgenic potato plants: analysis of the role of the 10 kDa protein. *EMBO J.* **9**, 3013–3021.
- Sundaresan, V., Springer, P., Volpe, T., Howard, S., Jones, J.D., Dean, C., Ma, H. and Martienssen, R. (1995) Patterns of gene action in plant development revealed by enhancer trap and gene trap transposable elements. *Genes Dev.* **9**, 1797–1810.
- Suorsa, M., Sirpio, S., Allahverdiyeva, Y., Paakkarinen, V., Mamedov, F., Styring, S. and Aro, E.M. (2006) PsbR, a missing link in the assembly of the oxygen-evolving complex of plant photosystem II. *J. Biol. Chem.* **281**, 145–150.
- Takabayashi, A., Ishikawa, N., Obayashi, T., Ishida, S., Obokata, J., Endo, T. and Sato, F. (2009) Three novel subunits of *Arabidopsis* chloroplast NAD(P)H dehydrogenase identified by bioinformatic and reverse genetic approaches. *Plant J.* **57**, 207–219.

- Thornton, L.E., Ohkawa, H., Roose, J.L., Kashino, Y., Keren, N. and Pakrasi, H.B. (2004) Homologs of plant PsbP and PsbQ proteins are necessary for regulation of photosystem II activity in the cyanobacterium *Synechocystis* 6803. *Plant Cell*, **16**, 2164–2175.
- Tikkanen, M., Piippo, M., Suorsa, M., Sirpio, S., Mulo, P., Vainonen, J., Vener, A.V., Allahverdiyeva, Y. and Aro, E.M. (2006) State transitions revisited – a buffering system for dynamic low light acclimation of *Arabidopsis*. *Plant Mol. Biol.* **62**, 779–793.
- Trotta, A., Redondo-Gomez, S., Pagliano, C., Clemente, M.E., Rascio, N., Rocca, N.L., Antonacci, A., Andreucci, F. and Barbato, R. (2012) Chloroplast ultrastructure and thylakoid polypeptide composition are affected by different salt concentrations in the halophytic plant *Arthrocnemum macrostachyum*. *J. Plant Physiol.* **169**, 111–116.
- Umena, Y., Kawakami, K., Shen, J.R. and Kamiya, N. (2011) Crystal structure of oxygen-evolving photosystem II at a resolution of 1.9 Å. *Nature*, **473**, 55–60.
- Vainonen, J.P., Sakuragi, Y., Stael, S. *et al.* (2008) Light regulation of CaS, a novel phosphoprotein in the thylakoid membrane of *Arabidopsis thaliana*. *FEBS J.* **275**, 1767–1777.
- Vass, I., Kirilovsky, D. and Etienne, A.L. (1999) UV-B radiation-induced donor- and acceptor-side modifications of photosystem II in the cyanobacterium *Synechocystis* sp. PCC 6803. *Biochemistry*, **38**, 12786–12794.
- Vergnolle, C., Vaultier, M.N., Taconnat, L., Renou, J.P., Kader, J.C., Zachowski, A. and Ruelland, E. (2005) The cold-induced early activation of phospholipase C and D pathways determines the response of two distinct clusters of genes in *Arabidopsis* cell suspensions. *Plant Physiol.* **139**, 1217–1233.
- Verwoerd, T.C., Dekker, B.M. and Hoekema, A. (1989) A small-scale procedure for the rapid isolation of plant RNAs. *Nucleic Acids Res.* **17**, 2362.
- Yi, X., McChargue, M., Laborde, S., Frankel, L.K. and Bricker, T.M. (2005) The manganese-stabilizing protein is required for photosystem II assembly/stability and photoautotrophy in higher plants. *J. Biol. Chem.* **280**, 16170–16174.
- Yi, X., Hargett, S.R., Frankel, L.K. and Bricker, T.M. (2006) The PsbQ protein is required in *Arabidopsis* for photosystem II assembly/stability and photoautotrophy under low light conditions. *J. Biol. Chem.* **281**, 26260–26267.
- Yi, X., Hargett, S.R., Liu, H., Frankel, L.K. and Bricker, T.M. (2007) The PsbP protein is required for photosystem II complex assembly/stability and photoautotrophy in *Arabidopsis thaliana*. *J. Biol. Chem.* **282**, 24833–24841.
- Yi, X., Hargett, S.R., Frankel, L.K. and Bricker, T.M. (2008) The effects of simultaneous RNAi suppression of PsbO and PsbP protein expression in photosystem II of *Arabidopsis*. *Photosynth. Res.* **98**, 439–448.
- Yi, X., Hargett, S.R., Frankel, L.K. and Bricker, T.M. (2009) The PsbP protein, but not the PsbQ protein, is required for normal thylakoid architecture in *Arabidopsis thaliana*. *FEBS Lett.* **583**, 2142–2147.

Plastid signaling involves GUN1-dependent formation of complexes containing plastid ribosomal protein S1 and Mg chelatase subunit D

Luca Tadini^{1,#}, Paolo Pesaresi^{2,#}, Tatjana Kleine¹, Fabio Rossi², Arthur Guljamow¹, Simona Masiero², Mathias Pribil¹, Maxi Rothbart³, Boris Hedtke³, Bernhard Grimm³, Gerhard Wanner⁴, Dario Leister^{1,5*}

¹*Plant Molecular Biology, Department Biology I, Ludwig-Maximilians-Universität München, 82152 Planegg-Martinsried, Germany*. ²*Department of Biosciences, University of Milan, 20133 Milano, Italy*. ³*Plant Physiology, Institute of Biology, Humboldt-University of Berlin, 10115 Berlin, Germany*. ⁴*Ultrastructural Research, Department Biology I, Ludwig-Maximilians-Universität München, 82152 Planegg-Martinsried, Germany*. ⁵*Copenhagen Plant Science Center (CPSC), University of Copenhagen, Copenhagen, 1871 Frederiksberg C, Denmark*.

[#]These authors contributed equally to this work.

*e-mail: leister@lmu.de

Plastid-to-nucleus retrograde signaling serves to coordinate nuclear gene expression with chloroplast functions. Genetic evidence suggests that the chloroplast protein GUN1 integrates signals derived from perturbations in plastid redox state, plastid gene expression (PGE) and tetrapyrrole biosynthesis (TPB). However, the molecular mechanism by which GUN1 integrates retrograde signaling in the chloroplast is unclear. Here we show that GUN1 physically interacts with several chloroplast proteins, including the plastid ribosomal protein S1 (PRPS1), Mg-chelatase subunit D (CHLD) and two other TPB enzymes known to activate retrograde signaling. The abundance of PRPS1 and CHLD, as well as their association with protein complexes, is modulated by GUN1. We postulate that GUN1 controls the formation of “retrosome” complexes, which contain components involved in PGE or TPB, and trigger retrograde signaling. Retrosomes may also serve to coordinate PGE and TPB activity at the protein level.

Developmental or metabolic changes in chloroplasts can have profound effects on the rest of the plant cell. Such intracellular responses are associated with signals that originate in chloroplasts and lead to large-scale changes in nuclear gene expression (retrograde signaling)¹⁻³. While norflurazon (NF) efficiently blocks expression of photosynthesis-associated nuclear genes (PhANGs) in wild-type (WT) plants, the so-called *genomes uncoupled* (*gun*) mutants⁴ are characterized by their capacity to express PhANGs after exposure to NF. Because the proteins GUN2, 3, 4, 5 and 6 are all involved in tetrapyrrole biosynthesis (TPB)⁵⁻⁷, one of the retrograde signaling pathways is clearly triggered by perturbations in TPB. Besides the TPB pathway, signals derived from plastid gene expression (PGE) and the thylakoid redox state (Redox), as well as products of secondary metabolism or carotenoid oxidation and mobile transcription factors have been implicated in retrograde signaling^{1,2,8-13}. Moreover, retrograde signals contribute both to the developmental control of

organelle biogenesis (biogenic control) and to rapid adjustments in energy metabolism (operational control)^{3,14}.

Genetic evidence suggests that GUN1 signaling activates the nuclear transcription factor ABI4¹⁵. GUN1-ABI4 integrates signals from three different retrograde signaling pathways: TPB, PGE and Redox¹⁵. Strikingly, only very young plants show the *gun* phenotype, so GUN1-ABI4 signaling is thought to operate mainly in the biogenic control circuit³. GUN1 contains two domains with putative nucleic acid-binding capacity - a pentatricopeptide repeat (PPR) and small MutS-related (SMR) domain; and, indeed, *in-vitro* experiments have suggested that GUN1 binds DNA¹⁵. Here, we analyzed the mechanism by which GUN1 integrates signals from different retrograde pathways and show that retrograde signaling appears to involve GUN1-dependent formation of protein complexes (which we call retrosomes) containing components of PGE or TPB. Such retrosomes might also coordinate PGE and TPB activities at the protein level.

Results

Genetic interactions of *gun1* with mutations affecting plastid ribosomal proteins

We found that *GUN1* is co-expressed with PGE genes, including *PRPS1* encoding the plastid ribosomal S1 protein (Supplementary Fig. 1a), and that GUN1 also operates in adult leaves (Supplementary Fig. 1b,c). However, although GUN1 is a PPR-SMR protein, we could not detect obvious interactions between GUN1 and nucleic acids (Supplementary Fig. 2a-c).

Therefore, we studied the functional relationship between GUN1 and selected plastid ribosomal subunits, in particular PRPS1. To this end, a T-DNA insertion based mutation of the *GUN1* gene (*gun1-102*) was introduced into genetic backgrounds carrying mutations in genes for components of the small (PRPS1 and PRPS21) and large (PRPL11) subunits of the plastid ribosome. Notably, while *gun1-102* plants displayed WT-like growth and photosynthesis, the three ribosomal mutants showed, to varying degrees, perturbations in

photosynthetic electron flow and decreased growth rates (Fig. 1a). Furthermore, while *gun1-102 prps21-1* behaved like the *prps21-1* single mutant, *gun1-102 prpl11-1* and *gun1-102 prps1-1* displayed either exacerbated (enhancer) or attenuated (suppressor) phenotypes (Fig. 1a,b). Thus, a strongly enhancing effect of *gun1-102* was observed in *gun1-102 prpl11-1*, which displayed a highly penetrant synthetic seedling-lethal phenotype (Fig. 1a,c). Only about 3% of the double mutants developed beyond the cotyledon stage and produced variegated plants (Fig. 1d) with chlorotic sectors, which contained small plastids with vacuolated structures and plastoglobuli (Fig. 1e) and were not affected by exposure to increasing light intensities with respect to their abundance and size (Fig. 1d). This indicates that the white sectors are due to a specific, genetically determined defect in chloroplast biogenesis. In contrast, the *gun1-102* mutation suppressed the effects of the *prps1-1* mutation; hence, in *gun1-102 prps1-1* plants, the negative effect of the *prps1-1* mutation on growth and photosynthetic performance was largely attenuated (Fig. 1a,b), indicating that a functional relationship exists between GUN1 and PRPS1. The genetic interactions between *gun1-102* and mutations affecting plastid ribosomes are specific, because *gun2*, *3*, *4* and *5* all failed to suppress the *prps1-1* phenotype and did not induce seedling lethality when combined with the *prpl11-1* mutation (Supplementary Fig. 3).

GUN1 controls PRPS1 accumulation at the protein level

Prokaryotic ribosomal S1 protein recognizes mRNA leaders and mediates binding of diverse mRNAs to the ribosome at the translation initiation step¹⁶. Given that this S1 function is conserved in chloroplasts, complete inactivation of PRPS1 can be expected to result in lethality in Arabidopsis, and such mutants have not been described yet. Accordingly, the *prps1-1* allele used here is leaky (providing 8% of WT *PRPS1* transcript levels¹⁷). Processing and abundance of plastid rRNAs is not altered in *gun1-102*, whereas both *prps21-1* and *prps1-1* strains exhibit aberrant processing of 23S and 4.5S precursor rRNAs (Fig. 2a). Intriguingly,

in *gun1-102 prps1-1*, but not in *gun1-102 prps21-1*, the changes in 23S and 4.5S processing were largely attenuated (Fig. 2a). At the protein level, reduced PRPS1 accumulation (~1/3 of WT levels) in *prps1-1* was associated with decreased levels of PRPS5 and PRPL2 (Fig. 2b). In *gun1-102 prps1-1*, the PRPS1 protein accumulated to WT-like levels, and amounts of PRPS5 and PRPL2 were near normal. The T-DNA in *prps1-1* disrupts the promoter region of the gene¹⁷, and in the *gun1-102 prps1-1* mutant *PRPS1* mRNA levels were similar to *prps1-1* (Fig. 2a), suggesting that the suppressor effects are based on posttranscriptional events. Again, the suppressor effects observed are specific to *gun1-102*, because *gun2*, *3*, *4* and *5* each failed to rescue the accumulation of PRPS1 when combined with the *prps1-1* mutation (Fig. 2c). In addition, the decreased formation of polysomes observed in *prps1-1* and *prps21-1* mutants was attenuated in *gun1-102 prps1-1*, but not in *gun1-102 prps21-1* leaves (Supplementary Fig. 4a). Accordingly, the drop in translation rates observed in *prps1-1* was also reversed in *gun1-102 prps1-1* plants (Supplementary Fig. 4b).

Effects of misregulation of *PRPS1* expression

Overexpression of a functional *GUNI:GFP* fusion (*oeGUNI-GFP*; Supplementary Fig. 5a-d) reduces PRPS1 accumulation to about two-thirds of WT (Fig. 3a and Supplementary Fig. 5c), which supports the idea that GUN1 negatively regulates PRPS1 levels. Moreover, since amounts of PRPS1 reach about 175% of WT levels in the *prpl11-1* mutant (Fig. 3a), a further increase upon removal of GUN1 in the *prpl11-1* background might account for the seedling-lethal phenotype seen in the double mutant. This would in turn imply that the surviving *gun1-102 prpl11-1* plants (see Fig. 1d) somehow managed to reduce PRPS1 concentrations to tolerable levels in sufficient cells during early development, before they experienced irreversible lethal effects. And indeed, levels of PRPS1 in surviving *gun1-102 prpl11-1* plants are lower than in WT (Fig. 3a).

Overexpression of the S1 protein in *E. coli* leads to the accumulation of “free” S1, which is thought to inhibit translation by sequestering mRNAs¹⁸. To investigate whether a similar mechanism takes place in Arabidopsis, the relative level of ribosome-bound and non-associated PRPS1 in Arabidopsis was investigated (Fig. 3b, Supplementary Fig. 5e). Only PRPS1 appeared in a ribosome-free form representing most likely PRPS1-mRNA complexes, whereas all other ribosomal proteins tested (S5, S7, L2 and L4) were exclusively detected in ribosomal complexes. Altered GUN1 levels in *gun1-102* and *oeGUN1-GFP* had no effect on the size of the pool of PRPS1-mRNA complexes (Fig. 3b).

To further corroborate the hypothesis that increased levels of PRPS1 negatively affect translation, we generated transgenic Arabidopsis lines that overexpressed the *PRPS1* gene (*35S:PRPS1 prps1-1* or *oePRPS1*). At low frequencies (<1%), *oePRPS1* plants showed albino cotyledons and were seedling lethal. The progeny (four sibling plants each) of two viable overexpressors were analyzed in detail (*oePRPS1_1.1* to *_1.4*, Fig. 3c,d; *oePRPS1_2.1* to *2_4*, Supplementary Fig. 5f,g). Interestingly, in most of the lines, photosynthetic rates in young emerging leaves were markedly reduced, indeed more so than in *prps1-1* plants in some cases. These photosynthetic defects were associated with pale-green leaf pigmentation. In contrast, older leaves and the old sections of younger leaves on the same plants showed WT-like photosynthetic performance and coloration. In young leaves of the four *oePRPS1_1* plants, wide variation in PRPS1 expression was detected, in the absence of any clear correlation between transcript and protein levels (Fig. 3d), implying that plants counterbalance increased expression of *PRPS1* both at the transcript and the protein level. In all *oePRPS1_1* plants, relatively more mRNA-associated PRPS1 was observed than in WT (Fig. 3b), indicating that – as in *E. coli* – overexpression of PRPS1 might interfere with translation owing to mRNA trapping by excess ribosome-free PRPS1.

Because accumulation of PRPS1 protein, but not of its RNA template, is induced by heat, and knockdown of PRPS1 results in significant loss of heat tolerance, chloroplast

translation capacity has been suggested to be a critical factor in heat-responsive retrograde signaling¹⁹. Therefore, both GUN1 function and the cellular response to heat involve PRPS1. However, *prps1-1* and *oePRPS1* are not *gun* mutants (Supplementary Fig. 5h), implying that PRPS1 is either not involved in PGE signaling or the alterations in the PRPS1 levels in *prps1-1* and *oePRPS1* are insufficient to perturb PGE signaling. Vice versa, *gun1-102* and *oeGUN1-GFP* lines showed WT-like phenotypes after heat challenge (Supplementary Fig. 5i), indicating that the ~30% drop in PRPS1 levels observed in *oeGUN1-GFP* plants (see Fig. 3a) does not alter heat tolerance sufficiently to be detectable by our assay.

GUN1 promotes formation of complexes containing PRPS1 or CHLD

We used several approaches to test for physical interactions of GUN1 with PRPS1 and other ribosomal proteins, and with several TPB enzymes, including the D subunit of the magnesium-chelatase (CHLD) and with protoporphyrinogen oxidase (PPOX) – both of which are tightly coregulated with GUN1 at the transcriptional level (see Supplementary Fig. 1a). Based on yeast two-hybrid (Y2H) analyses, mature GUN1 (GUN1₄₃₋₉₁₈) indeed interacts directly with PRPS1 and CHLD, but not with PPOX or any other ribosomal protein tested (Fig. 4a, Supplementary Fig. 6a). In addition, GUN1 interacts with three other TPB enzymes, namely porphobilinogen deaminase (PBGD), uroporphyrinogen III decarboxylase (UROD2) and ferrochelatase I (FC1) (Fig. 4a). Interestingly, mutants defective in three of these GUN1 interactors – CHLD, PBGD and FC1 – have been described as *gun* mutants^{7,20,21}. Two other *GUN* gene products, coproporphyrinogen III oxidase 1 (CPO1, ref. ²¹) and the I subunit of the Mg chelatase (CHLI, ref. ²⁰), as well as GUN2, 3, 4 and 5, all failed to interact with GUN1 in our Y2H assay (Fig. 4a). To identify the protein-interacting domain(s) of GUN1, the N-terminal portion of GUN1 (GUN1₄₃₋₂₅₁, GUN1_N), its PPR-containing domain (GUN1₂₅₂₋₆₈₇, GUN1_M) and the C-terminal segment containing the SMR domain (GUN1₆₈₈₋₉₁₈, GUN1_C) were tested for their capacity to interact with the five proteins that interact with GUN1₄₃₋₉₁₈

(Fig. 4b). These experiments showed that all three GUN1 domains can interact with one or more of these proteins, and GUN1_N interacts with four of them. GUN1-FC1 interactions appear to require more than one of the three GUN1 domains tested here.

BiFC assays in tobacco-leaf mesophyll cells corroborated the interactions of GUN1 with PRPS1, CHLD, PBGD, UROD2 and FC1, indicating that these interactions occur also in planta (Fig. 4c). The distribution of yellow fluorescence signals resulting from these protein-protein interactions were localized to distinct spots within chloroplasts, resembling the distribution of green fluorescence emitted by the GUN1-GFP construct (see Supplementary Fig. 5b). The combination GSA1^{YN}-GUN1^{YC}, used as negative control, failed to produce a YFP signal.

Because (i) GUN1 interacts with PRPS1 and (ii) changes in GUN1 levels affect the accumulation of PRPS1 at the protein level (see Fig. 3a), we tested whether the abundance of the other three GUN1 interactors for which antibodies were available (CHLD, PBGD and UROD2) is also affected by alterations in GUN1 levels (Fig. 4d). In all three independent *oeGUN1-GFP* lines (Supplementary Fig. 5c), accumulation of CHLD – but not of the corresponding transcript (Supplementary Fig. 6b) – was increased by about 50% (Fig. 4d). This effect was specific, because neither PBGD or UROD2 nor any other protein involved in TPB for which antibodies were available (CHLI, CHLH and GUN4) varied in its concentration in lines with different levels of GUN1.

In light of these GUN1-dependent changes in the abundance of PRPS1 and CHLD, we analysed the distribution of PRPS1 and CHLD in protein complexes by sucrose-gradient fractionation and BN/SDS-PAGE analysis followed by Western analysis in *gun1-102*, WT (Col-0) and *oeGUN1-GFP* plants. The two proteins were detected in molecular species with different masses (PRPS1, ~200 kDa; CHLD, ~400 kDa), indicating that they associate with distinct complexes. Interestingly, increased GUN1 dosage enhances the stability, or increases the molecular mass, of protein complexes containing PRPS1 or CHLD, as demonstrated by

both sucrose-gradient (Fig. 4e) and BN/SDS 2D-PAGE gel (Fig. 4f) analyses. Thus, in *gun1*, but not in WT or *oeGUNI-GFP*, PRPS1 monomers accumulate; in *oeGUNI-GFP* plants, PRPS1-containing complexes clearly have a higher molecular mass than in WT (Fig. 4f). For CHLD, increasing doses of GUN1 resulted in a shift of CHLD-containing complexes towards a higher molecular mass (Fig. 4f). Moreover, GUN1-GFP also accumulates in complexes, as demonstrated by analysing *oeGUNI-GFP* plants with a GFP-specific antibody.

Discussion

Only seven other proteins in Arabidopsis, all located in chloroplasts or mitochondria, are PPR-SMR domain proteins like GUN1, and functions in the promotion of transcription or RNA endonuclease activity have been suggested for them²². However, unlike the other PPR-SMR proteins, GUN1 seems to be expressed in very small amounts and has not yet been detected by proteomic approaches²². Previous analyses argued against a prominent role for GUN1 in plastid RNA metabolism²³, and our NIP-chip and one-hybrid experiments also failed to detect any significant GUN1-nucleic acid interaction. Instead, our study demonstrates that GUN1 interacts with several chloroplast proteins. Previous analyses have shown that GUN1 has a function in early plant development^{24,25}, and the seedling-lethal phenotype of *gun1-102 prpl11-1* reported here (see Fig. 1b) corroborates this. But additionally, GUN1 clearly modulates PhANG expression (see Supplementary Fig. 1b) and PRPS1 accumulation (Fig. 3a) in adult leaves, implying that GUN1 also contributes to operational control.

Because GUN1 physically interacts with PRPS1 and CHLD, and modulates the stability or formation of complexes containing these two proteins, we hypothesize that perturbations in PGE and TPB mobilize specific PGE- and TPB-related components, respectively, making them (more) available for interaction with GUN1 to trigger the formation of two different complexes. Each of these complexes can then elicit retrograde signaling, resulting into

downregulation of PhANG expression to match the decrease in activity of PGE or TPB in the chloroplast (Fig. 5a). We therefore designate these two types of complexes as “retrograde signaling triggering complexes” or “retrosomes”. In light of its low abundance, GUN1 might not be a component of retrosomes, but instead function as an assembly factor required for their formation. The GUN1-containing complexes that normally accumulate only transiently during complex assembly might grow in size and stability when GUN1 is overexpressed, which would explain their increase in molecular mass in *oeGUN1-GFP* plants (see Fig. 4f). Lack of GUN1 should interfere with the formation of both types of retrosomes, in order to accommodate the observation that *gun1* is the only mutation known to suppress the effect of both lincomycin and norflurazon on PhANG expression (Fig. 5b). In addition, the model predicts that, in the absence of GUN1, the “mobilized” PGE- and TPB-related components should persist as free proteins (Fig. 5b), and indeed PRPS1 accumulates as the free monomer in the *gun1-102* mutant (see Fig. 4f), as expected if GUN1 normally captures PRPS1 released from ribosomes to facilitate its integration into retrosomes. An intriguing possibility is that retrosomes might even be bifunctional and provide the organellar counterpart of the transcriptional coexpression of PGE and TPB genes in the nucleus²⁶, i.e. that they could also coordinate PGE and TPB activities at the protein level (Fig. 5a). In this scenario, such coordination should be inhibitory; for instance, when PGE is perturbed, the resulting retrosome might sequester enzymatic TPB activity from its substrate, thus concomitantly reducing TPB activity, and vice versa. Alternatively, PGE and TPB activities could also be diminished by proteolytic degradation of retrosomes. Indeed, many genes encoding peptidases or proteases are co-expressed with *GUN1* (see Supplementary Fig. 1a), explaining why PRPS1 levels decrease in *oeGUN1-GFP* plants and providing a means to switch off the retrograde signal as a prerequisite for dynamic signaling. In fact, associations between CHLD and ribosomes have been described in barley and *Rhodobacter*²⁷ and interpreted as reflecting a mechanism that coordinates PGE and TPB. Because PRPS1 and CHLD are highly abundant

in chloroplasts²⁸, the complexes they form (Fig. 4f) should be also sufficiently abundant to fulfil such a function in coordinating metabolic activities.

Methods

Plant material and cultivation. The *Arabidopsis thaliana* T-DNA insertion mutant lines *gun1-102* (SAIL_290_D09) and *prps21-1* (SAIL_1173_CO3) are both from the SAIL mutant collection²⁹. The regions flanking the T-DNA insertion in the vector pCSA110 were PCR-amplified and sequenced (primer sequences in Supplementary Table 1): *gun1-102* contains the T-DNA insertion in exon 2 (position 2313 relative to the start codon); the T-DNA in *prps21-1* lies in the only intron (position 1154). Both mutations prevent the accumulation of the respective transcripts, as determined by RT-PCR analyses (primer sequences in Supplementary Table 1), and the *gun1-102* line shows a *gun* phenotype (see Supplementary Fig. 4h). The *oeGUN1-GFP* lines were generated by introducing the *GUN1* coding sequence, under the control of the 35S promoter from the Cauliflower Mosaic Virus, into WT (Col-0) using the vector pB7FWG2 (Flanders Interuniversity Institute for Biotechnology, Gent, Belgium). All other mutants used here have been described previously, and are listed in Supplementary Methods. *Arabidopsis thaliana* plants were grown on soil in a climate chamber as described³⁰.

Electron microscopy. Pieces of leaf tissue from *gun1-102 prp111-1* plants, grown at 80 $\mu\text{mol photons m}^{-2}\text{s}^{-1}$, were fixed and postfixed as described³¹. All micrographs were taken using an EM 912 electron microscope (Zeiss, <http://zeiss.com>).

Coexpression analyses. To identify genes represented on the ATH1 microarray (22K) chip that show significant co-expression with *GUN1*, an expression correlation analysis with the “CoExSearch” tool implemented in ATTED-II (<http://atted.jp/>; refs. ^{32,33}) was performed. Hierarchical clustering was carried out with the single linkage method provided by the „HCluster“ tool in ATTED-II. Subcellular localizations for the different proteins were inferred from TAIR (<http://arabidopsis.org/>) and the “subcellular localization of proteins in Arabidopsis” database (SUBA3; <http://suba.plantenergy.uwa.edu.au/>).

Chlorophyll (Chl) a fluorescence measurements. In vivo Chl a fluorescence of leaves was measured as described³⁰ employing a Dual-PAM-100 (Walz, Effeltrich, Germany). Whole-plant Chl a fluorescence was recorded using an imaging chlorophyll fluorometer (Walz, Germany) as reported earlier³⁴.

Nucleic acid analyses. *Arabidopsis thaliana* genomic DNA was isolated³⁵ and RNA was purified from total leaf frozen tissue as before³⁶. Northern analysis was performed under stringent conditions³⁷ on 10- μ g samples of total RNA. Probes complementary to nuclear and chloroplast genes were used for the hybridizations. Primers used to amplify the probes are listed in Supplementary Table 1. All probes used were cDNA fragments labelled with ³²P. Quantitative real-time PCR (qRT-PCR) profiling was done as described previously³⁸. All reactions were performed in triplicate on three biological replicates, and primers are listed in Supplementary Table 1.

Immunoblot analyses. Immunoblot analyses were carried out as described³⁵ and immunodecorated with specific antibodies. Antibodies directed against plastid ribosomal proteins were obtained from Uniplastomic (Biviers, France), the GFP antibody from Life Technologies (Carlsbad, USA). Antibodies specific for TPB enzymes were obtained from

R.M. Larkin (Michigan State University; CHLI, CHLD and CHLH), P.E. Jensen (CHLD), B. Grimm (Humbolt University, GUN4) and A. Smith (University of Cambridge, PBGD and UROD).

Chloroplast isolation and sub-fractionation. Chloroplast isolation and preparation of soluble (stroma) and insoluble (thylakoids/envelope) fractions was performed as described³⁹.

Protein complex analyses. For sucrose gradient analysis, intact chloroplasts isolated as above were solubilized in Extraction Buffer (see above; ref. ³⁹) containing 0.6% (v/v) NP-40 detergent (15 min, 4°C). After centrifugation (16,000 g for 15 min), the supernatant was layered on a sucrose step-gradient (15%-55% (w/v)) and centrifuged (5 h, 240,000 g). Sixteen fractions were collected and analyzed by SDS-PAGE on a 12% PAA gel.

For BN/SDS-PAGE analysis of stromal protein complexes, chloroplasts from 4-week-old leaf material (corresponding to 60 µg of Chl) were isolated as described above, resuspended in 100 µl of 30 mM HEPES-KOH (pH 8.0), 60 mM KOAc and 10 mM MgOAc, and solubilized by adding NP-40 (final concentration 0.5% (v/v)) and centrifuged (16,000 g, 15 min, 4 °C). The supernatant was then analysed by BN/SDS PAGE as described previously⁴⁰.

For two-hybrid assays, the coding sequences for the proteins of interest, devoid of the chloroplast transit peptides (cTP) (see Supplementary Table 1 for primer sequences), were cloned into pGBKT7 (GUN1) and pGADT7 (PRPS1, S21, L11 and L24; CHLD; FC1 and 2; PBGD; UROD1 and 2; CPO1, GSA1 and 2, CHLI1 and 2) vectors (Clontech Otsu, Japan), or *vice versa*. Interactions in yeast were then analysed as described before⁴¹.

Bimolecular fluorescence complementation (BiFC) analyses. Cloning of genes into pVyNE or pVyCE (ref. ⁴²), which carry sequences encoding the N-terminal or the C-terminal

portion of the Venus protein (a YFP derivative), respectively, transformation of *Agrobacterium tumefaciens*, infiltration of *Nicotiana benthamiana* leaves and BiFC analyses were performed as described⁴³.

References

- 1 Chi, W., Sun, X. & Zhang, L. Intracellular signaling from plastid to nucleus. *Annu Rev Plant Biol* **64**, 559-582 (2013).
- 2 Nott, A., Jung, H. S., Koussevitzky, S. & Chory, J. Plastid-to-nucleus retrograde signaling. *Annu Rev Plant Biol* **57**, 739-759 (2006).
- 3 Pogson, B. J., Woo, N. S., Forster, B. & Small, I. D. Plastid signalling to the nucleus and beyond. *Trends Plant Sci* **13**, 602-609 (2008).
- 4 Susek, R. E., Ausubel, F. M. & Chory, J. Signal transduction mutants of Arabidopsis uncouple nuclear CAB and RBCS gene expression from chloroplast development. *Cell* **74**, 787-799 (1993).
- 5 Mochizuki, N., Brusslan, J. A., Larkin, R., Nagatani, A. & Chory, J. Arabidopsis genomes uncoupled 5 (GUN5) mutant reveals the involvement of Mg-chelatase H subunit in plastid-to-nucleus signal transduction. *Proc Natl Acad Sci U S A* **98**, 2053-2058 (2001).
- 6 Larkin, R. M., Alonso, J. M., Ecker, J. R. & Chory, J. GUN4, a regulator of chlorophyll synthesis and intracellular signaling. *Science* **299**, 902-906 (2003).
- 7 Woodson, J. D., Perez-Ruiz, J. M. & Chory, J. Heme synthesis by plastid ferrochelatase I regulates nuclear gene expression in plants. *Curr Biol* **21**, 897-903 (2011).
- 8 Woodson, J. D. & Chory, J. Coordination of gene expression between organellar and nuclear genomes. *Nat Rev Genet* **9**, 383-395 (2008).

- 9 Estavillo, G. M. *et al.* Evidence for a SAL1-PAP chloroplast retrograde pathway that functions in drought and high light signaling in Arabidopsis. *Plant Cell* **23**, 3992-4012 (2011).
- 10 Xiao, Y. *et al.* Retrograde signaling by the plastidial metabolite MEcPP regulates expression of nuclear stress-response genes. *Cell* **149**, 1525-1535 (2012).
- 11 Ramel, F. *et al.* Carotenoid oxidation products are stress signals that mediate gene responses to singlet oxygen in plants. *Proc Natl Acad Sci U S A* **109**, 5535-5540 (2012).
- 12 Isemer, R. *et al.* Recombinant Whirly1 translocates from transplastomic chloroplasts to the nucleus. *FEBS Lett* **586**, 85-88 (2012).
- 13 Sun, X. *et al.* A chloroplast envelope-bound PHD transcription factor mediates chloroplast signals to the nucleus. *Nat Commun* **2**, 477 (2011).
- 14 Jarvis, P. & Lopez-Juez, E. Biogenesis and homeostasis of chloroplasts and other plastids. *Nat Rev Mol Cell Biol* **14**, 787-802 (2013).
- 15 Koussevitzky, S. *et al.* Signals from chloroplasts converge to regulate nuclear gene expression. *Science* **316**, 715-719 (2007).
- 16 Hajnsdorf, E. & Boni, I. V. Multiple activities of RNA-binding proteins S1 and Hfq. *Biochimie* **94**, 1544-1553 (2012).
- 17 Romani, I. *et al.* Versatile roles of Arabidopsis plastid ribosomal proteins in plant growth and development. *Plant J* **72**, 922-934 (2012).
- 18 Delvillani, F., Papiani, G., Deho, G. & Briani, F. S1 ribosomal protein and the interplay between translation and mRNA decay. *Nucl Acids Res* **39**, 7702-7715 (2011).
- 19 Yu, H. D. *et al.* Downregulation of chloroplast RPS1 negatively modulates nuclear heat-responsive expression of HsfA2 and its target genes in Arabidopsis. *PLoS Genet* **8**, e1002669 (2012).

- 20 Huang, Y. S. & Li, H. M. Arabidopsis CHLI2 can substitute for CHLI1. *Plant Physiol* **150**, 636-645 (2009).
- 21 Strand, A., Asami, T., Alonso, J., Ecker, J. R. & Chory, J. Chloroplast to nucleus communication triggered by accumulation of Mg-protoporphyrinIX. *Nature* **421**, 79-83 (2003).
- 22 Liu, S., Melonek, J., Boykin, L. M., Small, I. & Howell, K. A. PPR-SMRs: ancient proteins with enigmatic functions. *RNA Biol* **10**, 1501-1510 (2013).
- 23 Woodson, J. D., Perez-Ruiz, J. M., Schmitz, R. J., Ecker, J. R. & Chory, J. Sigma factor-mediated plastid retrograde signals control nuclear gene expression. *Plant J* **73**, 1-13 (2012).
- 24 Cottage, A., Mott, E. K., Kempster, J. A. & Gray, J. C. The Arabidopsis plastid-signalling mutant *gun1* (*genomes uncoupled1*) shows altered sensitivity to sucrose and abscisic acid and alterations in early seedling development. *J Exp Bot* **61**, 3773-3786 (2010).
- 25 Ruckle, M. E., DeMarco, S. M. & Larkin, R. M. Plastid signals remodel light signaling networks and are essential for efficient chloroplast biogenesis in Arabidopsis. *Plant Cell* **19**, 3944-3960 (2007).
- 26 Leister, D., Wang, X., Haberer, G., Mayer, K. F. & Kleine, T. Intracompartamental and intercompartmental transcriptional networks coordinate the expression of genes for organellar functions. *Plant Physiol* **157**, 386-404 (2011).
- 27 Kannangara, C. G., Vothknecht, U. C., Hansson, M. & von Wettstein, D. Magnesium chelatase: association with ribosomes and mutant complementation studies identify barley subunit Xantha-G as a functional counterpart of *Rhodobacter* subunit BchD. *Mol Gen Genet* **254**, 85-92 (1997).
- 28 Zybilov, B. *et al.* Sorting signals, N-terminal modifications and abundance of the chloroplast proteome. *PLoS One* **3**, e1994 (2008).

- 29 Sessions, A. *et al.* A high-throughput Arabidopsis reverse genetics system. *Plant Cell* **14**, 2985-2994 (2002).
- 30 Pesaresi, P. *et al.* Arabidopsis STN7 kinase provides a link between short- and long-term photosynthetic acclimation. *Plant Cell* **21**, 2402-2423 (2009).
- 31 Aseeva, E. *et al.* Vipp1 is required for basic thylakoid membrane formation but not for the assembly of thylakoid protein complexes. *Plant Physiol Biochem* **45**, 119-128 (2007).
- 32 Obayashi, T., Hayashi, S., Saeki, M., Ohta, H. & Kinoshita, K. ATTED-II provides coexpressed gene networks for Arabidopsis. *Nucleic Acids Res* **37**, D987-991 (2009).
- 33 Obayashi, T. *et al.* ATTED-II: a database of co-expressed genes and cis elements for identifying co-regulated gene groups in Arabidopsis. *Nucleic Acids Res* **35**, D863-869 (2007).
- 34 Armbruster, U. *et al.* The photosynthesis affected mutant68-like protein evolved from a PSII assembly factor to mediate assembly of the chloroplast NAD(P)H dehydrogenase complex in Arabidopsis. *Plant Cell* **25**, 3926-3943 (2013).
- 35 Ihnatowicz, A. *et al.* Mutants for photosystem I subunit D of *Arabidopsis thaliana*: effects on photosynthesis, photosystem I stability and expression of nuclear genes for chloroplast functions. *Plant J* **37**, 839-852 (2004).
- 36 Armbruster, U. *et al.* The Arabidopsis thylakoid protein PAM68 is required for efficient D1 biogenesis and photosystem II assembly. *Plant Cell* **22**, 3439-3460 (2010).
- 37 Sambrook, J. & Russell, D. W. Molecular cloning: a laboratory manual. **3rd edn.** **Cold Spring Harbor, NY: Cold Spring Harbor Laboratory Press** (2001).
- 38 Voigt, C. *et al.* In-depth analysis of the distinctive effects of norflurazon implies that tetrapyrrole biosynthesis, organellar gene expression and ABA cooperate in the GUN-type of plastid signalling. *Physiol Plant* **138**, 503-519 (2010).

- 39 Kunst, L. Preparation of physiologically active chloroplasts from Arabidopsis. *Methods Mol Biol* **82**, 43-48 (1998).
- 40 Qi, Y. *et al.* Arabidopsis CSP41 proteins form multimeric complexes that bind and stabilize distinct plastid transcripts. *J Exp Bot* **63**, 1251-1270 (2012).
- 41 DalCorso, G. *et al.* A complex containing PGRL1 and PGR5 is involved in the switch between linear and cyclic electron flow in Arabidopsis. *Cell* **132**, 273-285 (2008).
- 42 Gehl, C., Waadt, R., Kudla, J., Mendel, R. R. & Hansch, R. New GATEWAY vectors for high throughput analyses of protein-protein interactions by bimolecular fluorescence complementation. *Mol Plant* **2**, 1051-1058 (2009).
- 43 Richter, A. S. *et al.* Posttranslational influence of NADPH-dependent thioredoxin reductase C on enzymes in tetrapyrrole synthesis. *Plant Physiol* **162**, 63-73 (2013).
- 44 Peltier, J. B. *et al.* The oligomeric stromal proteome of Arabidopsis thaliana chloroplasts. *Mol Cell Proteomics* **5**, 114-133 (2006).

Acknowledgements

We thank Sabrina Finster, Christiane Kupsch and Christian Schmitz-Linneweber for their support in NIP chip and PPR prediction analyses, and Poul Erik Jensen and Pablo Pulido for fruitful discussions.

Author contributions

L.T. and F.R. conceived and conducted the generation and analysis of double mutants; T.K. and M.P. conceived and conducted the bioinformatics analyses. A.G., S.M. and L.T. conceived and conducted yeast two-hybrid analyses, M.R., B.H. and B.G. conceived and conducted the BiFC experiments; G.W. conceived and conducted electron microscopy; L.T. conceived and conducted all other experiments not mentioned before; L.T., P.P. and D.L.

designed and conceived the study. D.L. wrote the manuscript. All authors discussed the results and commented on the manuscript.

Additional information

Supplementary information is available online. Reprints and permissions information is available online at www.nature.com/reprints. Correspondence and requests for materials should be addressed to D.L.

Competing interests

The authors declare no competing financial interests.

Figure legends

Figure 1 | Genetic interactions between *gun1-102* and mutations affecting individual ribosomal proteins. **a**, Phenotypes of WT (Col-0), single (*gun1-102*, *prps1-1*, *prps21-1* and *prpl11-1*) and double (*gun1-102 prps1-1*, *gun1-102 prps21-1* and *gun1-102 prpl11-1*) mutant plants. The effective quantum yield of photosystem II (Φ_{II}) is indicated for each plant (average \pm SD; $n \geq 12$). The photograph of the albinotic *gun1-102 prpl11-1* plants (white circles) was taken at 5 days after germination (d.a.g.), whereas all other plants shown were four weeks old. **b**, Growth kinetics of the different genotypes. For each time point, the average leaf area ($n \geq 12$ individuals) is provided. Standard deviations were $<10\%$. **c**, Images of fully mature embryos from WT (Col-0), *gun1-102 prpl11-1* and *gun1-102 prpl11-1* plants. Scale bar: 20 μm . **d**, Phenotypes of four-week-old WT (Col-0) and *gun1-102 prpl11-1* escapers grown under different lighting conditions (25 [LL], 80 [GL] and 400 [HL] $\mu\text{mol photons m}^{-2}\text{s}^{-1}$). **e**, Electron micrographs of green (GS) and white sectors (WS) and the

transition zone between them (G-WS) in leaves from surviving *gun1-102 prpl11-1* plants. V, vacuoles; P, plastoglobules (P). Scale bar: 1 μ m.

Figure 2 | Characterization of plastid ribosomes. **a**, RNA gel-blot analyses of total RNA from 4-week-old WT (Col-0) and mutant (*gun1-102*, *prps1-1*, *prps21-1*, *gun1-102 prps1-1* and *gun1-102 prps21-1*) plants with probes specific for plastid rRNAs (23S, 16S, 5S and 4.5S) and mRNAs (*psbA*, *rbcL*) and *PRPS1* transcripts. Transcript sizes (in Kb) are shown. As control, cytosolic 25S rRNA was stained with ethidium bromide. **b**, Immunoblot analyses, employing antibodies recognizing proteins of the 30S (PRPS1, S5 and S7) and 50S (PRPL2 and L5) ribosomal subunits. Decreasing levels of WT proteins were loaded in the lanes marked 0.5x and 0.25x Col-0. **c**, Immunoblot analyses as in panel b were performed on WT (Col-0), *prps1-1* and double mutants of *prps1-1* and *gun2-gun5* using a PRPS1-specific antibody.

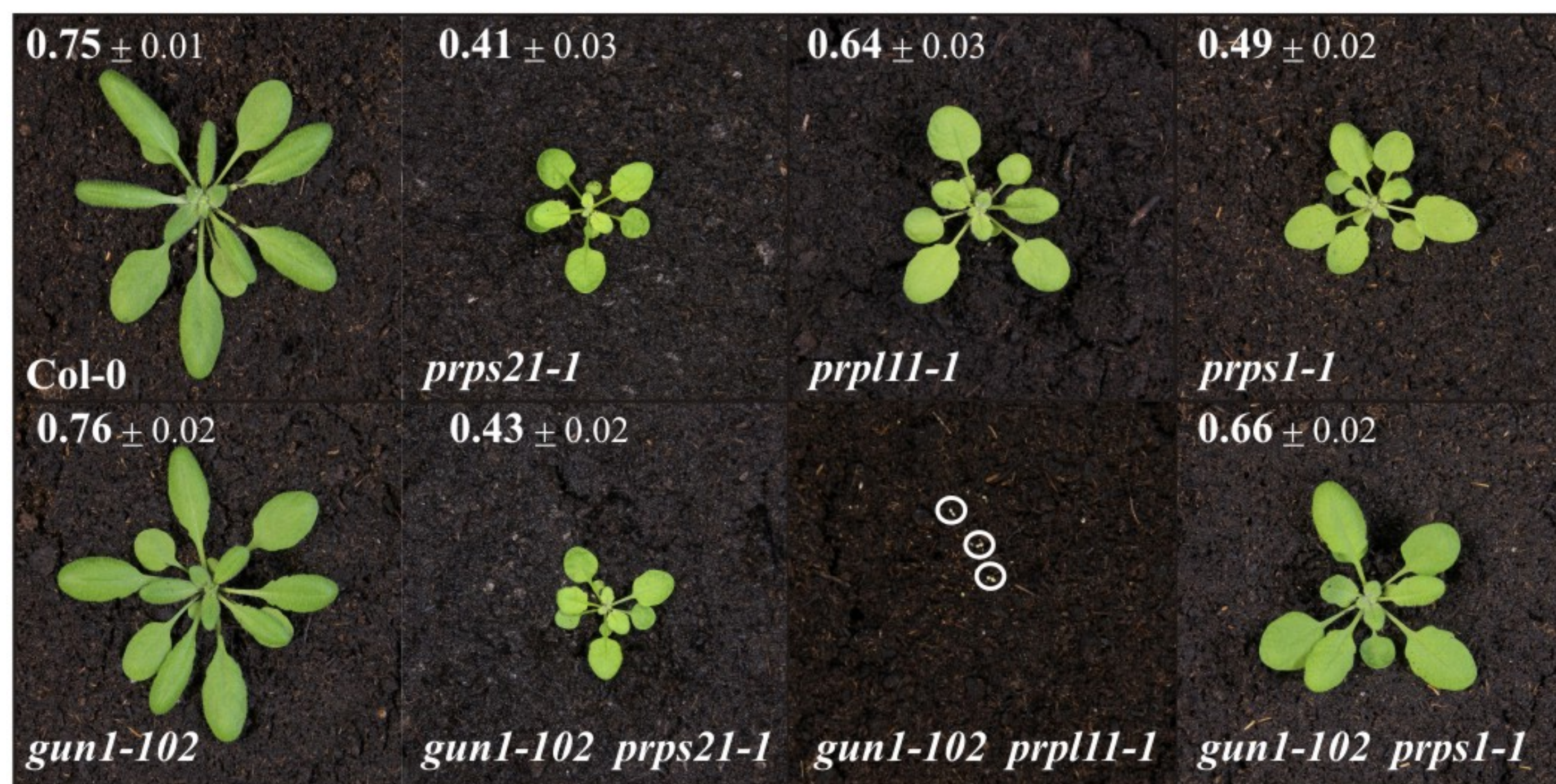
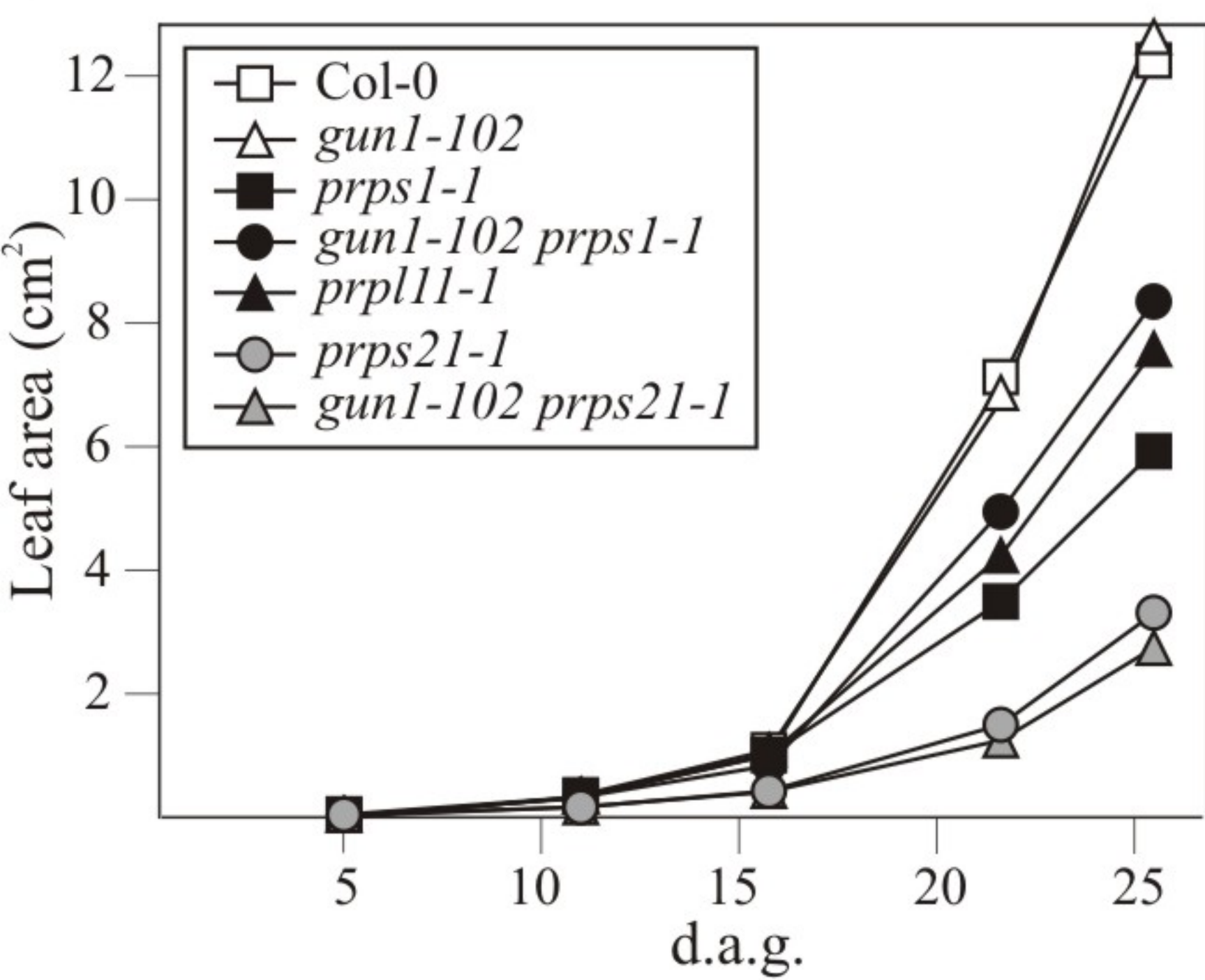
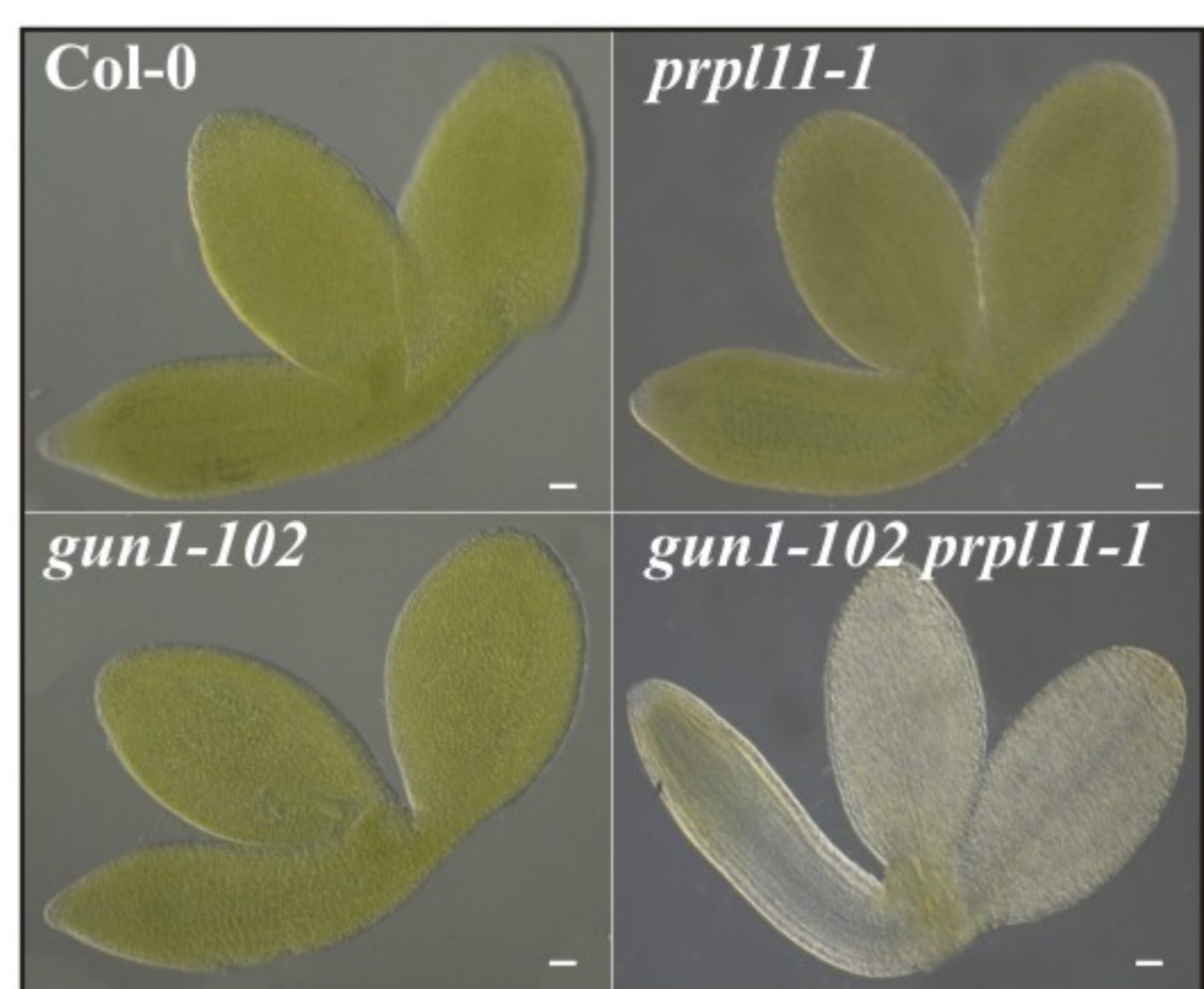
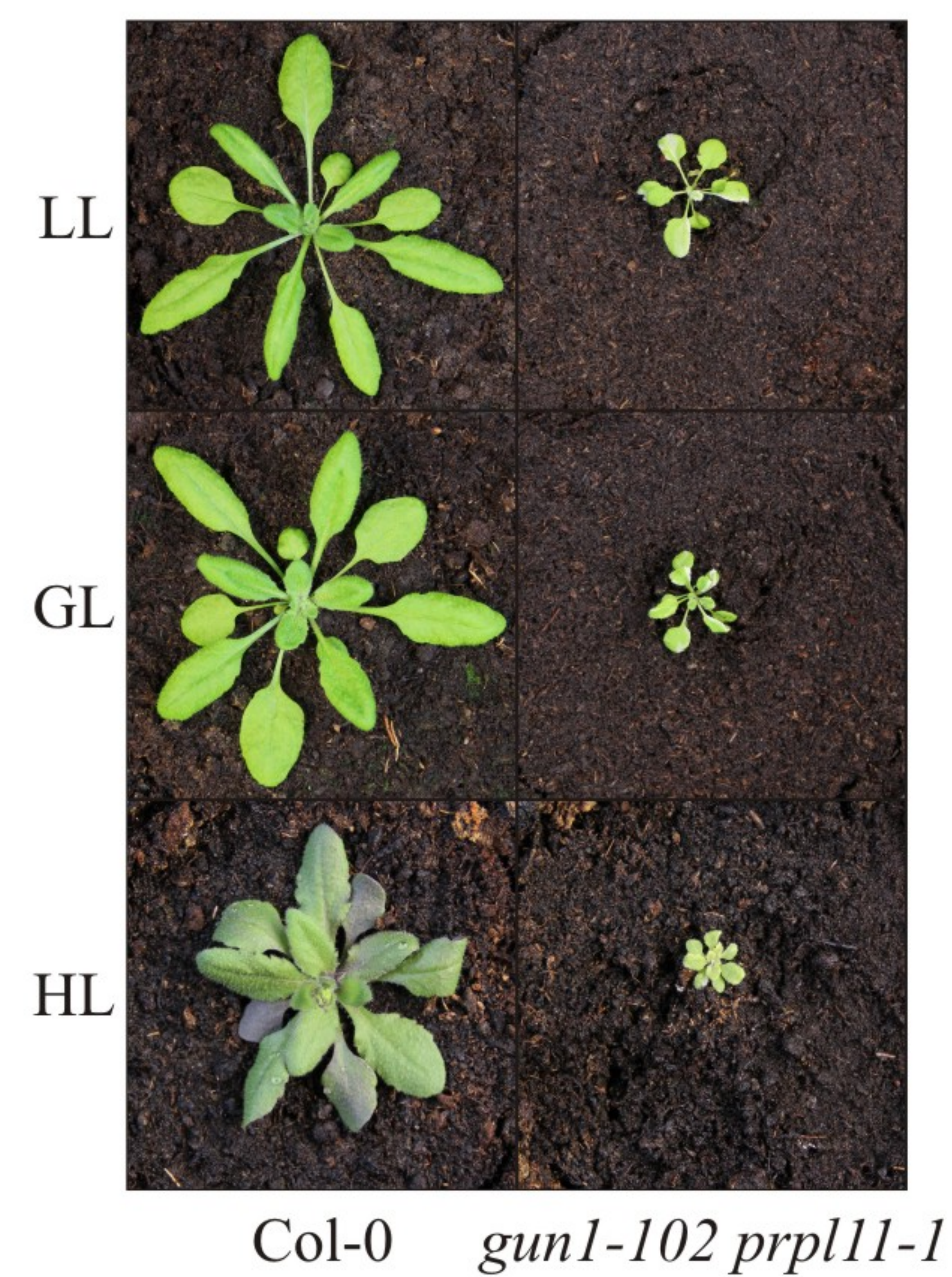
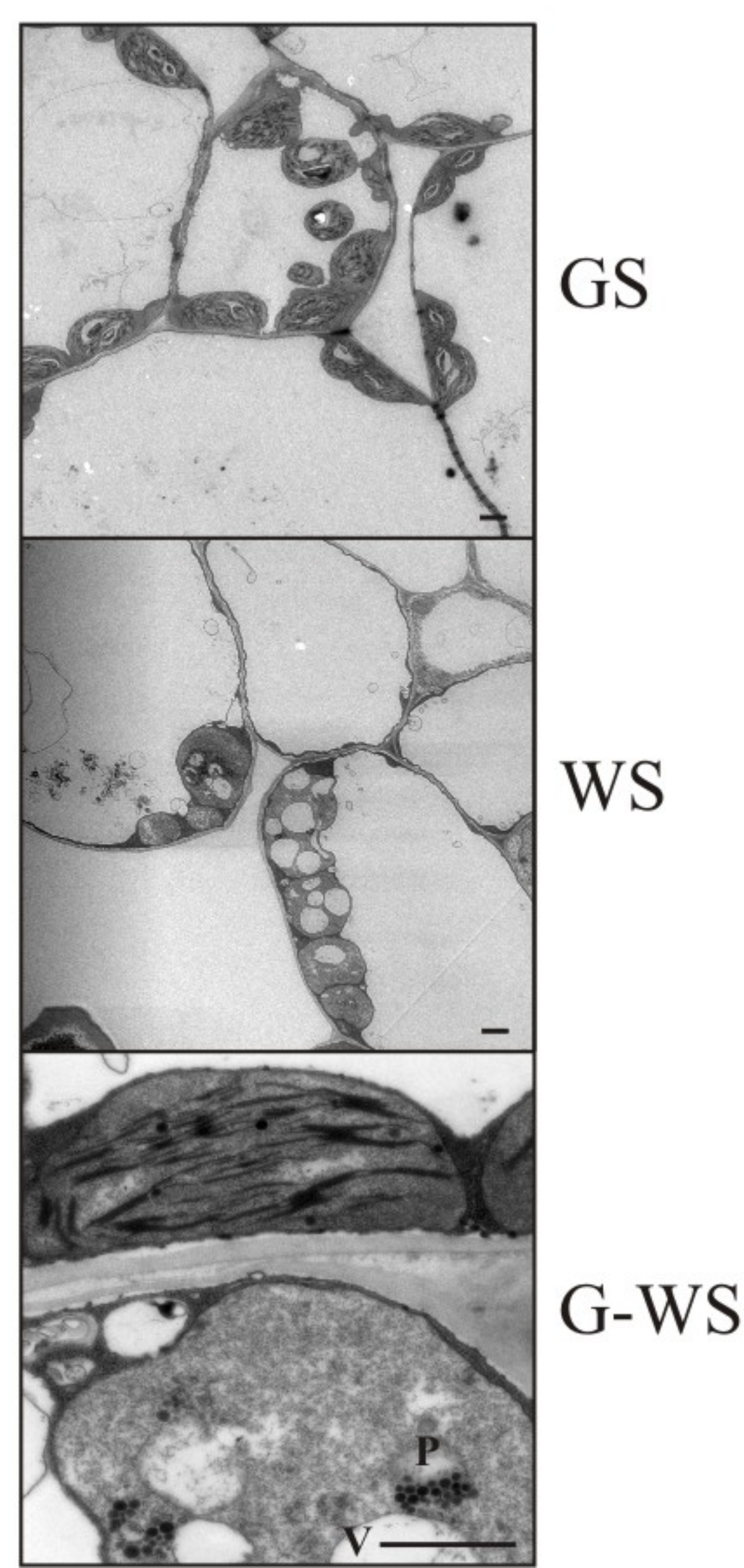
Figure 3 | Causes and effects of perturbations in PRPS1 levels. **a**, Immunoblot analyses of the PRPS1 protein in four-week-old leaves from WT (Col-0), mutants (*prps1-1*, *prpl11-1* and surviving *gun1-102 prpl11-1* individuals) and plants overexpressing *GUNI-GFP* (*oeGUNI-GFP*). **b**, Distribution of PRPS1, L2 and S7 among ribosome-bound and non-bound pools, as determined by sucrose gradient and Western analysis of proteins from WT (Col-0), *prps1-1*, *oePRPS1_1*, *gun1-102* and *oeGUNI-GFP* plants. Controls are shown in Supplementary Fig. 5e. **c**, Phenotypic characterization of four-week-old WT (Col-0), *prps1-1* and *PRPS1* overexpressors (*35S:PRPS1 prps1-1* or *oePRPS1_1*). The bottom panel shows the photosynthetic performance (measured as Φ_{II}), according to the colour scale. In addition, mean values (\pm SD) are provided. For plants with inhomogeneous Φ_{II} , values for young emerging leaves and older leaves are indicated separately. **d**, Relative expression levels of *PRPS1* transcripts (white bars) and protein (black bars) in *prps1-1* and *oePRPS1* plants (Col-

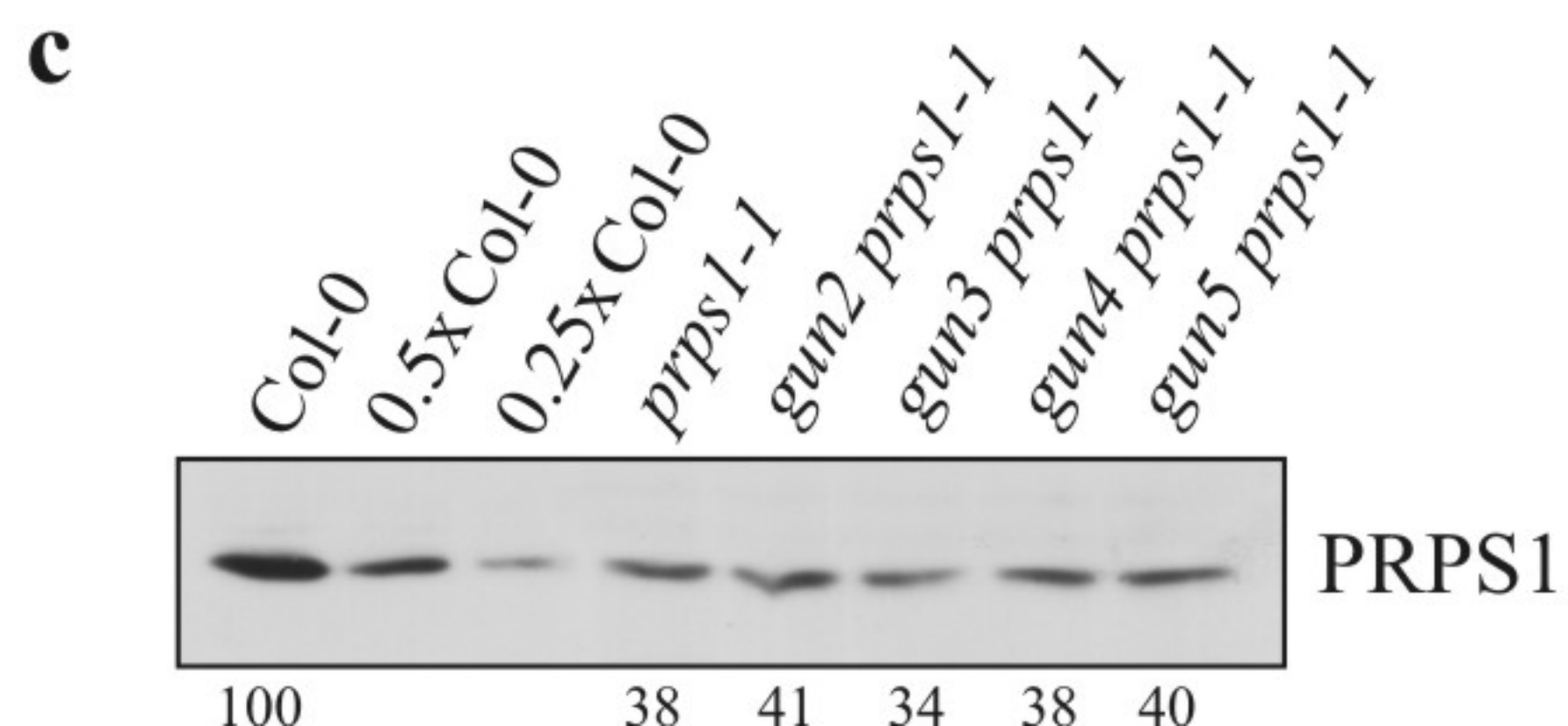
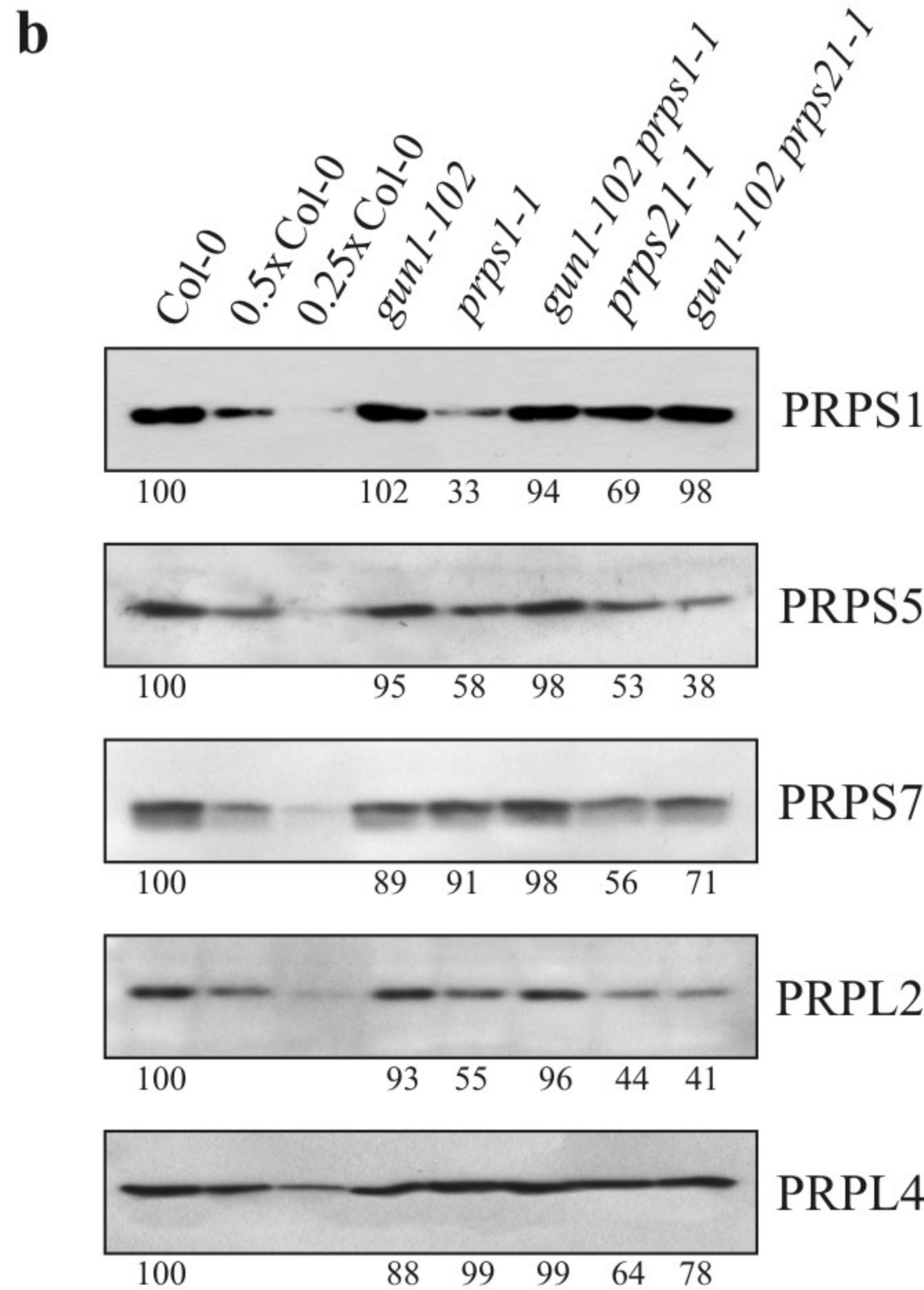
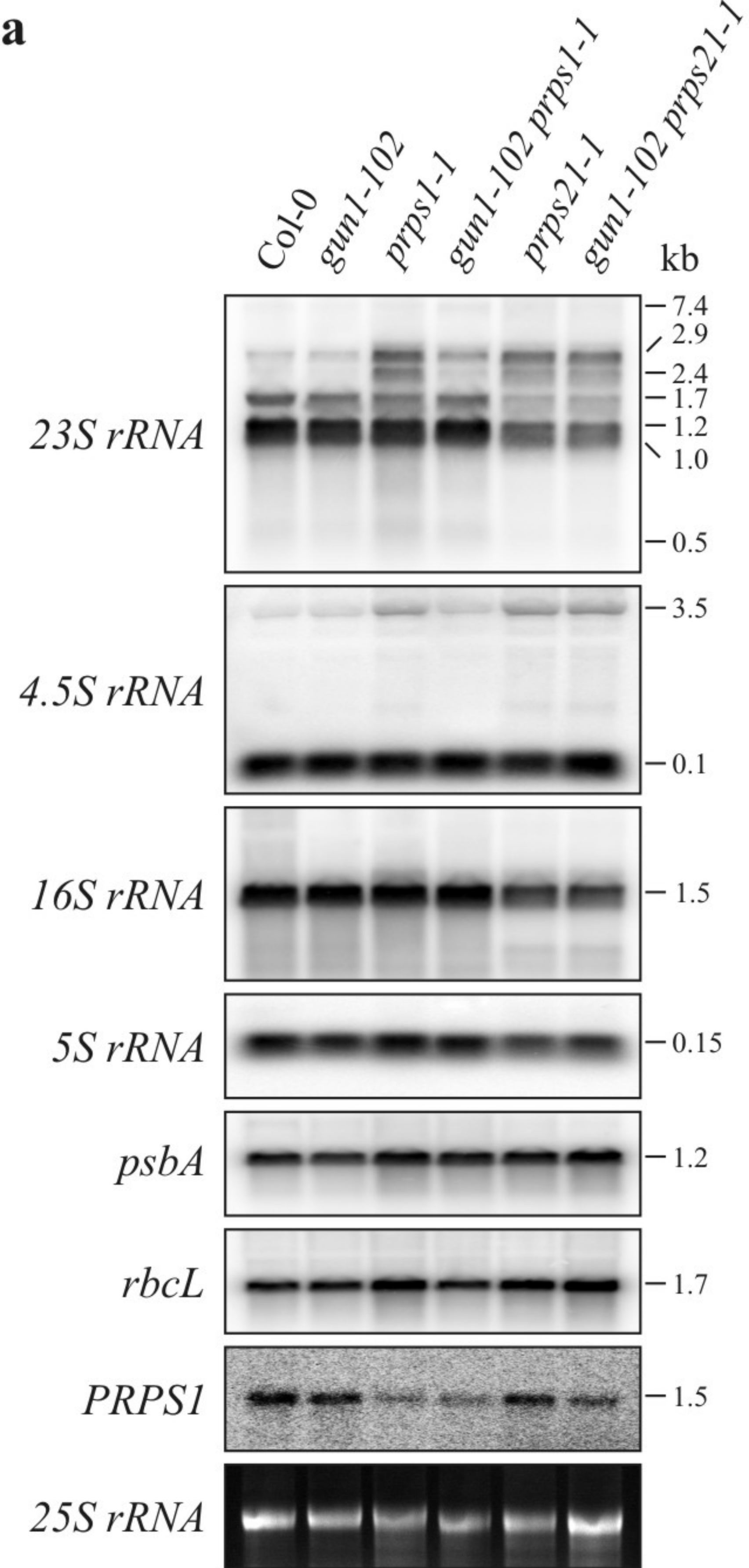
0=100%). *PRPS1* transcript accumulation was measured by real-time PCR of leaf cDNA; protein levels were quantified from Supplementary Fig. 5g.

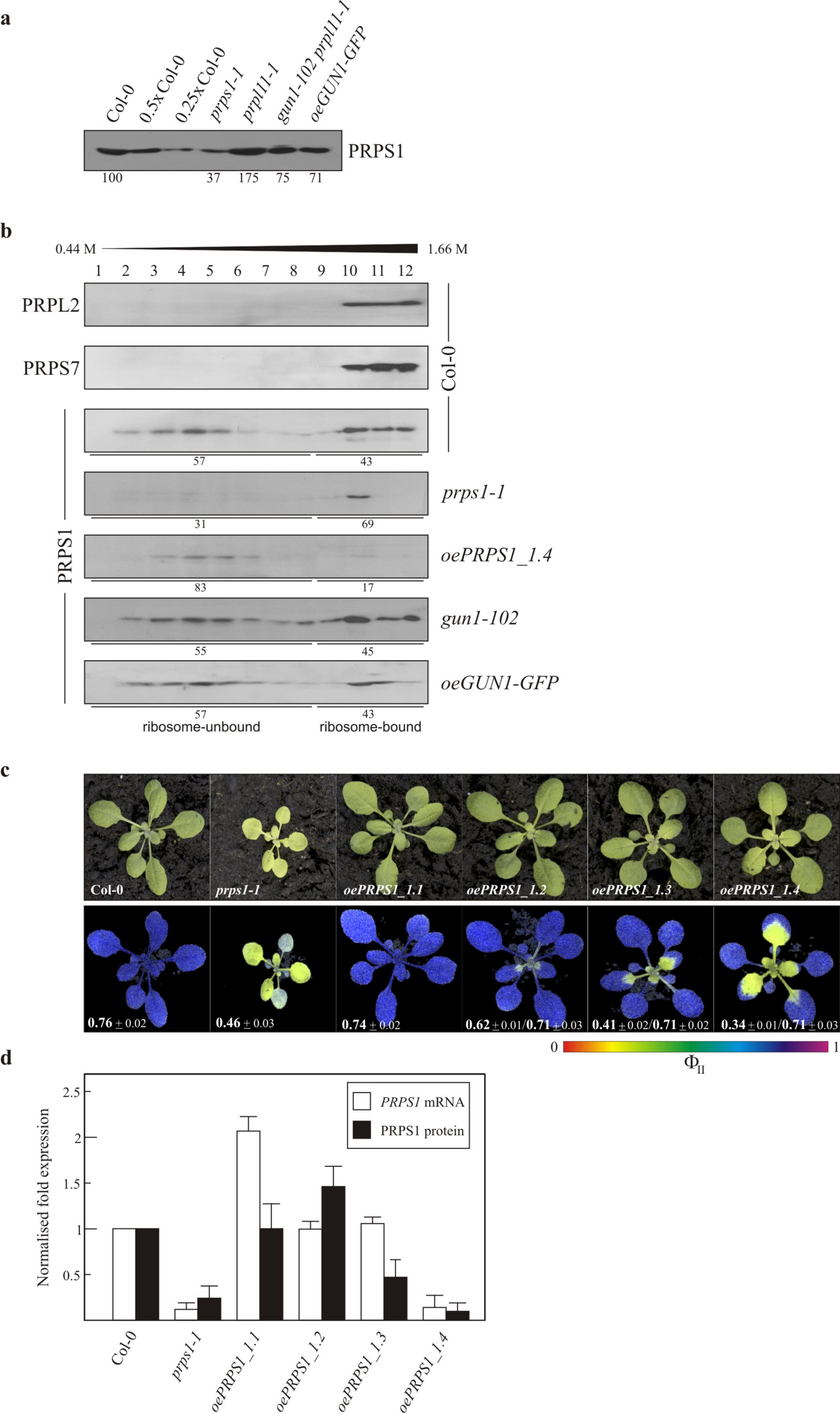
Figure 4 | Protein interactions of GUN1. **a** and **b**, Yeast two-hybrid assays. Cells were co-transformed with a plasmid expressing mature GUN1 (**a**) or its truncated versions (GUN1_N, GUN1_M, GUN1_C) (**b**) as bait protein and plasmids expressing potential interaction partners as prey proteins. Yeast cells were grown on permissive (-Trp-Leu) and selective (-Trp-Leu-His+5 mM 3-AT) medium (which reveals interactions). Asterisks indicate *GUN* gene products. Controls are shown in Supplementary Fig. 6a. **c**, Bimolecular fluorescence complementation (BiFC). GUN1 and test proteins were either fused to the N-terminal (YN) or C-terminal (YC) end of the Venus protein, respectively, and co-transformed into tobacco leaves. Reconstitution of YFP fluorescence (signaling positive interaction) Chl autofluorescence (Auto) and their overlay are shown. Scale bars = 20 μ m. **d**, Immunoblot analysis of TPB proteins from WT (Col-0), *gun1-102* and *oeGUN1-GFP* lines. Decreasing WT protein concentrations were loaded into lanes 0.5x and 0.25x Col-0. **e**, Sucrose-gradient analysis of PRPS1 and TPB proteins from WT (Col-0), *gun1-102* and *oeGUN1-GFP* plants. Proteins were detected by immunoblot analysis. **f**, Stromal proteins were fractionated by BN/SDS-PAGE, and proteins were detected with specific antibodies. Molecular masses of protein complexes were estimated according to ref. ⁴⁴. The ~40-kDa PRPS1 signal corresponds to monomeric PRPS1.

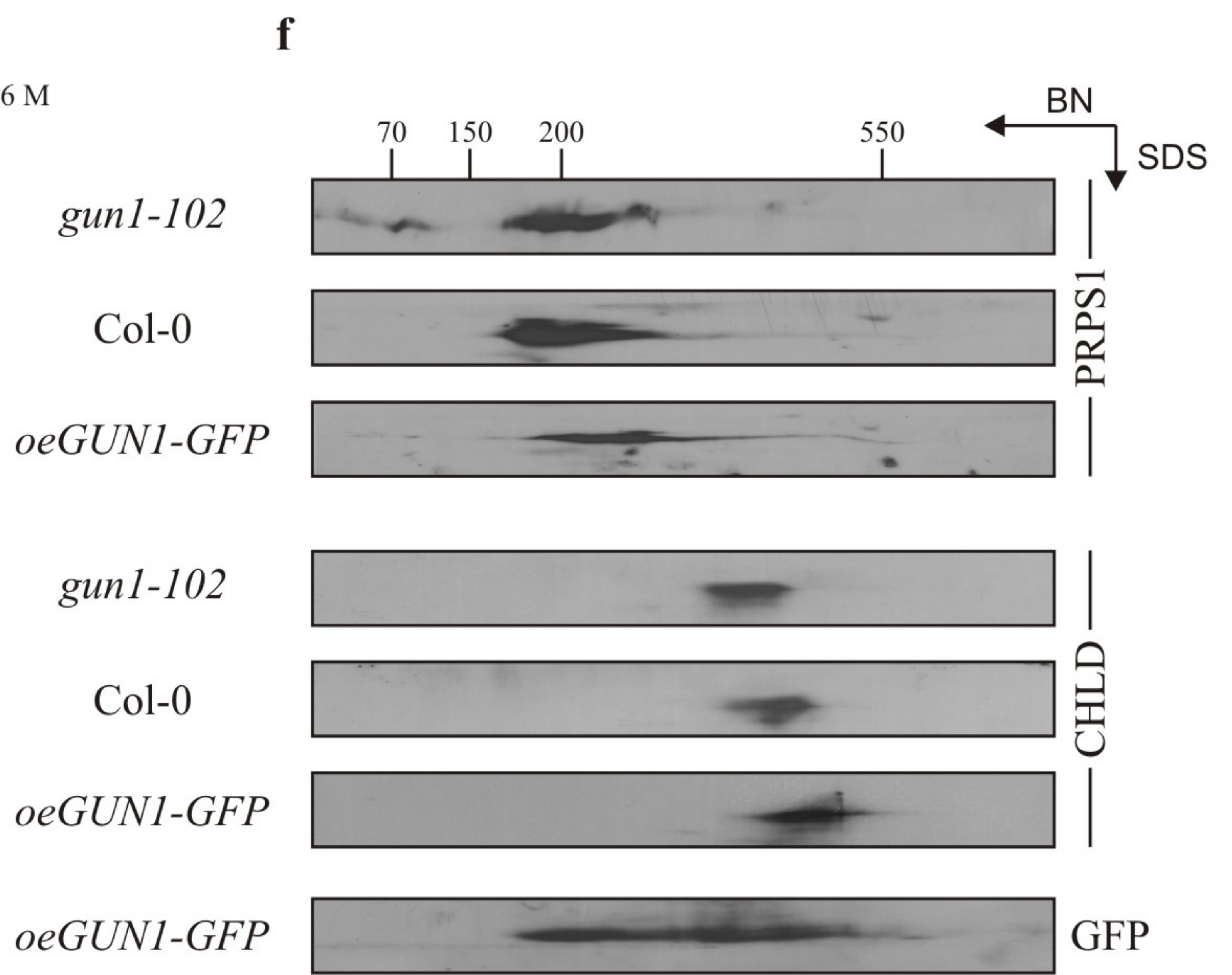
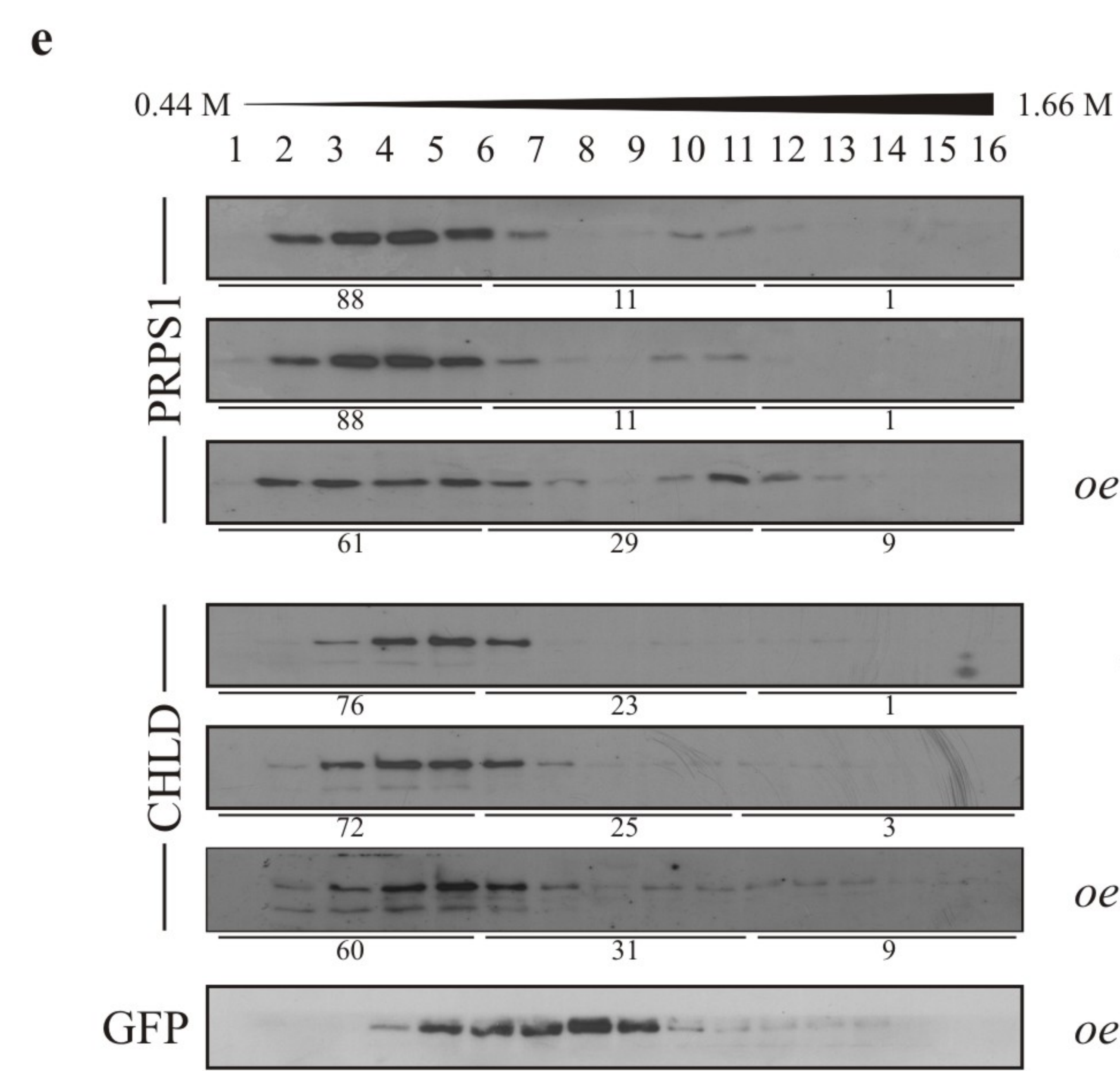
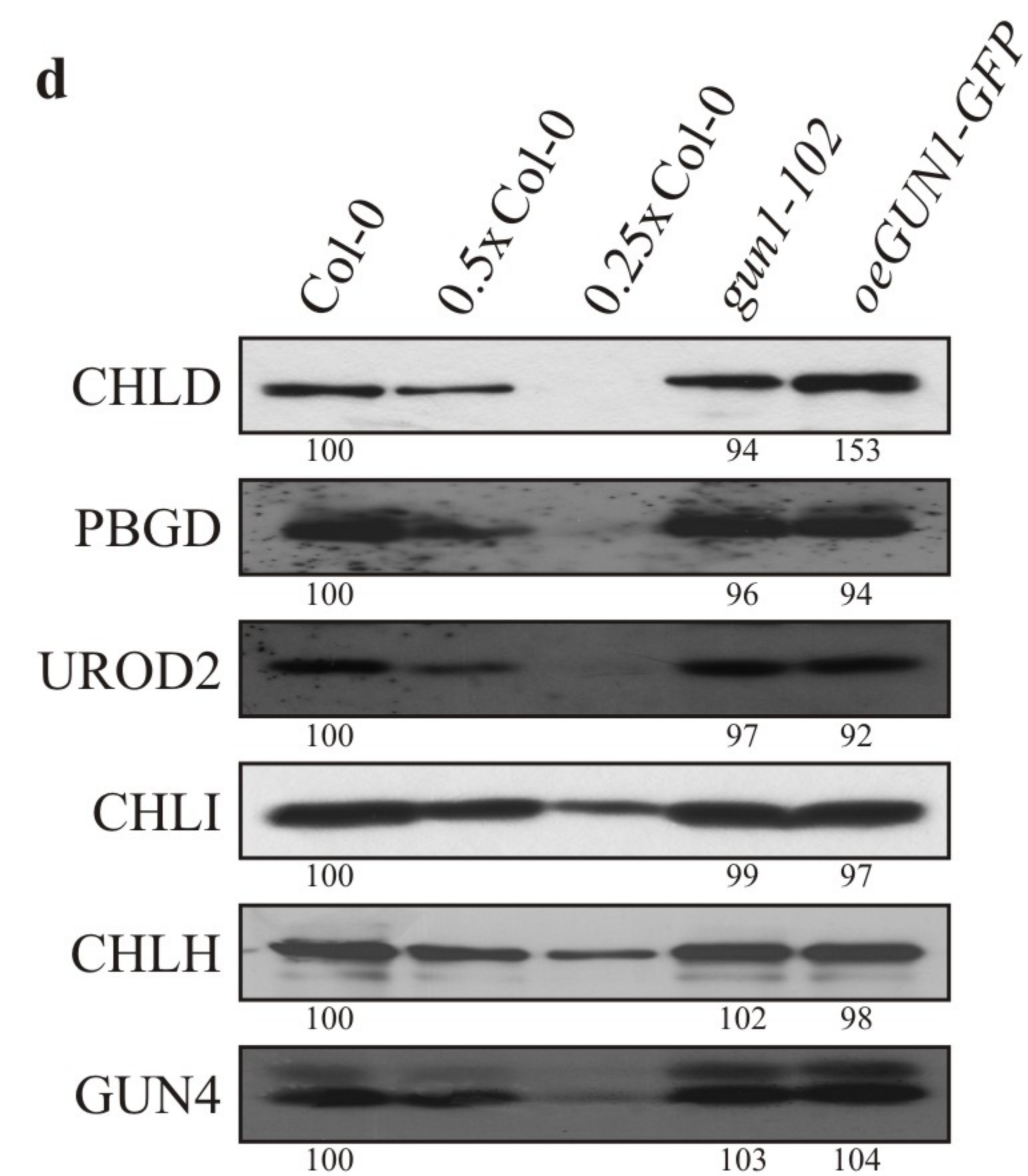
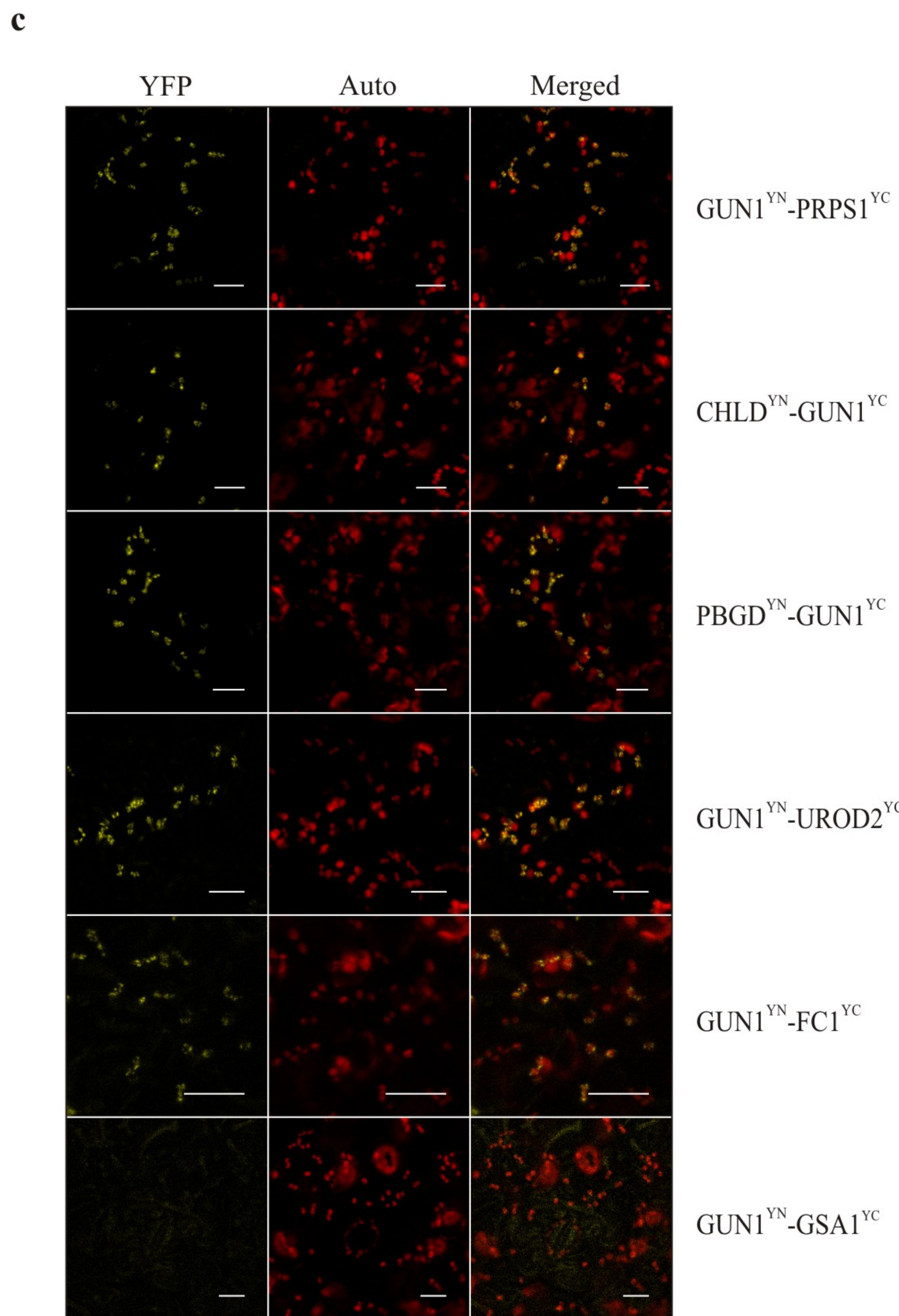
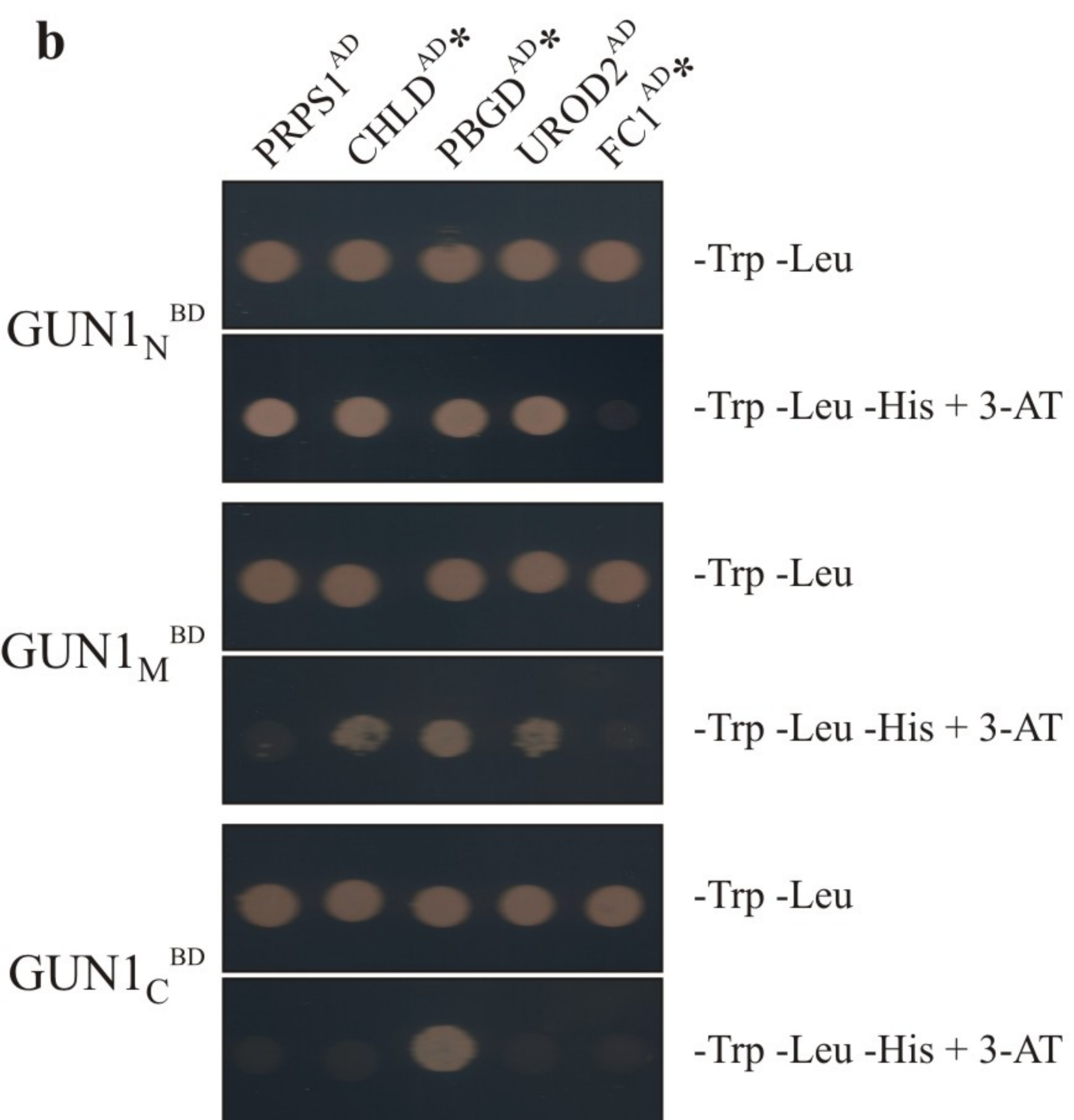
Figure 5 | The retrosome model. **a**, GUN1 can physically interact with certain components of PGE (grey shading) and TPB (green shading). Perturbations (symbolized by thin arrows) in PGE (e.g. by lincomycin treatment) or TPB (e.g. by NF treatment) might cause some of the components affected to interact with GUN1, thus promoting the formation of retrosomes that trigger retrograde signaling. If only involved in signaling, the abundance of retrosomes could

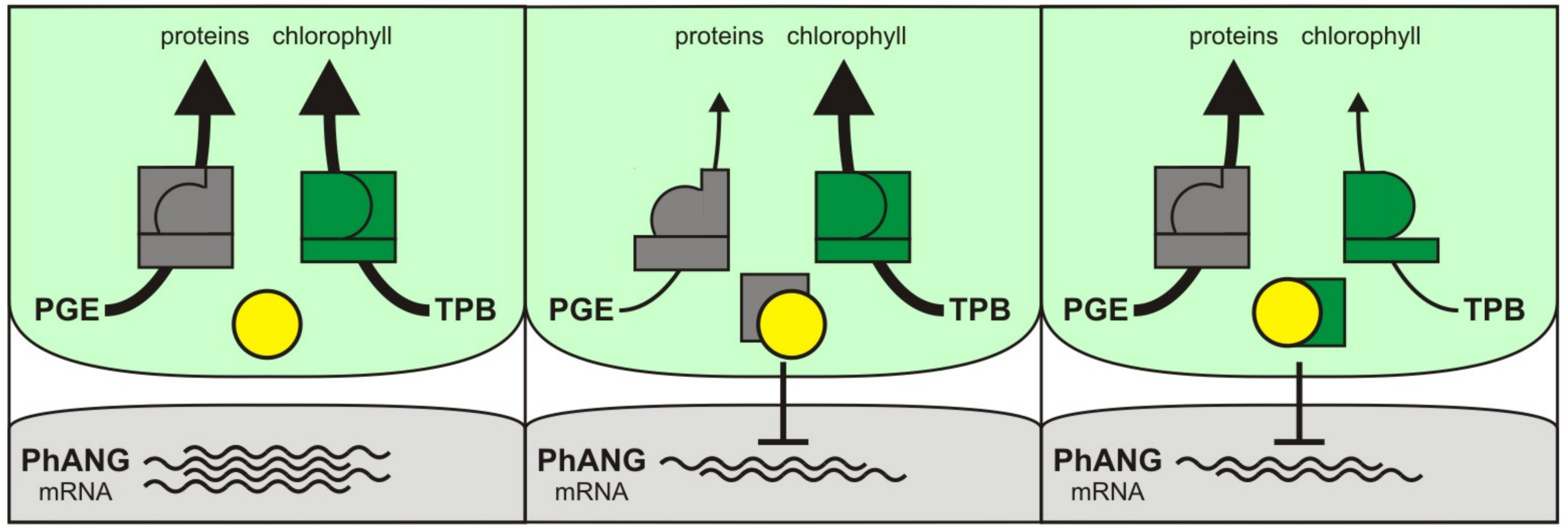
be limited by the – apparently low – concentration of GUN1, so that retrosomes might themselves contain GUN1 (upper panel). Retrosomes might also be bifunctional, i.e. they could also coordinate PGE and TPB activities at the protein level (lower panel) by down-regulating pathways (symbolized by the thick, tapering arrow). Bifunctional retrosomes should be relatively abundant so that GUN1 might serve as an assembly factor (indicated by the dotted yellow circle). **b**, In *gun1* mutants neither type of retrosomes is formed.

a**b****c****d****e**





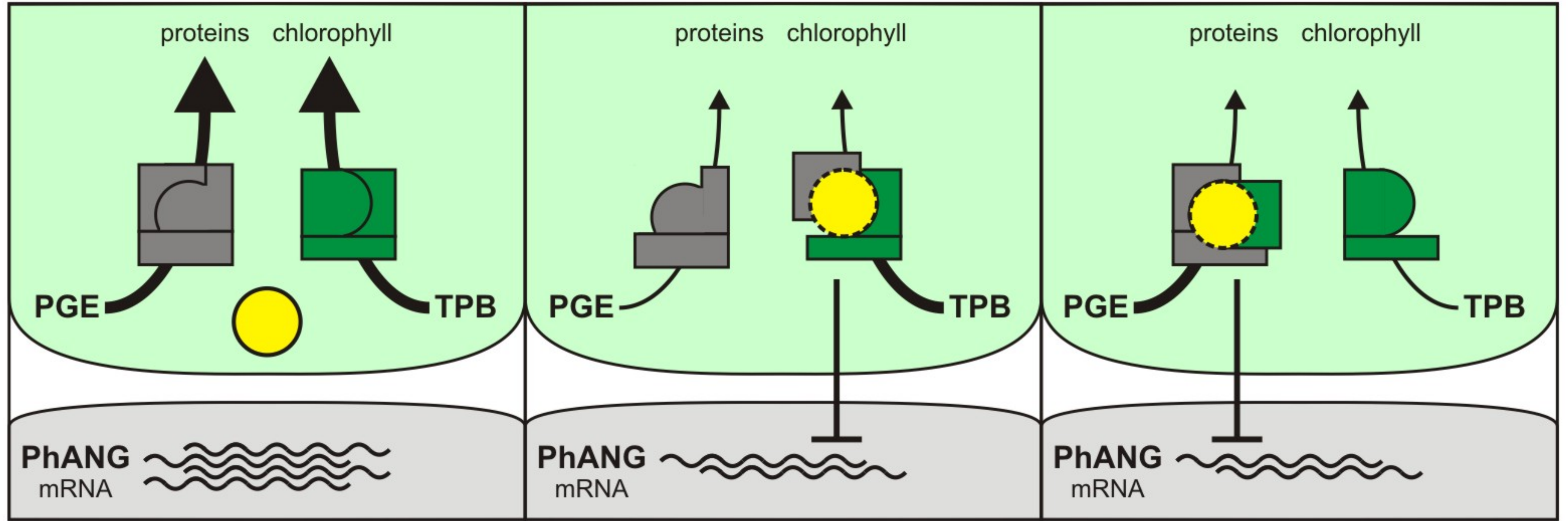
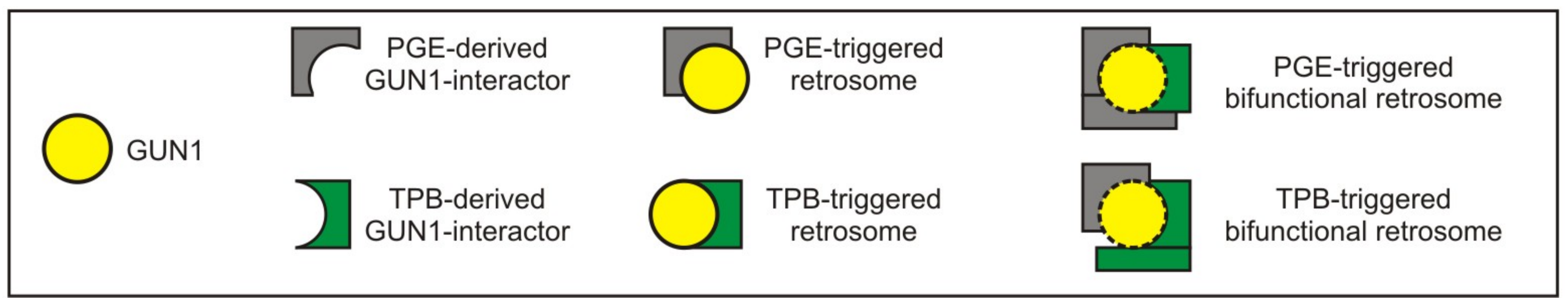
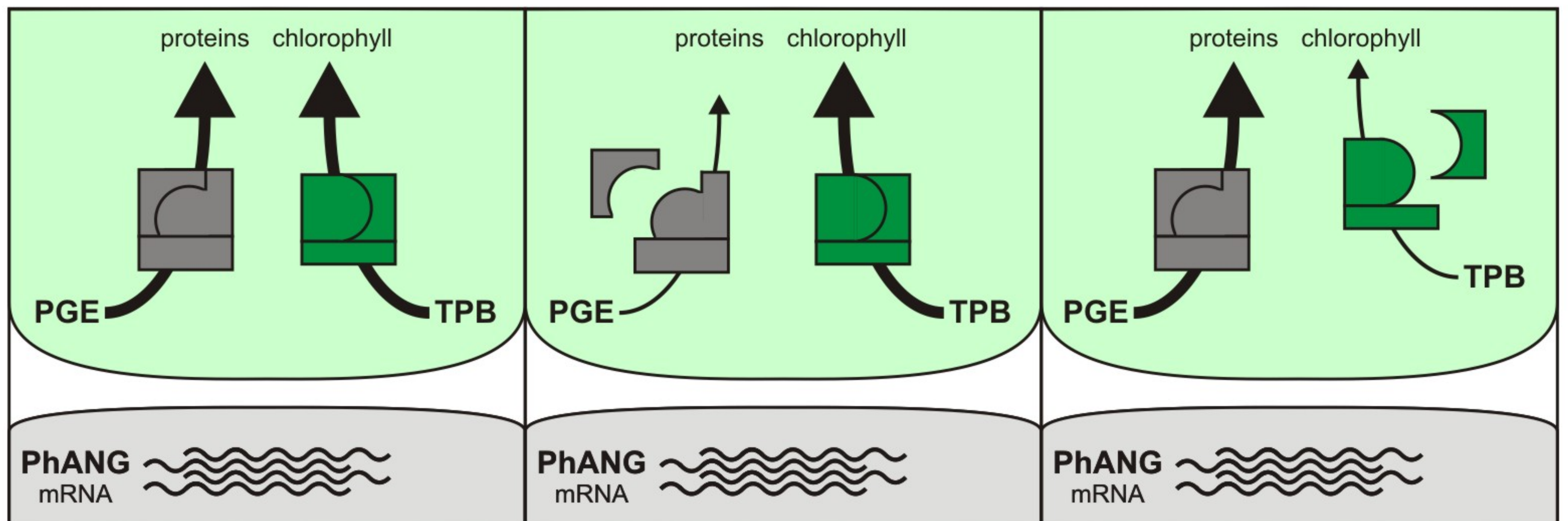


a**normal conditions****PGE limitation**
(e.g. +lincomycin)**TPB limitation**
(e.g. +norflurazon)

retosomes

bifunctional retosomes

WT

**b***gun1*

11. ACKNOWLEDGEMENTS

Siamo arrivati alla fine anche di questa avventura, ed è doveroso ringraziare tutti quelli che in un modo o nell'altro, mi hanno aiutato a raggiungere questo importante traguardo. Innanzitutto vorrei ringraziare il Professor Paolo Pesaresi, che mi ha accolto nel suo laboratorio ormai più di 6 anni fa, e che mi ha dato l'opportunità di imparare tutto quello che ora so in campo scientifico, e di conoscere magnifiche persone provenienti da ogni parte del mondo. Ringrazio anche queste persone, perché è stato un piacere avere conosciute, aver conosciuto le loro culture e lavorare con loro. Ringrazio Simona Masiero, anche se un semplice ringraziamento non è abbastanza. Simona è una persona straordinaria, è l'ingranaggio che fa funzionare qualsiasi cosa, è la mamma di tutti noi. Per qualsiasi cosa, che vada dai problemi in ambito lavorativo al supporto morale, si può sempre contare sul suo aiuto. Anche se sempre oberata di lavoro, trova sempre del tempo da dedicare a chi ne ha bisogno, e questo la rende una persona speciale. Ringrazio tutti i miei colleghi, Veronica, Ludovico, Valentina, Michela, che durante questi anni hanno condiviso con me le loro conoscenze, permettendomi di imparare sempre cose nuove. Ringrazio tanto Sara Simonini, perché oltre a essere stata una mia collega, è anche una mia grande amica. Mi ha insegnato molte cose in ambito lavorativo, e mi ha dato un grandissimo supporto morale nei momenti in cui avevo bisogno di qualcuno che mi ascoltasse e capisse. Ringrazio Tommaso Pellizzer, perché oltre a essere stato un compagno di corso e un collega, è una delle migliori amicizie che mi sono capitate in tutti i miei anni di università. Sono orgoglioso delle scelte che ha fatto e della strada che ha intrapreso, e gli auguro di raggiungere i traguardi che davvero si merita. Ringrazio tutti gli studenti a cui in questi anni ho cercato di trasmettere le mie conoscenze, perché questo mi ha permesso di crescere sia in ambito lavorativo che in ambito relazionale. Il rapporto con questi studenti non è mai stato un freddo rapporto professionale; con loro si sono condivise montagne di risate e di opinioni. In particolare ringrazio due persone: Francesca Ruperto, perché è stata la studentessa più espansiva e simpatica di tutti, e Claudia Arellano Fiore, perché è una ragazza eccezionale, con una determinazione incredibile. Nonostante tutti gli ostacoli che ha dovuto superare nella sua vita, è sempre riuscita a raggiungere i traguardi che si era prefissata senza mai vacillare. E' un'amica speciale da cui prendere esempio per affrontare la vita con una marcia in più. Ringrazio ora il mio ultimo studente Fabio Giulio Moratti, anche se ormai da tempo

non lo considero più un mio studente, ma un mio pari, se non superiore. La semplicità con cui affronta la vita, la sua determinazione, e la sua voglia di mettersi in gioco, credo non abbiano eguali. È stato un piacere conoscerlo e fare la sua amicizia, ed è stato per me un onore contribuire, seppur in minima parte, alla sua formazione scientifica. Sono sicuro che in un futuro non troppo lontano sentirò parlare di lui e dei suoi successi, e questo mi renderà orgoglioso dei traguardi che avrà raggiunto. Ringrazio il mio collega e in primis amico Roberto, per tutto il supporto lavorativo e non, che mi ha dato, soprattutto in questo ultimo anno. Ringrazio tutti gli amici che ho al di fuori dell'ambiente universitario, perché mi hanno dato un grandissimo supporto, perché mi sanno sempre capire e perché con loro ho passato e passerò dei momenti bellissimi. Ringrazio chi mi ha aiutato a preparare gli esami di matematica e fisica, chi mi tiene compagnia sul treno, chi si interessa alle mie cose. Un ringraziamento speciale va a uno di loro. Serena Signorelli, ti ringrazio per la stupenda amicizia che dura ormai da più di dieci anni. Servirebbero pagine di parole per descrivere la nostra amicizia, ma in realtà sappiamo entrambi che basta guardarci negli occhi per capire tutto. Basta solo una canzone per ricordare quanto è forte la nostra amicizia e per rievocare tutti i momenti e le situazioni che abbiamo condiviso. Grazie di far parte della mia vita. Grazie alla musica, che mi accompagna da tutta la vita, e che mi fa provare emozioni bellissime. Ringrazio la mia famiglia per avermi dato la possibilità di studiare, e in particolare mia sorella che ha sempre avuto una grandissima stima di me, e che io ho per lei. Ringrazio anche tutti quelli che mi hanno messo i bastoni fra le ruote, perché è stato un grandissimo piacere e un'immensa soddisfazione vincere contro di loro e uscire sempre a testa alta. Infine ringrazio anche me stesso, per non aver mai mollato di fronte agli ostacoli e ai problemi, per essermi impegnato a fondo e per aver sfruttato tutte le occasioni che la vita mi ha dato.